

**METABOLIC MANIPULATION OF GLUTATHIONE AS AN ANTICANCER
THERAPEUTIC TARGET**

PATRICK C TURNBULL

A DISSERTATION SUBMITTED TO THE FACULTY OF GRADUATE STUDIES IN
PARTIAL FULFILLMENT OF THE REQUIREMENTS FOR THE DEGREE OF DOCTOR
OF PHILOSOPHY

GRADUATE PROGRAM IN KINESIOLOGY AND HEALTH SCIENCES
YORK UNIVERSITY
TORONTO, ONTARIO

August 2019

© Patrick C Turnbull, 2019

Abstract

Many cancers rely on glycolysis rather than mitochondrial metabolism as their primary source of ATP. As such, altering this balance through forced mitochondrial activation has yielded promising results as anticancer therapies for specific cancers. In previous studies, stimulated mitochondrial activation through exposure to palmitoylcarnitine, a mitochondrial fatty-acid substrate, resulted in colon and prostate cancer-specific cell death, however, mitochondrial fatty-acid oxidation led to increased cervical cancer growth. The primary mechanism for promoting antineoplastic effects in response to palmitoylcarnitine is through oxidative stress, namely through production of superoxide and subsequently hydrogen peroxide (H_2O_2). However, H_2O_2 can be hormetic in nature, whereby elevated H_2O_2 can result in deleterious effects, yet modest H_2O_2 can promote growth. Therefore, the ability of the cell to regulate H_2O_2 is of apparent importance, highlighting glutathione, the most abundant intracellular antioxidant, as a potential determinant of cancer survival following palmitoylcarnitine. The purpose of this dissertation was to first determine the response of glutathione to palmitoylcarnitine within relation to cell survival. Following palmitoylcarnitine, glutathione responses seemingly dictated cell fate, whereby HT29 colorectal carcinoma cells displayed decreased cell survival, increased H_2O_2 and decreased glutathione. CCD 841 normal colon cells were insensitive to palmitoylcarnitine despite increased H_2O_2 , yet maintained glutathione. HepG2 hepatocarcinoma cells, cells associated with fatty-acid stimulated disease progression, increased cell growth with coordinated increases in glutathione following palmitoylcarnitine. This dissertation considered recent evidence that suggests combined inhibition of glutathione and thioredoxin, another intracellular antioxidant, is required for anticancer effects in established tumours. Auranofin is a putative inhibitor of the thioredoxin system. HCT 116 p53^{-/-} cells were resistant to auranofin at doses that

HCT 116 p53^{+/+} cells were sensitive to, however concurrent exposure of auranofin and glutathione depletion through serine and glycine starvation sensitized HCT 116 p53^{-/-} cells to decreased cell survival. This observation was repeated in a p53^{mutant} cell line, HT29. Taken together, this thesis identifies glutathione as an important regulator in determining cell fate in response to palmitoylcarnitine, the dual role of glutathione and thioredoxin in influencing cell fate in relation to p53, and highlights the potential of redox-buffering systems as therapeutic targets for selective antineoplastic growth.

Acknowledgements

The completion of this thesis represents not only the result of my time spent conducting research, but many experiences and lessons I have learned along the way. None of this would have been possible without the support of many people.

I would first like to thank my supervisor, Dr. Chris Perry for everything you've done for me, allowing me to learn and make my own mistakes and be there as a sounding board always willing to give advice. Your passion for science is contagious, and I consider myself lucky to have been able to learn from you these past several years. Not only have I grown as a scientist and a person, but also my ability to stretch a 2-minute joke into an 8-minute joke is a skill I will take with me and cherish forever.

I would like to thank the current and past members of the Perry lab, who I have worked with and who have helped me throughout my time at York. Sofia, we started off together as undergrad students in the same program, then as MSc students in the same lab and finally as PhD students at York. I can't wait to find out where you're taking us next! The key to being successful (according to Google) is to surround yourself with successful people, and I've been very fortunate (see: strategic) to be in the same lab as you for the last 10 years. To Meg (the Waldorf to my Statler?), I went running with you once and it was horrible. For someone so short, why do you run so fast? Thank you for pretending to listen to me when I started reasoning out problems out loud, and for eventually chiming in when I got to a logical answer. I stand by that most of our jokes were funny, and that everyone was better off for listening to us. To Ali, the loud and chatty student I had in one of my classes who became the loud and chatty undergrad in our lab; thank you for all of your hours of hard work and dedication. Whatever you decide to go on to next won't be ready for the volume that you're going to bring, but they'll be better off for it.

To my family, you guys are the smartest and hardworking individuals I know. Thank you for all of your support throughout this entire process. I would not have been able to do this without any of you.

To Judy and Ambo, I can never thank either one of you enough for all that you've done for me.

Finally, to Alicia, you have given me support and patience throughout this entire process. I have been told (by Meg and Sofia...) that I can be a little tough to deal with at times, thank you for always dealing with me. Your support has meant everything.

Table of contents

ABSTRACT	II
ACKNOWLEDGEMENTS	IV
TABLE OF CONTENTS	V
LIST OF FIGURES	VIII
LIST OF ABBREVIATIONS	X
CHAPTER 1 GENERAL INTRODUCTION	1
MITOCHONDRIA.....	2
TARGETING MITOCHONDRIA IN CANCER.....	3
THE ROLE OF GLUTATHIONE IN MEDIATING CELL SURVIVAL.....	4
PURPOSE.....	5
REFERENCES.....	6
CHAPTER 2 LITERATURE REVIEW	7
2.1 THE MITOCHONDRION	7
2.1.1 <i>Glycolysis</i>	9
2.1.2 <i>β-oxidation</i>	10
2.1.3 <i>The TCA cycle</i>	11
2.1.4 <i>Mitochondrial-mediated cell death</i>	11
2.2 REACTIVE OXYGEN SPECIES	12
2.2.1 <i>Oxidative stress</i>	16
2.3 MECHANISMS FOR REGULATING OXIDATIVE STRESS	17
2.3.1 <i>Decreasing mitochondrial ROS production</i>	17
Mitochondrial uncoupling.....	18
2.3.2 <i>Promoting ROS degradation</i>	18
Glutathione	19
Thioredoxin.....	23
NADPH	25
2.4 THE MITOCHONDRIA AND CANCER	25
2.4.1 <i>Cancer metabolism confers a pro-neoplastic environment</i>	28
Glycolytic intermediates promote a pro-neoplastic environment.....	30
TCA cycle intermediates are required for neoplastic growth.....	31
2.5 CANCER AND ANTIOXIDANT REGULATION	32
2.5.1 <i>Glutathione and thioredoxin are highly implicated in cancers</i>	33
2.5.2 <i>Cancer and glutathione</i>	34
Glutathione regulating cancer growth.....	34
Glutathione in chemoresistance.....	36
2.5.3 <i>Cancer and thioredoxin</i>	39
Thioredoxin regulating cancer growth	39
Thioredoxin in chemoresistance.....	41
2.5.4 <i>Antioxidant targeting for cancer therapy</i>	43
Glutathione inhibition for cancer therapy.....	44
Thioredoxin inhibition for cancer therapy.....	47
Dual targeting of glutathione and thioredoxin for cancer therapy.....	48
2.6 MITOCHONDRIAL TARGETED THERAPIES	49
2.6.1 <i>Mitochondrial activation as an anticancer therapy</i>	51
2.6.2 <i>Mitochondrial inhibition as an anticancer therapy</i>	53
2.7 CHAPTER 2 REFERENCES	55

CHAPTER 3 OBJECTIVES AND HYPOTHESIS	67
3.1 OVERVIEW OF THESIS.....	67
3.2 OBJECTIVES AND HYPOTHESIS FOR STUDY 1 (CHAPTER 4).....	67
<i>Hypothesis</i>	68
3.3 OBJECTIVES AND HYPOTHESIS FOR STUDY 2 (CHAPTER 5).....	68
<i>Hypothesis</i>	69
3.4 OBJECTIVES AND HYPOTHESIS FOR STUDY 3 (CHAPTER 6).....	69
<i>Hypothesis</i>	70
3.5 ADDITIONAL CONTRIBUTIONS	70
CHAPTER 4 THE FATTY ACID DERIVATIVE PALMITOYLCARNITINE ABROGATES COLORECTAL CANCER CELL SURVIVAL BY DEPLETING GLUTATHIONE.....	73
ABSTRACT.....	75
INTRODUCTION.....	76
EXPERIMENTAL PROCEDURES	78
RESULTS.....	83
DISCUSSION.....	94
CONFLICT OF INTEREST.....	101
REFERENCES.....	102
CHAPTER 5 SYNERGISTIC ACTIVATION OF MITOCHONDRIAL METABOLISM AND THE GLUTATHIONE REDOX COUPLE PROTECTS HEPG2 HEPATOCARCINOMA CELLS FROM PALMITOYLCARNITINE-INDUCED STRESS	105
ABSTRACT.....	107
INTRODUCTION.....	109
EXPERIMENTAL PROCEDURES	111
RESULTS.....	114
DISCUSSION.....	120
CONFLICT OF INTEREST.....	125
REFERENCES.....	126
CHAPTER 6 GLUTATHIONE DEPLETION THROUGH SERINE AND GLYCINE STARVATION SENSITIZES P53-NULL COLORECTAL CANCER CELLS TO AURANOFIN	128
ABSTRACT.....	130
INTRODUCTION.....	131
EXPERIMENTAL PROCEDURES	133
RESULTS.....	137
DISCUSSION.....	149
CONFLICT OF INTEREST.....	154
REFERENCES.....	155
CHAPTER 7 SUMMARY OF FINDINGS.....	157
7.1 GENERAL FINDINGS AND FUTURE DIRECTIONS.....	157
7.2 LIMITATIONS.....	168
7.3 CONCLUSIONS.....	172
7.4 CHAPTER 7 REFERENCES	174
APPENDIX A – ADDITIONAL FIGURES.....	177
APPENDIX B – FULL WESTERN BLOT IMAGES.....	178
APPENDIX C – OUTLINED EXPERIMENTAL METHODS.....	182
A.1 CELL LINES:	182

A.2 CRYSTAL VIOLET FOR RELATIVE CELL SURVIVAL	183
A.3 DIGESTED IN-WELL PROTEIN ASSAY	184
A.4 LIVE-CELL H ₂ O ₂ EMISSION	185
A.5 HIGH-RESOLUTION RESPIROMETRY	186
A.6 INTRACELLULAR LACTATE DETERMINATION	187
A.7 GLUTATHIONE.....	189
A.8 XTT FOR NAD(P)H DETERMINATION.....	193
A.9 CASPASE -3, -8 AND -9 ACTIVITY ASSAYS	194
A.10 TRYPAN BLUE EXCLUSION.....	196

List of figures

Chapter 1

Figure 1 1 Tumour formation as a result of uncontrollable cell growth..	1
--	---

Chapter 2

Figure 2 1 Schematic of mitochondrial ATP production through oxidative phosphorylation.	8
Figure 2 2 Schematic depicting the major components of glycolysis and β -oxidation ending in acetyl-CoA production.	9
Figure 2 3 Schematic depicting mitochondrial reactive oxygen species production from electron slip off of complex I and III.	14
Figure 2 4 Schematic depicting reactive oxygen species production leading to cellular damage.	15
Figure 2 5 Schematic depicting NADPH as the ‘master reducer’ of the cell.	20
Figure 2 6 Schematic of glutathione synthesis.	23
Figure 2 7 Schematic depiction of palmitoylcarnitine entry into the mitochondria	52

Chapter 4

Figure 4 1 Palmitoylcarnitine toxicity is greater in colorectal cancer HT29 and HCT 116 cells than normal CCD 841 cells.	84
Figure 4 2 Lower mitochondrial respiratory kinetics and impaired metabolic flexibility in HT29 cells compared to CCD 841 cells.	85
Figure 4 3 Elevated NAD(P)H production leads to increased H_2O_2 emission and caspase-3 induction in low oxidative capacity HT29 cells but not high oxidative capacity CCD 841 cells.	87
Figure 4 4 Palmitoylcarnitine lowers glutathione redox buffering capacity in HT29 cells but not CCD 841 cells.	89
Figure 4 5 Glutathione depletion sensitizes CCD 841 and HT29 cells to palmitoylcarnitine-induced decreasing cell survival.	91
Figure 4 6 MCF7 cells are insensitive to palmitoylcarnitine.	93
Figure 4 7 Palmitoylcarnitine induced decreases in cell survival are dictated by baseline mitochondrial reactive oxygen species and glutathione response	95

Chapter 5

Figure 5 1 Palmitoylcarnitine promotes selective growth in HepG2 cells compared to HT29, and HCT 116 cells and increases mitochondrial respiratory capacity in HepG2 cells.	116
Figure 5 2 Redox stress following palmitoylcarnitine exposure: maintenance of overall redox conditions (GSH/GSSG) in HepG2 cells but not in HT29 cells.	118
Figure 5 3 Palmitoylcarnitine alters H_2O_2 , glutathione and growth in HepG2 cells.	120
Figure 5 4 Proposed model of HepG2 cell adaptation to palmitoylcarnitine	121

Chapter 6

Figure 6 1 HCT 116 p53 ^{+/+} cells display greater oxidative characteristics despite lower glutathione relative to HCT 116 p53 ^{-/-} cells.	138
Figure 6 2 Auranofin-induced thioredoxin inhibition coupled with glutathione depletion through serine and glycine starvation renders the cell sensitive to oxidative stress.	139
Figure 6 3 Combined serine and glycine starvation sensitizes HCT 116 p53 ^{-/-} cells to auranofin.	141
Figure 6 4 Altering cell survival through manipulating antioxidant related pathways.	143
Figure 6 5 Serine and glycine starvation results in increased H_2O_2 emission and altered glutathione responses between HCT 116 p53 ^{+/+} and p53 ^{-/-} cells.	145
Figure 6 6 Auranofin induces a compensatory increase in glutathione in HCT 116 p53 ^{-/-} cells but not HCT 116 p53 ^{+/+} cells.	146

Figure 6 7 HT29 p53 ^{mutant} cell insensitivity to auranofin is overcome by coordinated serine and glycine starvation.	148
---	-----

Chapter 7

Figure 7 1 The change of glutathione in response to palmitoylcarnitine relates to the change in cell survival in response to palmitoylcarnitine.	159
Figure 7 2 The change H ₂ O ₂ emission in response to palmitoylcarnitine relates to the change in cell survival in response to palmitoylcarnitine concurrent with glutathione depletion by BSO.	160
Figure 7 3 Mitochondrial respiratory capacity relates to the susceptibility of cells to palmitoylcarnitine-induced changes in cell survival.	163
Figure 7 4 The combined effects of auranofin and buthionine sulfoximine (BSO) result in decreasing cell survival in cancer cells.	164

Appendix A

Figure A 1 N-acetylcysteine (NAC) provides marginal protection in HT29 cells against palmitoylcarnitine.	177
--	-----

Appendix B

Figure B 1 Total western blot images of UCP2 protein represented in Chapter 5.	178
Figure B 2 Total western blot images of p-p53 ^{ser46} protein represented in Chapter 6.	179
Figure B 3 Total western blot images of GR protein represented in Chapter 6.	180
Figure B 4 Total western blot images of 4HNE protein represented in Chapter 6.	181

List of abbreviations

2-HG	2-hydroxyglutarate
ACF	Aberrant crypt foci
ACL	ATP citrate lyase
ADP	Adenosine diphosphate
ATP	Adenosine triphosphate
β -oxidation	Beta-oxidation
BG	Brilliant green
BSO	Buthionine sulfoximine
CPT1	Carnitine palmitoyltransferase 1
CPT2	Carnitine palmitoyltransferase 2
CuZnSOD	Copper-zinc-superoxide dismutase
D3T	3H-1,2-dithiole-3-thione
DCA	Dichloroacetate
DHEA	Dehydroepiandrosterone
DHODH	Dihydroorotate dehydrogenase
DMH	1,2-dimethylhydrazine
DNA	Deoxyribonucleic acid
ETC	Electron transport chain
F1,6P	Fructose 1,6-bisphosphate
F6P	Fructose 6-phosphate
FABP4	Fatty acid binding protein 4
FADH ₂	Flavin adenine dinucleotide - Reduced
FDH	Folate dehydrogenase
FH	Fumarate hydratase
G6P	Glucose 6-phosphate
G6PD(H)	Glucose-6-phosphate dehydrogenase
GCL	Glutamate-cysteine ligase
GLUT1	Glucose transporter 1
Glutathione	γ -glutamyl-cysteinyl-glycine
GPx	Glutathione peroxidase
GR	Glutathione reductase
Grx	glutaredoxin
GS	glutathione synthetase
GSH	Glutathione - Reduced
GSSG	Glutathione disulfide
GST	Glutathione s-transferases
H ₂ O ₂	Hydrogen peroxide
HIF-1 α	Hypoxia-inducible factor 1-alpha

HKII	Hexokinase II
IDH	Isocitrate dehydrogenase
IL-6	Interleukin-6
IMM	Inner mitochondrial membrane
Keap1	Kelch Like ECH Associated Protein 1
LDH	Lactate dehydrogenase
ME	Malic enzyme
MEF	Mouse embryonic fibroblasts
ML 385	N-[4-[2,3-Dihydro-1-(2-methylbenzoyl)-1H-indol-5-yl]-5-methyl-2-thiazolyl]-1,3-benzodioxole-5-acetamide
mnSOD	Manganese-dependent superoxide dismutase
MOMP	Mitochondrial outer membrane permeabilization
mPTP	Mitochondrial permeability transition pore
MRP-1	Multidrug resistance protein-1
mtDNA	Mitochondrial DNA
NAC	N-acetylcysteine
NAD ⁺	Nicotinamide adenine dinucleotide - Oxidized
NADH	Nicotinamide adenine dinucleotide - Reduced
NADP ⁺	Nicotinamide adenine dinucleotide phosphate - Oxidized
NADPH	Nicotinamide adenine dinucleotide phosphate - Reduced
NOX	NADPH oxidase
NR	Nicotinamide riboside
Nrf2	Nuclear factor erythroid-derived 2-like 2 protein
NSCLC	Non-small-cell lung carcinoma (NSCLC)
O ₂ ^{•-}	Superoxide
ODH	2-oxoglutarate dehydrogenase
OH [•]	Hydroxyl radical
OMM	Outer mitochondrial membrane
OXPPOS	Oxidative phosphorylation
PDH	Pyruvate dehydrogenase
PDK	Pyruvate dehydrogenase kinase
PEP	Phosphoenolpyruvate
PFK	Phosphofructokinase
Pi	Inorganic phosphate
PKM2	Pyruvate Kinase M2 (PKM2)
PPP	Pentose phosphate pathway
Prx	Peroxiredoxin
PTEN	Phosphatase and tensin homolog deleted on chromosome 10

ROS	Reactive oxygen species
RR	Ribonucleotide reductase
SDH	Succinate dehydrogenase - complex II of the ETC
SOD	Superoxide dismutase
TCA cycle	Tricarboxylic acid cycle
TFAM	Mitochondrial transcription factor A
TP53	Tumor protein p53
Trx	Thioredoxin
TRx-S ₂	Thioredoxin - Oxidized
TRx-SH ₂	Thioredoxin - Reduced
Trx1	Cytosolic thioredoxin
Trx2	Mitochondrial thioredoxin
TRxR	Thioredoxin reductase
TrxR1	Cytosolic thioredoxin reductase
TrxR2	Mitochondrial thioredoxin reductase
TXNIP	Trx interacting protein
UCP1-5	Uncoupling proteins 1-5
xCT	Cysteine-glutamate antiporter
γGT	γ-glutamyltranspeptidase

Chapter 1 General introduction

Cancer is a disease of uncontrollable cell proliferation, and it is characterized by the development many possible mutations resulting in selective advantages allowing a cell to divide despite restraints on cell growth (Figure 1.1) [1].

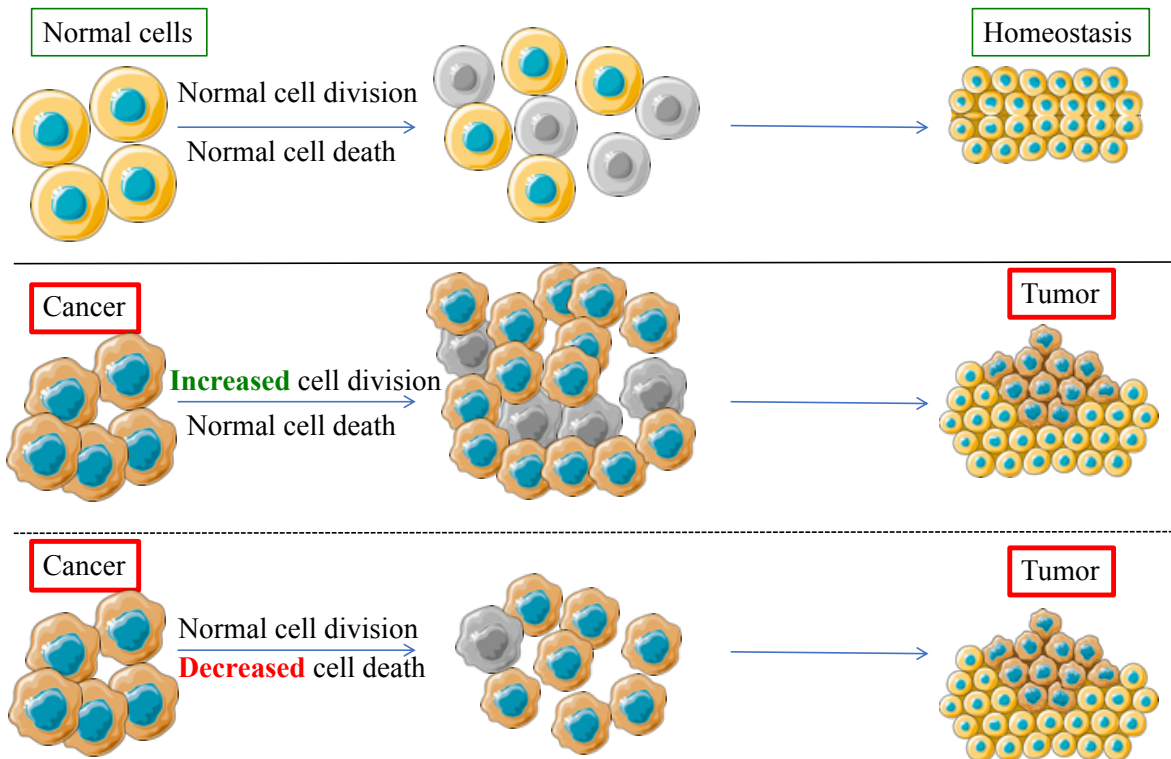


Figure 1 1 Tumour formation as a result of uncontrollable cell growth. Tumour growth is a result of a variety of mutations conferring pro-growth properties towards a cell, resulting in an increase in cellular division and/or avoidance in cell death pathways. Adapted from Alberts et al. [2].

This unrestrained cell growth allows for cancer cells to invade foreign tissues and reside and grow in areas reserved for other cells [2]. At our current abilities of cancer prognosis and therapies, roughly one in five people will die as a result of cancer [2]. The development of cancer is genetic in nature, however given that essentially an infinite variation of mutations may lead to cancer development, the search for both genetic and phenotypic-based therapies are warranted

[1]. Mitochondrion, although historically thought of as the primary source of ATP production throughout the cell, is a complex multifaceted organelle capable of influencing a variety of cellular functions and pathways such as cell *growth* and cell *death*. As such, altered mitochondrial and redox metabolism are key components in oncogenic behavior driving cancer growth and cell death avoidance, and presents an opportunity for selective cancer targeting for novel anticancer therapies. The dynamic relationship between mitochondrial metabolism and oxidative stress implicates glutathione, the most abundant intracellular antioxidant, as a potential pivotal agent in determining the success of mitochondrial targeted therapies as potential novel anticancer avenues.

Mitochondria

Mitochondria produce ATP through a process known as oxidative phosphorylation (OXPHOS), whereby the generation of an electrochemical gradient, or mitochondrial membrane potential, is harnessed to drive the production of ATP [3]. As mitochondrial membrane potential increases, reactive oxygen species (ROS) can be generated from the electron transport chain [4]. ROS production is a natural byproduct of OXPHOS and is linked to altered levels of mitochondrial ATP production and cell growth, where low levels of ROS can act as critical cell signaling molecules promoting growth, however high levels of ROS can be deleterious to the cell resulting in cell death. Given that cancer is ultimately a disease of sustained accelerated cell growth, cancer cells have developed different strategies to maintain high levels of ATP production while minimizing the deleterious effects of ROS.

Targeting mitochondria in cancer

Altered cancer mitochondrial metabolism was first observed almost 100 years ago when Otto Warburg noted that cancer cells produced excessive lactate despite the presence of oxygen [5, 6]. This was coined as ‘aerobic glycolysis’, and is directly observed through the high rates of glucose consumption in cancers and is currently exploited as a cancer diagnostic tool, whereby excessive ^{18}F -2-deoxyglucose (FDG) accumulation in cancer cells is detected by positron emission tomography [7, 8]. It appears that many cancers (although not all) rely on aerobic glycolysis as their primary source of ATP, concurrent with a decrease in reliance on mitochondrial OXPHOS [9]. These metabolic alterations vary greatly from normal cells and allow for several key adaptations ultimately resulting in a pro-growth cellular environment. The complete oxidation of glucose is a more efficient way to produce ATP compared to the fermentation of glucose; however, aerobic glycolysis is a less efficient yet faster source of ATP production [10]. The higher rate of glucose import in many cancers is able to offset lower mitochondrial ATP production, as well as the increased carbon flux through glycolysis allows for an increase in the production of biosynthetic precursors [9]. As such, countering the Warburg effect is thought to be a potential strategy to slow cancer progression resulting in cancer cell death. In this regard, it has been suggested that activating mitochondrial OXPHOS may redirect metabolic control away from glycolysis and stimulate mitochondrial ROS production in a manner that would be selectively toxic to highly glycolytic cancers but less toxic to non-transformed cells. The redirection of the end product of glycolysis, pyruvate, away from lactate and towards OXPHOS resulted in an increase in ROS and decreased cell growth in both lung and tongue cancer cells [11]. Whereas directly promoting fat oxidation has led to decreasing cell survival in several different cancer cell lines [12-15], however analogous normal cells were

resistant [14, 15]. This suggests that stimulating mitochondrial bioenergetics may serve as a therapeutic approach to selectively target cancer cells. Some cancer cells have however demonstrated a resistance to mitochondrial activation while others have increased cell growth rates when promoting OXPHOS [16, 17].

The role of glutathione in mediating cell survival

The influence of the mitochondria on determining cell fate is seemingly dichotomous: the provision of ATP promotes cell growth, whereas excessive ROS generation promotes cell death. Therefore, the ability of the cell to tolerate and respond to excess ROS may dictate the cell's response to mitochondrial-activation therapies. To combat high intracellular levels of ROS, cells produce antioxidant molecules capable of oxidant buffering. Glutathione is the most abundant intracellular antioxidant throughout the body [18]. Glutathione is critical in regulating the cellular redox environment by donating an electron at times of oxidative stress to an oxidized intracellular target [19]. The conversion of H_2O_2 to H_2O is catalyzed by glutathione peroxidase, whereby reduced glutathione (GSH) can donate an electron to H_2O_2 sacrificially self-oxidizing itself resulting in oxidized glutathione (GSSG). GSSG can be re-reduced by glutathione reductase using NADPH as an electron donor. Consequently, the redox state of glutathione is critical in determining the amount of oxidative stress the cell experiences, and the relative ratio of GSH/GSSG can be indicative of cellular oxidative stress. Therefore, an intriguing possibility is that heterogeneity in the glutathione response to mitochondrial challenges across cancers may dictate their susceptibility to cell death in response to mitochondrial ROS generated during oxidative phosphorylation.

Purpose

The purpose of this thesis is twofold: 1) Does the glutathione response to increasing mitochondrial substrates dictate cell fate? and 2) Can manipulating glutathione alter cell-fate and sensitize cancer cells to mitochondrial-influenced cell death?

References

1. Hanahan, D. and R.A. Weinberg, *Hallmarks of cancer: the next generation*. Cell, 2011. **144**(5): p. 646-74.
2. Alberts, B., *Molecular biology of the cell*, ed. A. Johnson, et al.: Garland Science, Taylor and Francis Group.
3. Nicholls, D.G. and S.J. Ferguson, in *Bioenergetics (Fourth Edition)*, D.G. Nicholls and S.J. Ferguson, Editors. 2013, Academic Press: Boston. p. ix-x.
4. Mailloux, R.J., *Teaching the fundamentals of electron transfer reactions in mitochondria and the production and detection of reactive oxygen species*. Redox Biol, 2015. **4**: p. 381-98.
5. Warburg, O., *The metabolism of carcinoma cells*. The Journal of Cancer Research, 1925. **9**(1): p. 148-163.
6. Warburg, O., *On the origin of cancer cells*. Science, 1956. **123**(3191): p. 309-14.
7. Lin, M., *Molecular imaging using positron emission tomography in colorectal cancer*. Discov Med, 2011. **11**(60): p. 435-47.
8. Lin, M., et al., *Positron emission tomography and colorectal cancer*. Crit Rev Oncol Hematol, 2011. **77**(1): p. 30-47.
9. Liberti, M.V. and J.W. Locasale, *The Warburg Effect: How Does it Benefit Cancer Cells?* Trends Biochem Sci, 2016. **41**(3): p. 211-8.
10. Shestov, A.A., et al., *Quantitative determinants of aerobic glycolysis identify flux through the enzyme GAPDH as a limiting step*. Elife, 2014. **3**.
11. Ayyanathan, K., et al., *Combination of sulindac and dichloroacetate kills cancer cells via oxidative damage*. PLoS One, 2012. **7**(7): p. e39949.
12. Blanquer-Rossello, M.D., et al., *Resveratrol induces mitochondrial respiration and apoptosis in SW620 colon cancer cells*. Biochim Biophys Acta Gen Subj, 2017. **1861**(2): p. 431-440.
13. Wenzel, U., A. Nickel, and H. Daniel, *alpha-Lipoic acid induces apoptosis in human colon cancer cells by increasing mitochondrial respiration with a concomitant O₂-*⁻generation*. Apoptosis, 2005. **10**(2): p. 359-68.
14. Wenzel, U., A. Nickel, and H. Daniel, *Increased carnitine-dependent fatty acid uptake into mitochondria of human colon cancer cells induces apoptosis*. J Nutr, 2005. **135**(6): p. 1510-4.
15. Al-Bakheit, A., et al., *Accumulation of Palmitoylcarnitine and Its Effect on Pro-Inflammatory Pathways and Calcium Influx in Prostate Cancer*. Prostate, 2016. **76**(14): p. 1326-37.
16. Nieman, K.M., et al., *Adipocytes promote ovarian cancer metastasis and provide energy for rapid tumor growth*. Nat Med, 2011. **17**(11): p. 1498-503.
17. Feuerecker, B., et al., *DCA promotes progression of neuroblastoma tumors in nude mice*. Am J Cancer Res, 2015. **5**(2): p. 812-20.
18. Balendiran, G.K., R. Dabur, and D. Fraser, *The role of glutathione in cancer*. Cell Biochem Funct, 2004. **22**(6): p. 343-52.
19. Lu, S.C., *Glutathione synthesis*. Biochim Biophys Acta, 2013. **1830**(5): p. 3143-53.

Chapter 2 Literature review

Cancer is a disease that is caused by a variety genetic mutations resulting in a state of rapid cell growth and resistance to cell death programming. In order to sustain accelerations in cell growth, cancers display highly adapted metabolic profiles resulting in altered ATP production, increased cyto-protective ability against ROS and apoptosis and an increased ability to produce biosynthetic precursors required for cell growth. The mitochondria is the main site for ATP production, yet it is involved in many other cellular processes such as ROS and apoptotic regulation, calcium handling and involved in DNA, fatty acid and protein synthesis. Therefore, understanding the role and regulation of the mitochondria is critically important in understanding bioenergetic regulation of cancer.

2.1 The mitochondrion

Over 1 billion years ago, protobacterial mitochondria and eukaryotes merged resulting in precursors to modern day cells [1]. Due to the ancient nature of the mitochondria within eukaryotic cells, mitochondria are involved in many cellular systems, however they are primarily responsible as the main source of ATP production accounting for ~95% of the ATP produced in the cell [2]. The mitochondria are double membrane structures consisting of an outer mitochondrial membrane (OMM), an intermembrane space and an inner mitochondrial membrane (IMM). As the mitochondria originated from a separate protobacterial origin, it has its own mitochondrial DNA (mtDNA) [3] which encodes essential components required for functional electron transport through the electron transport chain (ETC). The ETC comprises of five protein complexes (I through V) along with two electron carriers, coenzyme Q and cytochrome C. The ETC results in the production of ATP through an electrochemical gradient; a

concept that was first proposed by Peter Mitchell in 1961 [4], when, among several reasons, he failed to reconcile why ATP production was closely related to membranous structures within the cell. Originally, ATP synthesis was attributed to the release of high-energy bonds allowing for ADP and inorganic phosphate (P_i) to produce ATP [4]. Mitchell's chemiosmotic theory of oxidative phosphorylation explains the movement of ions generated in a series of redox reactions down an electrochemical gradient to produce ATP. The pumping of protons from the negative mitochondrial matrix into the positive intermembrane space produces a proton motive force capable of driving ATP synthase (complex V) to produce ATP from ADP and P_i through the protons flowing back through ATP synthase into the mitochondrial matrix [2]. The protons required for OXPHOS are generated through the reducing equivalents NADH and $FADH_2$ (Figure 2.1), and the generation of reducing equivalents is through the catabolism of fuel sources, primarily glucose and fat, through glycolysis and β -oxidation respectively.

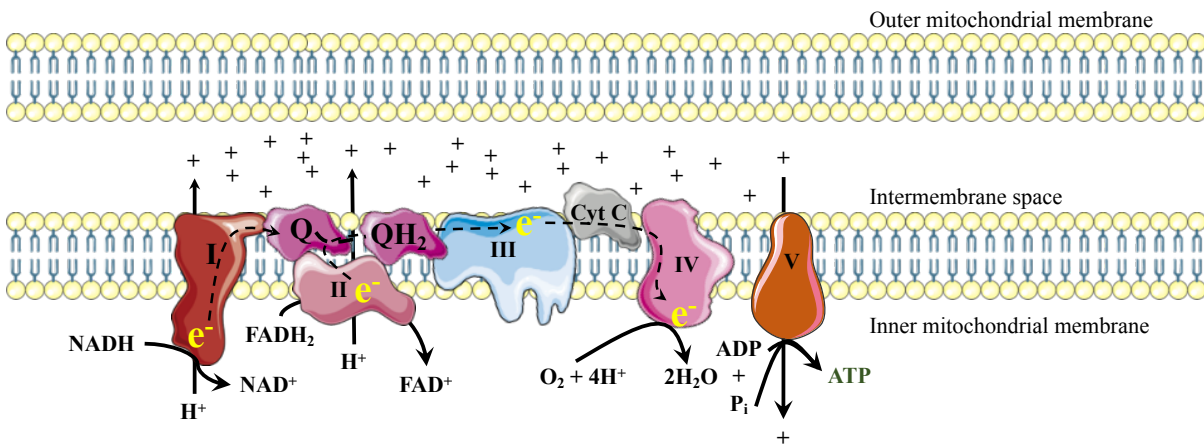


Figure 2 1 Schematic of mitochondrial ATP production through oxidative phosphorylation. There are five protein complexes and two electron carriers embedded within the inner mitochondrial membrane. These components are responsible for catalyzing redox-reactions transferring electrons to the eventual release of free energy, upon which protons are pumped into the intermembrane space from the mitochondrial matrix, to create an electrochemical gradient which is harnessed by complex V resulting in the phosphorylation of ADP into ATP, the energy currency of the cell.

2.1.1 Glycolysis

Glycolysis is the phosphorylation dependent breakdown of glucose to pyruvate (Figure 2.2). Gustav Embden first proposed our current understanding of glycolysis in 1933 [5] and it was further elucidated following Embden's death by Otto Meyerhof and Jakub Parnas (glycolysis is also referred to as the Embden-Meyerhof-Parnas pathway) [6]. Glucose enters the cell through glucose transporters where it undergoes a series of catabolic processes resulting in the formation of two pyruvate molecules. Glycolysis alone produces two net ATP molecules and two NADH molecules. Pyruvate ultimately has two distinct fates, fermentation or oxidation. Pyruvate can be converted to lactate through lactate dehydrogenase (LDH), or it can enter the mitochondria and be enzymatically converted into acetyl-CoA by pyruvate dehydrogenase (PDH) to stimulate mitochondrial OXPHOS.

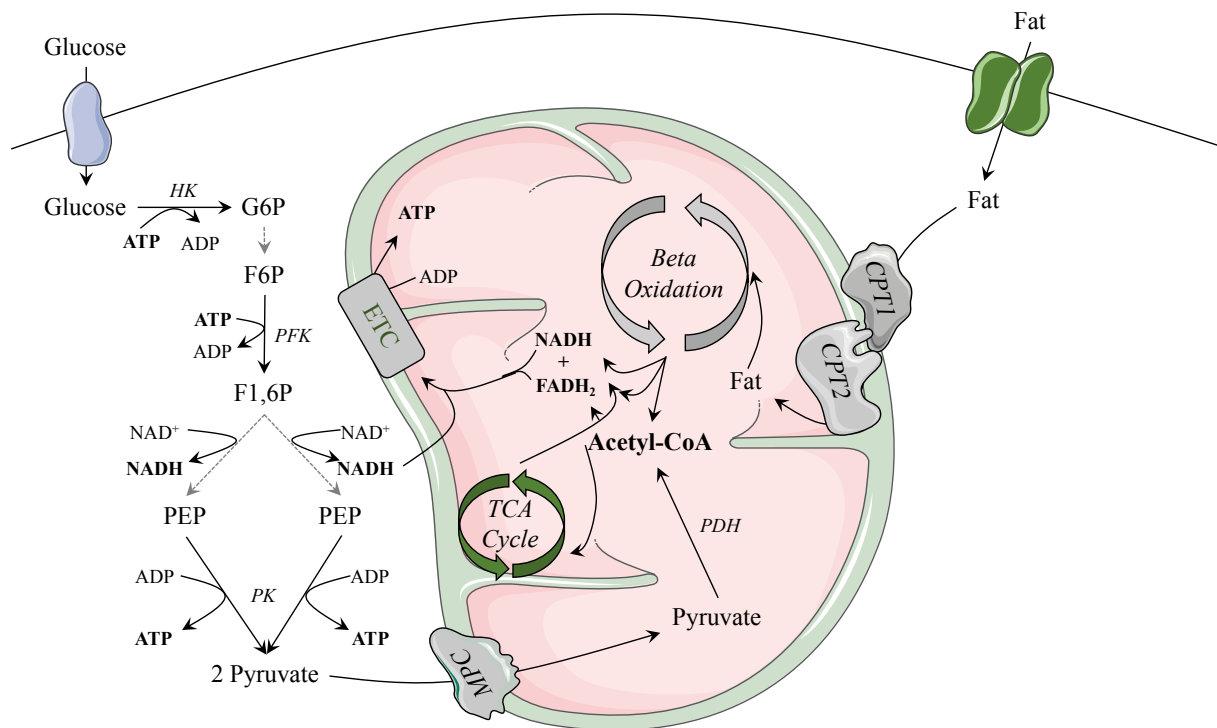


Figure 2 2 Schematic depicting the major components of glycolysis and β -oxidation ending in acetyl-CoA production. Glucose enters the cell through glucose transporters where it is immediately catalyzed by hexokinase (HK) into glucose-6-phosphate (G6P). Through a series of

enzymatic reactions, G6P gets converted to fructose-6-phosphate (F6P), where phosphofructokinase (PFK) converts F6P into fructose 1,6 bisphosphate (F1,6P). Over a series of reactions, F1,6P results in the production of two molecules of phosphoenolpyruvate (PEP) and eventual conversion by pyruvate kinase (PK) into 2 pyruvate molecules. Pyruvate is imported into the mitochondria, whereby it gets converted into acetyl-CoA by pyruvate dehydrogenase (PDH). Although fatty acids enter the mitochondria through different mechanisms, they result in a similar fate to glucose. Fatty acids are imported into the cell through fatty acid transporters. Once reaching the mitochondria, fatty acids get converted into acetylcarnitines by carnitine palmitoyltransferase 1 (CPT1), where they freely bypass the outer mitochondrial membrane. Once in the intermembrane space, acetylcarnitines are imported into the mitochondrial matrix and the carnitine group is removed by carnitine palmitoyltransferase 2 (CPT2). Fatty acids undergo beta-oxidation resulting in the production of reducing equivalents, NADH and FADH₂, as well as acetyl-CoA production. Acetyl-CoA, either from glucose or fatty acid sources, enters the TCA cycle where it undergoes cyclic degradation to produce further reducing equivalents, which stimulate oxidative phosphorylation and eventual ATP production.

2.1.2 β -oxidation

While fat enters the cell through different mechanisms than glucose, the catabolism of fat results in acetyl-CoA production through a process known as β -oxidation (Figure 2.2). Georg Knoop first discovered β -oxidation in 1904 where in which he theorized that the breakdown of fatty acids was through the successive removal of two carbon pairs starting at the β carbon [7]. β -oxidation is the cyclic removal of two carbon pairs resulting in the production of acetyl-CoA, NADH and FADH₂, as well as a fatty acyl-CoA (two carbons shorter than the original starting molecule) that is further continually degraded. Given that 1 molecule of each acetyl-CoA, NADH and FADH₂ are produced from a two carbon pair from the fatty acyl chain; β -oxidation yields more ATP in contrast to glycolysis. Palmitate, a 16-carbon long chain fatty acid, produces 129 ATP molecules compared to 36 ATP molecules from the oxidation of a glucose molecule [8]. Ultimately, both glycolysis and β -oxidation are able to stimulate mitochondrial OXPHOS through acetyl-CoA production entering the tricarboxylic acid (TCA) cycle.

2.1.3 The TCA cycle

Hans Adolf Krebs first proposed the TCA cycle (also known as the Krebs cycle) in 1937 [9]. The TCA cycle refers to the multi-step oxidation of acetyl-CoA in the mitochondrial matrix. The first step of the TCA cycle is the production of citrate from acetyl-CoA and oxaloacetate catalyzed by citrate synthase [10]. The subsequent production of reducing equivalents (NADH and FADH₂) from the serial catabolism of acetyl-CoA is able to stimulate OXPHOS to produce ATP (Figure 2.2). While our primary understanding of the TCA cycle is through the role of ATP production, the TCA cycle is crucial in supplying many biosynthetic molecules required for growth. Cataplerosis is the process by which TCA cycle intermediates are removed from the TCA cycle to be used in other cellular processes, while anapleurosis describes the replenishing of TCA cycle intermediates to account for molecules that were lost during cataplerosis [11]. As an avenue for fatty acid synthesis, citrate can be exported into the cytosol to produce cytosolic acetyl-CoA catalyzed by ATP citrate lyase (ACL). While mitochondrial acetyl-CoA stimulates the TCA cycle with the potential for ATP production, cytosolic acetyl-CoA is able to stimulate fatty acid synthesis, which is a key component to drive cell growth. As such, inhibition of ACL has demonstrated some antineoplastic properties [12], suggesting that mitochondrial cataplerosis is crucial in promoting cell growth in cancers.

2.1.4 Mitochondrial-mediated cell death

Along with the promotion of cell growth through generation of ATP and biosynthetic molecules, the mitochondria are key regulators in promoting cell death [13]. Mitochondrial-mediated cell death is triggered upon exposure of a death stimulus, where pro-apoptotic Bcl-2 proteins Bax and Bad on the OMM form dimers resulting in pore formation and mitochondrial

outer membrane permeabilization (MOMP) leading to cytochrome c release into the cytosol and mitochondrial dysfunction [14]. The release of cytochrome c results in the cleavage of a group of cysteine proteases, called caspases, which upon cleavage from their pro-caspase form, cleave and degrade intracellular substrates and cellular components. Under normal physiological conditions, anti-apoptotic proteins such as Bcl-X_L and Bcl-2 bind to and inhibit Bax and Bad. As a potential mechanism for resistance to cell death, many cancers typically display decreased levels of pro-apoptotic related genes and an increase in anti-apoptotic related genes such as breast cancer [15], colorectal cancer [16], ovarian cancer [17] and acute myeloid leukemia [18]. Along with MOMP, cell death can be initiated through formation of the mitochondrial permeability transition pore (mPTP) located on the IMM. While typically the IMM is fairly impermeable, following the promotion of cell death conditions (such as calcium overload or excessive oxidative stress) however, formation of the mPTP results in rapid mitochondrial swelling leading to the rupture of the OMM and a loss of mitochondrial ATP production. While the components and regulation of the mPTP are highly debated, it is clear that many solid tumours display drastic suppression of mPTP formation resulting in cell death avoidance [19].

2.2 Reactive oxygen species

Increased cell growth is linked to increased mitochondrial OXPHOS and increased mitochondrial OXPHOS can lead to an accumulation of oxidative damage. Interestingly, increased oxidative damage associated through mitochondrial OXPHOS is witnessed in many different organisms along with humans such as zebra finches [20], yellow-legged gulls [21] and coal tits [22]. The role of mitochondrial ROS in promoting cell growth and maturation is not entirely defined, however, in an attempt to determine whether mitochondrial ROS can regulate

cell growth in yellow-legged gulls, Velando et al. [23] administered the mitochondrial-targeted antioxidant, mitoQ (mitoubiquinone), to chicks and observed an increased growth rate. Lowering mitochondrial ROS and promoting growth suggests that while ATP is critical in promoting cell growth and maturation, mitochondrial ROS production can function to suppress growth. This highlights the link between mitochondrial ATP production and mitochondrial ROS emission.

Mitochondrial ROS is a natural byproduct of mitochondrial OXPHOS, and both mitochondrial ATP and ROS production are generated by electron transfer reactions [8]. During OXPHOS, electrons are transferred through the ETC to form H₂O at complex IV, however electrons are able to slip out of the ETC prior to complex IV. When electrons slip, they form a single electron reduction of O₂ resulting in the radical superoxide (O₂^{•-}). While O₂^{•-} is reactive, it does not cross lipid membranes easily. O₂^{•-} is degraded by superoxide dismutase (SOD) enzymes, manganese SOD (mnSOD) in the mitochondrial matrix, and copper/zinc SOD (CuZnSOD) throughout the rest of the cell [24]. The dismutation of O₂^{•-} by SOD results in the production of O₂ and hydrogen peroxide (H₂O₂) (Figure 2.3) [25]. H₂O₂ can bypass lipid membranes either through lipid solubility or through aquaporins, where it can elicit global cellular effects [26-28]. H₂O₂ in low levels can act as a critical signaling messenger throughout the cell, primarily through its ability to oxidize thiols on target proteins [25].

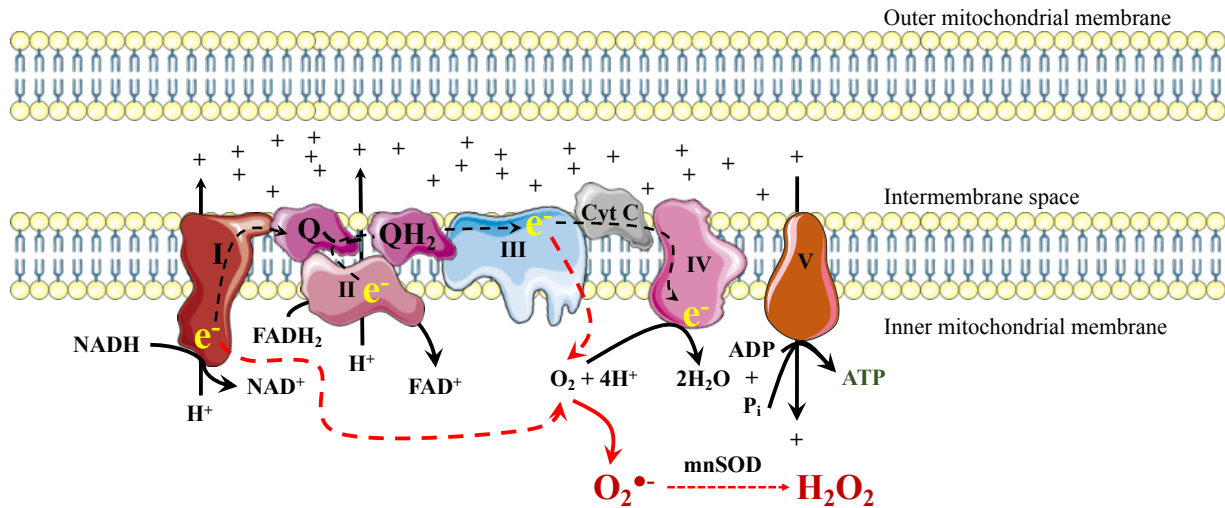


Figure 2 3 Schematic depicting mitochondrial reactive oxygen species production from electron slip off of complex I and III. Currently, 11 sites within the mitochondria have been identified as sites for electron slip and subsequent ROS production. As an electron slips out of the electron transport chain, it forces the semi-reduction of oxygen resulting in superoxide ($O_2^{\bullet-}$) formation. $O_2^{\bullet-}$ is quickly dismutated to hydrogen peroxide (H_2O_2) by superoxide dismutase (SOD), whereby H_2O_2 can leave the mitochondria resulting in global cellular effects.

As a response to oxidative stress, the Keap1-Nrf2 axis is a primary example of H_2O_2 signaling properties. Keap1 (Kelch-like ECH-associated protein 1) binds to and prevents the stabilization of Nrf2 (Nuclear factor erythroid-derived 2-like 2 protein) through Nrf2 ubiquitination and subsequent proteasomal degradation. H_2O_2 is able to stimulate an increase in Nrf2 stabilization and nuclear accumulation in HeLa cells through oxidation of two exposed cysteines found on Keap1 resulting in a disulfide bond preventing Keap1-targeted degradation of Nrf2 [29]. Furthermore, H_2O_2 is able to directly stabilize and prevent degradation of HIF-1 α (hypoxia inducible factor 1- α) in murine embryonic cells, thereby regulating the O_2 -sensing ability of the cell [30]. In addition, H_2O_2 is able to act as a second messenger in a variety of signaling pathways unrelated to cell protection against oxidative stress, such as angiogenesis, immune responses and cell proliferation [31]. However, in high enough levels, H_2O_2 can elicit deleterious effects throughout the cell. These harmful effects range from uncontrolled

oxidization of proteins, DNA damage, or the production of hydroxyl radicals (OH^\bullet) through Fenton chemistry reactions (Figure 2.4) [24]. OH^\bullet have a strong oxidizing potential, are lipid insoluble and have a very short half-life. They are recognized as molecules that are capable of doing irreversible oxidative damage to any macromolecular structure.

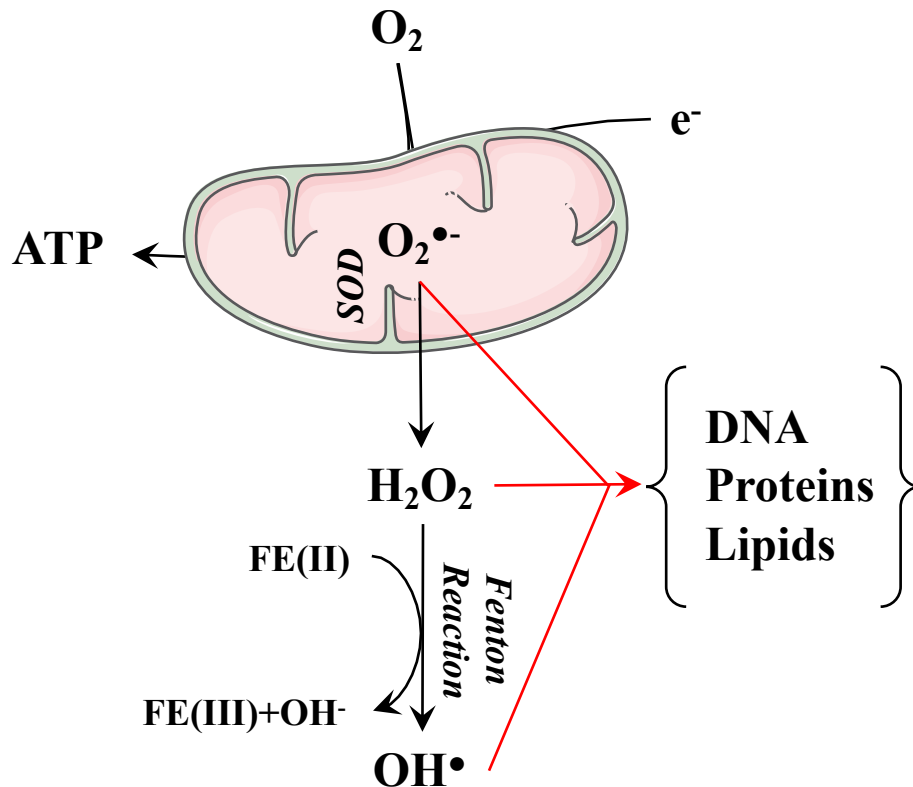


Figure 2 4 Schematic depicting reactive oxygen species production leading to cellular damage. Superoxide ($\text{O}_2^{\bullet-}$) is produced as a byproduct of mitochondrial oxidative phosphorylation where it is converted by superoxide dismutase into hydrogen peroxide (H_2O_2). H_2O_2 can freely diffuse out of the mitochondria, where upon expose to iron, can result in the production of hydroxyl radicals (OH^\bullet). $\text{O}_2^{\bullet-}$, H_2O_2 and OH^\bullet in high enough concentrations can lead to the oxidation of DNA, proteins and lipids result in cellular damage and eventual cell death.

Currently, there are 11 identified sites of $\text{O}_2^{\bullet-}$ production within the mitochondria [8]. This list includes isocitrate dehydrogenase (IDH), 2-oxoglutarate dehydrogenase (ODH), pyruvate dehydrogenase (PDH) [32], as well as two sites on complex I, one known site on each of

complex II and complex III among others [8]. NADPH oxidases (NOX) are further sources of $O_2^{\bullet-}$ generation throughout the cell, however NOX are commonly associated as critical signaling enzymes through an oxidative burst, or a transient production of $O_2^{\bullet-}$ [33]. The role of NOX varies based on cell type and subcellular distribution, however NOX has been implicated in a variety of non-pathological systems. NOX generation of $O_2^{\bullet-}$ contributes to a variety of signaling such as regulating blood pressure [34], renal function [35], smooth muscle contraction [36] and others [33]. NOX production of $O_2^{\bullet-}$ is not thought to be a primary contributor to the deleterious effects of ROS, therefore the role of mitochondrial ROS production appears to be critical for both cell signaling and oxidative stress.

2.2.1 Oxidative stress

In excess, accumulated ROS can lead to macromolecular damage, and disruption of key redox sensitive circuitry, this is termed as oxidative stress [37]. Common forms of macromolecular damage attributed to oxidative stress are lipid peroxidation, DNA and protein oxidation (Figure 2.4). $O_2^{\bullet-}$ is highly reactive, and a single oxidizing event has the potential to initiate chain oxidative reactions, whereby up to 200 to 400 lipid molecules can be oxidatively damaged upon a single $O_2^{\bullet-}$ initiating molecule [37]. $O_2^{\bullet-}$ is a 1-electron free radical, however $O_2^{\bullet-}$ is rapidly dismutated to H_2O_2 , a 2-electron oxidant, therefore this thesis focuses on H_2O_2 and H_2O_2 -specific antioxidant mechanisms. Between 1-4% of all O_2 consumed results in the formation of H_2O_2 [37]. H_2O_2 signaling is primarily through the reversible modification of protein function through the oxidation of thiols found on exposed cysteine residues [38]. While H_2O_2 production can lead to deleterious cellular effects such as single and double strand DNA breaks [39], the additional depletion of glutathione, the most abundant intracellular antioxidant

[40], through the use of buthionine sulfoximine (BSO) was able to lower the amount of H_2O_2 required to induce DNA strand breaks [39]. This suggests that while H_2O_2 can elicit cellular damages, the buffering and removal of H_2O_2 by glutathione is also of critical importance in determining cell fate when cells undergo oxidative stress.

2.3 Mechanisms for regulating oxidative stress

Many physiological and pathological conditions can increase the rate of $O_2^{\bullet-}$ production, resulting in an increase in H_2O_2 emission. The prevention of efficient ATP production through mitochondrial OXPHOS can result in an increase in the likelihood of electron slip, conditions such as elevated mitochondrial membrane potential, blockage of ETC components downstream of electron entry, high NADH/NAD⁺ ratio or simply low levels of ADP can all result in a build-up of electrons within the ETC allowing for $O_2^{\bullet-}$ and subsequent H_2O_2 production [41]. Without sufficient levels of ADP present within the mitochondria, complex V is unable to complete the final step of phosphorylating ADP into ATP. This results in a potential back-flow of electrons resulting in an increase in membrane pressure, resulting in elevated electron slip leading to the production of $O_2^{\bullet-}$ and H_2O_2 . Lowering mitochondrial H_2O_2 levels can be done through the degradation of H_2O_2 by antioxidant buffering systems, or through lowering the production mitochondrial H_2O_2 itself.

2.3.1 Decreasing mitochondrial ROS production

Mitochondrial ATP production is not perfectly coupled to mitochondrial OXPHOS, whereby proton-leak is able to dissipate mitochondrial membrane potential decreasing the pressure driving electron slip and $O_2^{\bullet-}$ and subsequent H_2O_2 emission. One of the most prevalent

mechanisms of decreasing mitochondrial $O_2^{\bullet-}$ and H_2O_2 emission is through mitochondrial uncoupling.

Mitochondrial uncoupling

A protein embedded in the IMM in brown adipose tissue was discovered in the early 1980s to be able to dissipate mitochondrial membrane potential [42] and elicit what is now termed as non-shivering thermogenesis [43]. This protein was called uncoupling protein-1 (UCP1). Since then, 5 different uncoupling proteins have been discovered throughout mammalian cells (UCP1-5). While the primary role of UCP1 appears to be the generation of heat, the role of the other uncoupling proteins appears to be that of attenuation of mitochondrial ROS production [44]. The tissue distribution and function of the various UCPs is still highly debated, however it appears that through various mechanisms, UCPs are able to dissipate mitochondrial membrane potential resulting in decreasing mitochondrial ROS production [44].

2.3.2 Promoting ROS degradation

In order to tightly control H_2O_2 levels, cells have evolved many antioxidant pathways designed to regulate intracellular H_2O_2 concentrations. It was originally believed that all enzymes had the power to catalytically degrade H_2O_2 . However, upon further exploration, it was determined that enzymes such as emulsion, pepsin and trypsin did not catalyze H_2O_2 degradation, it was therefore concluded that a specific enzyme functioned to degrade H_2O_2 , this enzyme was termed catalase [45]. Catalase is ubiquitously expressed in aerobic organisms and present in most mammalian cells [46]. Catalase functions through the enzymatic conversion of 2 H_2O_2 molecules into 2 H_2O and O_2 , however this function is primarily in the peroxisome [47], and catalase has

little function outside of peroxisome [48]. Many intracellular molecules are thought to contribute to the overall protection and regulation of oxidative stress, such as lactate [49], pyruvate [50, 51], certain vitamins [52] and free cysteine [53]. While many compounds can contribute to situational antioxidant defenses, there are two major antioxidant systems within mammalian cells: The glutathione and thioredoxin systems.

Glutathione

Glutathione was first discovered in 1888 when it was noted that yeast cells and yeast extract contained the property to reduce sulfur [54]. It wasn't until 1921 when the basic structure and function of glutathione was understood when Hopkins [55] concluded that glutathione was a dipeptide of cysteine and glutamate. It is now understood that glutathione (γ -glutamyl-cysteinyl-glycine) is non-nuclear encoded tri-peptide containing glutamate, cysteine and glycine [40]. Glutathione is the most abundant non-protein thiol and is present in all mammalian tissues in concentrations between 1-10mM with the highest concentrations being noted in the liver [56]. Glutathione has many critical functions beyond an antioxidant, such as promoting cell growth [57] through nuclear recruitment [58, 59], acting as a substrate for protein post-translational modifications [60], xenobiotic functions [61] and as a critical cysteine reservoir in the cell [62]. However, given that the mitochondria are the major source of ROS production, the role of glutathione in buffering and degrading H_2O_2 is of primary focus.

Glutathione as an antioxidant

H_2O_2 is enzymatically converted to H_2O by glutathione peroxidase (GPx) with reduced glutathione (GSH) as the electron donor. Glutathione is also able to function as the electron

donor to reduce lipid peroxides. The sacrificial oxidation of GSH results in a disulfide bond forming between two oxidized glutathione molecules creating the oxidized form of glutathione – GSSG. The redox cycle is completed by the re-reduction of GSSG to GSH catalyzed by glutathione reductase (GR) using NADPH as a master electron donor (Figure 2.5). The redox potential of the cell is largely determined by the amount of free GSH and the ratio of GSH to GSSG (GSH/GSSG), therefore the cell is able to tightly regulate levels of both GSH and GSSG [63]. If GSSG levels rise to a point to threaten the GSH/GSSG ratio, the cell has several possible mechanisms to lower GSSG. Along with the re-reduction of GSSG to GSH, the cell is able to export GSSG into the extracellular space, or GSSG can also react with proteins creating protein-glutathione adducts through a disulfide bond.

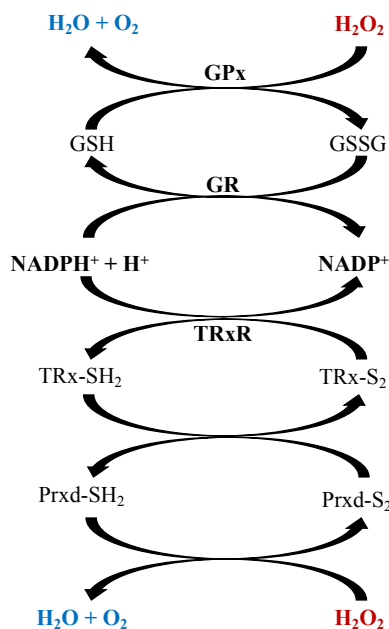


Figure 2 5 Schematic depicting NADPH as the ‘master reducer’ of the cell. Upon production of H_2O_2 , reduced glutathione (GSH) is able to act as a direct electron donor allowing for glutathione peroxidase (GPx) mediated reduction of H_2O_2 to H_2O , leading to the oxidation of GSH into oxidized glutathione (GSSG). GSSG can be re-reduced to GSH by glutathione reductase (GR) using NADPH as the ‘master’ electron donor. Thioredoxin is able to act as an indirect electron donor for the reduction of H_2O_2 to H_2O , whereby it donates an electron to reduced peroxiredoxin system. This leads to the oxidation of reduced thioredoxin (TRx-SH₂) to oxidized thioredoxin (TRx-S₂). TRx-S₂ can be re-reduced by thioredoxin reductase (TRxR) using NADPH as the ‘master’ electron donor.

Given the unique structure of glutathione, the only known enzyme capable of degrading glutathione is γ -glutamyltranspeptidase (γ GT). γ GT is only present on the external surface of cell membranes resulting in glutathione degradation occurring externally to cells that express γ GT [56]. Excess GSSG production can result in the cellular depletion of GSH through decreasing GSSG by cellular export and subsequent degradation by γ GT [56]. While catalase is able to enzymatically degrade H_2O_2 in the peroxisome, glutathione is a critical regulator of H_2O_2 in the cytosol, nucleus and the mitochondria. Excess mitochondrial H_2O_2 production can result in an increase in GSSG formation, however the mitochondria are unable to export elevated GSSG levels [64], and the re-reduction of GSSG to GSH by GR is critically important. Therefore, elevated levels of GSSG molecules can result in severe mitochondrial dysfunction through protein-glutathione adducts resulting in loss or change of function in critical mitochondrial proteins [65]. ROS generation by complex I within the mitochondria can result in certain subunits of complex I forming a disulfide bond with glutathione resulting in novel adduct formation [66]. Upon glutathionylation, complex I $O_2^{\bullet-}$ and subsequent H_2O_2 production are increased, and upon reduction by glutathione, $O_2^{\bullet-}$ and H_2O_2 return to steady-state levels. Interestingly, oxidation of the mitochondrial glutathione pool alone was able to increase complex I glutathionylation resulting in increased ROS emission, stressing the importance of the GSH/GSSG ratio in maintaining cellular redox balance [66]. Cellular glutathione depletion is a hallmark during apoptosis and cell death, however it is not simply a byproduct of cell death associated oxidative stress, rather a critical stimuli committing the cell to its fate [67]. The prevention of glutathione efflux upon an apoptotic stimuli was able to protect U937 and HepG2

cells [68] as well as Jurkat cells [69] from apoptosis. While glutathione depletion is able to promote cell death, glutathione synthesis is a critical regulator in cell protection and cell growth.

Glutathione synthesis

Glutathione synthesis occurs entirely in the cytosol. While there are several pathways involved in the production of the individual constituent parts of glutathione (glutamate, cysteine and glycine), glutathione synthesis is ultimately regulated by two enzymes; glutamate-cysteine ligase (GCL – formerly known as γ -glutamylcysteine synthetase) and glutathione synthetase (GS) (Figure 2.6) [56]. Glutathione synthesis is an energy consuming process, as both GCL and GS require ATP for catalytic function. The rate-limiting step in glutathione synthesis is the formation of γ -glutamylcysteine through the enzymatic joining of glutamate and cysteine by GCL. GCL activity, therefore glutathione synthesis, is influenced by the availability of cysteine [70] and feedback from intracellular glutathione levels [71]. The final step in glutathione synthesis is the addition of glycine to γ -glutamylcysteine by an ATP consuming process catalyzed by GS. GS is not subject to regulation by GSH levels, and overexpression of GS alone did not significantly increase GSH production [72]. Many factors are able to influence glutathione synthesis, such as glutathione and cysteine levels, cellular oxidative stress and nutrient availability. While both serine and glycine are non-essential amino acids, starvation of serine and glycine resulted in marked glutathione depletion in HCT 116 cells [73]. While glutathione itself is synthesized in the cytosol, many key enzymes involved in glutathione synthesis are transcriptionally regulated by Nrf2. Nrf2 is a redox sensor, whereby nuclear accumulation of Nrf2 through disassociation of Nrf2 from its negative regulator, Keap1, allows for a significant increase in many glutathione associated enzymes [56, 74, 75]. This results in

tight control on glutathione synthesis through both transcriptional and non-transcriptional regulation.

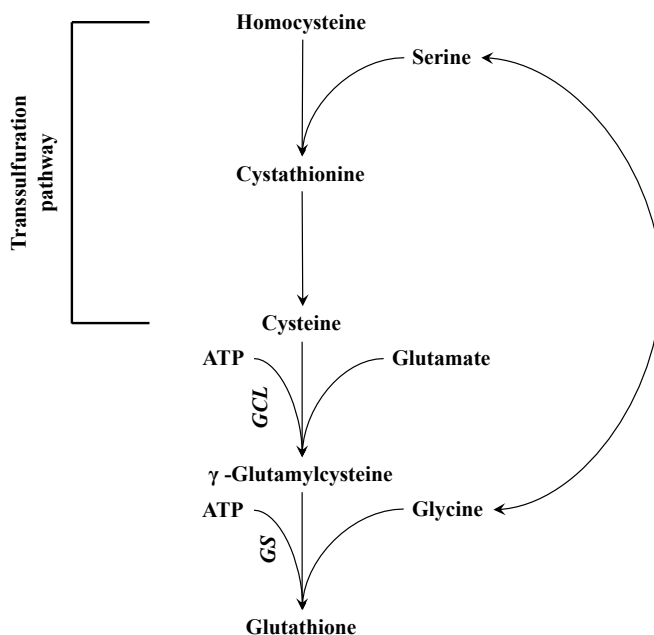


Figure 2 6 Schematic of glutathione synthesis. Glutathione comprises of glutamate, cysteine and glycine, and is enzymatically produced in a two-stage process. The rate-limiting enzyme, glutamate-cysteine ligase (GCL) produces γ -glutamylcysteine through the conversion of cysteine and glutamate. Glutathione synthetase (GS) produces glutathione through the additional joining to glycine. The rate of glutathione synthesis is controlled, in part, by the availability of cysteine, glutamate and glycine.

Thioredoxin

Along with the glutathione system, the other major intracellular antioxidant system is the thioredoxin (Trx) system. Unlike glutathione, Trx is unable to directly degrade H_2O_2 ; rather it supplies electrons for peroxiredoxin (Prx)-dependent removal of H_2O_2 [76]. Through successive crude fractionation of *E. Coli* samples, Trx was first identified and isolated in 1964 [77]. It is currently understood that mammalian cells contain two Trx systems, cytosolic (Trx1) and mitochondrial (Trx2). The function of Trx is through sacrificially donating electrons to

downstream donors going from a reduced form (Trx-SH₂) to an oxidized form (Trx-S₂). These downstream donors consist of several different redox sensitive compounds such as Prx for redox detoxification, or to certain transcription factors with redox-sensitive cysteine's [76]. The Trx-Prx system is able to degrade H₂O₂ as well as reduce oxidized protein targets and other forms of ROS such as peroxynitrite through NADPH-dependent electron regulation (Figure 2.5) [76]. The re-reduction of Trx-S₂ is enzymatically carried out by Trx-reductase (TrxR), however physiological levels of glutathione, NADPH and glutathione reductase have all been demonstrated to be able to re-reduce Trx-S₂ back to Trx-SH₂ in HeLa cells through the catalytic function of glutaredoxin (Grx – the enzyme responsible for regulating glutathione in protein-redox detoxification) [78]. This stresses that while the Trx and glutathione systems are typically viewed as separate antioxidant pathways, there does appear to be some degree of redundancy between the two. Trx is also involved in the regulation of cell death pathways. Upon response to oxidative stress, the Trx interacting protein (TXNIP) can leave the nucleus and enter the cytosol or mitochondria where it binds to and oxidizes Trx-SH₂. Under normal conditions, there is a pool of Trx-SH₂ bound to ASK1, preventing ASK1-initiated cell death pathways, however, upon binding of TXNIP, Trx dissociates from ASK1 promoting ASK1-initiated cell death [79, 80]. TXNIP is therefore viewed as an inhibitor of Trx resulting in Trx degradation, and the loss of TXNIP (and the subsequent removal of Trx inhibition) can lead to increases in cell proliferative rates, and is highly implicated in a variety of cancers [81, 82]. Furthermore, the inhibition of Trx resulted in a marked increase in Nrf2 activity [29], likely through increasing cellular oxidative stress, promoting the dissociation of Nrf2 and Keap1, and similar to the glutathione system, many key Trx-associated proteins are transcriptionally regulated by Nrf2 [76, 83]. Additionally,

both glutathione and Trx redox-systems function through NADPH-dependent mechanisms, implicating NADPH as the ‘master reducer’ of the cell.

NADPH

Nicotinamide adenine dinucleotide phosphate comes in an oxidized form (NADP⁺) or a reduced form (NADPH). NADPH serves as the master electron donor for the glutathione and Trx systems [84]. NADPH can be made through several metabolic pathways, such as malic enzyme (ME), isocitrate dehydrogenase (IDH), folate dehydrogenase (FDH), with the most prominent source of NADPH production stemming from the pentose phosphate pathway (PPP) [84]. The most crucial enzyme responsible for NADPH synthesis in the PPP is glucose-6-phosphate dehydrogenase (G6PD), where overexpression of G6PD led to increased NADPH and a more reduced GSH:GSSG ratio, resulting in an increased resistance to oxidative challenges and a prolonged lifespan in *drosophila melanogaster* [85]. Pyruvate Kinase M2 (PKM2) is a glycolytic enzyme (Figure 2.3) commonly overexpressed in cancers, and is associated with conferring much of the ‘aerobic glycolysis’ phenotype [86]. Upon mild oxidative stress, there was an increase PKM2 phosphorylation in HeLa cells resulting in an increase in carbon redirection into the PPP and subsequent NADPH production [87]. The metabolic implication of glycolytic and mitochondrial derived NADPH production conveys that key metabolic pathways are responsible for not only regulating ROS production, but also ROS buffering and degradation.

2.4 The mitochondria and cancer

Altered cancer metabolism was first observed almost 100 years ago, when Otto Warburg noted that cancers produce high levels of lactate, despite the presence of oxygen [88, 89].

Interestingly, Warburg proposed that aerobic glycolysis observed in cancers was a result of mitochondrial defects driving the increase in glycolysis. However, it has since been proven that while mitochondrial metabolism is often altered in cancers, the mitochondria in cancers are able to influence a variety of steps throughout oncogenesis [90]. There are many potential drivers of the Warburg effect, these factors have been defined as both direct mutations within metabolic genes, or through secondary influences of mutations upstream of glycolytic and mitochondrial pathways. Mutations in the p53 gene for example, are associated with conferring the ‘Warburg phenotype’, where mutant-p53 was able to increase glucose transporter 1 (GLUT1) expression in H1299 lung cancer cells and promote the Warburg effect and knockdown of wildtype-p53 in MCF7 breast, H460 and A549 lung cancers promoted increased glucose uptake and lactate production [91]. Kras-mediated tumourgenicity requires high levels of glucose consumption, mitochondrial derived ROS and TCA catapleurosis to promote elevated cancer cell proliferation [92]. The PI3K/Akt/mTOR pathway is highly implicated in promoting tumourgenisis, the Warburg effect and altered mitochondrial function [93]. Activation of Akt signaling via upstream influence of PIP₃ (phosphatidylinositol (3, 4, 5)-trisphosphate) promotes increased cell growth with suppression in cell death signaling [94]. The inhibition of PIP₃ therefore decreases Akt signaling. Phosphatase and tensin homolog deleted on chromosome 10 (PTEN) functions as the lipid phosphatase that dephosphorylates and inhibits PIP₃ [95]. Interestingly, PTEN has two exposed cysteines within its active site, and oxidation of cys¹²⁴ by H₂O₂ resulted in inhibition of PTEN activity through cysteine disulfide bond formation [96, 97]. Functionally, this inhibition is reversible through the reductive properties of Trx. While the role of PTEN is diverse, it is the most common deregulated phosphatase in cancers. PTEN may be additionally involved in mitochondrial apoptotic signaling, whereby upon staurosporine-induced apoptosis, PTEN can

translocate to the mitochondria where it may interact with Bax, promoting apoptosis, and knockdown of PTEN resulted in cell protection from apoptosis [98]. Additionally, Akt stimulation resulted in the promotion of glucose uptake and lactate production beyond the requirements needed to sustain cell growth, yet had no influence over mitochondrial oxygen consumption [99]. Additional to the PI3K/Akt/mTOR pathway stimulating aerobic glycolysis, oncogenic activation of PI3K/Akt was able to stimulate an increase in GSH (and presumably Trx) through the activation of Nrf2 [100].

Given that mitochondrial assembly is reliant on both mitochondrial and nuclear DNA, mutations in both have been implicated in altering cancer metabolism [101]. Mutations in the subunits of succinate dehydrogenase (SDH - complex II of the ETC) in humans have been implicated in increased risk of renal cell carcinoma development resulting in aggressive cancer growth [102], while mutations in isocitrate dehydrogenase (IDH) are common in acute myeloid leukemia's and glioma's [103]. Both SDH and IDH mutations can result in drastically altered mitochondrial function, along with altered rates of lipid synthesis and ROS production. Despite the root cause of altered mitochondrial metabolism in cancers, the mitochondria play an important role in all facets of cancer progression. In murine 4T1 breast cancer cells, chronic exposure of low-dose ethidium bromide resulted in mitochondrial ablation (mitochondrial-null cells were referred to as 4T1p⁰ cells) and subsequently blunted tumour formation of 4T1p⁰ cells following murine injection relative to the parental 4T1 cell line [104]. Unlike the findings of mitochondrial ablation decreasing tumourigenesis, Guo et al. [105] demonstrated that depletion of mtDNA was able to promote tumourigenesis and chemoresistance in certain colorectal carcinomas. While separately, increasing mtDNA in other colorectal carcinoma lines was able to increase cell proliferation and inhibit cell death [106]. It appears that the role of the mitochondria

in cancer is not as universally defined relative to what Warburg first proposed almost 100 years ago, in contrast to his initial argument, it appears that the mitochondria are involved in tumour formation and growth, although how the mitochondria is involved appears to be vary greatly between cancers. Inserting point mutations in mtDNA in HeLa cells coding for a subunit of ATP synthase resulted in conferring an advantage in tumour growth when these cells were xenographically implanted into nude mice. This was attributed to a significant decrease in apoptosis occurring in the mutant compared to the wild-type HeLa cell transplants [107]. Nutrient starvation resulted in decreased glucose uptake and lower ATP production in CT26 colorectal carcinoma cells, however this apparent decrease in glycolysis was accompanied by an increase in O₂ consumption and oxidative stress, which concurrently amplified the cytotoxic effects of the chemotherapy oxaliplatin [108]. In Rat-1 fibroblasts, human MCF7 breast and HepG2 hepatocellular carcinoma cell lines, inhibiting mitochondrial OXPHOS decreased mitochondrial apoptotic signaling brought upon by a variety of pro-apoptotic external stimuli [109]. This highlights the notion that normal mitochondrial function is required for proper regulation of apoptotic stimuli, and that aerobic glycolysis may confer a potential advantage to cancers through apoptotic evasion [110]. However, there is a misconception that cancers display intense apoptotic resistance. Many cancers display an increased sensitivity to a variety of external apoptotic stimuli (such as a variety of chemotherapies), and overcome this heightened sensitivity by constant and rapid cell division [111].

2.4.1 Cancer metabolism confers a pro-neoplastic environment

Mitochondria are linked to a variety of pro-growth events throughout the cell. Dihydroorotate dehydrogenase (DHODH) is an enzyme found on the outer leaflet of the IMM

and is critical for *de novo* pyrimidine biosynthesis [112]. In epithelial carcinoma cells, decreasing mitochondrial flux through the ETC resulted in a decrease in *de novo* pyrimidine biosynthesis through decreasing DHODH activity [113], suggesting that while cancers may elicit decreased mitochondrial flux through the ETC, some tonal level is required for *de novo* pyrimidine biosynthesis resulting in steady-state mitochondrial ROS production. Mitochondrial ROS emission is associated with an increase in HIF-1 α , and overexpression of HIF-1 α is linked to increased tumour aggression and growth [114]. Once increased, HIF-1 α can increase the transcription of many pro-glycolytic genes including GLUT1 and GLUT3 [115], pyruvate dehydrogenase kinase (PDK) [116], hexokinase II (HKII) and phosphofructokinase (PFK) [117]. Knocking down HIF-1 α resulted in decreased glycolytic metabolism [118] and increased the sensitivity of multiple myeloma cells to melphalan-induced cell death [119]. HIF-1 α is not the only driver of aerobic glycolysis, however it is certainly well characterized, regardless, the promotion of aerobic glycolysis can confer many pro-growth benefits to cancers. Overexpression of B7-H3, an immunoregulatory protein, resulted in the increase in glucose consumption, lactate production and HKII activity in colon cancer cells [120]. This increase in aerobic glycolysis conferred chemo resistant properties, and the inhibition of HKII prevented the increase in aerobic glycolysis and restored chemo sensitivity [120]. While understanding the role of B7-H3 in cancers is still in its infancy, the promotion of aerobic glycolysis is able to drive many pro-neoplastic adaptations. These adaptations are likely a result of both aerobic glycolysis and mitochondrial metabolism, as aerobic glycolysis can produce ATP and biosynthetic molecules, and through anapleurosis and catapleurosis, the mitochondria can supply the cell with other required molecules for growth and replenish TCA cycle intermediates through various alternate pathways.

Glycolytic intermediates promote a pro-neoplastic environment

Malignant tumour development is a process of micro-evolutionary events resulting in the cancer phenotype. Aerobic glycolysis likely stems from the micro-evolutionary adaptations to hypoxia during early stages of tumourigenesis [121]. During this initial hypoxic event, there is an increase in lactate production that is fatal to most cells, therefore the surviving cancer population typically display protective mechanisms against acidosis and a marked growth advantage associated with aerobic glycolysis [121]. Hypoxia, along with mitochondrial ROS, increases HIF-1 α which increases lactate dehydrogenase (LDH) expression [122]. LDH catalyzes the production lactate from pyruvate at the cost of the oxidation of NADH producing NAD⁺ in the process. Increased intratumoural lactate, which in itself is associated with increased aerobic glycolysis, is associated with an increased likelihood for metastasis in head and neck cancers [123] and cervical cancers [124]. In order to sustain elevated rates of aerobic glycolysis, a constant supply of NAD⁺ must be available. Therefore, one of the benefits of high rates of lactate production is through the restoration of the NAD⁺ pool through the oxidation of NADH [125]. Inhibition LDH by oxamate resulted in an increase in G2/M cell cycle arrest and an increase in apoptosis in two nasopharyngeal carcinoma cell lines, which was accompanied by an increase in mitochondrial ROS production, and N-acetylcysteine (NAC, an exogenous antioxidant) was able to partially blunt the effects [126]. However, the role of LDH in cancer progression is still debated, as LDH silencing led to the surprising increase in HIF-1 α in HT29 cells, yet HIF-1 α was unable to function properly as it was no longer able to promote expression of its regular targets [127]. Regardless, excess cancer lactate itself is a prominent pro-oncogenic signal, as it promotes vascularization through VEGF production in endothelial cells [125], inhibits T-cell

function through the prevention of T-cell lactic acid transport (disrupting T-cell metabolism) [128] and promotes cancer metastasis and migration [123, 124].

Along with excess lactate production, aerobic glycolysis also affords an increase in glycolytic-derived carbon flux through the pentose phosphate pathway (PPP). The PPP branches off of glycolysis following the first committed step of glucose. The PPP fulfills two main requirements of the cell, as it is required for the biosynthesis of ribonucleotides, and is a site of NADPH production [129]. Cancers display relatively high levels of glucose-6-phosphate dehydrogenase (G6PDH - the rate-limiting enzyme for initiating the PPP) protein content [130] and high levels of G6PDH enzymatic activity [131]. Dehydroepiandrosterone (DHEA) is an endogenous circulating steroid shown to display inhibitory properties towards G6PDH [132], and DHEA abrogated cell survival in several cancer cells. The inhibition of G6PDH rendered cells more susceptible to H₂O₂-induced decreasing cell survival, while overexpression G6PDH increased cellular proliferation [132]. This data highlights the importance of the PPP in regulating cancer growth, where the production of ribonucleotides is critical for constantly dividing cells, as is the production of NADPH for redox regulation and for other components of cell growth such as the requirement of NADPH to drive *de novo* lipid synthesis [129]. The *in vivo* efficacy of direct PPP inhibition is currently not well understood, however the PPP is the only known source of NADPH production in red blood cells, and G6PDH inhibition resulted in drastic red blood cell sensitization to ROS-induced cell damage [129], likely suggesting that G6PDH-inhibition through our current understanding may not be a viable therapeutic target given the potential for harmful deleterious off target effects.

TCA cycle intermediates are required for neoplastic growth

Alterations in IDH, SDH and fumarate hydratase (FH) have all been implicated in altering cancer metabolism and conferring pro-neoplastic properties [133]. Wild type IDH converts isocitrate to α -ketoglutarate, however mutant IDH gains the function to convert α -ketoglutarate to 2-hydroxyglutarate (2-HG) [134]. While the presence of 2-HG can serve as a potential biomarker for IDH-bearing mutant cancers to potentially guide therapies [135], mutated IDH and increased 2-HG resulted in the elevation of free amino acids and increased lipid precursors in human oligodendroglioma cells [136]. Activation of HIF-1 α is able to promote aerobic glycolysis through the increase in pyruvate shunting towards lactate instead of the mitochondria; the regulation of HIF-1 α can be manipulated by many of the TCA cycle intermediates [133]. Elevated levels of fumarate and succinate can stabilize and promote HIF-1 α activity [137], which in turn increases glutamate import into the mitochondria for anapleurotic replenishment of TCA cycle intermediates, while silencing FH resulted in an increase in HIF-1 α and a subsequent increase in aerobic glycolysis [133, 138]. FH-deficient human fibroblasts displayed altered metabolism through an increase in HKII, and a reduced redox state through a decrease in ROS and an increase in GSH [139]. Increased glycolysis corresponding to alterations in cellular redox conditions is common in cancer pathology, linking metabolism and redox regulation as properties involved in conferring a pro-neoplastic cellular environment.

2.5 Cancer and antioxidant regulation

ROS accumulation within cancers has long been associated as a mitogenic signal promoting tumourigenesis. Elevated ROS in cancers has been attributed to a variety of neoplastic functions such as altered metabolic activity, further oncogene activation and pseudo-hypoxic signaling [140]. At higher levels however, rather than promoting cell proliferation, mitochondrial

ROS can promote cell death if not countered by antioxidant defense systems [140]. Exogenous exposure of MCF7 cells to varying concentrations of H₂O₂ resulted in both an increase and decrease in cell proliferation compared to no H₂O₂ [141]. Chronic 25µM H₂O₂ exposure resulted in a drastic increase in MCF7 cell proliferation, however 250µM H₂O₂ resulted in a significant decrease in MCF7 cell proliferation. Given that low levels of H₂O₂ were able to stimulate growth yet high levels resulted in blunted proliferation, it is likely that the ability of the cell to buffer changes in ROS is an important factor in dictating cell fate upon exposure to potential oxidative stress. It has been previously reported in lung cancer patients (non-smoking population) that there was a significant increase in complex I associated mtDNA mutations [142], and given that complex I is a primary site for ROS generation in the mitochondria, it is a fair assumption that mutations in complex I may have resulted in abnormal mitochondrial ROS production. Furthermore, overexpression of the oncogene Ras promoted hyper proliferation in normal human fibroblasts despite increased DNA damage, which was accompanied by elevations in ROS [143]. However, the exogenous antioxidant NAC was able to prevent hyper proliferation induced by Ras overexpression restoring normal growth patterns in the Ras overexpressed cells. It is therefore apparent that the role of ROS in cancers is through promotion of both cell growth and cell death, and it is likely that if a cell can properly buffer elevations in ROS, ROS can potentially result in a pro-growth environment, yet if a cell is unable to buffer these elevations in ROS, the cell will undergo oxidative stress and cell death. As are many components associated with metabolism and redox signaling, the two main intracellular antioxidants, glutathione and Trx, are highly implicated in many cancers.

2.5.1 Glutathione and thioredoxin are highly implicated in cancers

Following the conversion of mitochondrial $O_2^{\bullet-}$ to H_2O_2 , the reduction of H_2O_2 to H_2O prevents the formation of hydroxyl radicals (OH^{\bullet}) through Fenton chemistry [8]. The peroxidase systems responsible for the reduction of H_2O_2 are the glutathione and Trx systems. Interestingly, both the Trx and glutathione system are highly implicated in cancer regulation.

2.5.2 Cancer and glutathione

Glutathione is often increased in many cancers [144], however the role of glutathione in cancer progression remains not entirely defined. Glutathione has many roles in regulating the progression of cancer other than redox regulation, as excess GSH can promote tumour growth and eventual metastases [145]. Elevated tumoural glutathione levels at the onset of diagnosis seemingly conferred with a worse prognosis in colorectal carcinoma patients [146]. While glutathione is implicated in a variety of cellular systems, it is highly implicated in promoting cancer growth and chemoresistance.

Glutathione regulating cancer growth

One of the main associative causes of death with cancer is through metastatic growth. Upon relocation of cancer cells to a new environment, metastatic cancer cells are exposed to a transient hypoxic environment resulting in the rapid production of ROS. Therefore, the ability of the cell to combat these elevations in ROS in part dictates cell survival during metastasis. Such that NB4 leukemia cells cultured in hypoxic conditions displayed an acute burst of ROS, resulting in marked cell death, however not cell extinction. Following 7 days of hypoxia, the surviving fraction of NB4 cells displayed significantly greater GSH levels to protect from excess ROS generation [147]. Cancer cell dormancy during metastasis allows for cancer cells to remain

in circulation for years, and despite the absence of cell proliferation in these cells, they can eventually lead to latent metastatic tumour formation. Havard et al. [148] demonstrated that elevated levels of GSH and citrate were able to re-animate previously dormant LNCaP prostate cells. While it currently remains undetermined, the combined role of increasing a mitochondrial substrate (citrate) and glutathione unifies cancer mitochondria and glutathione as critical regulators for cancer progression. In B16-F10 melanoma-bearing mice, elevated circulating GSH resulted in increased intratumoural GSH levels resulting in an increase in metastatic growth [149]. B16-F10 melanoma cells secreted interleukin-6 (IL-6), which resulted in increased hepatocyte release of GSH into the circulation, allowing for more GSH uptake by B16-F10 cells in a feedback loop. This is evidence that cancers are able to alter their redox environment through endocrine signaling. Following an increase in systemic glutathione, circulating glutathione is broken down at the target cell by cell membrane-bound γ GT, allowing for the import of the constituent ingredients required for intracellular glutathione reassembly. This pathway for glutathione synthesis is separate from *de novo* glutathione synthesis and is called the γ -glutamyl cycle. Interestingly, γ GT expression increases following oxidative stress and is commonly up-regulated in a variety of cancers. Additionally, in B16-F10 melanoma-bearing mice, the circulation of exogenously added GSH-ester promoted further metastasis, however the inhibition of γ GT by acivicin prevented GSH-ester induced cell metastasis [150]. Furthermore, inhibition of γ GT by acivicin resulted in increased tumour cytotoxicity to glutathione depletion [151]. As evidence that glutathione can directly promote cell division, glutathione has been previously demonstrated to co-localize with the nucleus as cells undergo proliferation. Nuclear translocation of glutathione serves to protect the nucleus during nuclear disintegration, as well as serve as a regulator of redox-dependent proteins involved in initiating and regulating cell cycle

[58, 59, 152]. While the role of glutathione directly regulating cell cycle progression has yet to be determined in cancers, it is fairly safe to assume that associative increases of glutathione in cancers is also likely involved in further progressing cell proliferation.

Glutathione in chemoresistance

Fujimori et al. [153] noted a relationship between cisplatin sensitivity and expression of GCL (the rate-limiting enzyme in *de novo* glutathione synthesis, Figure 2.6), whereby overexpression of the GCL subunits correlated with cisplatin resistance in human non-small-cell lung carcinoma (NSCLC) xenografts *in vivo*. While *de novo* glutathione synthesis is one mechanism for increasing GSH levels, another mechanism is through the breakdown and subsequent import of extracellular glutathione. Interestingly, when human ovarian tumour samples acquired chemoresistance, there was a corresponding ~10-fold increase in intratumoural GSH [154]. The notion of elevated GSH conferring chemoresistance has been confirmed in a variety of cancers to several different therapeutic compounds [145]. The role of glutathione in chemoresistance is primarily responsible for buffering chemotherapy-induced ROS and direct binding to xenobiotic compounds allowing for the export of anticancer compounds out of the cell. Many current cancer therapies elicit anticancer properties through either the generation of ROS or the depletion of antioxidant defenses [155]. To that point, Diehn et al. [156] reasoned that ionizing radiation kills cells through the rapid generation of ROS, and that radiation-resistant cancer could be sensitized to radiation through combined radiation and glutathione depletion by BSO. Indeed, they discovered that radiation-resistant tumours had higher levels of glutathione and contained cancer cells that were spared to ionizing radiation compared to non-transformed cells, yet glutathione depletion through BSO resulted in complete sensitization of the tumour to

radiation [156]. Additionally, many cancer cells have been demonstrated to be highly reliant on glutamine uptake to sustain elevated cell proliferation, where glutamine gets converted within the cell to glutamate by glutaminase. Upon enzymatic conversion, glutamate can function as a precursor to glutathione synthesis. Using radiolabeled glutamine, it was demonstrated that H460 and A549 lung cancer cells rapidly synthesize glutathione from cytosolic glutamine, and both glutaminase inhibition and glutamine starvation sensitized the cells to radiation-induced death [157]. Along with glutamine import, cancers typically have up-regulated xCT membrane expression. xCT is a cysteine-glutamate antiporter, and is critical in the development of many cancers such as colorectal, kidney, brain and breast cancer cells [145, 158]. While cysteine is typically viewed as a non-essential amino acid because it can be synthesized from methionine in many tissues, many cancers have demonstrated an inability to synthesize cysteine from methionine, and therefore rely on cysteine uptake. Likely stemming from the inability to synthesize *de novo* cysteine, many cancers have demonstrated an increase in both light and heavy chain subunits of the xCT antiporter, and this increase in xCT is seen as a primary mechanism for cysteine import for cell growth and glutathione synthesis to aid in chemoresistance. Interestingly, cysteine starvation or xCT inhibition has led to drastic glutathione depletion and cancer cell death [158]. The role of glutathione as an antioxidant during chemoresistance is fairly well defined, as certain therapies aim to increase intratumoural ROS to elicit anticancer effects, cancers combat this through elevations in GSH to prevent the deleterious effects of ROS. The other primary mechanism for glutathione-induced chemoresistance is mediated primarily through the family of enzymes known as glutathione S-transferases (GSTs).

Glutathione S-transferase

B16-F10 melanoma cells have high levels of GSH and display hyper proliferative qualities relative to B16-F1 low glutathione cells [150, 151], which is consistent with previous literature demonstrating high glutathione confers pro-growth properties. However, B16-F10 cells display inhibition towards glutathione efflux resulting in metastatic cell resistance to oxidative stress, while knocking out multidrug resistance protein-1 (MRP-1) resulted in the full prevention of glutathione efflux, suggesting that glutathione efflux is channeled through MRP-1 [151]. The regulation of glutathione efflux is critical in cancers not only to regulate extracellular glutathione levels, but also through the functioning role of glutathione as a xenobiotic regulator. MRP-1 is a member of a class of pumps called GS-X pumps, which serve to export glutathione conjugates out of the cell. Once a glutathione conjugate is formed through enzymatic regulation by GSTs, the glutathione conjugate is exported out of the cell for extracellular degradation and detoxification [159]. GSTs have been identified as commonly up-regulated in variety of cancers, and GST activity has been demonstrated to be elevated in a variety of breast cancers [160]. Interestingly, GST-null mutations lead to increased risk of cancer development as a consequence of cells losing the ability to remove carcinogenic compounds [161]. Furthermore, GST-null mutations result in a significantly worse prognosis and expected response to chemotherapies in breast cancer patients [162]. Contrary to this however, lower GST activity is associated with better survival in ovarian cancer patients, and there was a slight increase in survival advantage with GST-null mutations [163]. This demonstrates the complicated nature of GSTs in cancer, where the systemic lack of GSTs can result in an increase in cancer development due to increased cellular exposure to carcinogens; lower GST can result in either better or worse survival. Although speculative, it appears that the loss of GST on survival may be involved in the

systemic response to chemotherapies. Where lower survival with a GST-null mutation may result in systemic sensitization to chemotherapies resulting in negative systemic effects, however depending on the cancer itself, it may render the cancer more susceptible to therapy over surrounding tissue. Furthermore, high levels of GST expression have also been correlated to chemoresistance in ovarian cancer [164]. Future research will further elucidate the role of GSTs in cancers, currently however, therapeutic targeting of GSTs remain controversial given the contradictory nature of GSTs in determining survival.

2.5.3 Cancer and thioredoxin

Along with glutathione, Trx is commonly up-regulated in many cancers [165], and Trx expression is associated with aggressiveness of the tumours themselves, whereby the more aggressive tumours have greater levels of Trx [166]. Along with its antioxidant function, reduced thioredoxin is bound to ASK1, preventing ASK1 from initiating downstream apoptotic signaling. Trx disassociates from ASK1 upon oxidation, allowing for ASK1 to initiate apoptotic signaling [167]. Given the important role of Trx in redox and apoptotic signaling, emerging evidence highlights the importance of Trx in clinical cancer populations. In human primary gastric carcinoma samples, there was a positive correlation of Trx levels with cancer cell proliferation, and a negative correlation with DNA damage, suggesting that Trx is associated with both the promotion cancer cell growth and resistance to DNA damage [168]. Similar to glutathione, Trx is important in regulating both cancer growth and promoting chemoresistance.

Thioredoxin regulating cancer growth

Trx has been implicated through various pathways to promote both normal cell growth and cancer growth. Trx is a known inhibitor of PTEN, whereby an exposed cysteine on Trx can bind to an exposed cysteine on PTEN inhibiting PTEN inhibition on Akt [169]. Therefore, overexpression of Trx functions to increase the PI3K/Akt/mTOR pathway through inhibition of PTEN. While several different Akt inhibitors were able to decrease cancer cell viability, the coordinated exposure of cells to Akt inhibitors plus Trx rescued the original effect of the Akt inhibitors. Interestingly, Trx alone was able to promote an increase of cells in S and G2/M phase and decrease cells in G0/G1, suggesting that Trx is able to promote an increase in cell cycle progression [170]. Furthermore, overexpression of Trx in HeLa, HT29, MCF7 and EMT6 cells all resulted in an increase in HIF-1 α activity [171]. Beyond Trx itself, mitochondrial thioredoxin reductase (TrxR2) is up-regulated in NSCLC tumour samples. Knocking down TrxR2 in A549 and NCI-H1299 cells resulted in suppression of cell growth, induced apoptosis and decreased cell invasion, whereas overexpression of TrxR2 resulted in the opposite effects [172]. This suggests that TrxR2 can also promote cancer cell aggression. Interestingly, ribonucleotide reductase (RR) functions as the rate-limiting enzyme in DNA synthesis, however following the enzymatic reduction of a ribonucleotide to a deoxyribonucleotide by RR, cysteine residues on RR need to be re-reduced. RR physically interacts with Trx, and ectopically increased Trx expression increases RR expression (along with DNA synthesis, cell proliferation and migration). In human colorectal carcinoma tumours, Trx (but not glutaredoxin) and RR were coordinately up-regulated, and the expression of both Trx and RR were correlated with tumour aggression [173]. Beyond activation of Trx in cancers, the inhibition of Trx is also altered in many cancers. Thioredoxin interacting protein (TXNIP) is typically viewed as an inhibitor of Trx, resulting in decreasing Trx function. TXNIP expression is decreased in many cancers, and

lower TXNIP results in altered lipid metabolism [174], which in itself is a common phenotype in many cancers. The Trx system is a complex system in both normal and cancer cells. It is critical in regulating cell growth through normal cell development, and alterations in the Trx system further promote cancer progression.

Thioredoxin in chemoresistance

Similar to glutathione, Trx is highly implicated in cell protection from oxidative stress, this holds true in both normal cells as well as in cancer cells. Interestingly, Trx levels correlate to cisplatin resistance in human ovarian cancers [175]. Beyond simple correlation, the creation of cisplatin resistant HT29 and St-4 cell lines resulted in a ~2-2.5X increase in Trx relative to their parental lines. In line with resistance to cisplatin, levels of Trx prior to the exposure of docetaxel predicted chemoresistance, however there was no witnessed relationship between the levels of Trx after docetaxel exposure to the sensitivity of the cell to docetaxel-induced cell death [176]. This suggests that the adaption of Trx to anticancer therapies is less important than the starting levels of Trx. However, contrary to the notion of elevated Trx being able to confer chemoresistance, breast cancers that are resistant to anti-estrogen therapy are sensitized when mitochondrial thioredoxin (Trx2) is overexpressed. Anti-estrogen elicits an increase in intracellular H₂O₂ production; and modest increases in H₂O₂ may promote neoplastic growth. The overexpression of Trx2 may prevent the accumulation of modest levels of H₂O₂ allowing for non-ROS inducing cell death mechanisms to kill the cell [177]. While the role of Trx in promoting chemoresistance appears to be diverse, evidence suggests that alterations in Trx is highly involved in cell protection [178]. Androgen deprivation therapy (ADT) is the standard-of-care for prostate cancers when surgical or radiation options fail. While ADT initially results in

tumour regression, prostate cancer relapse typically occurs between ~1-3 years later. The relapsed prostate cancer is considered incurable and is termed castration-resistant prostate cancer. Samaranayake et al. [178] demonstrated that Trx is significantly increased in castration-resistant prostate cancer cells and shRNA knockdown of Trx impedes cell growth and promotes cell death, and early Trx knockdown in castration-resistant prostate cancer prevented tumour formation [178]. Additionally, diffuse Large B cell lymphomas have a fairly high initial therapy success rate, however similar to ADT treated prostate cancers, diffuse Large B cell lymphomas have a high rate of relapse and a low patient survival rate following cancer return. This is largely attributed to diffuse Large B cell lymphoma chemoresistance. Interestingly, in both derived and primary lines, diffuse Large B cell lymphoma cells have higher levels of cytosolic thioredoxin (Trx1), and Trx1 expression is associated with decreased patient survival. Further inhibition of Trx1 by siRNA or a specific Trx1 inhibitor (PX-12) resulted in the blunting of diffuse Large B cell lymphoma cell growth and sensitized diffuse Large B cell lymphoma cells to doxorubicin-induced cell death *in vitro* [179]. In doxorubicin-resistant McA diffuse Large B cell lymphoma cells, it was noted that Trx1 was significantly higher compared to the parental cell line that was not generated to be resistant to doxorubicin, yet the doxorubicin-resistant cells were more sensitive to Trx1-inhibition induced decreasing cell survival compared to the parental doxorubicin-sensitive line. This is particularly interesting because it suggests a form of Trx addiction in cancers, where the heightened levels of Trx likely means cancers have a heightened reliance on cyto-protective Trx properties. Beyond Trx itself, the regulators of Trx also appear to be important to promote chemoresistance. To this point, selenite is used as an anticancer therapy that functions through the induction of cellular oxidative stress. Interestingly, selenite seems to be more potent in cancer cells relative to non-transformed cells. Preventing the

reduction of Trx-S₂ by decreasing cytosolic thioredoxin reductase (TrxR1) resulted in increased sensitivity to selenite, despite TrxR1 knockdown resulting in a compensatory increase in glutathione (which in turn elicited marginal cyto-protective effects) [180]. The role of Trx in promoting cancer growth and chemoresistance is still not entirely defined. However, it appears that elevated levels of Trx and Trx-related proteins are able to alter cell growth and cell death dynamics, and manipulations in both glutathione and Trx offer potential potent therapeutic options given the heightened reliance of cancers both for ROS production to promote cell growth, but also Trx and glutathione to regulate and manage ROS levels.

2.5.4 Antioxidant targeting for cancer therapy

Much work has been conducted on examining the potential of exogenous antioxidant supplementation as an adjunct anti-cancer therapy. Exposure of HT1080 fibrosarcoma and RD rhabdomyosarcoma cells *in vitro* to the mitochondrial-targeted antioxidant, SkQ1, resulted in drastic tumour growth suppression [181]. However, several different clinical trials have demonstrated that dietary antioxidant supplementation were able to mitigate treatment-related off-target effects [182-187]. Interestingly, several reports have suggested that exogenous antioxidant supplementation may not only confer protective benefits to normal tissues, but also to cancer tissues rendering anticancer therapies less potent [188-190]. Bairati et al. [186] administered oral α -tocopherol and β -carotene in a clinical trial with patients with head and neck cancers. While β -carotene administration was ceased during the trial, α -tocopherol was administered during treatment and up to three years after. Interestingly, α -tocopherol administration resulted in an increase in cancer-specific mortality compared to placebo; resulting in the conclusion that high-dose α -tocopherol could be harmful to cancer survival [186].

However, given the role of glutathione and Trx in promoting both cancer progression and chemoresistance, and the potential addiction of cancers to endogenous antioxidant systems, rather than the administration of exogenous antioxidants to patients with cancer, selective targeting of glutathione and Trx has gained more recognition in recent years as a potential for anticancer therapies.

Glutathione inhibition for cancer therapy

Many studies have demonstrated that genetic manipulation of glutathione can alter cancer survival (see section 2.5.2 Cancer and Glutathione). The use of glutathione-specific depleting agents or inhibitors has demonstrated potentially beneficial results towards anticancer growth, and warrants further exploration.

Buthionine sulfoximine (BSO)

BSO is an inhibitor of glutamate cysteine ligase (GCL – Figure 2.6), resulting in the inhibition of glutathione synthesis leading to a rapid decrease in intracellular glutathione levels [191]. BSO-induced glutathione depletion can result in decreasing cancer growth and survival, as well as act in combination with a variety of other anticancer therapies to provide beneficial effects [192]. Using Auger electron emitting thymidine (I-125-ITdU) as a cancer specific radiotherapy (I-125-ITdU incorporates into the DNA of target cells, but radiation of the Auger electron has the capacity of only nanometers, therefore it only degrades DNA of the host cell, with minimal side effects, this is called nanosurgery), GSH depletion by BSO was able to markedly sensitize triple-negative breast cancer stem cells to DNA damage and death from I-125-ITdU, suggesting a potential avenue for concurrent glutathione depletion in novel anticancer

therapies [193]. However, while phase I clinical trials demonstrated that BSO was safe, it did not however result in marked decreases in intracellular glutathione levels [194]. This was likely due to rapid elimination of BSO from plasma resulting in a short half-life minimizing the effects of BSO on glutathione depletion [195]. While BSO remains an important compound to test the influence of glutathione depletion in cancer, it is unlikely that BSO is a viable option for an anticancer therapy; therefore other mechanisms to induce glutathione depletion are required.

Serine and glycine starvation

Serine and glycine are integral for glutathione synthesis (Figure 2.6). During serine starvation, glycolysis is redirected towards the one-carbon cycle for *de novo* serine synthesis, and typically a compensatory increase in mitochondrial activity is observed to counteract decreasing glycolytic ATP supply. To that point, serine and glycine starvation resulted in glutathione depletion in HCT 116 colorectal cancer cells [73]. Upon serine and glycine starvation and glutathione depletion, HCT 116 p53^{+/+} cells were able to promote a cell cycle arrest, resulting in the decreased demand for serine and glycine for pro-growth synthesis, allowing for *de novo* serine synthesis through one-carbon metabolism and the restoration of glutathione levels. However, in HCT 116 p53^{-/-} cells, there was no witnessed cell cycle arrest, therefore serine and glycine were required to sustain growth rather than being redirected towards glutathione replenishment, resulting in a further decrease in glutathione levels [73]. Interestingly, Kras-driven mouse models of both pancreatic and intestinal cancers were less sensitive to serine and glycine starvation due to increased expression of enzymes involved in serine synthesis [196]. The therapeutic potential for serine and glycine starvation in anticancer therapies is incredibly high, as serine and glycine are non-essential amino acids, and serine and glycine starvation is

likely systemically well tolerated. However, given that some cancers are able to modulate serine synthesis related enzymes, adjunct therapy is required to increase the sensitivity of serine and glycine starvation in order to promote glutathione depletion.

Other novel glutathione-depleting compounds

There are many compounds known to alter or deplete intracellular glutathione systems. Compounds such as telcya (an inhibitor of GSTs), disulfiram (causes an increase in GSSG relative to GSH) and NOV-002 (GSSG conjugated to cisplatin) have been met with various successes as anticancer therapies [192]. Flavonoids have been demonstrated to induce glutathione depletion in A549 lung cancer cells, HL-60 myeloid cancer cells and PC3 prostate cancer cells resulting in decreasing cell survival [197]. However, the role of flavonoids on glutathione depletion *in vivo* remains unknown. One such novel compound to undergo clinical trials is imexon. Imexon incubations resulted in cytotoxic effects in 8226 myeloma cells at varying concentrations with long duration, low-concentrations of imexon eliciting the most potent effects [198]. Imexon elicited oxidative stress through cellular depletion of glutathione, and NAC partially blunted imexon-induced cytotoxicity, whereas concurrent BSO and Imexon incubations increased cytotoxic effects on 8226 myeloma cells [198]. Phase I trials demonstrated a relatively safe dosage with encouraging anticancer properties in patients with advanced pancreatic cancer [199], however, phase II trials with imexon and gemcitabine resulted in no observable improved outcome in patients with advanced pancreatic cancer [200]. Interestingly, in a phase II trial of imexon in patients with B-cell non-Hodgkin lymphoma, patient success with imexon was correlated with baseline levels of redox-related genes such as SOD1 and glutathione peroxidase, such that patients with cancers that a higher 'redox-score' were more likely to be

sensitive to imexon-induced partial responses compared to patients with cancers with a lower ‘redox-score’ [201]. Which is in alignment with the notion of antioxidant addiction, where cancer cells with higher antioxidant function are more sensitive to antioxidant inhibition.

Thioredoxin inhibition for cancer therapy

Many studies have demonstrated that genetic manipulation of Trx can alter cancer survival (see section 2.5.3 Cancer and Thioredoxin). The use of Trx-specific depleting agents or inhibitors has demonstrated potentially beneficial results towards anticancer growth, and warrants further exploration.

Auranofin

Auranofin is a gold compound originally deployed for the treatment of rheumatoid arthritis [202]. Auranofin displays potent inhibition on thioredoxin reductase (TrxR) through the putative inhibition of the active site selenocysteine on TrxR [203]. Given that auranofin has a recognized toxicity profile and is considered safe for human consumption, auranofin is now being repurposed towards anticancer therapies [204]. There are currently 6 clinical trials involving auranofin and cancer according to the NCI database, to date however there are currently no reports on the efficacy of auranofin in humans towards anticancer therapies.

PX-12

Unlike auranofin, which binds with TrxR, PX-12 inhibits Trx through binding to an exposed cysteine residue on Trx itself [192]. In A549 lung cancer cells, PX-12 resulted in an

increase in ROS generation leading to apoptosis, while NAC was able to partially blunt the cytotoxic effects of PX-12 [205]. A phase I clinical trial demonstrated that PX-12 is safe for administration and resulted in a stable disease state for ~18% of patients for up to a year [206]. However, PX-12 displayed a lack of anticancer activity in a phase II clinical trial in patients with advanced pancreatic cancer likely due to these patients having low baseline Trx levels [207].

Brilliant green

Brilliant green (BG) functions through the targeted inhibition of mitochondrial thioredoxin (Trx2) resulting in cell death at nanomolar concentrations. In HeLa cells, BG resulted in selective cancer cell death because fibroblasts appeared resistant to BG [208]. Furthermore, knocking down Trx2 increased sensitivity to BG-induced cell death in HeLa cells, however knocking down Trx2 had no effect in altering BG sensitivity in fibroblasts.

Dual targeting of glutathione and thioredoxin for cancer therapy

Glutathione and Trx are often viewed in part as redundant systems. Transformed mouse embryonic fibroblasts (MEFs) taken from TrxR knockout mice displayed no difference in tumorigenic potential relative to MEFs isolated from control mice [209]. However, TrxR knockout MEFs were significantly more sensitive to BSO induced cell death relative to control MEFs [209]. This highlights the redundancy between systems given that TrxR knockout MEFs were solely reliant on glutathione for antioxidant defense purposes. To that end, Harris et al. [210] demonstrated in mice that generated spontaneous mammary tumours that while glutathione depletion with BSO was able to prevent tumour formation, only combined BSO + auranofin resulted in cancer death following established tumour formation. Separately, disulfiram has

demonstrated potent anticancer effects in PCa prostate cancer cells through the induction of miR-17 that in turn suppresses expression of both glutathione peroxidase-2 and mitochondrial TrxR (TrxR2) [211]. Dual targeting of glutathione and Trx systems may lead to potent anticancer therapies, however, given the importance of both glutathione and Trx in normal cell development, potential cancer specific targeting of glutathione and/or Trx may be required to minimize deleterious off-target effects.

2.6 Mitochondrial targeted therapies

Mitochondria are attractive therapeutic targets for a number of reasons, in particular because it is highly debated whether cancers display metabolic flexibility [212]. Given the hyper-reliance of cancers on ATP production along with other growth requirements, it is still unknown whether cancers are able to adapt and alter these pathways. Interestingly, it appears that ATP is not rate-limiting for cancer growth, rather the carbon distribution to glycolytic biosynthetic pathways (see section *2.4.1 Cancer metabolism confers a pro-neoplastic environment*) appears to be crucial. In line with the importance of carbon sparing, one theory as to why pyruvate is not fully oxidized in many cancers is to prevent carbon loss through the oxidation product of CO₂ [212]. Some cancer metabolic adaptations are due to direct irreversible genetic mutations [101]; it appears that most alterations in cancer metabolism are due to upstream adaptive phenotypes, such as the overexpression of PKM2 which results in slower carbon flux through glycolysis allowing for greater carbon redirection to glycolytic biosynthetic pathways such as the PPP. While these adaptive phenotypes may be theoretically reversible, the reversion of these metabolic phenotypes would come at a significant cost towards neoplastic growth. The impact of mitochondrial targeted anticancer therapies are based on the principle that alterations in cancer

metabolism are in fact irreversible, or indeed would be too costly to the cancer and arrest further cell division. However, there is a wide variety of mitochondrial-targeted therapies, some are designed to inhibit mitochondrial activity, while some therapies are targeted towards mitochondrial activation. What remains unclear is why some cancers are sensitive to mitochondrial inhibition, whereas some cancers are sensitive to mitochondrial activation. Increasing mitochondrial OXPHOS through forced overexpression of frataxin in MIP101, DLD2 and HT29 colorectal cancer cells resulted in decreased growth rates, inhibited colony formation and decreased tumourigenic properties when xenographically implanted into nude mice [213]. Contrary to the findings of increasing mitochondrial metabolism to slow cancer growth, decreasing mitochondrial metabolism through the formation of mitochondrial-null B16 mouse melanoma cells (B16p⁰) resulted in impaired tumourigenesis when xenographically implanted and significantly impaired the population doubling time under normoxic conditions [214]. However, under hypoxic conditions, there was no major difference between doubling time of B16p⁰ cells relative to the parental B16 cell line largely due to impaired population doubling of the parental B16 cell line. Further to this complication, elevated mitochondrial transcription factor A (TFAM), which promotes expression of mtDNA, is correlated to both increased cancer aggression and decreasing cancer progression. In 336 human breast cancer samples, patients with elevated levels of TFAM in cancer tissues correlated to poorer clinical outcomes and survival [215], whereas lower TFAM expression was correlated to a greater cell invasion in melanoma cell lines and human metastatic melanoma samples [216]. The efficacy of mitochondrial activation or inhibition appears to vary greatly between cancers. While debated, it appears that cancers may be susceptible to therapies designed at altering their metabolic profile whereas normal cells are able to display metabolic flexibility and are more resistant to mitochondrial

targeted therapies. Through detailed genetic manipulation, it can be ascertained that mitochondrial manipulation may provide a novel therapeutic target area selective for cancers, and many compounds have been examined to elicit desired effects.

2.6.1 Mitochondrial activation as an anticancer therapy

Dichloroacetate (DCA) is perhaps the most commonly studied compound for mitochondrial activating therapies. In 2007, Bonnet et al. discovered that DCA displayed potent anticancer properties through the forced oxidation of pyruvate in A549 NSCLC cells, M059K glioblastoma cells and MCF7 breast cancer cells, despite resulting in no witnessed negative effects to non-cancerous cells [217]. DCA functions through the inhibition of PDH kinase (PDK), resulting in the conversion of pyruvate to acetyl-CoA by PDH whereby acetyl-CoA stimulates mitochondrial OXPHOS. While many trials have demonstrated selective potent anticancer effects of DCA, Feurecker et al. [218] demonstrated that DCA stimulated cancer growth in Neuro-2a neuroblastoma xenografts *in vivo*, while stimulating increased cell growth in Neuro-2A and SkBr3 breast carcinoma cells *in vitro*, but had no effect on cell growth in the neuroblastoma cell lines Kelly and SK-N-SH *in vitro*. Additionally, DCA has been associated with peripheral nerve and hepatocellular toxicity [219]. The possibility of forced pyruvate oxidation is still currently under examination as phenyl butyrate has also demonstrated inhibitory properties towards PDK [219]. However, another avenue for forcing mitochondrial OXPHOS is through the supply of mitochondrial substrates. One intriguing example is through the provision of free carnitine and palmitoylcarnitine, a mitochondrial fatty-acid substrate able to bypass inhibition of carnitine palmitoyltransferase-1 (CPT-1, Figure 2.7), which has demonstrated

selective anticancer properties in HT29 colorectal cancer cells [220], as well as PC3 prostate cancer cells [221], while leaving normal cells healthy.

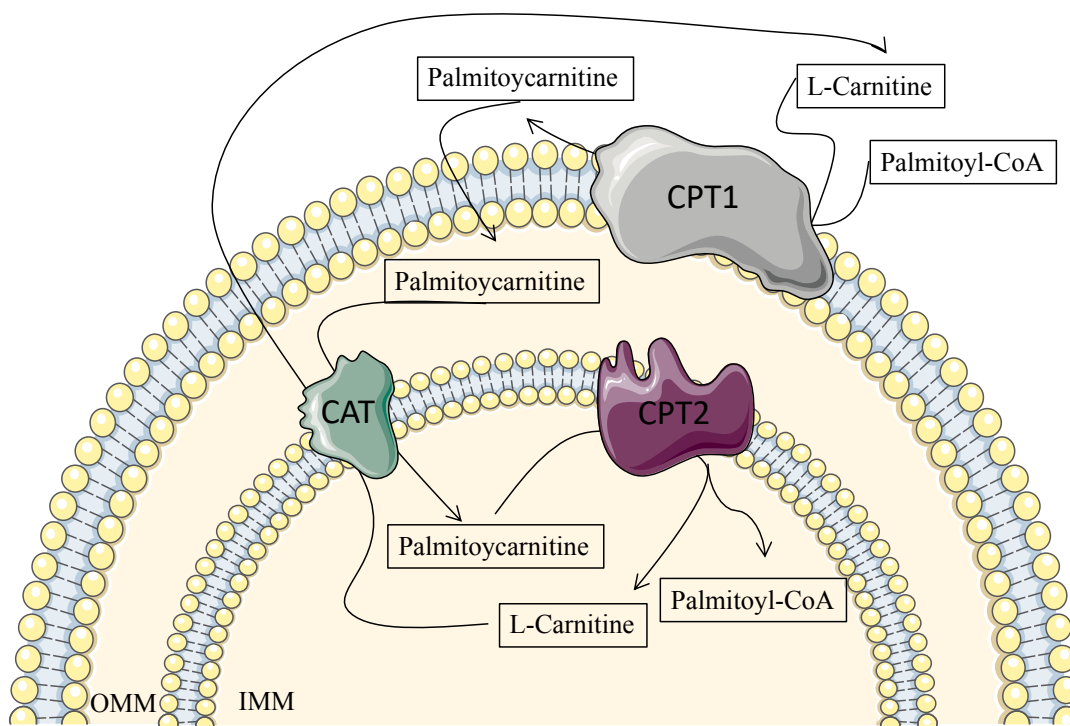


Figure 2 7 Schematic depiction of palmitoylcarnitine entry into the mitochondria. Palmitoyl-CoA and L-carnitine get converted to palmitoylcarnitine by carnitine palmitoyltransferase 1 (CPT1), whereby palmitoylcarnitine can freely diffuse into the intermembrane space, where it is imported into the mitochondrial matrix by carnitine acetyltransferase (CAT) through the antiporter function of palmitoylcarnitine against L-carnitine. Once in the mitochondrial matrix, palmitoylcarnitine gets broken down into palmitoyl-CoA and L-carnitine by carnitine palmitoyltransferase 2 (CPT2), allowing for L-carnitine cycling back out of the mitochondria.

When mice were treated with 1,2-dimethylhydrazine (DMH) to induce colon carcinogenesis, the addition of orally administered acetylcarnitine was able to significantly reduce the formation of DMH-induced colorectal neoplastic lesions, with no deleterious side effects reported [222]. Additionally, following 4-weeks of azoxymethane injections used to elicit carcinogen-induced colon cancer, a diet high in butterfat resulted in an increase in aberrant crypt foci (ACF), however when butterfat was combined with free carnitine, it appears that there was a significant

decrease in ACF formation compared to control [223]. As an alternative to both pyruvate oxidation and oversupply of mitochondrial substrates, Maddocks et al. [73] demonstrated that serine and glycine starvation resulted in the increase in mitochondrial reliance due to glycolytic redirection away from pyruvate and towards *de novo* serine synthesis. This redirection of glycolysis likely resulted in a decrease in ATP production, stimulating mitochondrial OXPHOS to generate ATP. Interestingly, serine is an allosteric regulator for PKM2, and serine starvation resulted in inhibition of PKM2 causing carbon backflow into *de novo* serine synthesis [224].

2.6.2 Mitochondrial inhibition as an anticancer therapy

Work by Nieman et al. [225] demonstrated that primary human ovarian cancer cells and SKOV3ip1 human ovarian cancer cells utilize neighboring fatty acids from the omentum to stimulate fatty acid oxidation and drive metastasis, potentially through the up-regulation of fatty acid binding protein 4 (FABP4). In line with the theory of cancer metabolic inflexibility, the inhibition of mitochondrial fatty acid import by etomoxir resulted in complete ablation of SKOV3ip1 cell growth with or without the presence of omental adipocytes [225]. Furthermore, inhibition of mitochondrial fatty acid oxidation by avocatin B selectively killed human primary acute myeloid leukemia cells without harming normal cells, and functioning mitochondria are critical for avocatin B-induced cell death in Jurkat T cells as well as TEX leukemia cells [226]. Further research has demonstrated that mitochondrial inhibition can selectively kill cancers in a mitochondrial dependent fashion using the compound ONC201 in many cancer lines [227] as well phenethyl isothiocyanate in LNCaP and PC3 prostate cancer cells [228]. Interestingly, in both cell models of brain cancer and acute myeloid leukemia cells, a novel clinical grade small molecule, IACS-010759, directly inhibited complex I, resulting in a decrease in mitochondrial

ATP and nucleotide biosynthesis leading to cell death, and was further validated in a murine tumour model where IACS-010759 inhibited tumour growth *in vivo* [229]. These findings are consistent with previous research demonstrating that direct complex I inhibition in MCF7 breast cancer cells with rotenone (a putative complex I inhibitor resulting in elevated H₂O₂ emission) elicited potent apoptotic signaling responses resulting in decreasing MCF7 cell survival [230].

2.7 Chapter 2 references

1. Pittis, A.A. and T. Gabaldon, Late acquisition of mitochondria by a host with chimaeric prokaryotic ancestry. *Nature*, 2016. **531**(7592): p. 101-4.
2. Nicholls, D.G. and S.J. Ferguson, in *Bioenergetics (Fourth Edition)*, D.G. Nicholls and S.J. Ferguson, Editors. 2013, Academic Press: Boston. p. ix-x.
3. Nass, M.M., The circularity of mitochondrial DNA. *Proc Natl Acad Sci U S A*, 1966. **56**(4): p. 1215-22.
4. Mitchell, P., Coupling of Phosphorylation to Electron and Hydrogen Transfer by a Chemi-Osmotic type of Mechanism. *Nature*, 1961. **191**(4784): p. 144-148.
5. Cori, C.F., Embden and the glycolytic pathway. *Trends in Biochemical Sciences*, 1983. **8**(7): p. 257-259.
6. Lenzen, S., A fresh view of glycolysis and glucokinase regulation: history and current status. *J Biol Chem*, 2014. **289**(18): p. 12189-94.
7. Houten, S.M. and R.J. Wanders, A general introduction to the biochemistry of mitochondrial fatty acid beta-oxidation. *J Inherit Metab Dis*, 2010. **33**(5): p. 469-77.
8. Mailloux, R.J., Teaching the fundamentals of electron transfer reactions in mitochondria and the production and detection of reactive oxygen species. *Redox Biol*, 2015. **4**: p. 381-98.
9. Krebs, H.A., The history of the tricarboxylic acid cycle. *Perspect Biol Med*, 1970. **14**(1): p. 154-70.
10. Akram, M., Citric acid cycle and role of its intermediates in metabolism. *Cell Biochem Biophys*, 2014. **68**(3): p. 475-8.
11. Owen, O.E., S.C. Kalhan, and R.W. Hanson, The key role of anaplerosis and cataplerosis for citric acid cycle function. *J Biol Chem*, 2002. **277**(34): p. 30409-12.
12. Hatzivassiliou, G., et al., ATP citrate lyase inhibition can suppress tumor cell growth. *Cancer Cell*, 2005. **8**(4): p. 311-321.
13. Bhola, P.D. and A. Letai, Mitochondria-Judges and Executioners of Cell Death Sentences. *Mol Cell*, 2016. **61**(5): p. 695-704.
14. Jourdain, A. and J.C. Martinou, Mitochondrial outer-membrane permeabilization and remodelling in apoptosis. *Int J Biochem Cell Biol*, 2009. **41**(10): p. 1884-9.
15. Binder, C., et al., Expression of Bax in relation to Bcl-2 and other predictive parameters in breast cancer. *Ann Oncol*, 1996. **7**(2): p. 129-33.
16. Hattori, T., et al., Heterodimerization of Bcl-2 and Bcl-X(L) with Bax and Bad in colorectal cancer. *Acta Oncol*, 2000. **39**(4): p. 495-500.
17. Marx, D., et al., Differential expression of apoptosis associated genes bax and bcl-2 in ovarian cancer. *Anticancer Res*, 1997. **17**(3C): p. 2233-40.
18. Kohler, T., et al., High Bad and Bax mRNA expression correlate with negative outcome in acute myeloid leukemia (AML). *Leukemia*, 2002. **16**(1): p. 22-9.
19. Bonora, M. and P. Pinton, The mitochondrial permeability transition pore and cancer: molecular mechanisms involved in cell death. *Front Oncol*, 2014. **4**: p. 302.
20. ALONSO-ALVAREZ, C., et al., Increased susceptibility to oxidative damage as a cost of accelerated somatic growth in zebra finches. *Functional Ecology*, 2007. **21**(5): p. 873-879.

21. Kim, S.-Y., et al., *Quantitative genetic evidence for trade-off between growth and resistance to oxidative stress in a wild bird. Evolutionary Ecology*, 2011. **25**(2): p. 461-472.
22. Stier, A., et al., *Elevation impacts the balance between growth and oxidative stress in coal tits. Oecologia*, 2014. **175**(3): p. 791-800.
23. Velando, A., et al., *Redox-regulation and life-history trade-offs: scavenging mitochondrial ROS improves growth in a wild bird. Scientific Reports*, 2019. **9**(1): p. 2203.
24. Halliwell, B., *Reactive species and antioxidants. Redox biology is a fundamental theme of aerobic life. Plant Physiol*, 2006. **141**(2): p. 312-22.
25. Liochev, S.I. and I. Fridovich, *The effects of superoxide dismutase on H₂O₂ formation. Free Radic Biol Med*, 2007. **42**(10): p. 1465-9.
26. Bienert, G.P. and F. Chaumont, *Aquaporin-facilitated transmembrane diffusion of hydrogen peroxide. Biochim Biophys Acta*, 2014. **1840**(5): p. 1596-604.
27. Bienert, G.P., et al., *Specific aquaporins facilitate the diffusion of hydrogen peroxide across membranes. J Biol Chem*, 2007. **282**(2): p. 1183-92.
28. Bienert, G.P., J.K. Schjoerring, and T.P. Jahn, *Membrane transport of hydrogen peroxide. Biochim Biophys Acta*, 2006. **1758**(8): p. 994-1003.
29. Fourquet, S., et al., *Activation of NRF2 by nitrosative agents and H₂O₂ involves KEAP1 disulfide formation. J Biol Chem*, 2010. **285**(11): p. 8463-71.
30. Mansfield, K.D., et al., *Mitochondrial dysfunction resulting from loss of cytochrome c impairs cellular oxygen sensing and hypoxic HIF- α activation. Cell Metab*, 2005. **1**(6): p. 393-9.
31. Veal, E. and A. Day, *Hydrogen peroxide as a signaling molecule. Antioxid Redox Signal*, 2011. **15**(1): p. 147-51.
32. Quinlan, C.L., et al., *The 2-oxoacid dehydrogenase complexes in mitochondria can produce superoxide/hydrogen peroxide at much higher rates than complex I. J Biol Chem*, 2014. **289**(12): p. 8312-25.
33. Panday, A., et al., *NADPH oxidases: an overview from structure to innate immunity-associated pathologies. Cell Mol Immunol*, 2015. **12**(1): p. 5-23.
34. Datla, S.R. and K.K. Griendling, *Reactive oxygen species, NADPH oxidases, and hypertension. Hypertension*, 2010. **56**(3): p. 325-30.
35. Sedeek, M., et al., *NADPH oxidases, reactive oxygen species, and the kidney: friend and foe. J Am Soc Nephrol*, 2013. **24**(10): p. 1512-8.
36. Ferreira, L.F. and O. Laitano, *Regulation of NADPH oxidases in skeletal muscle. Free Radic Biol Med*, 2016. **98**: p. 18-28.
37. Jones, D.P., *Radical-free biology of oxidative stress. Am J Physiol Cell Physiol*, 2008. **295**(4): p. C849-68.
38. Reczek, C.R. and N.S. Chandel, *ROS-dependent signal transduction. Curr Opin Cell Biol*, 2015. **33**: p. 8-13.
39. Driessens, N., et al., *Hydrogen peroxide induces DNA single- and double-strand breaks in thyroid cells and is therefore a potential mutagen for this organ. Endocr Relat Cancer*, 2009. **16**(3): p. 845-56.
40. Jefferies, H., et al., *Glutathione. ANZ J Surg*, 2003. **73**(7): p. 517-22.
41. Mailloux, R.J., S.L. McBride, and M.E. Harper, *Unearthing the secrets of mitochondrial ROS and glutathione in bioenergetics. Trends Biochem Sci*, 2013. **38**(12): p. 592-602.

42. Lin, C.S. and M. Klingenberg, *Characteristics of the isolated purine nucleotide binding protein from brown fat mitochondria. Biochemistry*, 1982. **21**(12): p. 2950-6.
43. Nicholls, D.G. and E. Rial, *A history of the first uncoupling protein, UCP1. J Bioenerg Biomembr*, 1999. **31**(5): p. 399-406.
44. Jezek, P., et al., *Mitochondrial Uncoupling Proteins: Subtle Regulators of Cellular Redox Signaling. Antioxid Redox Signal*, 2018. **29**(7): p. 667-714.
45. LOEW, O., *A NEW ENZYME OF GENERAL OCCURRENCE IN ORGANISMIS. Science*, 1900. **11**(279): p. 701-702.
46. Djordjevic, V.B., *Free radicals in cell biology. Int Rev Cytol*, 2004. **237**: p. 57-89.
47. Sepasi Tehrani, H. and A.A. Moosavi-Movahedi, *Catalase and its mysteries. Prog Biophys Mol Biol*, 2018. **140**: p. 5-12.
48. Jones, D.P., et al., *Metabolism of hydrogen peroxide in isolated hepatocytes: relative contributions of catalase and glutathione peroxidase in decomposition of endogenously generated H₂O₂. Arch Biochem Biophys*, 1981. **210**(2): p. 505-16.
49. Groussard, C., et al., *Free radical scavenging and antioxidant effects of lactate ion: an in vitro study. J Appl Physiol (1985)*, 2000. **89**(1): p. 169-75.
50. Ramos-Ibeas, P., et al., *Pyruvate antioxidant roles in human fibroblasts and embryonic stem cells. Mol Cell Biochem*, 2017. **429**(1-2): p. 137-150.
51. Wang, X., et al., *Pyruvate protects mitochondria from oxidative stress in human neuroblastoma SK-N-SH cells. Brain Res*, 2007. **1132**(1): p. 1-9.
52. Sies, H., W. Stahl, and A.R. Sundquist, *Antioxidant functions of vitamins. Vitamins E and C, beta-carotene, and other carotenoids. Ann NY Acad Sci*, 1992. **669**: p. 7-20.
53. Netto, L.E., et al., *Reactive cysteine in proteins: protein folding, antioxidant defense, redox signaling and more. Comp Biochem Physiol C Toxicol Pharmacol*, 2007. **146**(1-2): p. 180-93.
54. Meister, A., *On the discovery of glutathione. Trends Biochem Sci*, 1988. **13**(5): p. 185-8.
55. Hopkins, F.G., *On an Autoxidisable Constituent of the Cell. Biochem J*, 1921. **15**(2): p. 286-305.
56. Lu, S.C., *Glutathione synthesis. Biochim Biophys Acta*, 2013. **1830**(5): p. 3143-53.
57. Huang, Z.Z., et al., *Mechanism and significance of increased glutathione level in human hepatocellular carcinoma and liver regeneration. FASEB J*, 2001. **15**(1): p. 19-21.
58. Vivancos, P.D., et al., *Recruitment of glutathione into the nucleus during cell proliferation adjusts whole-cell redox homeostasis in Arabidopsis thaliana and lowers the oxidative defence shield. Plant J*, 2010. **64**(5): p. 825-38.
59. Vivancos, P.D., T. Wolff, and C.H. Foyer, *A nuclear glutathione cycle within the cell cycle. Biochemical Journal*, 2010. **431**(2): p. 169-178.
60. Dalle-Donne, I., et al., *S-glutathionylation in protein redox regulation. Free Radic Biol Med*, 2007. **43**(6): p. 883-98.
61. Sipes, I.G., D.A. Wiersma, and D.J. Armstrong, *The role of glutathione in the toxicity of xenobiotic compounds: metabolic activation of 1,2-dibromoethane by glutathione. Adv Exp Med Biol*, 1986. **197**: p. 457-67.
62. Cho, E.S., N. Sahyoun, and L.D. Stegink, *Tissue glutathione as a cyst(e)ine reservoir during fasting and refeeding of rats. J Nutr*, 1981. **111**(5): p. 914-22.
63. Forman, H.J., H. Zhang, and A. Rinna, *Glutathione: overview of its protective roles, measurement, and biosynthesis. Mol Aspects Med*, 2009. **30**(1-2): p. 1-12.

64. Olafsdottir, K. and D.J. Reed, Retention of oxidized glutathione by isolated rat liver mitochondria during hydroperoxide treatment. *Biochim Biophys Acta*, 1988. **964**(3): p. 377-82.
65. Ribas, V., C. Garcia-Ruiz, and J.C. Fernandez-Checa, Glutathione and mitochondria. *Front Pharmacol*, 2014. **5**: p. 151.
66. Taylor, E.R., et al., Reversible glutathionylation of complex I increases mitochondrial superoxide formation. *J Biol Chem*, 2003. **278**(22): p. 19603-10.
67. Franco, R. and J.A. Cidlowski, Apoptosis and glutathione: beyond an antioxidant. *Cell Death Differ*, 2009. **16**(10): p. 1303-14.
68. Ghibelli, L., et al., Rescue of cells from apoptosis by inhibition of active GSH extrusion. *FASEB J*, 1998. **12**(6): p. 479-86.
69. van den Dobbelsteen, D.J., et al., Rapid and specific efflux of reduced glutathione during apoptosis induced by anti-Fas/APO-1 antibody. *J Biol Chem*, 1996. **271**(26): p. 15420-7.
70. Stipanuk, M.H., et al., Cysteine concentration regulates cysteine metabolism to glutathione, sulfate and taurine in rat hepatocytes. *J Nutr*, 1992. **122**(3): p. 420-7.
71. Richman, P.G. and A. Meister, Regulation of gamma-glutamyl-cysteine synthetase by nonallosteric feedback inhibition by glutathione. *J Biol Chem*, 1975. **250**(4): p. 1422-6.
72. Grant, C.M., F.H. MacIver, and I.W. Dawes, Glutathione synthetase is dispensable for growth under both normal and oxidative stress conditions in the yeast *Saccharomyces cerevisiae* due to an accumulation of the dipeptide gamma-glutamylcysteine. *Mol Biol Cell*, 1997. **8**(9): p. 1699-707.
73. Maddocks, O.D., et al., Serine starvation induces stress and p53-dependent metabolic remodelling in cancer cells. *Nature*, 2013. **493**(7433): p. 542-6.
74. Wild, A.C., H.R. Moinova, and R.T. Mulcahy, Regulation of gamma-glutamylcysteine synthetase subunit gene expression by the transcription factor Nrf2. *J Biol Chem*, 1999. **274**(47): p. 33627-36.
75. Moinova, H.R. and R.T. Mulcahy, Up-regulation of the human gamma-glutamylcysteine synthetase regulatory subunit gene involves binding of Nrf-2 to an electrophile responsive element. *Biochem Biophys Res Commun*, 1999. **261**(3): p. 661-8.
76. Lu, J. and A. Holmgren, The thioredoxin antioxidant system. *Free Radic Biol Med*, 2014. **66**: p. 75-87.
77. Laurent, T.C., E.C. Moore, and P. Reichard, Enzymatic Synthesis of Deoxyribonucleotides. Iv. Isolation and Characterization of Thioredoxin, the Hydrogen Donor from *Escherichia Coli* B. *J Biol Chem*, 1964. **239**: p. 3436-44.
78. Du, Y., et al., Glutathione and glutaredoxin act as a backup of human thioredoxin reductase 1 to reduce thioredoxin 1 preventing cell death by aurothioglucose. *J Biol Chem*, 2012. **287**(45): p. 38210-9.
79. Yu, Y., et al., Overexpression of thioredoxin-binding protein 2 increases oxidation sensitivity and apoptosis in human lens epithelial cells. *Free Radic Biol Med*, 2013. **57**: p. 92-104.
80. Saxena, G., J. Chen, and A. Shalev, Intracellular shuttling and mitochondrial function of thioredoxin-interacting protein. *J Biol Chem*, 2010. **285**(6): p. 3997-4005.
81. Zhou, J. and W.J. Chng, Roles of thioredoxin binding protein (TXNIP) in oxidative stress, apoptosis and cancer. *Mitochondrion*, 2013. **13**(3): p. 163-9.
82. Lane, T., et al., TXNIP shuttling: missing link between oxidative stress and inflammasome activation. *Front Physiol*, 2013. **4**: p. 50.

83. Sakurai, A., et al., *Transcriptional regulation of thioredoxin reductase 1 expression by cadmium in vascular endothelial cells: role of NF-E2-related factor-2*. *J Cell Physiol*, 2005. **203**(3): p. 529-37.
84. Fernandez-Marcos, P.J. and S. Nobrega-Pereira, *NADPH: new oxygen for the ROS theory of aging*. *Oncotarget*, 2016. **7**(32): p. 50814-50815.
85. Legan, S.K., et al., *Overexpression of glucose-6-phosphate dehydrogenase extends the life span of Drosophila melanogaster*. *J Biol Chem*, 2008. **283**(47): p. 32492-9.
86. Luo, W. and G.L. Semenza, *Emerging roles of PKM2 in cell metabolism and cancer progression*. *Trends Endocrinol Metab*, 2012. **23**(11): p. 560-6.
87. Kumar, B. and R.N. Bamezai, *Moderate DNA damage promotes metabolic flux into PPP via PKM2 Y-105 phosphorylation: a feature that favours cancer cells*. *Mol Biol Rep*, 2015. **42**(8): p. 1317-21.
88. Warburg, O., *The metabolism of carcinoma cells*. *The Journal of Cancer Research*, 1925. **9**(1): p. 148-163.
89. Warburg, O., *On the origin of cancer cells*. *Science*, 1956. **123**(3191): p. 309-14.
90. Pavlova, N.N. and C.B. Thompson, *The Emerging Hallmarks of Cancer Metabolism*. *Cell Metab*, 2016. **23**(1): p. 27-47.
91. Zhang, C., et al., *Tumour-associated mutant p53 drives the Warburg effect*. *Nat Commun*, 2013. **4**: p. 2935.
92. Weinberg, F., et al., *Mitochondrial metabolism and ROS generation are essential for Kras-mediated tumorigenicity*. *Proc Natl Acad Sci U S A*, 2010. **107**(19): p. 8788-93.
93. Courtney, R., et al., *Cancer metabolism and the Warburg effect: the role of HIF-1 and PI3K*. *Mol Biol Rep*, 2015. **42**(4): p. 841-51.
94. Engelman, J.A., *Targeting PI3K signalling in cancer: opportunities, challenges and limitations*. *Nat Rev Cancer*, 2009. **9**(8): p. 550-62.
95. Stiles, B.L., *Phosphatase and tensin homologue deleted on chromosome 10: extending its PTENacles*. *Int J Biochem Cell Biol*, 2009. **41**(4): p. 757-61.
96. Kwon, J., et al., *Reversible oxidation and inactivation of the tumor suppressor PTEN in cells stimulated with peptide growth factors*. *Proc Natl Acad Sci U S A*, 2004. **101**(47): p. 16419-24.
97. Lee, S.R., et al., *Reversible inactivation of the tumor suppressor PTEN by H₂O₂*. *J Biol Chem*, 2002. **277**(23): p. 20336-42.
98. Zhu, Y., et al., *PTEN: a crucial mediator of mitochondria-dependent apoptosis*. *Apoptosis*, 2006. **11**(2): p. 197-207.
99. Elstrom, R.L., et al., *Akt stimulates aerobic glycolysis in cancer cells*. *Cancer Res*, 2004. **64**(11): p. 3892-9.
100. Lien, E.C., et al., *Glutathione biosynthesis is a metabolic vulnerability in PI(3)K/Akt-driven breast cancer*. *Nat Cell Biol*, 2016. **18**(5): p. 572-8.
101. Brandon, M., P. Baldi, and D.C. Wallace, *Mitochondrial mutations in cancer*. *Oncogene*, 2006. **25**(34): p. 4647-62.
102. Ricketts, C.J., et al., *Succinate dehydrogenase kidney cancer: an aggressive example of the Warburg effect in cancer*. *J Urol*, 2012. **188**(6): p. 2063-71.
103. Reitman, Z.J. and H. Yan, *Isocitrate dehydrogenase 1 and 2 mutations in cancer: alterations at a crossroads of cellular metabolism*. *J Natl Cancer Inst*, 2010. **102**(13): p. 932-41.

104. Tan, A.S., et al., Mitochondrial genome acquisition restores respiratory function and tumorigenic potential of cancer cells without mitochondrial DNA. *Cell Metab*, 2015. **21**(1): p. 81-94.
105. Guo, J., et al., Frequent truncating mutation of TFAM induces mitochondrial DNA depletion and apoptotic resistance in microsatellite-unstable colorectal cancer. *Cancer Res*, 2011. **71**(8): p. 2978-87.
106. Sun, X., et al., Increased mtDNA copy number promotes cancer progression by enhancing mitochondrial oxidative phosphorylation in microsatellite-stable colorectal cancer. *Signal Transduct Target Ther*, 2018. **3**: p. 8.
107. Shidara, Y., et al., Positive contribution of pathogenic mutations in the mitochondrial genome to the promotion of cancer by prevention from apoptosis. *Cancer Res*, 2005. **65**(5): p. 1655-63.
108. Bianchi, G., et al., Fasting induces anti-Warburg effect that increases respiration but reduces ATP-synthesis to promote apoptosis in colon cancer models. *Oncotarget*, 2015. **6**(14): p. 11806-19.
109. Tomiyama, A., et al., Critical role for mitochondrial oxidative phosphorylation in the activation of tumor suppressors Bax and Bak. *J Natl Cancer Inst*, 2006. **98**(20): p. 1462-73.
110. Taylor, R.C., S.P. Cullen, and S.J. Martin, Apoptosis: controlled demolition at the cellular level. *Nat Rev Mol Cell Biol*, 2008. **9**(3): p. 231-41.
111. Lopez, J. and S.W. Tait, Mitochondrial apoptosis: killing cancer using the enemy within. *Br J Cancer*, 2015. **112**(6): p. 957-62.
112. Fang, J., et al., Dihydro-orotate dehydrogenase is physically associated with the respiratory complex and its loss leads to mitochondrial dysfunction. *Biosci Rep*, 2013. **33**(2): p. e00021.
113. Khutornenko, A.A., et al., Pyrimidine biosynthesis links mitochondrial respiration to the p53 pathway. *Proc Natl Acad Sci U S A*, 2010. **107**(29): p. 12828-33.
114. Galanis, A., et al., Reactive oxygen species and HIF-1 signalling in cancer. *Cancer Lett*, 2008. **266**(1): p. 12-20.
115. Lu, H., R.A. Forbes, and A. Verma, Hypoxia-inducible factor 1 activation by aerobic glycolysis implicates the Warburg effect in carcinogenesis. *J Biol Chem*, 2002. **277**(26): p. 23111-5.
116. Kirito, K., Y. Hu, and N. Komatsu, HIF-1 prevents the overproduction of mitochondrial ROS after cytokine stimulation through induction of PDK-1. *Cell Cycle*, 2009. **8**(17): p. 2844-9.
117. Marin-Hernandez, A., et al., HIF-1alpha modulates energy metabolism in cancer cells by inducing over-expression of specific glycolytic isoforms. *Mini Rev Med Chem*, 2009. **9**(9): p. 1084-101.
118. Del Rey, M.J., et al., Hif-1alpha Knockdown Reduces Glycolytic Metabolism and Induces Cell Death of Human Synovial Fibroblasts Under Normoxic Conditions. *Sci Rep*, 2017. **7**(1): p. 3644.
119. Hu, Y., et al., Inhibition of hypoxia-inducible factor-1 function enhances the sensitivity of multiple myeloma cells to melphalan. *Mol Cancer Ther*, 2009. **8**(8): p. 2329-38.
120. Shi, T., et al., B7-H3 promotes aerobic glycolysis and chemoresistance in colorectal cancer cells by regulating HK2. *Cell Death Dis*, 2019. **10**(4): p. 308.

121. Gatenby, R.A. and R.J. Gillies, *Why do cancers have high aerobic glycolysis?* *Nat Rev Cancer*, 2004. **4**(11): p. 891-9.
122. Cui, X.G., et al., *HIF1/2alpha mediates hypoxia-induced LDHA expression in human pancreatic cancer cells.* *Oncotarget*, 2017. **8**(15): p. 24840-24852.
123. Brizel, D.M., et al., *Elevated tumor lactate concentrations predict for an increased risk of metastases in head-and-neck cancer.* *Int J Radiat Oncol Biol Phys*, 2001. **51**(2): p. 349-53.
124. Walenta, S., et al., *High lactate levels predict likelihood of metastases, tumor recurrence, and restricted patient survival in human cervical cancers.* *Cancer Res*, 2000. **60**(4): p. 916-21.
125. San-Millan, I. and G.A. Brooks, *Reexamining cancer metabolism: lactate production for carcinogenesis could be the purpose and explanation of the Warburg Effect.* *Carcinogenesis*, 2017. **38**(2): p. 119-133.
126. Zhai, X., et al., *Inhibition of LDH-A by oxamate induces G2/M arrest, apoptosis and increases radiosensitivity in nasopharyngeal carcinoma cells.* *Oncol Rep*, 2013. **30**(6): p. 2983-91.
127. Langhammer, S., et al., *LDH-A influences hypoxia-inducible factor 1alpha (HIF1 alpha) and is critical for growth of HT29 colon carcinoma cells in vivo.* *Target Oncol*, 2011. **6**(3): p. 155-62.
128. Fischer, K., et al., *Inhibitory effect of tumor cell-derived lactic acid on human T cells.* *Blood*, 2007. **109**(9): p. 3812-9.
129. Patra, K.C. and N. Hay, *The pentose phosphate pathway and cancer.* *Trends Biochem Sci*, 2014. **39**(8): p. 347-54.
130. Jonas, S.K., et al., *Increased activity of 6-phosphogluconate dehydrogenase and glucose-6-phosphate dehydrogenase in purified cell suspensions and single cells from the uterine cervix in cervical intraepithelial neoplasia.* *Br J Cancer*, 1992. **66**(1): p. 185-91.
131. Wang, J., et al., *Overexpression of G6PD is associated with poor clinical outcome in gastric cancer.* *Tumour Biol*, 2012. **33**(1): p. 95-101.
132. Tian, W.N., et al., *Importance of glucose-6-phosphate dehydrogenase activity for cell growth.* *J Biol Chem*, 1998. **273**(17): p. 10609-17.
133. Raimundo, N., B.E. Baysal, and G.S. Shadel, *Revisiting the TCA cycle: signaling to tumor formation.* *Trends Mol Med*, 2011. **17**(11): p. 641-9.
134. Dang, L., et al., *Cancer-associated IDH1 mutations produce 2-hydroxyglutarate.* *Nature*, 2009. **462**(7274): p. 739-44.
135. Sim, H.W., et al., *Tissue 2-Hydroxyglutarate as a Biomarker for Isocitrate Dehydrogenase Mutations in Gliomas.* *Clin Cancer Res*, 2019. **25**(11): p. 3366-3373.
136. Reitman, Z.J., et al., *Profiling the effects of isocitrate dehydrogenase 1 and 2 mutations on the cellular metabolome.* *Proc Natl Acad Sci U S A*, 2011. **108**(8): p. 3270-5.
137. Koivunen, P., et al., *Inhibition of hypoxia-inducible factor (HIF) hydroxylases by citric acid cycle intermediates: possible links between cell metabolism and stabilization of HIF.* *J Biol Chem*, 2007. **282**(7): p. 4524-32.
138. Isaacs, J.S., et al., *HIF overexpression correlates with biallelic loss of fumarate hydratase in renal cancer: novel role of fumarate in regulation of HIF stability.* *Cancer Cell*, 2005. **8**(2): p. 143-53.
139. Raimundo, N., et al., *Differential metabolic consequences of fumarate hydratase and respiratory chain defects.* *Biochim Biophys Acta*, 2008. **1782**(5): p. 287-94.

140. Sabharwal, S.S. and P.T. Schumacker, Mitochondrial ROS in cancer: initiators, amplifiers or an Achilles' heel? *Nat Rev Cancer*, 2014. **14**(11): p. 709-21.
141. Mahalingaiah, P.K. and K.P. Singh, Chronic oxidative stress increases growth and tumorigenic potential of MCF-7 breast cancer cells. *PLoS One*, 2014. **9**(1): p. e87371.
142. Dasgupta, S., et al., Mitochondrial DNA mutations in respiratory complex-I in never-smoker lung cancer patients contribute to lung cancer progression and associated with EGFR gene mutation. *J Cell Physiol*, 2012. **227**(6): p. 2451-60.
143. Ogrunc, M., et al., Oncogene-induced reactive oxygen species fuel hyperproliferation and DNA damage response activation. *Cell Death Differ*, 2014. **21**(6): p. 998-1012.
144. Gamcsik, M.P., et al., Glutathione levels in human tumors. *Biomarkers*, 2012. **17**(8): p. 671-91.
145. Bansal, A. and M.C. Simon, Glutathione metabolism in cancer progression and treatment resistance. *J Cell Biol*, 2018. **217**(7): p. 2291-2298.
146. Barranco, S.C., et al., Relationship between colorectal cancer glutathione levels and patient survival: early results. *Dis Colon Rectum*, 2000. **43**(8): p. 1133-40.
147. Goto, M., et al., Adaptation of leukemia cells to hypoxic condition through switching the energy metabolism or avoiding the oxidative stress. *BMC Cancer*, 2014. **14**: p. 76.
148. Havard, M., F. Dautry, and T. Tchenio, A dormant state modulated by osmotic pressure controls clonogenicity of prostate cancer cells. *J Biol Chem*, 2011. **286**(51): p. 44177-86.
149. Obrador, E., et al., Intertissue flow of glutathione (GSH) as a tumor growth-promoting mechanism: interleukin 6 induces GSH release from hepatocytes in metastatic B16 melanoma-bearing mice. *J Biol Chem*, 2011. **286**(18): p. 15716-27.
150. Obrador, E., et al., gamma-Glutamyl transpeptidase overexpression increases metastatic growth of B16 melanoma cells in the mouse liver. *Hepatology*, 2002. **35**(1): p. 74-81.
151. Benlloch, M., et al., Acceleration of glutathione efflux and inhibition of gamma-glutamyltranspeptidase sensitize metastatic B16 melanoma cells to endothelium-induced cytotoxicity. *J Biol Chem*, 2005. **280**(8): p. 6950-9.
152. Pallardo, F.V., et al., Role of nuclear glutathione as a key regulator of cell proliferation. *Mol Aspects Med*, 2009. **30**(1-2): p. 77-85.
153. Fujimori, S., et al., The subunits of glutamate cysteine ligase enhance cisplatin resistance in human non-small cell lung cancer xenografts in vivo. *Int J Oncol*, 2004. **25**(2): p. 413-8.
154. Britten, R.A., J.A. Green, and H.M. Warenius, Cellular glutathione (GSH) and glutathione S-transferase (GST) activity in human ovarian tumor biopsies following exposure to alkylating agents. *Int J Radiat Oncol Biol Phys*, 1992. **24**(3): p. 527-31.
155. Yang, H., et al., The role of cellular reactive oxygen species in cancer chemotherapy. *J Exp Clin Cancer Res*, 2018. **37**(1): p. 266.
156. Diehn, M., et al., Association of reactive oxygen species levels and radioresistance in cancer stem cells. *Nature*, 2009. **458**(7239): p. 780-3.
157. Sappington, D.R., et al., Glutamine drives glutathione synthesis and contributes to radiation sensitivity of A549 and H460 lung cancer cell lines. *Biochim Biophys Acta*, 2016. **1860**(4): p. 836-43.
158. Lo, M., Y.Z. Wang, and P.W. Gout, The x(c)- cystine/glutamate antiporter: a potential target for therapy of cancer and other diseases. *J Cell Physiol*, 2008. **215**(3): p. 593-602.
159. Singh, S., Cytoprotective and regulatory functions of glutathione S-transferases in cancer cell proliferation and cell death. *Cancer Chemother Pharmacol*, 2015. **75**(1): p. 1-15.

160. Oguztuzun, S., et al., *GST isoenzymes in matched normal and neoplastic breast tissue. Neoplasma*, 2011. **58**(4): p. 304-10.
161. de Aguiar, E.S., et al., *GSTM1, GSTT1, and GSTP1 polymorphisms, breast cancer risk factors and mammographic density in women submitted to breast cancer screening. Rev Bras Epidemiol*, 2012. **15**(2): p. 246-55.
162. Howells, R.E., et al., *Association of glutathione S-transferase GSTM1 and GSTT1 null genotypes with clinical outcome in epithelial ovarian cancer. Clin Cancer Res*, 1998. **4**(10): p. 2439-45.
163. Nagle, C.M., et al., *The role of glutathione-S-transferase polymorphisms in ovarian cancer survival. Eur J Cancer*, 2007. **43**(2): p. 283-90.
164. Kolwijck, E., et al., *GSTP1-1 in ovarian cyst fluid and disease outcome of patients with ovarian cancer. Cancer Epidemiol Biomarkers Prev*, 2009. **18**(8): p. 2176-81.
165. Jia, J.J., et al., *The role of thioredoxin system in cancer: strategy for cancer therapy. Cancer Chemother Pharmacol*, 2019.
166. Lincoln, D.T., et al., *The thioredoxin-thioredoxin reductase system: over-expression in human cancer. Anticancer Res*, 2003. **23**(3B): p. 2425-33.
167. Saitoh, M., et al., *Mammalian thioredoxin is a direct inhibitor of apoptosis signal-regulating kinase (ASK) 1. EMBO J*, 1998. **17**(9): p. 2596-606.
168. Grogan, T.M., et al., *Thioredoxin, a putative oncogene product, is overexpressed in gastric carcinoma and associated with increased proliferation and increased cell survival. Hum Pathol*, 2000. **31**(4): p. 475-81.
169. Meuillet, E.J., et al., *Thioredoxin-1 binds to the C2 domain of PTEN inhibiting PTEN's lipid phosphatase activity and membrane binding: a mechanism for the functional loss of PTEN's tumor suppressor activity. Arch Biochem Biophys*, 2004. **429**(2): p. 123-33.
170. Sartelet, H., et al., *Activation of the phosphatidylinositol 3'-kinase/AKT pathway in neuroblastoma and its regulation by thioredoxin 1. Hum Pathol*, 2011. **42**(11): p. 1727-39.
171. Naranjo-Suarez, S., et al., *Regulation of HIF-1alpha activity by overexpression of thioredoxin is independent of thioredoxin reductase status. Mol Cells*, 2013. **36**(2): p. 151-7.
172. Bu, L., et al., *Inhibition of TrxR2 suppressed NSCLC cell proliferation, metabolism and induced cell apoptosis through decreasing antioxidant activity. Life Sci*, 2017. **178**: p. 35-41.
173. Lou, M., et al., *Physical interaction between human ribonucleotide reductase large subunit and thioredoxin increases colorectal cancer malignancy. J Biol Chem*, 2017. **292**(22): p. 9136-9149.
174. Kaimul, A.M., et al., *Thioredoxin and thioredoxin-binding protein-2 in cancer and metabolic syndrome. Free Radic Biol Med*, 2007. **43**(6): p. 861-8.
175. Yamada, M., et al., *Increased expression of thioredoxin/adult T-cell leukemia-derived factor in cisplatin-resistant human cancer cell lines. Clin Cancer Res*, 1996. **2**(2): p. 427-32.
176. Kim, S.J., et al., *High thioredoxin expression is associated with resistance to docetaxel in primary breast cancer. Clin Cancer Res*, 2005. **11**(23): p. 8425-30.
177. Penney, R.B. and D. Roy, *Thioredoxin-mediated redox regulation of resistance to endocrine therapy in breast cancer. Biochim Biophys Acta*, 2013. **1836**(1): p. 60-79.

178. Samaranayake, G.J., et al., *Thioredoxin-1 protects against androgen receptor-induced redox vulnerability in castration-resistant prostate cancer*. *Nat Commun*, 2017. **8**(1): p. 1204.
179. Li, C., et al., *Over-expression of Thioredoxin-1 mediates growth, survival, and chemoresistance and is a druggable target in diffuse large B-cell lymphoma*. *Oncotarget*, 2012. **3**(3): p. 314-26.
180. Tobe, R., et al., *Thioredoxin reductase 1 deficiency enhances selenite toxicity in cancer cells via a thioredoxin-independent mechanism*. *Biochem J*, 2012. **445**(3): p. 423-30.
181. Titova, E., et al., *Mitochondria-targeted antioxidant SkQ1 suppresses fibrosarcoma and rhabdomyosarcoma tumour cell growth*. *Cell Cycle*, 2018. **17**(14): p. 1797-1811.
182. Pace, A., et al., *Neuroprotective effect of vitamin E supplementation in patients treated with cisplatin chemotherapy*. *J Clin Oncol*, 2003. **21**(5): p. 927-31.
183. Sieja, K., *Protective role of selenium against the toxicity of multi-drug chemotherapy in patients with ovarian cancer*. *Pharmazie*, 2000. **55**(12): p. 958-9.
184. Conklin, K.A., *Coenzyme q10 for prevention of anthracycline-induced cardiotoxicity*. *Integr Cancer Ther*, 2005. **4**(2): p. 110-30.
185. Branda, R.F., et al., *Effect of vitamin B12, folate, and dietary supplements on breast carcinoma chemotherapy--induced mucositis and neutropenia*. *Cancer*, 2004. **101**(5): p. 1058-64.
186. Bairati, I., et al., *Randomized trial of antioxidant vitamins to prevent acute adverse effects of radiation therapy in head and neck cancer patients*. *J Clin Oncol*, 2005. **23**(24): p. 5805-13.
187. Ferreira, P.R., et al., *Protective effect of alpha-tocopherol in head and neck cancer radiation-induced mucositis: a double-blind randomized trial*. *Head Neck*, 2004. **26**(4): p. 313-21.
188. D'Andrea, G.M., *Use of antioxidants during chemotherapy and radiotherapy should be avoided*. *CA Cancer J Clin*, 2005. **55**(5): p. 319-21.
189. Seifried, H.E., et al., *The antioxidant conundrum in cancer*. *Cancer Res*, 2003. **63**(15): p. 4295-8.
190. Lawenda, B.D., et al., *Should supplemental antioxidant administration be avoided during chemotherapy and radiation therapy?* *J Natl Cancer Inst*, 2008. **100**(11): p. 773-83.
191. Drew, R. and J.O. Miners, *The effects of buthionine sulfoximine (BSO) on glutathione depletion and xenobiotic biotransformation*. *Biochem Pharmacol*, 1984. **33**(19): p. 2989-94.
192. Kirkpatrick, D.L. and G. Powis, *Clinically Evaluated Cancer Drugs Inhibiting Redox Signaling*. *Antioxid Redox Signal*, 2017. **26**(6): p. 262-273.
193. Miran, T., et al., *Modulation of glutathione promotes apoptosis in triple-negative breast cancer cells*. *FASEB J*, 2018. **32**(5): p. 2803-2813.
194. Bailey, H.H., et al., *Phase I clinical trial of intravenous L-buthionine sulfoximine and melphalan: an attempt at modulation of glutathione*. *J Clin Oncol*, 1994. **12**(1): p. 194-205.
195. Smith, A.C., et al., *Pharmacokinetics of buthionine sulfoximine (NSC 326231) and its effect on melphalan-induced toxicity in mice*. *Cancer Res*, 1989. **49**(19): p. 5385-91.
196. Maddocks, O.D.K., et al., *Modulating the therapeutic response of tumours to dietary serine and glycine starvation*. *Nature*, 2017. **544**(7650): p. 372-376.

197. Kachadourian, R. and B.J. Day, Flavonoid-induced glutathione depletion: potential implications for cancer treatment. *Free Radic Biol Med*, 2006. **41**(1): p. 65-76.
198. Dvorakova, K., et al., Induction of oxidative stress and apoptosis in myeloma cells by the aziridine-containing agent imexon. *Biochem Pharmacol*, 2000. **60**(6): p. 749-58.
199. Cohen, S.J., et al., A phase I study of imexon plus gemcitabine as first-line therapy for advanced pancreatic cancer. *Cancer Chemother Pharmacol*, 2010. **66**(2): p. 287-94.
200. Cohen, S.J., et al., A Phase 2 Randomized, Double-Blind, Multicenter Trial of Imexon Plus Gemcitabine Versus Gemcitabine Plus Placebo in Patients With Metastatic Chemotherapy-naive Pancreatic Adenocarcinoma. *Am J Clin Oncol*, 2018. **41**(3): p. 230-235.
201. Barr, P.M., et al., Phase 2 study of imexon, a prooxidant molecule, in relapsed and refractory B-cell non-Hodgkin lymphoma. *Blood*, 2014. **124**(8): p. 1259-65.
202. Finkelstein, A.E., et al., Auranofin. New oral gold compound for treatment of rheumatoid arthritis. *Ann Rheum Dis*, 1976. **35**(3): p. 251-7.
203. Gabbiani, C., et al., Thioredoxin reductase, an emerging target for anticancer metallodrugs. Enzyme inhibition by cytotoxic gold(III) compounds studied with combined mass spectrometry and biochemical assays. *MedChemComm*, 2011. **2**(1): p. 50-54.
204. Roder, C. and M.J. Thomson, Auranofin: repurposing an old drug for a golden new age. *Drugs R D*, 2015. **15**(1): p. 13-20.
205. You, B.R., H.R. Shin, and W.H. Park, PX-12 inhibits the growth of A549 lung cancer cells via G2/M phase arrest and ROS-dependent apoptosis. *Int J Oncol*, 2014. **44**(1): p. 301-8.
206. Ramanathan, R.K., et al., A Phase I pharmacokinetic and pharmacodynamic study of PX-12, a novel inhibitor of thioredoxin-1, in patients with advanced solid tumors. *Clin Cancer Res*, 2007. **13**(7): p. 2109-14.
207. Ramanathan, R.K., et al., A randomized phase II study of PX-12, an inhibitor of thioredoxin in patients with advanced cancer of the pancreas following progression after a gemcitabine-containing combination. *Cancer Chemother Pharmacol*, 2011. **67**(3): p. 503-9.
208. Zhang, X., et al., Disruption of the mitochondrial thioredoxin system as a cell death mechanism of cationic triphenylmethanes. *Free Radic Biol Med*, 2011. **50**(7): p. 811-20.
209. Mandal, P.K., et al., Loss of thioredoxin reductase 1 renders tumors highly susceptible to pharmacologic glutathione deprivation. *Cancer Res*, 2010. **70**(22): p. 9505-14.
210. Harris, I.S., et al., Glutathione and thioredoxin antioxidant pathways synergize to drive cancer initiation and progression. *Cancer Cell*, 2015. **27**(2): p. 211-22.
211. Xu, Y., et al., miR-17* suppresses tumorigenicity of prostate cancer by inhibiting mitochondrial antioxidant enzymes. *PLoS One*, 2010. **5**(12): p. e14356.
212. Olson, K.A., J.C. Schell, and J. Rutter, Pyruvate and Metabolic Flexibility: Illuminating a Path Toward Selective Cancer Therapies. *Trends Biochem Sci*, 2016. **41**(3): p. 219-230.
213. Schulz, T.J., et al., Induction of oxidative metabolism by mitochondrial frataxin inhibits cancer growth: Otto Warburg revisited. *J Biol Chem*, 2006. **281**(2): p. 977-81.
214. Berridge, M.V. and A.S. Tan, Effects of mitochondrial gene deletion on tumorigenicity of metastatic melanoma: reassessing the Warburg effect. *Rejuvenation Res*, 2010. **13**(2-3): p. 139-41.
215. Gao, W., et al., Increased expression of mitochondrial transcription factor A and nuclear respiratory factor-1 predicts a poor clinical outcome of breast cancer. *Oncol Lett*, 2018. **15**(2): p. 1449-1458.

216. Araujo, L.F., et al., Mitochondrial transcription factor A (TFAM) shapes metabolic and invasion gene signatures in melanoma. *Sci Rep*, 2018. **8**(1): p. 14190.
217. Bonnet, S., et al., A mitochondria-K⁺ channel axis is suppressed in cancer and its normalization promotes apoptosis and inhibits cancer growth. *Cancer Cell*, 2007. **11**(1): p. 37-51.
218. Feurecker, B., et al., DCA promotes progression of neuroblastoma tumors in nude mice. *Am J Cancer Res*, 2015. **5**(2): p. 812-20.
219. Ferriero, R. and N. Brunetti-Pierri, Phenylbutyrate increases activity of pyruvate dehydrogenase complex. *Oncotarget*, 2013. **4**(6): p. 804-5.
220. Wenzel, U., A. Nickel, and H. Daniel, Increased carnitine-dependent fatty acid uptake into mitochondria of human colon cancer cells induces apoptosis. *J Nutr*, 2005. **135**(6): p. 1510-4.
221. Al-Bakheit, A., et al., Accumulation of Palmitoylcarnitine and Its Effect on Pro-Inflammatory Pathways and Calcium Influx in Prostate Cancer. *Prostate*, 2016. **76**(14): p. 1326-37.
222. Roscilli, G., et al., Carnitines slow down tumor development of colon cancer in the DMH-chemical carcinogenesis mouse model. *J Cell Biochem*, 2013. **114**(7): p. 1665-73.
223. Dionne, S., et al., Studies on the chemopreventive effect of carnitine on tumorigenesis in vivo, using two experimental murine models of colon cancer. *Nutr Cancer*, 2012. **64**(8): p. 1279-87.
224. Chaneton, B., et al., Serine is a natural ligand and allosteric activator of pyruvate kinase M2. *Nature*, 2012. **491**(7424): p. 458-462.
225. Nieman, K.M., et al., Adipocytes promote ovarian cancer metastasis and provide energy for rapid tumor growth. *Nat Med*, 2011. **17**(11): p. 1498-503.
226. Lee, E.A., et al., Targeting Mitochondria with Avocatin B Induces Selective Leukemia Cell Death. *Cancer Res*, 2015. **75**(12): p. 2478-88.
227. Greer, Y.E., et al., ONC201 kills breast cancer cells in vitro by targeting mitochondria. *Oncotarget*, 2018. **9**(26): p. 18454-18479.
228. Xiao, D., et al., Phenethyl isothiocyanate inhibits oxidative phosphorylation to trigger reactive oxygen species-mediated death of human prostate cancer cells. *J Biol Chem*, 2010. **285**(34): p. 26558-69.
229. Molina, J.R., et al., An inhibitor of oxidative phosphorylation exploits cancer vulnerability. *Nat Med*, 2018. **24**(7): p. 1036-1046.
230. Deng, Y.T., H.C. Huang, and J.K. Lin, Rotenone induces apoptosis in MCF-7 human breast cancer cell-mediated ROS through JNK and p38 signaling. *Mol Carcinog*, 2010. **49**(2): p. 141-51.

Chapter 3 Objectives and hypothesis

Cancers display irreversible or costly alterations in bioenergetics geared towards sustained accelerated growth. While previous research has extensively examined the response of many cancers to forced mitochondrial activation as a possible route for anticancer therapy, it currently remains unknown why some cancers are able to tolerate mitochondrial activation, whereas others are not. Increased mitochondrial ROS is a well-established byproduct of increasing mitochondrial OXPHOS, therefore, perhaps the ability of the cell to tolerate alterations in mitochondrial-derived ROS can in part dictate cell survival during forced mitochondrial activation.

3.1 Overview of thesis

The overall purpose of this thesis is to determine the response of glutathione following metabolic alterations, and whether experimental manipulation of glutathione can alter cell survival. The specific objectives and hypothesis for each study are outlined below.

3.2 Objectives and hypothesis for study 1 (Chapter 4)

Palmitoylcarnitine has previously been demonstrated to selectively decrease cell survival in HT29 colorectal carcinoma cells and prostate cancer cells, but not in analogous normal cells. It has been demonstrated that palmitoylcarnitine (with the addition of L-carnitine) enters the mitochondria where it stimulates ROS production leading to caspase activity and HT29 specific cell death, but not in NCOL-1 normal epithelial cells. The purpose of Chapter 4 was to evaluate the degree to which palmitoylcarnitine abrogates cell survival in HT29 colorectal cancer cells vs. non-transformed cells as previously demonstrated, and to determine whether cell-specific susceptibilities to palmitoylcarnitine are due to intrinsic differences in the glutathione response.

Hypothesis

- 1) Following palmitoylcarnitine incubations, HT29 cells will display decreased glutathione levels corresponding to decreasing cell survival, whereas CCD 841 cells will maintain glutathione levels resulting in no change in cell survival.
- 2) Concurrent glutathione depletion will sensitize CCD 841 cells to palmitoylcarnitine-induced decreasing cell survival and further sensitize HT29 cells.
- 3) Palmitoylcarnitine will have no effect on glutathione levels and cell survival in MCF7 cells, which have been previously demonstrated to be reliant on mitochondrial activity for survival.

3.3 Objectives and hypothesis for study 2 (Chapter 5)

Obesity and high-fat diets are associated with increased risk of developing hepatocellular carcinoma (HCC), and high-fat diets during HCC result in a more aggressive cancer phenotype. While systemic inflammatory effects of high-fat diets and obesity are often cited as key regulators promoting HCC growth, several studies have identified direct effects of fatty acids on promoting HepG2 (a HCC cell line) cell growth. Interestingly, HepG2 cells require glutathione to grow and depletion of glutathione stagnates HepG2 cell growth, while increasing glutathione in HepG2 cells is able to promote cell growth. Based on the findings of Chapter 4, the mitochondrial substrate palmitoylcarnitine resulted in drastic decreases in cell survival in HT29 and HCT 116 colon cancer cells, whereas MCF7 breast cancer and CCD 841 colon epithelial cells were insensitive to palmitoylcarnitine. The purpose of this study is to examine the early effects of a mitochondrial fatty acid challenge on HepG2 cells, and to better understand the underlying mechanisms associated with HepG2 cell resistance to palmitoylcarnitine, and whether glutathione is implicated in mediating this insensitivity.

Hypothesis

- 1) Palmitoylcarnitine will promote a unique HepG2 cell growth response while causing varying degrees of decreasing cell growth in other cancer cell lines.
- 2) Palmitoylcarnitine will cause an adaptive increase in mitochondrial reliance in HepG2 cells.
- 3) Glutathione levels will increase in HepG2 cells following palmitoylcarnitine, and glutathione depletion will prevent palmitoylcarnitine-induced HepG2 cell growth.

3.4 Objectives and hypothesis for study 3 (Chapter 6)

The response of glutathione to a metabolic challenge seemingly dictates cell fate. Building upon the results of Chapters 4 and 5, whereby palmitoylcarnitine resulted in a corresponding decrease in both cell survival and glutathione in HT29 cells, yet a corresponding increase in cell growth and glutathione in HepG2 cells. Glutathione depletion in HT29 cells resulted in further palmitoylcarnitine-induced decreasing cell survival and abrogated palmitoylcarnitine-induced cell growth in HepG2 cells. Recent evidence has suggested that the abolishment of both glutathione and thioredoxin is required to elicit anticancer effects in established tumours. In this regard, the repurposing of auranofin towards anticancer therapy has gained popularity. Auranofin functions through inhibition of thioredoxin reductase, ultimately inhibiting the thioredoxin system. Auranofin is an established drug historically used to target rheumatoid arthritis. While thioredoxin inhibition is effectively achieved through auranofin administration, there is currently a lack of a concrete method for glutathione inhibition/depletion. While buthionine sulfoximine (BSO) is a potent glutathione-depleting agent *in vitro*, it appears that it has limited functionality *in vivo*. To that end, serine and glycine starvation appears to be a novel approach for glutathione depletion, with heightened sensitivity in p53-null cells.

Interestingly, p53-null cells are more likely to be chemo resistant, as p53 is a common cell cycle inhibitor and apoptosis inducer. Therefore, the purpose of this study was twofold: 1) Are p53-null cells resistant to auranofin-induced anticancer effects? and 2) Can concurrent serine and glycine starvation along with auranofin sensitize p53-null cells to auranofin?

Hypothesis

- 1) It stands to reason that inhibiting thioredoxin within a cell sensitizes that cell to ROS. As p53 responds to excessive ROS to trigger cell cycle arrest or apoptosis, the loss of p53 may allow a cell to withstand higher levels of ROS, allowing instead of compensatory increases in antioxidant pathways mediated by the ROS-sensitive Nrf2. Therefore, HCT 116 p53^{-/-} will be more insensitive to auranofin relative to HCT 116 p53^{+/+} cells.
- 2) While auranofin will result in ROS mediated-decreasing cell survival in HCT 116 p53^{+/+} cells, auranofin will cause a compensatory increase in glutathione allowing for continuation of cell survival in HCT 116 p53^{-/-} cells, and depletion of glutathione through serine and glycine starvation will sensitize HCT 116 p53^{-/-} cells to auranofin.

3.5 Additional contributions

The following work encompasses significant contributions that I made during my PhD that are not included in my dissertation.

Co-Author: Published

1. Polidovitch N, Yang S, Sun H, Lakin R, Ahmad F, Gao X, **Turnbull PC**, Chiarello C, Perry CGR, Manganiello V, Yang P, and Backx PH. Phosphodiesterase type 3A (PDE3A), but not type 3B (PDE3B), contributes to the adverse cardiac remodeling induced by pressure overload. *Journal of molecular and cellular cardiology* 2019.
2. Hughes MC, Ramos SV, **Turnbull PC**, Rebalka IA, Cao A, Monaco CMF, Varah NE, Edgett BA, Huber JS, Tadi P, Delfinis LJ, Schlattner U, Simpson JA, Hawke TJ, and

Perry CGR. Early myopathy in Duchenne muscular dystrophy is associated with elevated mitochondrial H₂O₂ emission during impaired oxidative phosphorylation. *Journal of cachexia, sarcopenia and muscle* 2019.

3. Hughes MC, Ramos SV, **Turnbull PC**, Edgett BA, Huber JS, Polidovitch N, Schlattner U, Backx PH, Simpson J, and Perry CGR. Impairments in left ventricular mitochondrial bioenergetics precede overt cardiac dysfunction and remodelling in Duchenne muscular dystrophy. *The Journal of Physiology*.
4. Song E, Ramos SV, Huang X, Liu Y, Botta A, Sung HK, **Turnbull PC**, Wheeler MB, Berger T, Wilson DJ, Perry CGR, Mak TW, and Sweeney G. Holo-lipocalin-2-derived siderophores increase mitochondrial ROS and impair oxidative phosphorylation in rat cardiomyocytes. *Proceedings of the National Academy of Sciences of the United States of America* 2018.
5. Mandel ER, Dunford EC, Abdifarkosh G, **Turnbull PC**, Perry CGR, Riddell MC, and Haas TL. The superoxide dismutase mimetic tempol does not alleviate glucocorticoid-mediated rarefaction of rat skeletal muscle capillaries. *Physiological reports* 5: 2017.
6. Hughes MC, Ramos SV, **Turnbull PC**, Nejatbakhsh A, Baechler BL, Tahmasebi H, Laham R, Gurd BJ, Quadriatero J, Kane DA, and Perry CG. Mitochondrial Bioenergetics and Fiber Type Assessments in Microbiopsy vs. Bergstrom Percutaneous Sampling of Human Skeletal Muscle. *Frontiers in physiology* 6: 360, 2015.

Co-Author: In Submission

1. Islam H, Bonafiglia JT, **Turnbull PC**, Simpson CA, Perry CGR, Gurd BJ. The impact of acute and chronic exercise on Nrf2 expression in relation to markers of mitochondrial biogenesis in human skeletal muscle. *European journal of applied physiology* 2019. – In submission

Co-Author: In progress

1. Ramos SV, Hughes MC, Teich T, **Turnbull PC**, Perry CGR. Divergent muscle function and mitochondrial bioenergetic effects of microtubule targeted chemotherapy in oxidative and glycolytic skeletal muscles.
2. Bellissimo CA, Delfinis LJ, **Turnbull PC**, Hughes MC, Tadi P, Amaral C, Dehghani A, Perry CGR. The mitochondrial-enhancing drug Olesoxime improves quadriceps mitochondrial function and force recovery but not diaphragm function in a mouse model of Duchenne muscular dystrophy.
3. Hughes MC, Ramos SV, Teich T, Tadi P, **Turnbull PC**, Polidovitch N, Schlatter U, Backx PH, Simpson JA, Perry CGR. Mitochondrial creatine kinase deficits evident in Duchenne muscular dystrophy are ameliorated through treatment with cardioplin-

targeting peptide SBT-20.

4. **Turnbull PC**, Kane DA. H₁/H₂ Histamine Receptor Blockade Alters the Glutathione Redox Status in Skeletal Muscle Following a Bout of Prolonged Exercise.
5. Hughes MC, Ramos SV, Bellissimo CA, Dial AG, Tin E, **Turnbull PC**, Tadi P, Schlatter U, Hawke TJ, Perry CGR. The mitochondrial targeted peptide SBT-20 improves diaphragm and skeletal muscle pathophysiology in dystrophin-deficient mice.

Chapter 4 The fatty acid derivative palmitoylcarnitine abrogates colorectal cancer cell survival by depleting glutathione

This chapter is an original published article. It is presented in its published form.

Turnbull PC, Hughes MC, and Perry CGR. The fatty acid derivative palmitoylcarnitine abrogates colorectal cancer cell survival by depleting glutathione. *American journal of physiology Cell physiology* 2019.

Author Contributions: Patrick C. Turnbull (PCT) carried out the majority of experiments for this project, with the exception of the following. MCH performed caspase-3 measurements on treated cell lysates as prepared by PCT. PCT and CGRP wrote the manuscript.

The fatty acid derivative palmitoylcarnitine abrogates colorectal cancer cell survival by depleting glutathione

Patrick C. Turnbull^{1*}, Meghan C. Hughes¹, and Christopher G.R. Perry¹

From the ¹School of Kinesiology and Health Science, Muscle Health Research Center, York University, 4700 Keele Street, Toronto, ON, Canada, M3J 1P3.

Running title: *Colorectal cancer susceptibility to palmitoylcarnitine*

To whom correspondence should be addressed: Christopher G.R. Perry: School of Kinesiology & Health Science, York University, Toronto, Ontario, Canada. M3J 1P3; cperry@yorku.ca; Tel 1 (416) 736-2100 x33232

Keywords: Cancer, Warburg effect, mitochondria, reactive oxygen species (ROS), glutathione.

Abstract

Previous evidence suggests that palmitoylcarnitine incubations trigger mitochondrial-mediated apoptosis in HT29 colorectal adenocarcinoma cells, yet non-transformed cells appear insensitive. The mechanism by which palmitoylcarnitine induces cancer cell death is unclear. The purpose of this investigation was to examine the relationship between mitochondrial kinetics and glutathione buffering in determining the effect of palmitoylcarnitine on cell survival. HT29 and HCT 116 colorectal adenocarcinoma cells, CCD 841 non-transformed colon cells and MCF7 breast adenocarcinoma cells were exposed to 0 μ M, 50 μ M and 100 μ M palmitoylcarnitine for 24-48 hours. HCT 116 and HT29 cells showed decreased cell survival following palmitoylcarnitine compared to CCD 841 cells. Palmitoylcarnitine stimulated H₂O₂ emission in HT29 and CCD 841 cells but increased it to a greater level in HT29 cells due largely to a higher basal H₂O₂ emission. This greater H₂O₂ emission was associated with lower glutathione buffering capacity and caspase-3 activation in HT29 cells. The glutathione depleting agent, buthionine sulfoximine, sensitized CCD 841 cells and further sensitized HT29 cells to palmitoylcarnitine-induced decreases in cell survival. MCF7 cells did not produce H₂O₂ when exposed to palmitoylcarnitine and were able to maintain glutathione levels. Furthermore, HT29 cells demonstrated the lowest mitochondrial oxidative kinetics vs CCD 841 and MCF7 cells. The results demonstrate that colorectal cancer is sensitive to palmitoylcarnitine due in part to an inability to prevent oxidative stress through glutathione-redox coupling thereby rendering the cells sensitive to elevations in H₂O₂. These findings suggest that the relationship between inherent metabolic capacities and redox regulation is altered early in response to palmitoylcarnitine.

Introduction

It is believed that cancer cell proliferation can be influenced by the interaction between cellular metabolism and redox conditions (reviewed in (14, 35)). As mitochondria generate reactive oxygen species during oxidative phosphorylation, it follows that the balance between glycolysis and oxidative metabolism may influence the cellular redox environment by altering the demands placed on the glutathione redox couple. This highly regulated antioxidant system is essential for both cancer cell growth and protection from cell death in response to a variety of cellular stressors, including certain chemotherapeutic compounds (reviewed in (6, 31)). As such, the effectiveness of targeting cancer metabolism to attenuate cancer survival may depend on the efficiency of glutathione buffering mechanisms in response to changes in metabolically derived reactive oxygen species generation.

As many cancers are inherently glycolytic (25, 36, 37), numerous studies have attempted to promote the generation of mitochondrial reactive oxygen species by activating oxidative phosphorylation in various models. For example, redirecting pyruvate away from lactate and towards oxidative phosphorylation through the activation of pyruvate dehydrogenase increases reactive oxygen species production and reduces cell proliferation in lung and tongue cancer cell lines (4). Likewise, resveratrol promotes fat oxidation and triggers reactive oxygen species-induced death in SW620 colon cancer cells, (7) and orally administered acetylcarnitine reduces the formation of colorectal neoplastic lesions in a mouse model with no apparent deleterious side effects (32). Additionally, a diet high in butterfat causes an increase in aberrant crypt foci in another mouse model of colon cancer, which is partially prevented by the addition of free carnitine in the diet (10). While it is not fully clear how targeting mitochondrial oxidative phosphorylation decreased survival in these cancer models, several different groups have also

demonstrated that the fatty acid-derived mitochondrial substrate, palmitoylcarnitine, selectively decreased cell survival in colorectal (38) and prostate cancer cells (1). Specifically, Wenzel et al. (38) reported augmented superoxide production during palmitoylcarnitine oxidation that was lethal to colorectal HT29 cancer cells yet tolerated by preneoplastic NCOL-1 epithelial cells. This approach is intriguing in that palmitoylcarnitine oxidation may be less toxic to healthy cells given it is a natural metabolite oxidized by mitochondria. Collectively, these findings suggest approaches that stimulate mitochondrial bioenergetics may serve as a therapeutic avenue to selectively target cancer cells, but the mechanism for why non-transformed cells may be insensitive remains unclear. It seems possible that heterogeneous effects of palmitoylcarnitine on cell survival could be linked to inherent differences in glutathione redox buffering responses.

The purpose of this investigation was to evaluate the early time course by which palmitoylcarnitine abrogates cell survival in HT29 colorectal cancer cells vs non-transformed cells as reported by Wenzel et al. (38), and to determine whether cell-specific susceptibilities to palmitoylcarnitine are due to intrinsic differences in the glutathione response. We also determined whether differences in mitochondrial oxidative characteristics are related to the redox response to palmitoylcarnitine. Palmitoylcarnitine elicited HT29 specific decreases in cell survival, concurrent with a decrease in glutathione levels, despite no effect on non-transformed CCD 841 cell survival or glutathione. However, both HT29 and CCD 841 cells increased H_2O_2 in response to palmitoylcarnitine, despite HT29 cells having ~2-fold greater baseline steady-state H_2O_2 . By pharmacologically depleting glutathione concurrently with palmitoylcarnitine incubations, we rendered CCD 841 cells sensitive to palmitoylcarnitine and further sensitized HT29 cells to the deleterious effects of palmitoylcarnitine. This data supports the notion that

glutathione is a critical regulator in determining cell survival in HT29 and CCD 841 cells when exposed to palmitoylcarnitine.

Experimental procedures

Cell lines

CCD 841 Con primary colon epithelial cells were purchased from the American Type Culture Collection (ATCC, Manassas, VA, USA). HT29 and HCT 116 colorectal adenocarcinoma cells and MCF7 breast adenocarcinoma cells were a generous gift from Dr. Samuel Benchimol (York University, Toronto, Canada). CCD 841 cells were grown in EMEM (Wisent Inc, Saint-Jean-Baptiste, QC, Canada), HT29 and HCT 116 cells were grown in DMEM (Wisent Inc) and MCF7 cells were grown in AMEM (Wisent Inc). All media was supplemented with 10% fetal bovine serum (Wisent Inc) and 1% penicillin/streptomycin (Wisent Inc) and grown at 37°C in 5% CO₂.

Palmitoylcarnitine incubations

For palmitoylcarnitine treatments, cells were treated with 2mM L-carnitine (Sigma-Aldrich) and increasing palmitoyl-L-carnitine (palmitoylcarnitine, 0µM, 50µM and 100µM, Toronto Research Chemicals) for 24 hours or 48 hours in phenol-red free versions of their respective growth media (Wisent Inc).

Relative Cell Survival Assay

The crystal violet assay was used to determine relative cell survival (13). Following 24 hours or 48 hours of palmitoylcarnitine incubations, with or without and 50µM L-buthionine-

sulfoximine (BSO, Sigma-Aldrich), cells plated in 96-well optical bottom black walled plates (ThermoFisher Scientific) were incubated in 10% formalin (Sigma-Aldrich) for 10 minutes. Formalin was removed and a 0.5% Crystal Violet (Sigma-Aldrich) solution in 25% MeOH was added for 10 minutes. Following crystal violet staining, wells were rinsed clean with water and allowed to dry overnight. Visualization of crystal violet as a marker for relative cell survival was conducted using the LiCor odyssey scanner (Licor Biosciences, Lincoln, NE, USA) and fluorescent density analyses was conducted using LiCor software.

XTT as a measure of NAD(P)H

XTT is a negatively charged tetrazolium salt that changes colour and becomes soluble following reduction, particularly in response to NADH (12, 19). Therefore, XTT serves as an indirect measure of either NADH or NAD(P)H concentration which are collectively referred to as NAD(P)H. In this study, it is assumed that a change in XTT signal in response to palmitoylcarnitine reflects a change in NADH. To perform the assay, cells were treated with increasing amounts of palmitoylcarnitine for 24 hours or 48 hours in 96-well plates. In the final 4 hours of each treatment, 50µl of XTT solution comprising of 1mg/ml XTT (BioShop Canada Inc.) dissolved in media with 25µM phenazine methosulfate (Sigma-Aldrich,) was added directly into each well. Cells were incubated for 4 hours at 37°C at 5% CO₂ and then absorbance at 450nm was read using the VICTOR³ 1420 Multilabel Counter plate reader (PerkinElmer, Waltham, MA, USA). NAD(P)H absorbance was made relative to 0µM palmitoylcarnitine. In order to account for variations in cell number, cells were then digested in-well using 10% RIPA (Sigma-Aldrich,) while protein was assessed with BCA (ThermoFisher Scientific) according to kit instructions.

Live-cell H₂O₂ measurements

Cells were seeded in a 96-well optical bottom black-walled plate (ThermoFisher Scientific). For H₂O₂ determination, cells were treated with palmitoylcarnitine for 24 hours and 48 hours. Cells were then incubated with 10µM Amplex® UltraRed and 1 U/ml horseradish peroxidase for 20 minutes and then fluorescent intensity (EX568/EM581) was taken using the BioTek Cytation 3 fluorescent plate reader (BioTek, Winooski, VT, USA). A single read after these timepoints reflected the net accumulated fluorescent resorufin product of oxidized Amplex Ultrared and therefore represents the ‘net emission’ or ‘net pressure’ of H₂O₂ that cells experienced throughout this time period. This measurement was then made relative to a H₂O₂ standard curve. To account for variations in cell number, cells were then digested in-well using 10% RIPA (Sigma-Aldrich) while protein was assessed with BCA (ThermoFisher Scientific) according to kit instructions.

Glutathione analysis

Glutathione was measured as previously published (17, 18, 27). Both reduced (GSH) and oxidized (GSSG) glutathione were measured using an Agilent HPLC 1100 (Agilent Technologies, Mississauga, ON, Canada) and separation was achieved using a Zorbax C18 column (Agilent Technologies). Cells were trypsin lifted, washed with PBS then re-suspended in 50mM TRIS buffer with 20mM boric acid (Sigma-Aldrich), 2mM L-serine (Sigma-Aldrich), 20µM acivicin (Enzo Life Sciences) and 5mM N-ethylmaleimide (Sigma-Aldrich), pH at 8.0 with HCl. Glutathione concentrations were calculated using standard concentration curves for GSH and GSSG (Sigma-Aldrich) and normalized to total protein.

GSH: This method was adapted from Giustriani et al. (15). Cells were deproteinated in 100µl trichloroacetic acid with 100µl cells in TRIS buffer suspension. GSH samples were run under isocratic conditions using a 0.25% glacial acetic acid mobile phase with 6% acetonitrile with a flow rate of 1.25ml/min. GSH was detected using a using a modular variable wavelength detector (Agilent Technologies) at 265nm wavelength.

GSSG: This method was adapted from Kand'ar et al. (21). Cells were deproteinated in equal parts 15% perchloric acid to sample volume. 100µl of deproteinated sample was added to 500µl of 0.5M NaOH. 37.5µl of 0.1% o-phthalimide (Sigma-Aldrich) in methanol was added to the 600µl sample volume and incubated for 15 minutes rocking in the dark creating a GS-OPA conjugate. Following incubation, samples were transferred to an HPLC autosampler vial for column separation. GSSG mobile phase was 25mM Na₂HPO₄ in HPLC grade water with 15% methanol at a flow rate of 0.5ml/min. Following column separation, the eluent flowed through a Firefly Sci 8830 flow-through cuvette (Firefly Sci Inc, NY, USA) and GSSG peak was detected using a QuantaMaster 40 spectrofluorometer (Horiba, Edison, NJ, USA). GS-OPA was excited at 350nm and emission was detected at 420nm.

Caspase activity assay

Enzymatic activity of caspase-3 was determined using the substrate Ac-DEVD-AMC (Enzo Life Sciences), as previously described (8, 9). Following palmitoylcarnitine incubations, cells were isolated using lysis buffer containing (mM): 20 mM HEPES, 10 mM NaCl, 1.5 mM MgCl, 1 mM DTT, 20% glycerol, and 0.1% Triton-X100, pH 7.4, without addition of protease inhibitors and were sonicated for 3x3 seconds. Cells were incubated in 96-well plates with Ac-DEVD-AMC at 37°C. Fluorescence was measured with excitation and emission wavelengths of

360 nm and 440 nm respectively. Caspase-3 activity was normalized to total protein content and expressed as fluorescence intensity in arbitrary units (AU) per milligram protein.

Intracellular lactate determination

Following palmitoylcarnitine incubations, adherent cells were trypsin harvested, washed twice in PBS and re-suspended in 0.5M perchloric acid, vortexed and free-thawed in liquid nitrogen three times. Following centrifugation, 2.2M KHCO₃ was added and centrifuged at 4°C for 15 minutes at 7,000 rpm and the supernatant was collected. 20µl of supernatant was added to 258µl lactate buffer (1M glycine, 500mM hydrazine sulphate (Sigma-Aldrich), 5mM EDTA pH 9.5) and 20µl NAD (Sigma-Aldrich) and 2µl of heart lactate dehydrogenase (LDH, Sigma-Aldrich). Each sample was rocked briefly, and 300µl was inserted into a 96-well plate, in triplicate, and compared to a non-LDH added mirroring sample. Absorption of NADH was measured at 340nm on a BioTek Cytation 3 plate reader and made relative to total protein.

Cell permeabilization and high-resolution respirometry

Cells were seeded in 10 cm dishes for 48 hours, trypsin harvested, washed in PBS and re-suspended in mitochondrial respiration media (MIRO5, in mM): 0.5 EGTA, 10 KH₂PO₄, 3 MgCl₂·6 H₂O, 60 K-lactobionate, 20 Hepes, 20 Taurine, 110 sucrose and 1 mg/ml fatty acid free BSA (pH 7.1) supplemented with 20mM creatine. Cells were then permeabilized with 10µg/ml digitonin (Sigma-Aldrich) for 30 minutes rocking at room temperature. Following centrifugation for 5 minutes at 2,000 RPM, cells were re-suspended in 105µl MIRO5, with 5µl subsequently removed to determine protein content, while the remaining 100µl was used for high-resolution respirometry.

Cells were loaded into the Oroboros Oxygraph-2k (Oroboros Instruments, Corp., Innsbruck, Austria) system. Total volume was 2 ml, with spinning at 750 rpm and temperature at 37°C. To determine ADP-stimulated respiration, 5mM pyruvate and 2mM malate were added as complex I substrates (NADH), followed by ADP titrations of 25µM, 500µM and 5mM ADP. Polarographic oxygen measurements were acquired in 2 s intervals with the rate of respiration derived from 40 data points and expressed as pmol/s/mg protein.

Statistics

All results are expressed as means \pm SEM. Significance was determined as $p < 0.05$ for all measures. Each 'N' signifies an individual experiment, with each experiment conducted in triplicate where appropriate. For the comparison of only two groups, unpaired t-tests were used. For the comparison of more than two groups, ANOVA's were conducted. Following significance with a one-way ANOVA, a Dunnett's *post-hoc* analysis was performed, and following a significant two-way ANOVA a Fisher's LSD *post-hoc* was performed. All statistics were performed using GraphPad Prism 7 (San Diego, CA, USA).

Results

HT29 cells are sensitive to palmitoylcarnitine induced cell death

In order to determine the influence of palmitoylcarnitine on relative cell survival, HT29 and HCT 116 cells and non-transformed colon epithelial CCD 841 cells were incubated for 24 hours (Figure 4.1A) and 48 hours (Figure 4.1B) with 0µM, 50µM and 100µM palmitoylcarnitine, similar to concentrations used in previous literature (1, 38). While CCD 841 cells had a modest ~10% decrease in relative cell survival with 100µM, HT29 and HCT 116 cells had more robust

decreases in relative cell survival at 50 μ M (~20%) and 100 μ M (~90%) palmitoylcarnitine ($p < 0.05$), with HT29 and HCT 116 cells showing decreased relative cell survival compared to CCD 841 cells at each palmitoylcarnitine concentration ($p < 0.05$) (Figure 4.1A and 4.1B).

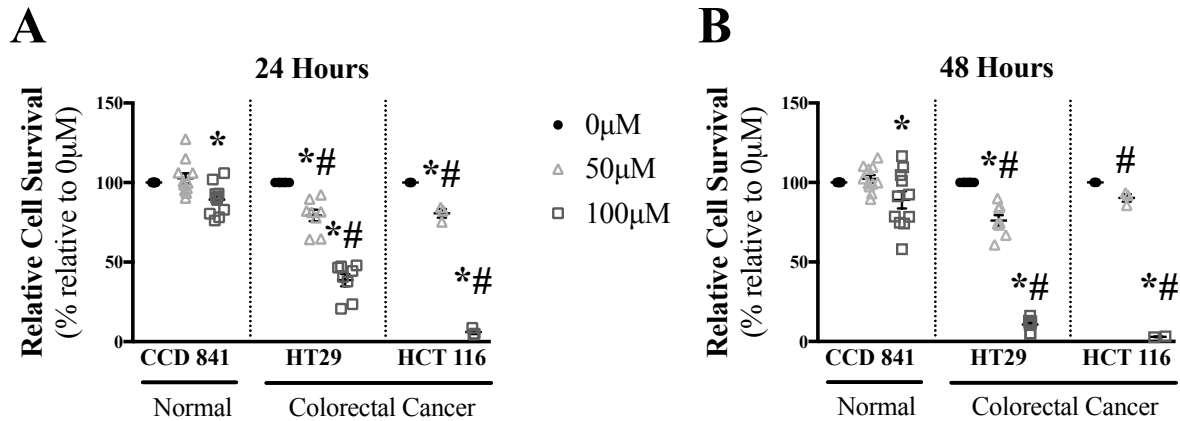


Figure 4.1 Palmitoylcarnitine toxicity is greater in colorectal cancer HT29 and HCT 116 cells than normal CCD 841 cells. Relative cell survival was measured in non-transformed CCD 841 cells (N=11) as well as HT29 (N=8) and HCT 116 cells (N=3) for **A** 24 hours and **B** 48 hours. Data are reported as means \pm SEM with ‘*’ representing a significant difference relative to 0 μ M palmitoylcarnitine within the same cell type, and ‘#’ representing a significant difference of the same palmitoylcarnitine concentration relative to CCD 841, $P < 0.05$.

We next determined whether colorectal cancer displayed altered mitochondrial oxidative capacities and metabolic flexibilities in order to explain their sensitivity to palmitoylcarnitine. HT29 cells had significantly lower coupled oxidative kinetics (ADP-stimulation of ATP synthesis) relative CCD 841 cells ($p < 0.05$) (Figure 4.2A and 4.2B). CCD 841 cells demonstrated increased net lactate levels in response to 24 hours of palmitoylcarnitine ($p < 0.05$), which is in line with the expected redirection of glucose-derived pyruvate away from the mitochondria when excess fatty acids are present (Figure 4.2C). At 48 hours, there was no difference in intracellular lactate levels. While difficult to explain, this may suggest that CCD 841 cells had exhausted the exogenously added palmitoylcarnitine supply. This metabolic flexibility was not observed in

HT29 cells given no change in net lactate concentrations were observed in response to palmitoylcarnitine (Figure 4.2D).

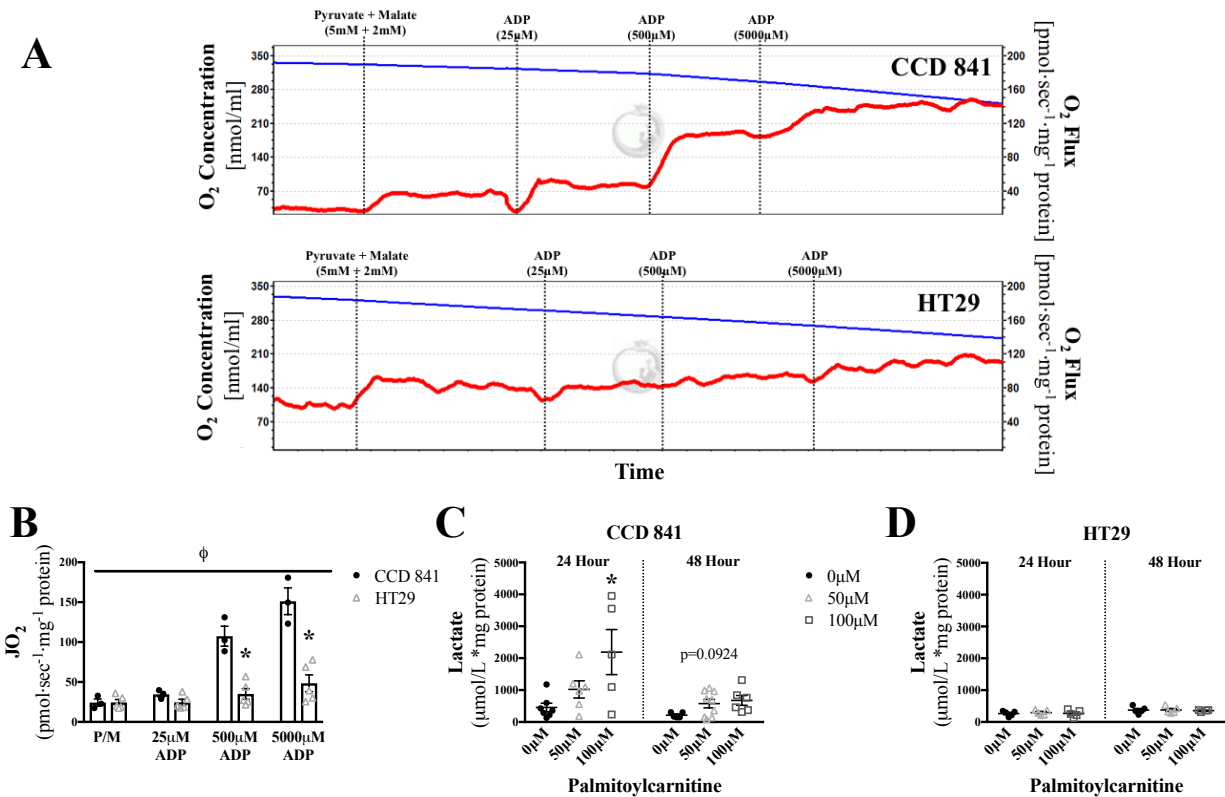


Figure 4.2 Lower mitochondrial respiratory kinetics and impaired metabolic flexibility in HT29 cells compared to CCD 841 cells. Mitochondrial respiratory kinetics and the cell lactate concentrations were assessed in response to palmitoylcarnitine in CCD 841 and HT29 cells. **A** a representative high resolution respirometric trace showing oxygen consumption (red line) that is calculated by the change in slope of oxygen concentration in the respiratory chamber (blue line; top, CCD 841 cells; bottom, HT29 cells). The blue line represents in-chamber oxygen concentration that is used to calculate the rate of oxygen consumption (red line). **B** Mitochondrial respiratory kinetics of CCD 841 cells compared to HT29 cells across a range of ADP concentrations reflecting low and high metabolic demands. ‘*’ represents a significant difference between HT29 and CCD 841 cells of a given substrate, $P < 0.05$. ‘Φ’ represents a main effect of cell type. $P < 0.05$. (N=5). Net intracellular lactate was determined in **C** CCD 841 cells (N=8-9) and **D** HT29 cells (N=5) for 24 and 48 hours. ‘*’ represents a significant difference relative to 0μM palmitoylcarnitine of the same time point, $P < 0.05$. Data are reported as means \pm SEM.

Excessive NADH generation relative to low rates of oxidative phosphorylation can lead to H₂O₂ production, which can trigger deleterious cellular effects such as caspase-3 activation

(Figure 4.3A) (29). Given the lower oxidative capacities shown in Figure 4.2, we next tested the hypothesis that NADH generation from palmitoylcarnitine remained intact in HT29 cells such that excess NADH provision to the electron transport chain would increase H₂O₂ emission (Figure 4.3A). Indeed, palmitoylcarnitine resulted in greater accumulations in NAD(P)H in HT29 cells at both 24 and 48 hours (*100μM*: +~35%), with only a modest increase in NAD(P)H observed at 48 hours in CCD 841 (*50μM*: +~20%) as detected by XTT (*p*<0.05) (Figure 4.3B and 4.3C). This was associated with greater H₂O₂ emission (*p*<0.05) (Figure 4.3D and 4.3E) and induction of caspase-3 activity (*p*<0.05) (Figure 4.3F and 4.3G) in HT29 cells at 24 hours, yet there was no observable change in caspase-3 activity at 48 hours, suggesting an early activation of caspase-3 resulting in cell death leading to the cessation of caspase-3 activity. This relationship of NAD(P)H to H₂O₂ emission was not observed in all conditions, such as 50μM at 24 hours (Figure 4.3B and 4.3D), but may be related to the difficulty in capturing the precise temporal relationship between NADH and H₂O₂ kinetics.

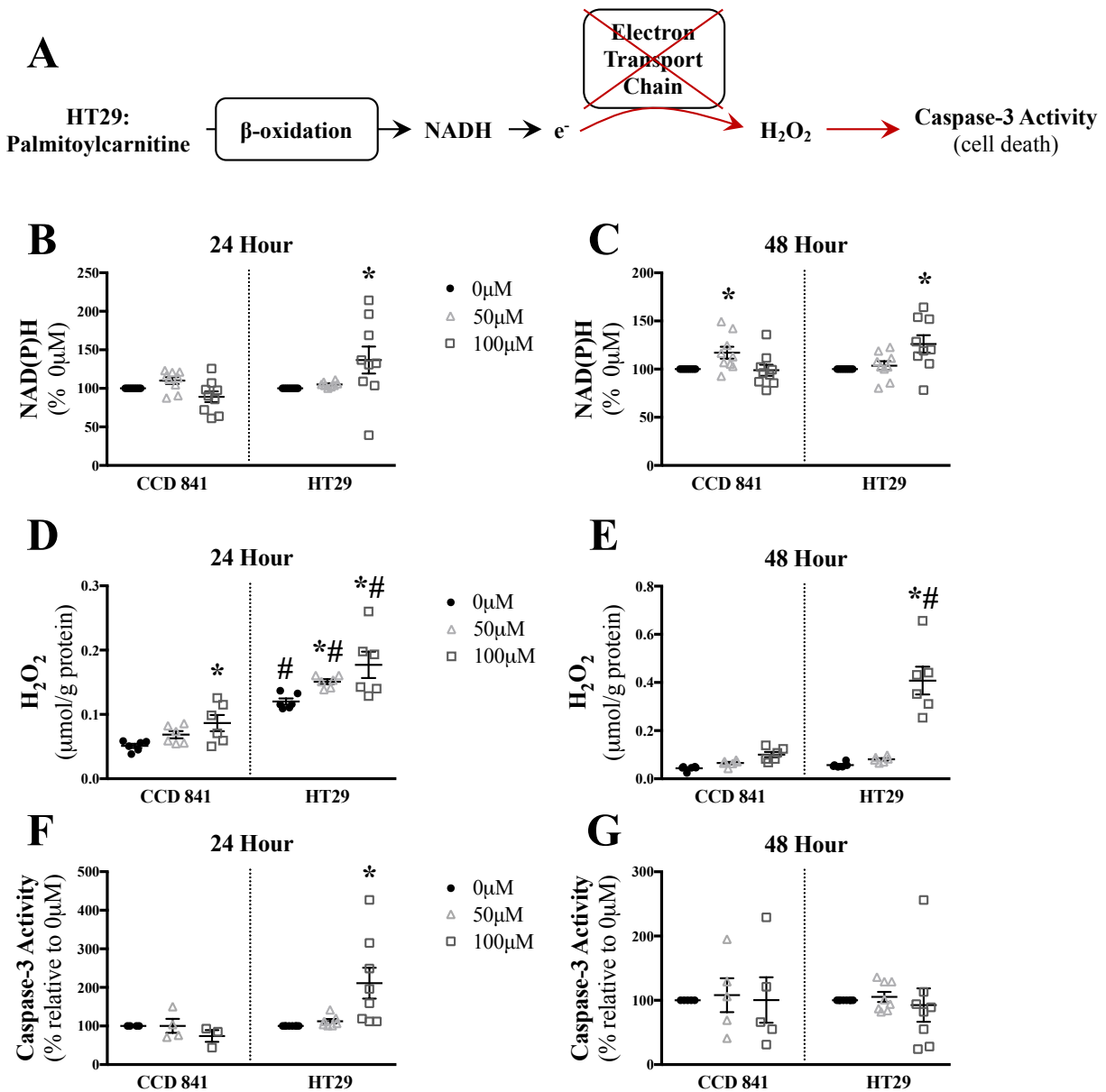


Figure 4 3 Elevated NAD(P)H production leads to increased H_2O_2 emission and caspase-3 induction in low oxidative capacity HT29 cells but not high oxidative capacity CCD 841 cells. A Proposed schematic of how palmitoylcarnitine may result in elevated caspase-3 activity through H_2O_2 generation in a state of low oxidative capacity. NAD(P)H levels were measured in CCD 841 (N=9) and HT29 (N=9) cells for **B** 24 hours and **C** 48 hours. Total H_2O_2 emission was measured in CCD 841 (N=6) and HT29 (N=6) cells after **D** 24 hours and **E** 48 hours. $P < 0.05$. Caspase-3 activity was measured in CCD 841 (N=4-5) and HT29 (N=8) cells for **F** 24 hours and **G** 48 hours. Data are reported as means \pm SEM with ‘*’ representing a significant difference relative to $0\mu M$ palmitoylcarnitine of the same time point and ‘#’ representing a significant difference relative to CCD 841 of the same palmitoylcarnitine concentration, $P < 0.05$.

Elevated H₂O₂ emission in relation to decreased cell survival in HT29 cells suggested that glutathione redox buffering might be insufficient to protect HT29 cells from palmitoylcarnitine-induced stress. In HT29 cells, 24 hours of palmitoylcarnitine lowered the reduced/oxidized glutathione ratio ($p < 0.05$) (Figure 4.4A and 4.4B), reduced ($p < 0.05$) (Figure 4.4C and 4.4D) and total glutathione ($p < 0.05$) (Figure 4.4G and 4.4H) without changing total oxidized glutathione (Figure 4.4E and 4.4F), suggesting a net attenuation of glutathione redox buffering dynamics, despite no changes in CCD 841 cell glutathione response to palmitoylcarnitine.

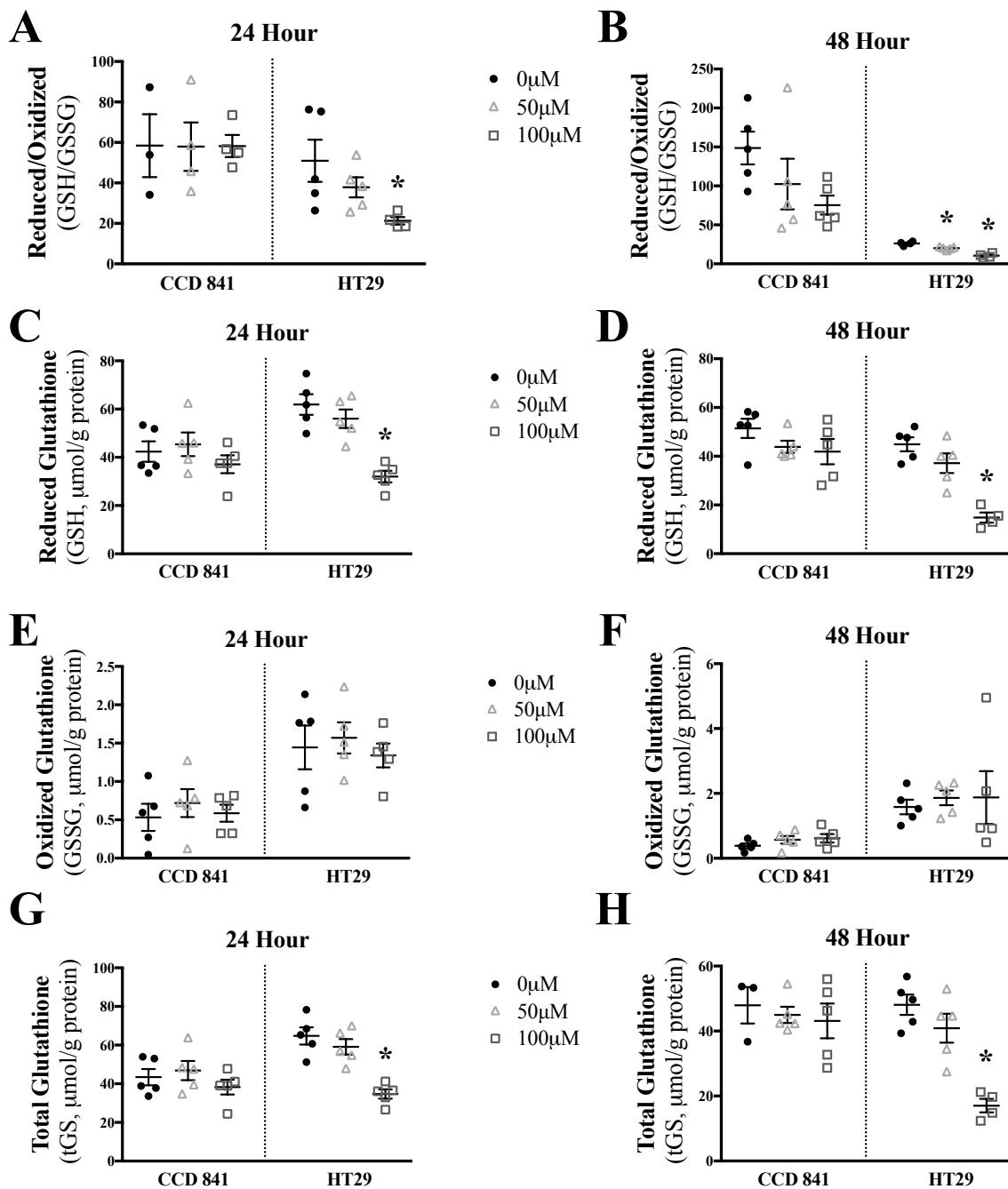


Figure 4 Palmitoylcarnitine lowers glutathione redox buffering capacity in HT29 cells but not CCD 841 cells. The following parameters of glutathione redox buffering were assessed after 24 and 48 hours of palmitoylcarnitine respectively: ratio of reduced to oxidized glutathione (GSH/GSSG) (A, B), reduced glutathione (GSH) (C, D), oxidized glutathione (GSSG) (E, F), and total glutathione (tGS) (G, H) (n=5). Data are reported as means \pm SEM with ‘*’ representing a significant difference relative to 0μM palmitoylcarnitine of the same cell type, $P < 0.05$.

Based on these associations, we then determined whether glutathione redox buffering directly determined cell survival in response to palmitoylcarnitine. The glutathione synthesis inhibitor buthionine sulfoximine (BSO) (Figure 4.5A) nearly eliminated reduced glutathione in CCD 841 and HT29 cells ($p < 0.05$) (Figure 4.5B) and sensitized CCD 841 cells to palmitoylcarnitine-induced decreasing cell survival ($p < 0.05$) (Figure 4.5C and 4.5D) while further sensitizing HT29 cells to decreasing cell survival ($p < 0.05$) (Figure 4.5E and 4.5F).

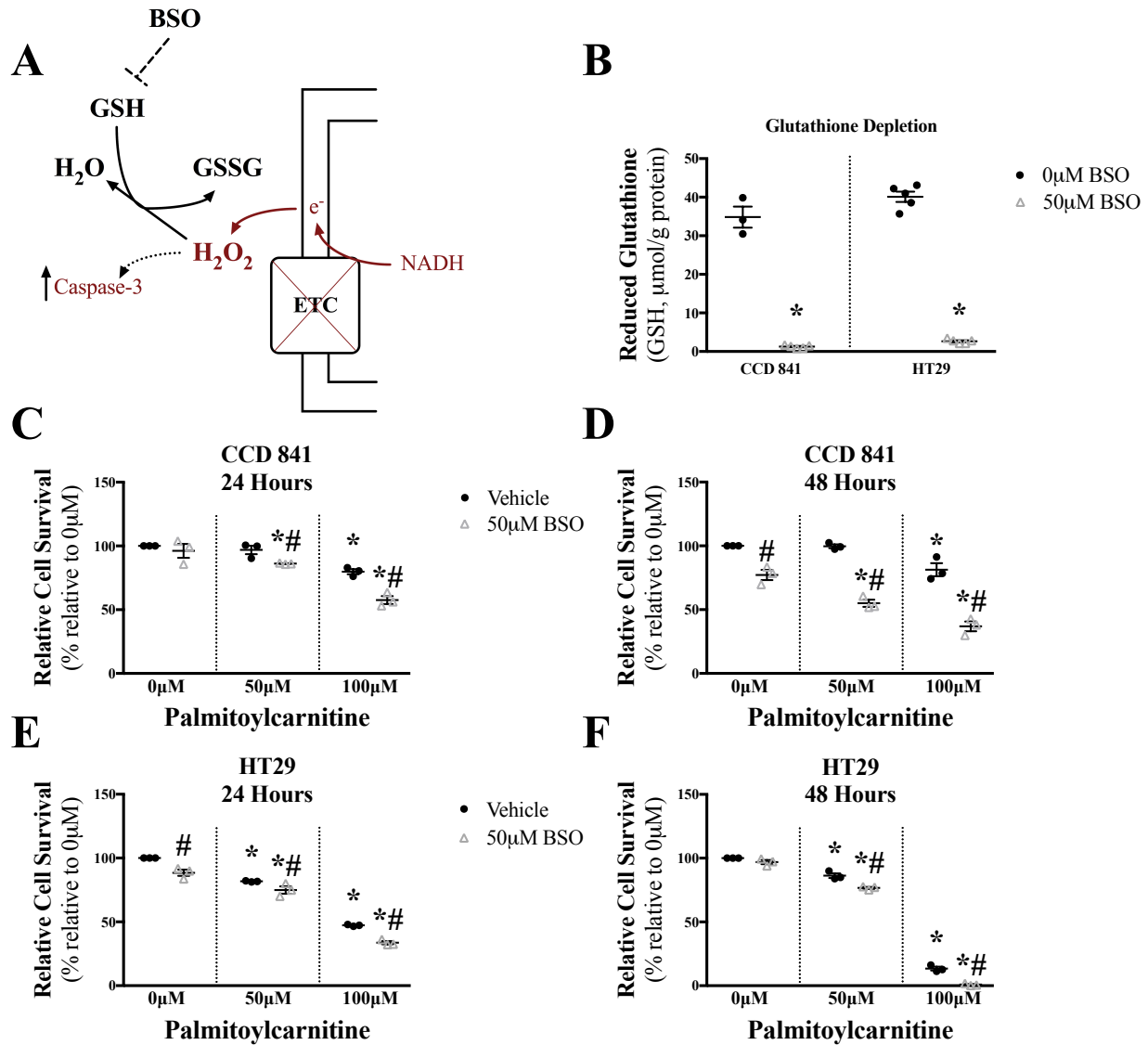


Figure 4 5 Glutathione depletion sensitizes CCD 841 and HT29 cells to palmitoylcarnitine-induced decreasing cell survival. **A** Schematic depicting the influence of buthionine sulfoximine (BSO, inhibitor of glutathione synthesis) on glutathione levels. ETC – electron transport chain, GSH – reduced glutathione, GSSG – oxidized glutathione. **B** Reduced glutathione was measured in CCD 841 and HT29 cells following 24 hours with 0μM or 50μM BSO, ‘*’ representing a significant difference relative to 0μM BSO. Following palmitoylcarnitine incubations concurrent with BSO, relative cell survival was measured in CCD 841 cells for 24 and 48 hours respectively (**C**, **D**) and in HT29 cells (**E**, **F**) (N=3). Data are reported as means ±SEM with ‘*’ representing a significant difference relative to 0μM palmitoylcarnitine, with ‘#’ representing a significant difference between vehicle and 50μM BSO of the same palmitoylcarnitine concentration. *P* < 0.05.

We then explored whether the susceptibility of HT29 cells to palmitoylcarnitine was observed in a cancer line previously shown to be reliant on mitochondrial function (2), the MCF7 breast cancer cell line. In so doing, the role of metabolic and redox flexibility in determining the degree of (in)sensitivity to palmitoylcarnitine could be compared between cell lines. Palmitoylcarnitine had a small effect on cell survival in MCF7 cells after 24 hours ($p < 0.05$) but not 48 hours (Figure 4.6A), indicating that MCF7 cells are more insensitive to palmitoylcarnitine than HT29 cells. In order to validate whether MCF7 cells displayed greater mitochondrial respiratory kinetics compared to HT29 cells (consistent with the notion that MCF7 cells are reliant on mitochondrial metabolism), mitochondrial respiration was compared across HT29, MCF7 and CCD 841 cells. MCF7 cell mitochondrial respiration was greater than HT29 cells at physiological 25 μ M ADP, yet not statistically different than CCD 841 cells at 25 μ M and 500 μ M ADP (Figure 4.6B). However, no changes in intracellular lactate were observed in response to palmitoylcarnitine (Figure 4.6C) suggesting MCF7 cells lack metabolic flexibility in response to fatty acid challenges. Indeed, an increase in NAD(P)H was observed at 48 hours (Figure 4.6D) similar to that seen previously with HT29 cells suggesting the generated NADH is not oxidized by the attenuated rates of oxidative phosphorylation. However, this NADH generation was not sufficient to stimulate H₂O₂ emission (Figure 4.6E), which was consistent with no increases in caspase-3 activity (Figure 4.6F) and no changes in glutathione redox buffering responses (Figures 4.6G-4.6J).

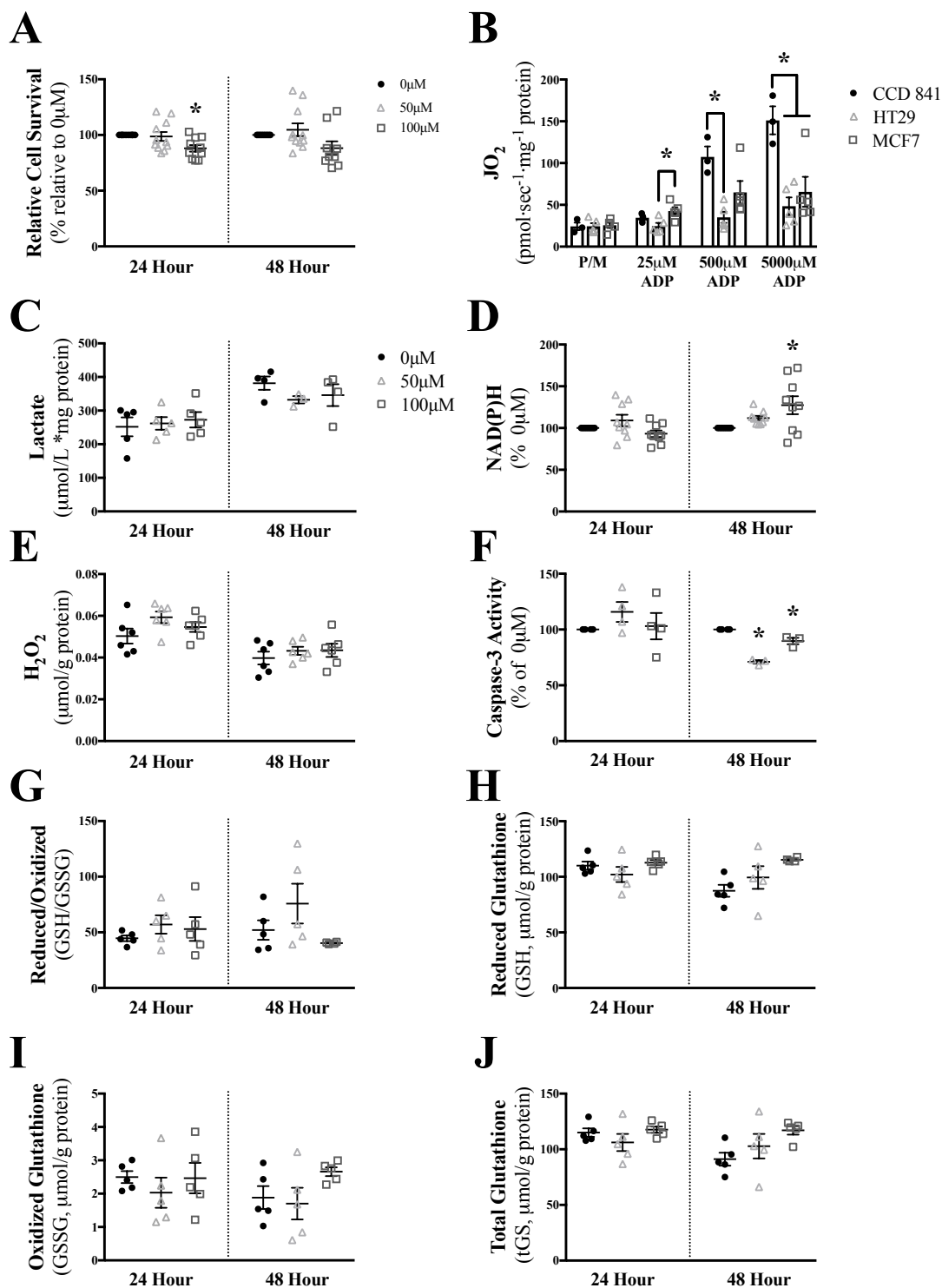


Figure 4 6 MCF7 cells are insensitive to palmitoylcarnitine. A MCF7 cells were incubated with palmitoylcarnitine for 24 and 48 hours and assessed for relative cell survival (N=11). B Mitochondrial respiratory kinetics in MCF7 cells was compared to CCD 841 and HT29 cells (from Fig 2A) (N=5). MCF7 cells were incubated with palmitoylcarnitine for 24 and 48 hours

and assessed for **C** net intracellular lactate (N=5) **D** NAD(P)H (N=9) **E** H₂O₂ (N=6) **F** caspase-3 activity (N=4) **G** GSH/GSSG (N=5) **H** reduced glutathione (N=5) **I** oxidized glutathione (N=5) **J** total glutathione (N=5). Data are reported as means ±SEM with ‘*’ representing a significant difference relative to 0μM palmitoylcarnitine of the same time point, *P* <0.05.

Overall, these results indicate that the susceptibilities of HT29 cells to palmitoylcarnitine are linked to insufficient redox buffering that is not observed in MCF7 breast cancer cells or non-transformed CCD 841 cells.

Discussion

Palmitoylcarnitine caused marked reductions in cell survival in HT29 and HCT 116 colorectal cancer cells with minor reductions in non-transformed CCD 841 colon cells and MCF7 breast cancer cells. The degree of response was related to oxidative kinetics, H₂O₂ emission and the ability to maintain glutathione redox buffering (Figure 4.7). Specifically, the greatest H₂O₂ emission occurred in HT29 cells in association with a collapse in glutathione redox buffering capacity and attenuated cell survival. These results suggest cancer-specific mitochondrial oxidative kinetics and glutathione may influence cell-specific responses to palmitoylcarnitine-induced oxidative stress.

Response to palmitoylcarnitine induced H₂O₂

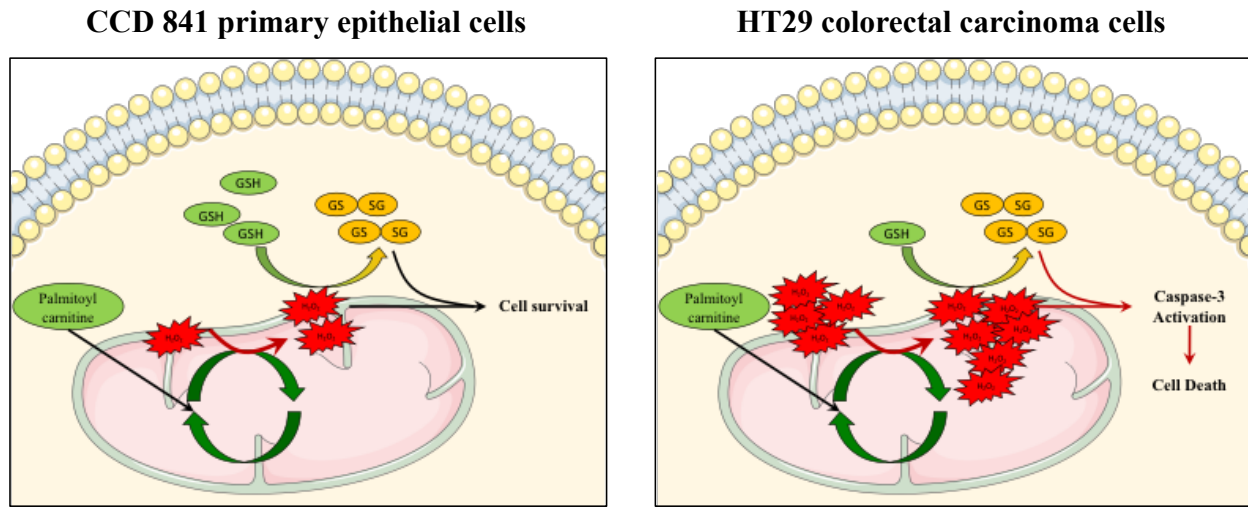


Figure 4 7 Palmitoylcarnitine induced decreases in cell survival are dictated by baseline mitochondrial reactive oxygen species and glutathione response. Upon exposure to palmitoylcarnitine, there is an increase in reactive oxygen species production, however this increase in reactive oxygen species is sufficiently buffered by glutathione resulting in maintaining CCD 841 cell survival. HT29 cells however have significantly higher baseline reactive oxygen species production; therefore upon exposure to palmitoylcarnitine, the additional increase in reactive oxygen species production leads to decreases in glutathione and subsequent caspase-3 activation and cell death.

Oxidative kinetics and redox flexibility determines susceptibility to palmitoylcarnitine

In the present study, we considered classic bioenergetic principles which posit that an over-supply of reducing equivalents (NADH, FADH₂) from excess fat oxidation relative to the metabolic demands for oxidative phosphorylation leads to increased membrane potential and concurrent electron slip onto oxygen to generate superoxide and subsequently H₂O₂ (29). With these bioenergetic principles in mind, cells with low dependencies on mitochondrial oxidative phosphorylation may generate higher rates of H₂O₂ emission when provided with excess substrate. Bypassing CPT-1 in HT29 cells with palmitoylcarnitine increased NADH steady state levels possibly because the lower reliance on oxidative phosphorylation in this cell line caused

NADH production to exceed its oxidation in the electron transport chain, thereby stimulating H₂O₂ emission. In contrast, highly oxidative CCD 841 non-transformed epithelial cells may have been able to oxidize the NADH that was generated in response to palmitoylcarnitine, although this is speculative. As CCD 841 cells demonstrated lower baseline H₂O₂ emission kinetics, the subsequent increase in H₂O₂ emission with palmitoylcarnitine reached a lower absolute rate than seen in HT29 cells. The data suggests that this lower H₂O₂ was effectively buffered by the glutathione redox couple and resulted in no caspase-3 induction and markedly less effects on overall cell survival. Conversely, the higher rates of H₂O₂ emission generated in HT29 cells were related to a concurrent collapse in glutathione buffering capacity which further reveals an inferior redox buffering response in this cancer. This is in line with previous literature demonstrating that cells with higher baseline or steady-state reactive oxygen species production are more susceptible to further elevations in reactive oxygen species through glucose starvation, likely resulting in an increased reliance on mitochondrial metabolism (3).

However, several observations are not entirely in agreement with our previous conclusions. For example, while palmitoylcarnitine resulted in an increase in NAD(P)H in MCF7 cells, there was no associated increase in H₂O₂ emission, perhaps due to glutathione levels successfully buffering changes in palmitoylcarnitine-induced H₂O₂ preventing any associated change in fluorescent signal. Furthermore, there was no statistical increase in NAD(P)H levels at 24 hours following 50μM palmitoylcarnitine in HT29 cells despite an associated increase in H₂O₂ emission and a corresponding decrease in cell survival. While difficult to explain, this perhaps could be attributed to the temporal nature of bioenergetics, such that an earlier increase in NAD(P)H may have preceded the increase in H₂O₂ emission. The highly dynamic turnover of NAD(P)H, H₂O₂ and glutathione particularly during oxidative phosphorylation poses a challenge

in capturing the precise temporal relationship at any given palmitoylcarnitine challenge and time point. Nevertheless, as noted above, the responses following 100 μ M palmitoylcarnitine suggest that the lower cell survival in HT29 cells were related to insufficient glutathione homeostasis.

While palmitoylcarnitine is naturally produced within the cell, exogenous palmitoylcarnitine has been demonstrated to increase intracellular palmitoylcarnitine levels in neuroblastoma NB-2a cells (28), and has previously been demonstrated to cause an adaptive increase in oxidative capacity in mouse embryonic fibroblasts (26). Elevating mitochondrial oxidative phosphorylation has also been mimicked in experiments designed to force pyruvate shuttling towards mitochondria either through inhibiting lactate production (23) or by activating pyruvate dehydrogenase (4). It is therefore possible that similar relative increases in mitochondrial reactive oxygen species production between cancerous and non-transformed cells result in different fates, whereby increasing reactive oxygen species in cells with higher baseline levels would cause great attenuations in glutathione resulting in cell death, whereas cells with lower baseline levels would be able to combat similar relative elevations in reactive oxygen species production through glutathione buffering.

A key finding in this study is that glutathione depletion by BSO amplified the reduction in cell survival following palmitoylcarnitine incubations in HT29 cells and sensitized non-transformed CCD 841 cells. BSO is a selective inhibitor of glutamate cysteine ligase (previously known as γ -glutamylcysteine synthetase), resulting in a rapid decrease in intracellular glutathione levels by preventing its synthesis (11, 16), which was effective at inhibiting growth of a mammary adenocarcinoma cell line *in vivo* (34). The decreased cell survival in HT29 cells in the present study reveals an insufficient ability of this cancer to maintain glutathione-based redox buffering capacity that is otherwise intact in CCD 841 cells. This suggests that

assessments of glutathione redox buffering capacity may serve as a biomarker to predict cancer-specific sensitivity to palmitoylcarnitine as a therapy.

Intriguingly, selective leukemia cell death in acute myeloid leukemia (AML) cells was achieved by inhibiting mitochondrial fat oxidation with Avocatin B (24), mitochondrial complex I with mubritinib (5), amino acid mitochondrial oxidation (20) and BCL-2 dependent mitochondrial metabolism (22). These findings seem to be opposite to the present data whereby the provision of excess mitochondrial substrates resulted in colorectal cancer cell death. While we cannot fully explain the heterogeneity in cancer cell responses toward mitochondrial-targeted therapies, the response of glutathione to metabolic-targeting therapies may provide insight into determining cell fate. Many current chemotherapies elevate intracellular levels of reactive oxygen species or target redox-homeostasis to elicit anticancer effects (39). However, given that we are currently unable to detect *in vivo* kinetics of reactive oxygen species production in cancer patients, the present results may serve as a foundation to explore the possibility that unique glutathione redox buffering capacities within tumours may yield predictive value for guiding future therapies which trigger mitochondrial reactive oxygen species by targeting mitochondrial metabolism.

We note two limitations of the present work. First, the respiratory kinetics observed in the present study may be under-estimations given the respirometric protocols were performed with cells in suspension rather than in an adherent environment as they are accustomed to given their epithelial origin. While palmitoylcarnitine-supported respiration was not detected in any cell lines likely due to this reason (data not shown), the increased ADP-stimulated respiration nonetheless demonstrates a robust difference in mitochondrial oxidative phosphorylation between cell lines. Second, the lactate concentrations reflect intracellular lactate rather than

efflux, which would otherwise require assessments of acidification rates of local media in combination with lactate efflux assessments. However, changes in intracellular lactate concentrations serve as an index of altered glycolytic flux and support the present interpretation.

Perspectives and Conclusions

Collectively, HT29 cells demonstrate greater reductions in cell survival in response to palmitoylcarnitine in association with lower oxidative kinetics, higher baseline H₂O₂ and inferior glutathione redox flexibility. These relationships were observed in less than 48 hours suggesting metabolic and redox processes occur early in response to palmitoylcarnitine challenges. Previous literature demonstrates a paradoxical role of mitochondrial activation in cancer survival, whereby some cancers rely on mitochondrial metabolism to drive cell growth, such as MCF7 cells (2), ovarian cancers (30) and leukemia cells (24), whereas other cancers demonstrate decreased survival if forced to rely on mitochondrial oxidative phosphorylation (3, 23, 33, 38). A striking corollary is the potential for non-transformed cells to tolerate changes in metabolism, as was observed in CCD 841 cells. In contrast, it may be that certain cancers lack such metabolic flexibility by developing a stronger reliance on dedicated metabolic pathways through a myriad of micro-evolutionary adaptations in order to maximize growth rates. The metabolic flexibilities of cancers are likely heterogeneous, as seen in the present study whereby HCT 116 and HT29 cell deleterious responses to palmitoylcarnitine were not seen in MCF7 breast cancer cells which otherwise maintained cell proliferation rates without an increase in H₂O₂ emission. These findings also guide new directions into the role of H₂O₂ and glutathione-based redox signaling of specific pathways that regulate cell fate. Finally, MCF7 cells also demonstrated greater oxidative kinetics at physiological levels of ADP relative to HT29 cells, and maintained glutathione-

buffering capacities throughout palmitoylcarnitine incubations. This finding highlights the possibility that heterogeneous responses of cancers to metabolic therapies may be linked to a dynamic relationship between their inherent metabolic capacities and redox regulation. This discovery guides additional research to determine whether a combination of lower mitochondrial oxidative kinetics and inferior redox buffering couples may represent a biomarker that predicts whether a cancer will be uniquely susceptible to palmitoylcarnitine-mediated reductions in survival.

Author contributions

P.C.T. and C.G.R.P. designed the study. P.C.T. and M.C.H. conducted experiments and analyzed data. P.C.T. and C.G.R.P. wrote the manuscript. All authors approved the manuscript.

Conflict of interest

The authors declare that they have no conflicts of interest with the contents of this article.

Acknowledgments

We thank Dr. Samuel Benchimol for kindly providing the HT29, HCT 116 and MCF7 cells.

Funding

Funding was provided to C.G.R.P. by the National Science and Engineering Research Council (#436138-2013), with infrastructure supported by Canada Foundation for Innovation, the James. H. Cummings foundation and the Ontario Research Fund. P.C.T and M.C.H. were supported by NSERC CGS-PhD scholarships.

References

1. **Al-Bakheit A, Traka M, Saha S, Mithen R, and Melchini A.** Accumulation of Palmitoylcarnitine and Its Effect on Pro-Inflammatory Pathways and Calcium Influx in Prostate Cancer. *The Prostate* 76: 1326-1337, 2016.
2. **Andrzejewski S, Gravel SP, Pollak M, and St-Pierre J.** Metformin directly acts on mitochondria to alter cellular bioenergetics. *Cancer & metabolism* 2: 12, 2014.
3. **Aykin-Burns N, Ahmad IM, Zhu Y, Oberley LW, and Spitz DR.** Increased levels of superoxide and H₂O₂ mediate the differential susceptibility of cancer cells versus normal cells to glucose deprivation. *The Biochemical journal* 418: 29-37, 2009.
4. **Ayyanathan K, Kesaraju S, Dawson-Scully K, and Weissbach H.** Combination of sulindac and dichloroacetate kills cancer cells via oxidative damage. *PLoS one* 7: e39949, 2012.
5. **Baccelli I, Gareau Y, Lehnertz B, Gingras S, Spinella JF, Corneau S, Mayotte N, Girard S, Frechette M, Blouin-Chagnon V, Leveille K, Boivin I, MacRae T, Krosil J, Thiollier C, Lavalley VP, Kanshin E, Bertomeu T, Coulombe-Huntington J, St-Denis C, Bordeleau ME, Boucher G, Roux PP, Lemieux S, Tyers M, Thibault P, Hebert J, Marinier A, and Sauvageau G.** Mubritinib Targets the Electron Transport Chain Complex I and Reveals the Landscape of OXPHOS Dependency in Acute Myeloid Leukemia. *Cancer cell* 36: 84-99 e88, 2019.
6. **Bansal A, and Simon MC.** Glutathione metabolism in cancer progression and treatment resistance. *The Journal of cell biology* 217: 2291-2298, 2018.
7. **Blanquer-Rossello MD, Hernandez-Lopez R, Roca P, Oliver J, and Valle A.** Resveratrol induces mitochondrial respiration and apoptosis in SW620 colon cancer cells. *Biochimica et biophysica acta General subjects* 1861: 431-440, 2017.
8. **Bloemberg D, and Quadrilatero J.** Mitochondrial pro-apoptotic indices do not precede the transient caspase activation associated with myogenesis. *Biochimica et biophysica acta* 1843: 2926-2936, 2014.
9. **Dam AD, Mitchell AS, and Quadrilatero J.** Induction of mitochondrial biogenesis protects against caspase-dependent and caspase-independent apoptosis in L6 myoblasts. *Biochimica et biophysica acta* 1833: 3426-3435, 2013.
10. **Dionne S, Elimrani I, Roy MJ, Qureshi IA, Sarma DR, Levy E, and Seidman EG.** Studies on the chemopreventive effect of carnitine on tumorigenesis in vivo, using two experimental murine models of colon cancer. *Nutrition and cancer* 64: 1279-1287, 2012.
11. **Drew R, and Miners JO.** The effects of buthionine sulphoximine (BSO) on glutathione depletion and xenobiotic biotransformation. *Biochemical pharmacology* 33: 2989-2994, 1984.
12. **Dunigan DD, Waters SB, and Owen TC.** Aqueous soluble tetrazolium/formazan MTS as an indicator of NADH- and NADPH-dependent dehydrogenase activity. *BioTechniques* 19: 640-649, 1995.
13. **Feoktistova M, Geserick P, and Leverkus M.** Crystal Violet Assay for Determining Viability of Cultured Cells. *Cold Spring Harbor protocols* 2016: pdb prot087379, 2016.
14. **Gatenby RA, and Gillies RJ.** Why do cancers have high aerobic glycolysis? *Nature reviews Cancer* 4: 891-899, 2004.

15. **Giustarini D, Dalle-Donne I, Milzani A, Fanti P, and Rossi R.** Analysis of GSH and GSSG after derivatization with N-ethylmaleimide. *Nature protocols* 8: 1660-1669, 2013.
16. **Griffith OW, and Meister A.** Potent and specific inhibition of glutathione synthesis by buthionine sulfoximine (S-n-butyl homocysteine sulfoximine). *The Journal of biological chemistry* 254: 7558-7560, 1979.
17. **Hughes MC, Ramos SV, Turnbull PC, Edgett BA, Huber JS, Polidovitch N, Schlattner U, Backx PH, Simpson JA, and Perry CGR.** Impairments in left ventricular mitochondrial bioenergetics precede overt cardiac dysfunction and remodelling in Duchenne muscular dystrophy. *J Physiol* 2019.
18. **Hughes MC, Ramos SV, Turnbull PC, Rebalka IA, Cao A, Monaco CMF, Varah NE, Edgett BA, Huber JS, Tadi P, Delfinis LJ, Schlattner U, Simpson JA, Hawke TJ, and Perry CGR.** Early myopathy in Duchenne muscular dystrophy is associated with elevated mitochondrial H₂ O₂ emission during impaired oxidative phosphorylation. *Journal of cachexia, sarcopenia and muscle* 2019.
19. **Ishiyama M, Miyazono Y, Sasamoto K, Ohkura Y, and Ueno K.** A highly water-soluble disulfonated tetrazolium salt as a chromogenic indicator for NADH as well as cell viability. *Talanta* 44: 1299-1305, 1997.
20. **Jones CL, Stevens BM, D'Alessandro A, Reisz JA, Culp-Hill R, Nemkov T, Pei S, Khan N, Adane B, Ye H, Krug A, Reinhold D, Smith C, DeGregori J, Pollyea DA, and Jordan CT.** Inhibition of Amino Acid Metabolism Selectively Targets Human Leukemia Stem Cells. *Cancer cell* 34: 724-740 e724, 2018.
21. **Kand'ar R, Zakova P, Lotkova H, Kucera O, and Cervinkova Z.** Determination of reduced and oxidized glutathione in biological samples using liquid chromatography with fluorimetric detection. *Journal of pharmaceutical and biomedical analysis* 43: 1382-1387, 2007.
22. **Lagadinou ED, Sach A, Callahan K, Rossi RM, Neering SJ, Minhajuddin M, Ashton JM, Pei S, Grose V, O'Dwyer KM, Liesveld JL, Brookes PS, Becker MW, and Jordan CT.** BCL-2 inhibition targets oxidative phosphorylation and selectively eradicates quiescent human leukemia stem cells. *Cell stem cell* 12: 329-341, 2013.
23. **Le A, Cooper CR, Gouw AM, Dinavahi R, Maitra A, Deck LM, Royer RE, Vander Jagt DL, Semenza GL, and Dang CV.** Inhibition of lactate dehydrogenase A induces oxidative stress and inhibits tumor progression. *Proceedings of the National Academy of Sciences of the United States of America* 107: 2037-2042, 2010.
24. **Lee EA, Angka L, Rota SG, Hanlon T, Mitchell A, Hurren R, Wang XM, Gronda M, Boyaci E, Bojko B, Minden M, Sriskanthadevan S, Datti A, Wrana JL, Edginton A, Pawliszyn J, Joseph JW, Quadrilatero J, Schimmer AD, and Spagnuolo PA.** Targeting Mitochondria with Avocatin B Induces Selective Leukemia Cell Death. *Cancer research* 75: 2478-2488, 2015.
25. **Liberti MV, and Locasale JW.** The Warburg Effect: How Does it Benefit Cancer Cells? *Trends in biochemical sciences* 41: 211-218, 2016.
26. **Lin Z, Liu F, Shi P, Song A, Huang Z, Zou D, Chen Q, Li J, and Gao X.** Fatty acid oxidation promotes reprogramming by enhancing oxidative phosphorylation and inhibiting protein kinase C. *Stem cell research & therapy* 9: 47, 2018.
27. **Mandel ER, Dunford EC, Abdifarkosh G, Turnbull PC, Perry CGR, Riddell MC, and Haas TL.** The superoxide dismutase mimetic tempol does not alleviate

glucocorticoid-mediated rarefaction of rat skeletal muscle capillaries. *Physiol Rep* 5: 2017.

28. **Nalecz KA, Szczepankowska D, Czeredys M, Kulikova N, and Grzeskiewicz S.** Palmitoylcarnitine regulates estrification of lipids and promotes palmitoylation of GAP-43. *FEBS letters* 581: 3950-3954, 2007.

29. **Nicholls DG, and Ferguson SJ.** In: *Bioenergetics (Fourth Edition)*, edited by Nicholls DG, and Ferguson SJ. Boston: Academic Press, 2013, p. ix-x.

30. **Nieman KM, Kenny HA, Penicka CV, Ladanyi A, Buell-Gutbrod R, Zillhardt MR, Romero IL, Carey MS, Mills GB, Hotamisligil GS, Yamada SD, Peter ME, Gwin K, and Lengyel E.** Adipocytes promote ovarian cancer metastasis and provide energy for rapid tumor growth. *Nature medicine* 17: 1498-1503, 2011.

31. **Ortega AL, Mena S, and Estrela JM.** Glutathione in cancer cell death. *Cancers* 3: 1285-1310, 2011.

32. **Roscilli G, Marra E, Mori F, Di Napoli A, Mancini R, Serlupi-Crescenzi O, Virmani A, Aurisicchio L, and Ciliberto G.** Carnitines slow down tumor development of colon cancer in the DMH-chemical carcinogenesis mouse model. *Journal of cellular biochemistry* 114: 1665-1673, 2013.

33. **Schulz TJ, Thierbach R, Voigt A, Drewes G, Mietzner B, Steinberg P, Pfeiffer AF, and Ristow M.** Induction of oxidative metabolism by mitochondrial frataxin inhibits cancer growth: Otto Warburg revisited. *The Journal of biological chemistry* 281: 977-981, 2006.

34. **Terradez P, Asensi M, Lasso de la Vega MC, Puertes IR, Vina J, and Estrela JM.** Depletion of tumour glutathione in vivo by buthionine sulphoximine: modulation by the rate of cellular proliferation and inhibition of cancer growth. *The Biochemical journal* 292 (Pt 2): 477-483, 1993.

35. **Wallace DC.** Mitochondria and cancer. *Nature reviews Cancer* 12: 685-698, 2012.

36. **Warburg O.** The metabolism of carcinoma cells. *The Journal of Cancer Research* 9: 148-163, 1925.

37. **Warburg O.** On the origin of cancer cells. *Science* 123: 309-314, 1956.

38. **Wenzel U, Nickel A, and Daniel H.** Increased carnitine-dependent fatty acid uptake into mitochondria of human colon cancer cells induces apoptosis. *The Journal of nutrition* 135: 1510-1514, 2005.

39. **Yang H, Villani RM, Wang H, Simpson MJ, Roberts MS, Tang M, and Liang X.** The role of cellular reactive oxygen species in cancer chemotherapy. *Journal of experimental & clinical cancer research : CR* 37: 266, 2018.

Chapter 5 Synergistic activation of mitochondrial metabolism and the glutathione redox couple protects HepG2 hepatocarcinoma cells from palmitoylcarnitine-induced stress

This chapter is formatted for publication in the American Journal of Physiology – Cell physiology, rapid reports.

Turnbull PC, Dehghani AC, Theriau CF, Connor MK, and Perry CGR. Synergistic activation of mitochondrial metabolism and the glutathione redox couple protects HepG2 hepatocarcinoma cells from palmitoylcarnitine-induced stress. *AJP-Cell rapid reports*, 2019. – *In revision*.

Author Contributions: The majority of experiments for this project were carried out by Patrick C. Turnbull (PCT), with the exception of the following. PCT, CGRP and MKC contributed to the rationale and study design. ACD and PCT performed intracellular lactate assays. CFT was involved in cell handling and unpublished additional data. PCT and CGRP wrote the manuscript.

Synergistic activation of mitochondrial metabolism and the glutathione redox couple protects HepG2 hepatocarcinoma cells from palmitoylcarnitine-induced stress

Authors: Patrick C. Turnbull, Ali C. Dehghani, Christopher F. Theriau, Michael K. Connor, and Christopher G.R. Perry

Affiliations:

School of Kinesiology, York University, 4700 Keele Street, Toronto, ON, Canada, M6J 1P3.

†Address for Correspondence:

Christopher Perry, PhD

School of Kinesiology and Health Science

Muscle Health Research Centre

344 Norman Bethune College

York University

4700 Keele Street

Toronto, Ontario M3J 1P3

(P) 416 736 2100 ext. 33232

cperry@yorku.ca

Abstract

Fatty acid stress can have divergent effects in various cancers. We explored how metabolic and redox flexibility in HepG2 hepatocarcinoma cells mediate protection from palmitoylcarnitine. HepG2 cells, along with HCT 116 and HT29 colorectal cancer cells were incubated with 100 μ M palmitoylcarnitine for up to 48 hours. Mitochondrial H₂O₂ emission, glutathione and cell survival were assessed in HT29 and HepG2 cells. 100 μ M palmitoylcarnitine promoted early growth in HepG2 cells by ~8% after 48 hours vs decreased cell survival observed in HT29 and HCT 116 cells. Palmitoylcarnitine increased mitochondrial respiration at physiological and maximal concentrations of ADP while lowering cellular lactate content in HepG2 cells, suggesting a switch to mitochondrial metabolism. HepG2 cell growth was associated with an early increase in H₂O₂ emission by 10 minutes followed by a decrease in H₂O₂ at 24 hours that corresponded with increased glutathione content, suggesting a redox-based compensatory mechanism. In contrast, abrogation of HT29 cell proliferation was related to decreased mitochondrial respiration (likely due to cell death) and decreased glutathione. Concurrent glutathione depletion with BSO prevented palmitoylcarnitine-induced growth in HepG2 cells indicating that glutathione was critical for promoting growth following palmitoylcarnitine. Inhibiting UCP2 with genipin sensitized HepG2 cells to palmitoylcarnitine, suggesting that activation of UCP2 may be a 2nd redox-based mechanism conferring protection. These findings suggest that HepG2 cells possess inherent metabolic and redox flexibility that confers protection from palmitoylcarnitine-induced stress via adaptive increases in mitochondrial respiratory control, glutathione buffering and induction of UCP2.

Keywords: redox flexibility, cancer, mitochondria, uncoupling, oxidative stress

Introduction

Fatty acid challenges have been shown to induce cell death in some cancers, such as HT29 colorectal (20) and PC3 prostate carcinoma cells (1), while other cells appear resistant to this stress. In fact, excess hepatic fat accumulation is associated with increased risk of hepatocellular carcinoma (HCC) development (18). Likewise, a high-fat diet induced HCC in rodents, and reversal back to a low-fat diet prevented HCC development (9). Vendel Nielsen et al. (19) also observed that the unsaturated fatty acid, oleic acid, increased growth in HepG2 HCC cells. However, the mechanisms that confer resistance to fatty-acid stress in HCC remain unresolved.

One possibility is the influence of fatty acid metabolism on the cellular redox environment through mitochondrial H_2O_2 emission – a natural byproduct of oxidative phosphorylation (OXPHOS). This concept is intriguing given cellular redox conditions can dictate cell fate, whereby an excess of H_2O_2 can invoke deleterious effects on cell function and fate, (reviewed by (13)), yet low levels of H_2O_2 can act as a hormetic signal that drives cancer cell growth (8). This suggests that the influence of metabolically derived H_2O_2 on cell fate will depend on the ability of the cell to maintain cellular redox conditions. In this regard, the main cellular antioxidant glutathione is essential in maintaining cell survival. Indeed, pharmacological increases in glutathione stimulated HepG2 cell growth, whereas glutathione depletion prevented HepG2 cell proliferation (10).

Evidence also suggests that uncoupling protein-2 (UCP2) attenuates mitochondrial H_2O_2 emission potentially by dissipating membrane potential and preventing increases in superoxide production (the precursor to mitochondrial H_2O_2

emission) from fatty acid oxidation (review by (2, 4, 14)). While there is controversy over the specific mechanistic function of UCP2 (3, 5, 15), it appears that UCP2 is able to dissipate H_2O_2 emission. However, it remains to be determined whether UCP2 mediates a redox-dependent compensation in response to fatty acid challenges that ultimately prevents oxidative stress and creates a pro-growth reduced environment in HCC. Indeed, palmitic acid increased superoxide production in HepG2 cells, which was amplified by genipin, a selective UCP2 inhibitor (12). Likewise, transgenic overexpression of UCP2 in HepG2 cells prevented oxidative modifications of membranes and proteins, which is indicative of attenuated reactive oxygen species production (6).

The degree to which UCP2 determines cell fate in response to fatty acid stress remains uncertain, as does the potential synergistic responses of the glutathione redox couple. Such dynamic relationships make it difficult to predict whether HepG2 cells would fail or succeed at invoking sufficient metabolic and redox adaptations to survive fatty acid stress. In this study, we determined the response of HepG2 cells to palmitoylcarnitine-induced stress and explored potential metabolic and redox-based mechanisms. The results demonstrate that palmitoylcarnitine stimulates early growth in HepG2 cells that contrasted with decreased cell survival in HT29 and HCT 116 cells. This protection from palmitoylcarnitine stress in HepG2 cells was dependent on glutathione and UCP2, and was related to rapid changes in mitochondrial bioenergetics. These findings reveal a dynamic metabolic and redox response system that ultimately confers protection against palmitoylcarnitine stress in HepG2 cells.

Experimental procedures

Cell culture conditions

HepG2 hepatocarcinoma cells were gifted by Dr. Paul Spagnuolo (University of Guelph, Guelph, Canada). HT29 and HCT 116 colorectal carcinoma cells were gifted by Dr. Samuel Benchimol (York University, Toronto, Canada). HepG2 cells were grown in EMEM, whereas both HT29 and HCT 116 cells were grown in DMEM. All media was supplemented with 10% fetal bovine serum and 1% penicillin/streptomycin (Wisent Inc, Saint-Jean-Baptiste, Canada).

Palmitoylcarnitine incubations

Cells were cultured with 2mM L-carnitine (Sigma-Aldrich) and 0 μ M or 100 μ M palmitoylcarnitine (Toronto Research Chemicals, Toronto, Canada).

Relative Cell Survival Assay

Following 24 or 48 hours of palmitoylcarnitine incubations, with or without buthionine-sulfoximine (BSO) and genipin (Sigma-Aldrich), cells plated in 96-well optical bottom black walled plates were fixed using 10% formalin and then stained using 0.5% Crystal Violet (Sigma-Aldrich) in 25% MeOH. Visualization and fluorescent analyses of Crystal Violet as a measure of relative cell survival was conducted using the LiCor odyssey scanner (LiCor Biosciences, Lincoln, NE, USA).

NAD(P)H

The reduction of XTT can serve as an indirect measure of NADH and NADPH, collectively referred to as NAD(P)H (7). During the final 4 hours of palmitoylcarnitine incubations, 50µl of XTT solution (1mg/ml XTT, 25µM phenazine methosulfate; BioShop Canada Inc.) was added into each well and incubated at 37°C with 5% CO₂. Absorbance was read at 450nm using the VICTOR³ 1420 Multilabel Counter plate reader (PerkinElmer, Waltham, MA, USA). Cells were digested in-well using 10% RIPA (Sigma-Aldrich) and protein was assessed with BCA (ThermoFisher) to normalize NAD(P)H signal.

Live-cell H₂O₂ measurements

HepG2 cells were seeded in a 96-well optical bottom black-walled plate (ThermoFisher Scientific). Following palmitoylcarnitine incubations, 10µM Amplex® UltraRed and 1 U/ml horseradish peroxidase was added to each well for 10 minutes and fluorescence (EX568/EM581) was measured using the BioTek Cytation 3 fluorescent platereader (BioTek, Winooski, VT, USA). A single read after these time points reflected the net accumulated fluorescent resorufin product of oxidized Amplex Ultrared and therefore represents the ‘net emission’ of H₂O₂ that cells accumulated which was made relative to a H₂O₂ standard curve. Cells were then normalized to protein by BCA as described above.

Glutathione analysis

Analysis was performed as previously demonstrated (11) with alterations for cell culture. Following palmitoylcarnitine incubations, cells were trypsin-lifted, washed with

PBS and re-suspended in final buffer (50mM TRIS, 20mM boric acid, 2mM L-serine, 20 μ M acivicin, 5mM N-ethylmaleimide) for reduced (GSH) and oxidized (GSSG) glutathione determination.

Intracellular lactate determination

Cells were trypsin-harvested, washed with PBS and re-suspended in 0.5M perchloric acid, vortexed and freeze-thawed in liquid nitrogen. Supernatant was collected, centrifuged (4°C, 5 minutes, 5,700rcf), treated with 2.2M KHCO₃, and subsequently centrifuged with new supernatant collected. Supernatant was added in triplicate in a 96-well plate and incubated for 1hr with lactate buffer (1M glycine, 500mM hydrazine sulphate, 5mM EDTA, pH 9.5), NAD⁺ and LDH (Sigma-Aldrich). Absorption of NADH was measured at 340nm on a BioTek Cytation 3 fluorescent plate reader (BioTek, Winooski, VT, USA). Signal was normalized to pre-perchloric acid protein determination as described above.

Mitochondrial Bioenergetic Assessments

Following palmitoylcarnitine incubations, cells were trypsin-harvested from 10cm dishes, washed in PBS and re-suspended in mitochondrial respiration media (11) supplemented with 20mM creatine. Cells were permeabilized with 10 μ g/ml digitonin (Sigma-Aldrich) for 30 minutes rocking at room temperature. Following centrifugation (5 minutes, 500rcf), cells were re-suspended for high-resolution respirometry as previously described (11) with an aliquot removed to determine protein concentration for normalization as outlined above.

Western Blotting

SDS-PAGE was performed as previously described (11) with alterations for cell culture. Cells were trypsin harvested, PBS washed, and re-suspended in lysis buffer (0.5% IGEPAL, 50mM TRIS, 10% glycerol, 0.1mM EDTA, 150mM NaCl, 1mM DTT) with protease and phosphatase inhibitors (Sigma-Aldrich). Monoclonal anti-UCP2 antibody produced in rabbit (1:1000 dilution, D105V, Cell Signaling Technology) was used to determine UCP2 protein content, polyclonal anti-TXNRD2 produced in rabbit (1:200, HPA003323, Sigma-Aldrich) was used to determine thioredoxin reductase-2 protein content.

Statistics

All results are expressed as means \pm SEM. Significance was determined as $p < 0.05$ for all measures. Unpaired t-tests and ANOVA's were conducted where appropriate. A Fisher's LSD *post-hoc* test was conducted following significant interactions in a two-way ANOVA. All statistics were performed using GraphPad Prism 7 (San Diego, CA, USA).

Results

Unique HepG2 cell growth response to palmitoylcarnitine compared to HT29 and HCT

116

HepG2, HT29, and HCT 116 cells were exposed to 0 μ M and 100 μ M palmitoylcarnitine (Figure 5.1A) for 24 and 48 hours. While HT29 and HCT 116 cells

displayed varying degrees of decreased relative cell survival (Figure 5.1B, $p < 0.05$) following 24 and 48 hours of 100 μ M palmitoylcarnitine, in contrast, HepG2 cells displayed an ~8% increase in relative cell growth (Figure 5.1B, $p < 0.05$). This response is notable considering HepG2 cells have a population doubling time of ~44 hours. These responses were related to increased mitochondrial respiration kinetics in HepG2 cells at 24 hours (Figure 5.1C, $p < 0.05$) vs decreased respiration in HT29 cells (Figure 5.1D, $p < 0.05$). To gain insight into whether the increased respiration was linked to greater content of electron transport system proteins, we stimulated maximal electron flux by uncoupling the inner mitochondrial membrane with FCCP. Indeed, the greater respiration seen following palmitoylcarnitine in HepG2 cells demonstrates a greater capacity of the electron transport system (Figure 5.1E, $p < 0.05$). Consistent with previous data, HT29 cells displayed a decrease in FCCP-stimulated capacity (Figure 5.1F, $p < 0.05$) likely signifying that HT29 cells were non-viable rather than a direct decrease in mitochondrial respiratory kinetics following palmitoylcarnitine.

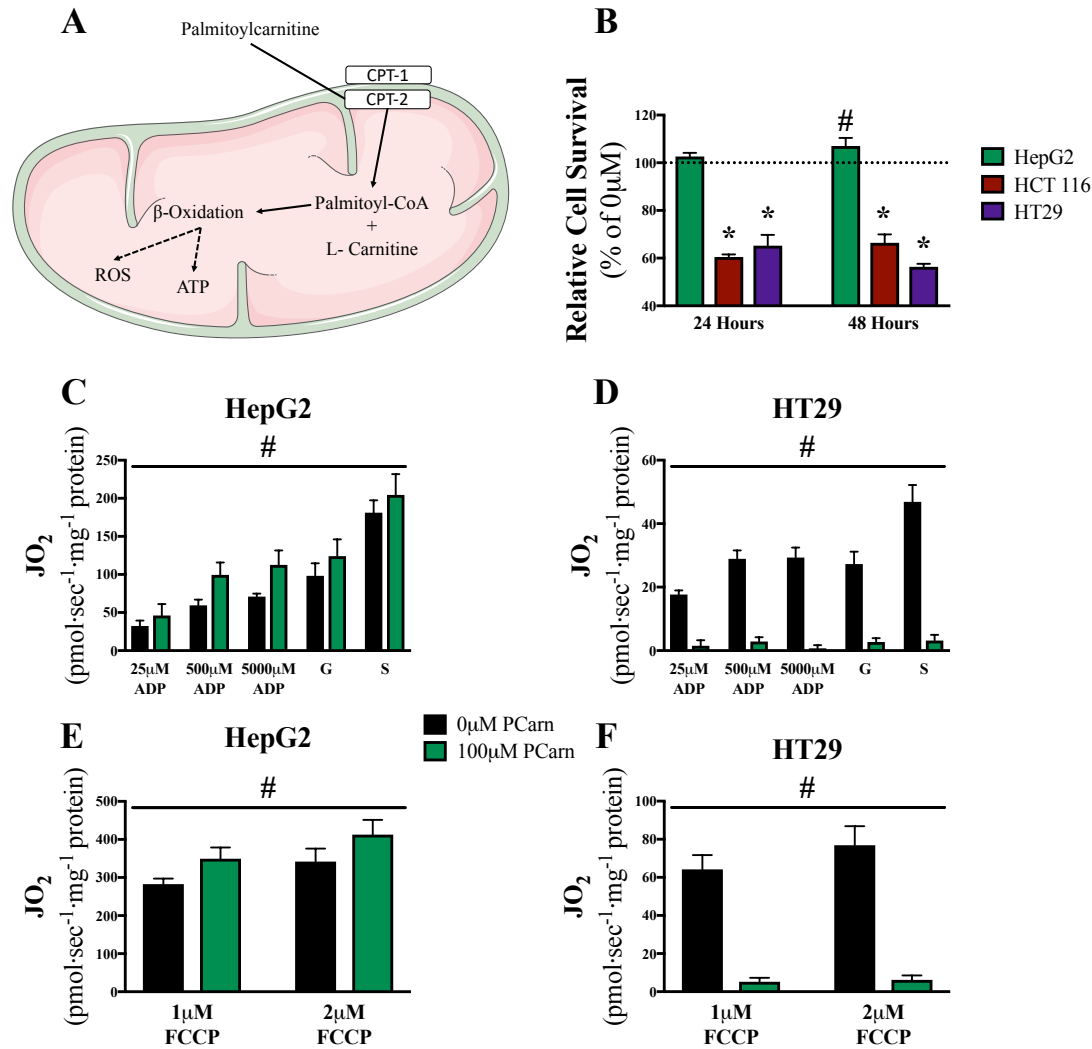


Figure 5 1 Palmitoylcarnitine promotes selective growth in HepG2 cells compared to HT29, and HCT 116 cells and increases mitochondrial respiratory capacity in HepG2 cells. **A** Schematic showing palmitoylcarnitine bypassing CPT-1, whereby it enters the mitochondria and stimulates β -oxidation resulting ATP and reactive oxygen species (ROS) production. **B** Relative cell survival was measured in HepG2 (N=14), HT29 (N=3) and HCT 116 (N=3) cells following 24 and 48 hours of 100 μ M palmitoylcarnitine relative to 0 μ M palmitoylcarnitine at same time points. Data are reported as means \pm SEM with ‘*’ representing a significant decrease and ‘#’ representing a significant increase relative to 0 μ M palmitoylcarnitine of the same cell type within the same time point. $P < 0.05$. HepG2 and HT29 cells were incubated with 0 μ M or 100 μ M palmitoylcarnitine for 24 hours and mitochondrial respiration was measured following **C and D** ADP, glutamate (G) and succinate (S) (N=4) and **E and F** maximal uncoupled rate of respiration following FCCP as an index of electron transport chain content (N=4). Data are reported as means \pm SEM with ‘#’ representing a main effect for palmitoylcarnitine. $P < 0.05$.

Redox responses to palmitoylcarnitine in HepG2 cells

Considering that fatty acids have been demonstrated to stimulate mitochondrial superoxide and H₂O₂ emission (12, 17), and excess H₂O₂ emission can lead to deleterious effects throughout the cell such as glutathione depletion and cell death (13), we then measured reduced (GSH) and oxidized (GSSG) glutathione following palmitoylcarnitine for 24 hours in HT29 and HepG2 cells. HT29 cells displayed signs of oxidative stress, as there was a palmitoylcarnitine-induced decrease in GSH (Figure 5.2A, $p < 0.05$), an increase in GSSG (Figure 5.2B, $p < 0.05$) and a decrease in the GSH/GSSG ratio (Figure 5.2C, $p < 0.05$). However, HepG2 cells showed an increase in both GSH (Figure 5.2D, $p < 0.05$) and GSSG (Figure 5.2E, $p < 0.05$) and no changes in GSH/GSSG (Figure 5.2F, $p < 0.05$).

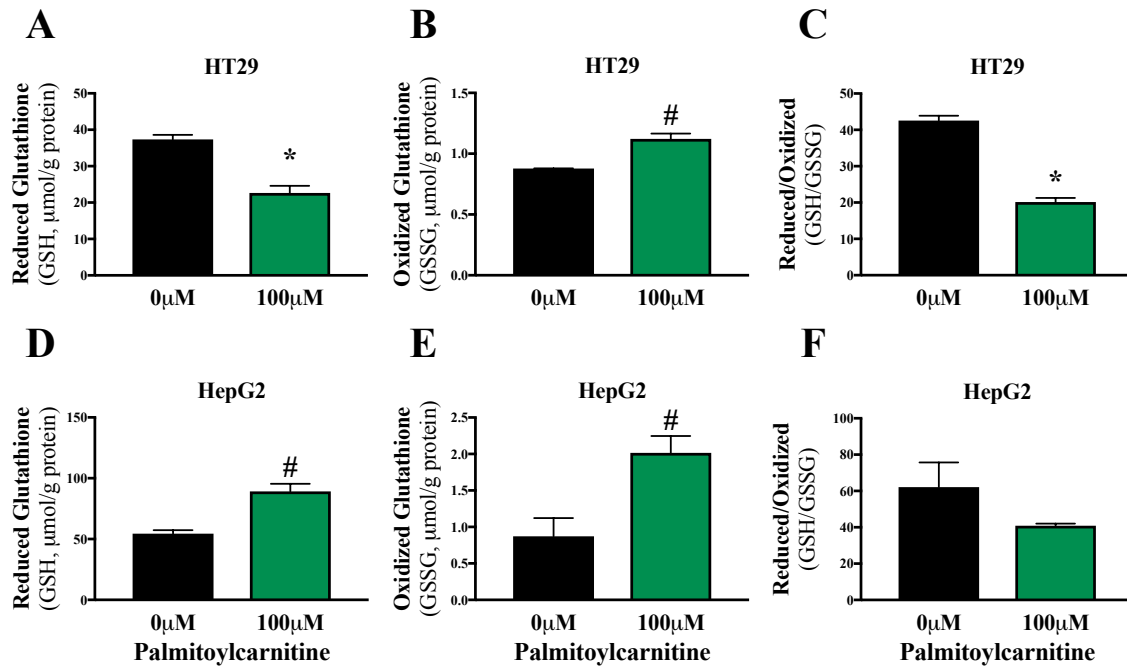


Figure 5.2 Redox stress following palmitoylcarnitine exposure: maintenance of overall redox conditions (GSH/GSSG) in HepG2 cells but not in HT29 cells. HepG2 and HT29 cells were incubated with 0 μM and 100 μM palmitoylcarnitine for 24 hours. **A and D** reduced glutathione (GSH), **B and E** oxidized glutathione (GSSG), **C and F** the ratio of reduced-to-oxidized glutathione (GSH/GSSG) was assessed (N=5). Data are reported as means ± SEM with ‘*’ representing a significant decrease and ‘#’ representing a significant increase with 100 μM palmitoylcarnitine compared to 0 μM. $P < 0.05$.

In agreement with HepG2 cells displaying an increase in mitochondrial respiratory kinetics following palmitoylcarnitine, HepG2 cells displayed a decrease in intracellular lactate (Figure 5.3A, $p < 0.05$). The decrease in lactate and increase in mitochondrial respiratory control suggests a shift from glycolysis to aerobic metabolism. However, despite these responses, there was a decrease in NAD(P)H following palmitoylcarnitine (Figure 5.3B, $p < 0.05$).

In HepG2 cells, H_2O_2 emission increased transiently by 10 minutes followed by a decrease at 24 hours (Figure 5.3C, $p < 0.05$). This reversal was related to an increase in total glutathione in HepG2 cells contrasted to decreasing total glutathione in HT29 cells

(Figure 5.3D, $p < 0.05$), suggesting a redox buffering mechanism may have been triggered by the initial H_2O_2 emission. To test this possibility, HepG2 cells were co-incubated with palmitoylcarnitine and the glutathione depleting agent buthionine sulfoximine (BSO). BSO prevented palmitoylcarnitine-induced growth (Figure 5.3E, $p < 0.05$, Figure 5.3G), but did not sensitize HepG2 cells to decreasing cell survival as observed in HT29 and HCT 116 cells. We then determined whether the reversal in H_2O_2 emission was related to a 2nd mechanism of mitochondrial uncoupling. The UCP2 inhibitor genipin caused marked sensitization of HepG2 cells to palmitoylcarnitine resulting in a drastic decrease in cell survival (Figure 5.3E, $p < 0.05$, Figure 5.3G), despite no change in UCP2 protein content in HepG2 cells (Figure 5.3F). Collectively, these findings support a model whereby palmitoylcarnitine stimulates acute increases in H_2O_2 , which leads to both an increase in total glutathione and UCP2 activation to ultimately decrease H_2O_2 and protect HepG2 cells (Figure 5.3H).

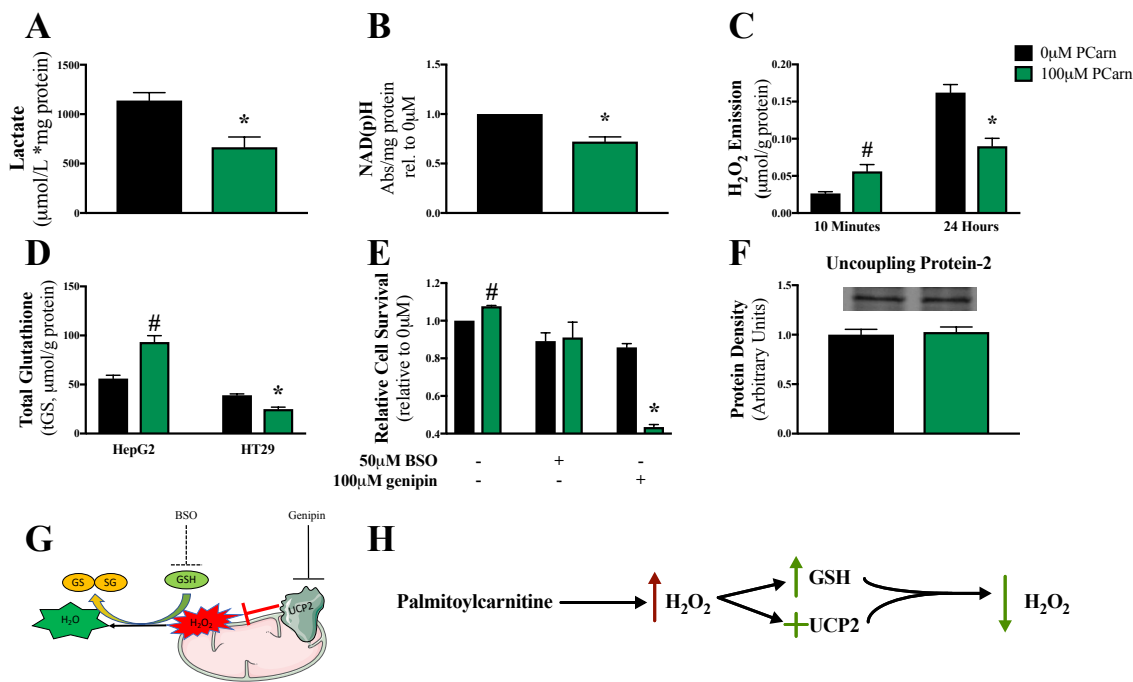


Figure 5 3 Palmitoylcarnitine alters H₂O₂, glutathione and growth in HepG2 cells. **A** Intracellular lactate (N=5) and **B** NAD(p)H (N=9) was measured in HepG2 cells following 24 hours of 0 μM or 100 μM palmitoylcarnitine. **C** H₂O₂ was assessed following 10 minutes and 24 hours of 0 μM and 100 μM palmitoylcarnitine (N=15). **D** Total glutathione was measured in HepG2 cells following 24 and 48 hours of 0 μM or 100 μM palmitoylcarnitine (N=5). **E** Relative cell survival was assessed in HepG2 cells following 48 hours of 0 μM or 100 μM palmitoylcarnitine as well as concurrent incubated with 50 μM buthionine sulfoximine or 100 μM genipin (N=3). **F** HepG2 cells were incubated with 0 μM and 100 μM palmitoylcarnitine for 24 hours and uncoupling protein-2 (UCP2) protein content was determined (N=5). **G** Schematic depicting the selective inhibition of UCP2 by genipin and the depletion of glutathione with buthionine sulfoximine (BSO). **H** Schematic of palmitoylcarnitine acutely triggering an increase in H₂O₂ emission, resulting in UCP2 activation and an increase in GSH, which in turn lowers H₂O₂ as well as stimulates an increase in growth. Data are reported as means \pm SEM with ‘*’ representing a significant decrease and ‘#’ representing a significant increase relative to 0 μM palmitoylcarnitine. $P < 0.05$.

Discussion

Unlike HT29 and HCT 116 colorectal carcinoma cells, HepG2 HCC cells were resistant to palmitoylcarnitine-induced decreases in cell survival and demonstrated a

small increase in growth by 48 hours. This protection in HepG2 cells was associated with increased mitochondrial respiratory kinetics concurrent with decreased intracellular lactate content, suggesting a shift towards a greater reliance on OXPHOS. Furthermore, inhibition of the glutathione redox couple prevented palmitoylcarnitine-induced HepG2 cell growth and UCP2 inhibition sensitized HepG2 cells to palmitoylcarnitine stress. These findings support a model that HepG2 cells invoke a cytoprotective response to palmitoylcarnitine that is associated with a mitochondrial and redox-based flexibility system (Figure 5.4).

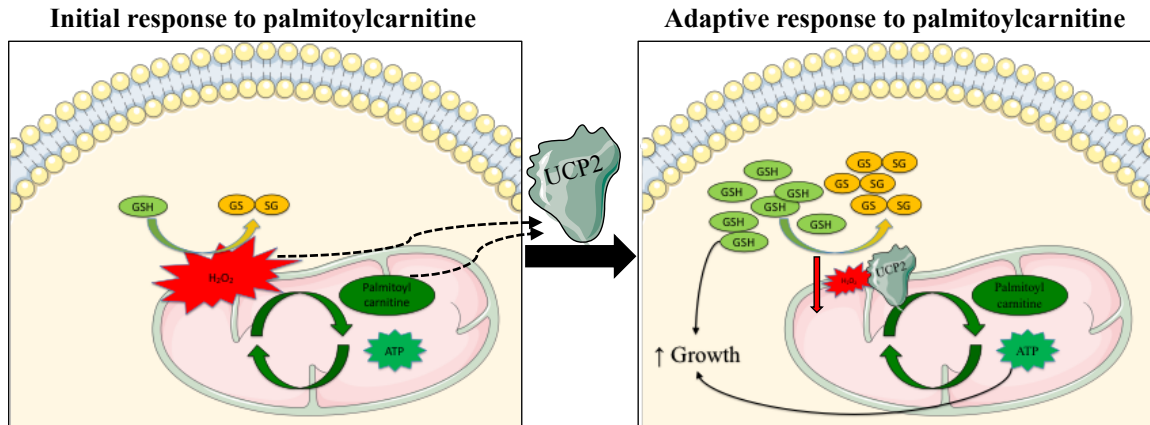


Figure 5.4 Proposed model of HepG2 cell adaptation to palmitoylcarnitine. The mitochondrial substrate, palmitoylcarnitine, stimulates an acute increase in H_2O_2 . A compensatory increase in glutathione and activation of UCP2 eventually lead to lower H_2O_2 emission. These hormetic responses to palmitoylcarnitine result in an increase in glutathione redox buffering capacity. An increase in oxidative capacity also improves ATP synthesis. Collectively, the metabolic and redox flexibility of HepG2 cells results in improved proliferation in response to palmitoylcarnitine in contrast to the abrogations observed in HT29 and HCT 116 cells.

Metabolic adaptations in HepG2 responses to palmitoylcarnitine

A dynamic series of metabolic and redox adaptations occurred within 48hr of palmitoylcarnitine exposure. First, a transient increase in H_2O_2 emission by 10 minutes was noted. This suggests that the reducing equivalents (NADH, $FADH_2$) generated by β -

oxidation may have exceeded a relatively low rate of OXPHOS in HepG2 cells consistent with the concept of electron slip in situations of excess reducing equivalent supply (16). The stimulation of H₂O₂ emission by 10 minutes may have preceded the increase in glutathione content at 24 hours that coincided with the maintenance of cell survival, in conjunction with the UCP2 dependency observed at 48 hours. While evidence suggests that UCP2 may not be a direct uncoupler of membrane potential (16), inhibition of UCP2 by genipin in HepG2 cells was previously shown to increase superoxide generation in response to palmitoylcarnitine in HepG2 cells (12), suggesting that UCP2 attenuates mitochondrial H₂O₂ emission in response to fatty acids (3). Collectively, the present findings suggest that the initial H₂O₂ emission at 10 minutes was related to activation of uncoupling via UCP2, although this latter point is speculative without measures of proton conductance (16).

In support of the current proposed model of redox flexibility in HepG2 cells, in mice fed a high fat diet, inhibition of UCP2 by genipin was able to prevent high fat diet induced liver damage (21), suggesting that UCP2 may be involved in the pathogenesis and progression of liver damage towards HCC development. Likewise, Huang et al. (10) demonstrated that glutathione is a critical regulator in HepG2 cell growth whereby depletion of glutathione through BSO stagnated growth whereas increasing glutathione levels triggered increases in HepG2 proliferation. Collectively, these previous findings align with the present study and support the proposed model that early induction of H₂O₂ by palmitoylcarnitine in HepG2 cells mediated cell survival through a UCP2-dependent attenuation of redox stress concurrent with increased glutathione content.

Another possible mechanism pertains to the increased mitochondrial respiratory capacity observed after palmitoylcarnitine treatment in HepG2 cells. 24 hours of palmitoylcarnitine increased ADP-stimulated mitochondrial respiration in conjunction with lower NAD(P)H content, which might suggest that NADH was oxidized to greater extents following this adaptive period. While NAD(P)H content on its own does not represent rate of generation or oxidation by the mitochondria, the greater respiratory kinetics following palmitoylcarnitine suggests the lower NAD(P)H was related to a greater rate of utilization. Indeed, lower lactate accumulation support this notion of a switch to mitochondrial OXPHOS following palmitoylcarnitine incubations. The lower NADH could, in theory, place less pressure on membrane potential-dependent superoxide generation, thereby explaining the lower H₂O₂ emission observed by 24 hours in addition to UCP2 induction discussed above.

Perspectives and Conclusions

The results in HepG2 cells suggest that fatty acid stress survival mechanisms through a dynamic relationship between oxidant generation and compensatory increases in glutathione redox buffering capacity. These observations may explain previous reports of HepG2 cell survival following direct exposure to fatty acids (19) and that glutathione is a critical regulator in not only promoting HepG2 survival but also driving the early induction of HepG2 cell growth (10). The present findings highlight how the interplay between metabolism and redox biology is not necessarily a predictable event of simple oxidative stress, but rather could manifest as a hormetic system that triggers an advantageous compensation promoting cancer cell growth. As such, this model could be

applied to determine how inherent metabolic and redox flexibility through H₂O₂ emission, OXPHOS, UCP2 activity and glutathione dynamics could confer protection from fatty acid stress.

Author contributions

P.C.T. and C.G.R.P. designed the study. P.C.T., C.F.T. and A.C.D. conducted experiments and analyzed data. All authors interpreted the findings. P.C.T. and C.G.R.P. wrote the manuscript. All authors approved the manuscript.

Conflict of interest

The authors declare that they have no conflicts of interest with the contents of this article.

Acknowledgements

We would like to thank Linda May of Dr. Mark Tarnopolsky's lab (McMaster University, Hamilton, Canada) for her technical assistance.

Funding

Funding was provided to C.G.R.P. by the National Science and Engineering Research Council (#436138-2013), with infrastructure supported by Canada Foundation for Innovation, the James. H. Cummings foundation and the Ontario Research Fund. P.C.T was supported by a NSERC CGS-PhD scholarship.

References

1. **Al-Bakheit A, Traka M, Saha S, Mithen R, and Melchini A.** Accumulation of Palmitoylcarnitine and Its Effect on Pro-Inflammatory Pathways and Calcium Influx in Prostate Cancer. *The Prostate* 76: 1326-1337, 2016.
2. **Baffy G.** Uncoupling protein-2 and non-alcoholic fatty liver disease. *Frontiers in bioscience : a journal and virtual library* 10: 2082-2096, 2005.
3. **Berardi MJ, and Chou JJ.** Fatty acid flippase activity of UCP2 is essential for its proton transport in mitochondria. *Cell metabolism* 20: 541-552, 2014.
4. **Boss O, Hagen T, and Lowell BB.** Uncoupling proteins 2 and 3: potential regulators of mitochondrial energy metabolism. *Diabetes* 49: 143-156, 2000.
5. **Brand MD, and Esteves TC.** Physiological functions of the mitochondrial uncoupling proteins UCP2 and UCP3. *Cell metabolism* 2: 85-93, 2005.
6. **Collins P, Jones C, Choudhury S, Damelin L, and Hodgson H.** Increased expression of uncoupling protein 2 in HepG2 cells attenuates oxidative damage and apoptosis. *Liver international : official journal of the International Association for the Study of the Liver* 25: 880-887, 2005.
7. **Dunigan DD, Waters SB, and Owen TC.** Aqueous soluble tetrazolium/formazan MTS as an indicator of NADH- and NADPH-dependent dehydrogenase activity. *BioTechniques* 19: 640-649, 1995.
8. **Galadari S, Rahman A, Pallichankandy S, and Thayyullathil F.** Reactive oxygen species and cancer paradox: To promote or to suppress? *Free radical biology & medicine* 104: 144-164, 2017.
9. **Hill-Baskin AE, Markiewski MM, Buchner DA, Shao H, DeSantis D, Hsiao G, Subramaniam S, Berger NA, Croniger C, Lambris JD, and Nadeau JH.** Diet-induced hepatocellular carcinoma in genetically predisposed mice. *Human molecular genetics* 18: 2975-2988, 2009.
10. **Huang ZZ, Chen C, Zeng Z, Yang H, Oh J, Chen L, and Lu SC.** Mechanism and significance of increased glutathione level in human hepatocellular carcinoma and liver regeneration. *FASEB journal : official publication of the Federation of American Societies for Experimental Biology* 15: 19-21, 2001.
11. **Hughes MC, Ramos SV, Turnbull PC, Edgett BA, Huber JS, Polidovitch N, Schlattner U, Backx PH, Simpson JA, and Perry CGR.** Impairments in left ventricular mitochondrial bioenergetics precede overt cardiac dysfunction and remodelling in Duchenne muscular dystrophy. *J Physiol* 2019.
12. **Ma S, Yang D, Li D, Tan Y, Tang B, and Yang Y.** Inhibition of uncoupling protein 2 with genipin exacerbates palmitate-induced hepatic steatosis. *Lipids in health and disease* 11: 154, 2012.
13. **Mailloux RJ.** Teaching the fundamentals of electron transfer reactions in mitochondria and the production and detection of reactive oxygen species. *Redox biology* 4: 381-398, 2015.
14. **Nedergaard J, and Cannon B.** The 'novel' 'uncoupling' proteins UCP2 and UCP3: what do they really do? Pros and cons for suggested functions. *Experimental physiology* 88: 65-84, 2003.
15. **Nicholls DG.** The Pancreatic beta-Cell: A Bioenergetic Perspective. *Physiological reviews* 96: 1385-1447, 2016.

16. **Nicholls DG, and Ferguson SJ.** In: *Bioenergetics (Fourth Edition)*, edited by Nicholls DG, and Ferguson SJ. Boston: Academic Press, 2013, p. ix-x.
17. **Seifert EL, Estey C, Xuan JY, and Harper ME.** Electron transport chain-dependent and -independent mechanisms of mitochondrial H₂O₂ emission during long-chain fatty acid oxidation. *The Journal of biological chemistry* 285: 5748-5758, 2010.
18. **Simon TG, King LY, Chong DQ, Nguyen LH, Ma Y, VoPham T, Giovannucci EL, Fuchs CS, Meyerhardt JA, Corey KE, Khalili H, Chung RT, Zhang X, and Chan AT.** Diabetes, metabolic comorbidities, and risk of hepatocellular carcinoma: Results from two prospective cohort studies. *Hepatology* 67: 1797-1806, 2018.
19. **Vendel Nielsen L, Krogager TP, Young C, Ferreri C, Chatgililoglu C, Norregaard Jensen O, and Enghild JJ.** Effects of elaidic acid on lipid metabolism in HepG2 cells, investigated by an integrated approach of lipidomics, transcriptomics and proteomics. *PloS one* 8: e74283, 2013.
20. **Wenzel U, Nickel A, and Daniel H.** Increased carnitine-dependent fatty acid uptake into mitochondria of human colon cancer cells induces apoptosis. *The Journal of nutrition* 135: 1510-1514, 2005.
21. **Zhong H, Liu M, Ji Y, Ma M, Chen K, Liang T, and Liu C.** Genipin Reverses HFD-Induced Liver Damage and Inhibits UCP2-Mediated Pyroptosis in Mice. *Cellular physiology and biochemistry : international journal of experimental cellular physiology, biochemistry, and pharmacology* 49: 1885-1897, 2018.

Chapter 6 Glutathione depletion through serine and glycine starvation sensitizes p53-null colorectal cancer cells to auranofin

Turnbull PC, Dehghani AC, Deep B, Hughes MC, Delfinis L, Abdul-Sater AA, and Perry CGR. Glutathione depletion through serine and glycine starvation sensitizes p53-null colorectal cancer cells to auranofin. 2019 – *In preparation*

Author Contributions: Patrick C. Turnbull (PCT) carried out the majority of experiments for this project, with the exception of the following. ACD performed many of the HT29 cell experiments. BD and AAAS helped with non-published additional shRNA knockdown experiments and overall cell handling. MCH and LD conducted much of the mitochondrial respiration experiments. PCT and CGRP wrote the manuscript.

Glutathione depletion through serine and glycine starvation sensitizes p53-null colorectal cancer cells to auranofin

Authors: Patrick C. Turnbull, Ali C. Dehghani, Bipin Deep, Meghan C. Hughes, Luca Delfinis, Ali A. Abdul-Sater, Christopher G. R. Perry

Affiliations:

School of Kinesiology and Health Science, Muscle Health Research Centre, York University, 4700 Keele Street, Toronto, ON, Canada, M3J 1P3.

†Address for Correspondence:

Christopher Perry

School of Kinesiology and Health Science

Muscle Health Research Centre

344 Norman Bethune College

York University

4700 Keele Street

Toronto, Ontario M3J 1P3

(P) 416 736 2100 ext. 33232

cperry@yorku.ca

Abstract

Auranofin inhibits thioredoxin reductase, rendering the thioredoxin antioxidant system incapable of functioning, and has gained recent popularity as a potential antineoplastic therapy. However, it is likely that the coordinated inhibition of thioredoxin and glutathione, the main intracellular antioxidant, is required for potent anticancer effects. Serine and glycine (S&G) starvation has been demonstrated to elicit p53^{-/-} glutathione depletion, whereas p53^{+/+} cells were less sensitive. Therefore, the purpose of this study was to determine whether thioredoxin inhibition with auranofin coupled with S&G starvation selectively abrogates p53^{-/-} colorectal cancer proliferation. HCT 116 p53^{+/+} and p53^{-/-} cells were incubated with or without auranofin and S&G. p53^{-/-} cells were resistant to auranofin relative to p53^{+/+}, however this was overcome by the coordinated starvation of S&G. N-acetylcysteine and exogenous glutathione were able to rescue both p53^{+/+} and p53^{-/-}. Auranofin treatment resulted in a compensatory increase in glutathione in p53^{-/-} cells, this compensatory increase was prevented when p53^{-/-} cells were incubated with auranofin but without S&G. Nrf2 is a transcription factor responsible for increasing many antioxidant response genes. When Nrf2 was pre-activated prior to auranofin exposure, p53^{+/+} cells were dose-dependently rescued primarily when S&G were present, yet when Nrf2 was concurrently inhibited along with auranofin; p53^{-/-} cells were sensitized to auranofin-induced decreasing cell survival. This data suggests that p53^{-/-} are resistant to auranofin through a compensatory increase in glutathione and that S&G starvation renders p53^{-/-} cells susceptible to auranofin. This demonstrates the potential for overriding p53^{-/-} cell insensitivity to auranofin through coordinated glutathione depletion by S&G starvation.

Introduction

Despite the presence of oxygen, many cancers rely on non-mitochondrial glycolysis as their main source of ATP production, this is known as the Warburg effect [1]. These associated alterations in energy metabolism confer many cellular benefits resulting in a pro-growth environment [2]. The generation of reactive oxygen species (ROS), such as hydrogen peroxide (H_2O_2), is often associated as a byproduct of growth. As cancers are in a state of constant growth, they are reliant on antioxidant buffering systems, which utilize intracellular antioxidants, glutathione and thioredoxin, to combat elevations in H_2O_2 [3]. Both glutathione and thioredoxin have previously been implicated in conferring pro-growth advantages and chemoresistance in cancers. For example, relationships between both glutathione [4] and thioredoxin [5] systems and levels of cisplatin resistance have been established in a variety of cancers. Thioredoxin system proteins are often elevated in cancers [6], and the experimental generation of cisplatin-resistant HT29 and St-4 cells resulted in an adaptive ~2.5-fold increase in thioredoxin in the cisplatin-resistant cell lines relative to their parental controls [7]. Similar to thioredoxin, glutathione is also often elevated in many cancers [8], and increased intratumoural glutathione levels at the time of diagnosis conferred with worse disease progression in colorectal carcinoma patients [9].

Auranofin is a gold complex drug historically used to treat rheumatoid arthritis [10]. It has gained recent popularity as a cancer therapeutic as it functions through the inhibition of thioredoxin reductase [11], effectively inhibiting the thioredoxin system. However, glutathione compensation is a concern with thioredoxin inhibition as glutathione is the most abundant intracellular antioxidant, and is therefore implicated in

both ROS handling and cell fate [12]. Harris et al. [13] demonstrated that glutathione is a critical regulator for cancer initiation. However, it appears that glutathione becomes less important in later stages of cancer progression due to the redundant action of thioredoxin. Coordinated inhibition of both glutathione (through buthionine sulfoximine – BSO) and thioredoxin (through auranofin) was able to display potent cancer cell death in spontaneous tumour forming mice [13]. However, systemic inhibition of both glutathione and thioredoxin may lead to off-target effects given the importance of redox buffering for healthy cell function. Furthermore, while BSO is a potent mechanistic glutathione-depleting agent, it appears to have limited efficacy in humans, as intravenous human BSO administration failed to deplete glutathione levels to a significant degree [14].

Serine and glycine are two non-essential amino acids and are critical components in glutathione synthesis [15]. It has been previously demonstrated that serine and glycine starvation leads to a marked depletion of glutathione levels and eventual cell death, and this response was significantly heightened in HCT 116 p53^{-/-} cells relative to HCT 116 p53^{+/+} cells [15]. This is critical given that ~50% of human cancers display mutations in the *TP53* gene, resulting in hyper-aggressive cancer growth and apoptotic and chemoresistance [16]. Preliminary data from our lab demonstrates that HCT 116 p53^{-/-} cells relative to HCT 116 p53^{+/+} cells are significantly less sensitive to auranofin. Which is consistent with previous data demonstrating increased chemoresistance in p53^{-/-} cells such that HCT 116 p53^{-/-} cells were less sensitive to 5-FU and oxaliplatin relative to HCT 116 p53^{+/+} cells [17]. As such, it is possible that targeted depletion of glutathione in p53^{-/-} cancer cells by serine and glycine deprivation would uniquely sensitize these cells to

thioredoxin inhibition by auranofin, which is otherwise tolerated by non-cancerous p53^{+/+} cells.

The purpose of this study was to first determine whether HCT 116 p53^{-/-} cells are less sensitive to auranofin compared to HCT 116 p53^{+/+} cells, and secondly, to determine whether HCT 116 p53^{-/-} cells could be sensitized to auranofin through coordinated glutathione depletion by serine and glycine starvation. While we were unable to recapitulate previous results that demonstrated increased sensitivity of HCT 116 p53^{-/-} cells to serine and glycine starvation [15], we demonstrate that HCT 116 p53^{-/-} cells are insensitive to auranofin-induced cell death at a concentration that is effective in HCT 116 p53^{+/+} cells. Using serine and glycine deprivation, we show that this resistance in p53^{-/-} is attributed to a compensatory increase in glutathione, resulting in heightened cell protection from H₂O₂. This heightened cell protection can be over-ridden by starvation of serine and glycine and exploited as a means of sensitizing these cells to auranofin-induced cell death.

Experimental procedures

Cell culture

HCT 116 p53^{+/+} and HCT 116 p53^{-/-} colon adenocarcinoma cells and HT29 colon adenocarcinoma cells were generously gifted from Dr. Samuel Benchimol (York University, Toronto, Canada). Cells were passaged in DMEM supplemented with 10% fetal bovine serum (Wisent Inc, Saint-Jean-Baptiste, QC, Canada) and 1% penicillin/streptomycin (Wisent Inc). For experimental conditions, cells were seeded in desired culture dishes in condition media similar to previously published [15] with serine

and glycine. Following up to 72 hours, cells were exposed to condition media with or without serine and glycine and 1 μ M auranofin (Tocris Bioscience, Bristol, UK). In addition to auranofin and serine and glycine manipulations, in separate experiments cells were also treated with N-acetyl cysteine (NAC), reduced glutathione (GSH), 3H-1,2-dithiole-3-thione (D3T) and *N*-[4-[2,3-Dihydro-1-(2-methylbenzoyl)-1*H*-indol-5-yl]-5-methyl-2-thiazolyl]-1,3-benzodioxole-5-acetamide (ML 385) (Sigma-Aldrich).

Relative cell survival

The crystal violet assay was used to determine relative cell survival [18]. Cells were treated for up to 72 hours in 96-well optical bottom black walled plates (ThermoFisher Scientific). Following treatment time, cells were fixed using 10% formalin (Sigma-Aldrich) for 10 minutes. Formalin was subsequently removed and 0.5% crystal violet (Sigma-Aldrich) solution in 25% MeOH was added for 10 minutes. Following crystal violet staining, wells were rinsed clean with water and dried overnight. Relative cell survival was visualized as crystal violet fluorescence conducted using the LiCor odyssey scanner (LiCor Biosciences, Lincoln, NE, USA) and fluorescent density analysis was conducted using LiCor software.

Glutathione

Glutathione was measured as previously published [19]. Both reduced (GSH) and oxidized (GSSG) glutathione were measured using a Shimadzu Nexera X2 UPLC system (Mandel Scientific Company inc. Guelph, Canada) and separation was achieved using a Zorbax C18 column (Agilent Technologies, Mississauga, ON, Canada). Following

experimental conditions for 24 and 48 hours, cells were washed with PBS and scraped in 50mM TRIS based buffer (pH 8.0 with HCl) with 20mM boric acid (Sigma-Aldrich), 2mM L-serine (Sigma-Aldrich), 20µM acivicin (Enzo Life Sciences, NY, USA) and 5mM N-ethylmaleimide (Sigma-Aldrich). Cell suspension was used for GSH and GSSG determination as well as protein concentration was assessed with BCA (ThermoFisher Scientific) according to kit instructions.

GSH

This method was adapted from Giustriani et al. [20]. Following cell scraping, cells were deproteinated in 10µl trichloroacetic acid with 100µl cells in suspension. GSH samples were run under isocratic conditions using a 0.25% glacial acetic acid mobile phase with 6% acetonitrile at a flow rate of 1.05ml/min. GSH was detected using a modular UV-VIS detector (Shimadzu) detector at 265nm wavelength.

GSSG

This method was adapted from Kand'ar et al. [21]. Cells were deproteinated in equal parts 15% perchloric acid to sample volume. 100µl of deproteinated sample was added to 500µl of 0.5M NaOH. 37.5µl of 0.1% o-phthalimide in methanol was added and incubated for 15 minutes rocking in the dark creating a GS-OPA conjugate. Following incubation, samples were transferred to HPLC autosampler vials and ready for column separation. GSSG samples were run under isocratic conditions using a 25mM Na₂HPO₄ in HPLC grade water with 15% methanol mobile phase at a flow rate of 0.5ml/min.

GSSG was excited at 350nm and emission was detected at 420nm using a HPLC/UHPLC fluorescence detector (Shimadzu).

Mitochondrial bioenergetics assessment

Cell preparation

Cells were seeded in 10cm dishes for 24 hours. Cells were trypsin harvested, washed in PBS and re-suspended in mitochondrial respiration media (MIRO5, in mM): 0.5 EGTA, 10 KH₂PO₄, 3 MgCl₂·6 H₂O, 60 K-lactobionate, 20 HEPES, 20 Taurine, 110 sucrose and 1 mg/ml fatty acid free BSA (pH 7.1) supplemented with 20mM creatine. Cells were then permeabilized with 10ug/ml digitonin (Sigma-Aldrich, St. Louis, MO, USA) for 30 minutes rocking at room temperature. Cells were pelleted, and re-suspended in 105µl MIRO5, with 5µl subsequently removed to determine protein content, while the remaining 100µl was used for high-resolution respirometry.

Cells suspended in mitochondrial respiration media (MIRO5) were loaded into the Oroboros Oxygraph-2k (Oroboros Instruments, Corp., Innsbruck, Austria) system. Total volume was 2mls, spinning at 750 rpm at 37°C. To determine ADP-stimulated respiration, 5mM pyruvate and 2mM malate were added as complex I substrates, followed by ADP titrations of 25µM, 500µM and 5mM ADP. Polarographic oxygen measurements were acquired in 2 s intervals with the rate of respiration derived from 40 data points and expressed as pmol/s/mg protein.

Western blotting

Cells were seeded in 6-well plates. Following experimental conditions, cells were washed with PBS then scraped into 68mM TRIS-HCl buffer containing 2% SDS, 10% glycerol, protease and phosphatase inhibitors (Sigma-Aldrich), on ice and subsequently boiled for 10 minutes. Cells were then vortexed and centrifuged at 10,000RPM for 10 minutes. Supernatant was collected and stored in -80°C until further analysis. Hybridoma generated PAb 421 p53 antibody was provided by Dr. Samuel Benchimol. Cleaved Parp and p-p53^{ser46} antibody cocktail (p53 mediated apoptosis WB cocktail, Abcam ab140360), 4-hydroxynoneal (4-HNE, Abcam ab ab46545), glutathione reductase antibody (SAB4200182, Sigma-Aldrich), were used.

Statistics

Data is reported as mean \pm SEM. Significance is reported as $p < 0.05$ for all measures. Each 'N' signifies an individual experiment, with each experiment conducted in triplicate where appropriate. For the comparison of only two groups, unpaired t-tests were used. For the comparison of more than two groups, ANOVA's were performed. Following significance of a two-way ANOVA, a Fisher's LSD *post-hoc* was performed on appropriate groups. All statistics were performed using GraphPad Prism 7 (San Diego, CA, USA).

Results

p53 knockout results in decreased complex I capacity, decreased steady-state H₂O₂ and increased glutathione

In order to determine baseline metabolic phenotypic alterations, HCT 116 p53^{+/+} and p53^{-/-} cells (Figure 6.1A) were subject to examination of mitochondrial oxygen consumption, glutathione and steady-state H₂O₂ emission. Consistent with previous data demonstrating that HCT 116 p53^{-/-} cells displayed decreased O₂ consumption relative to HCT 115 p53^{+/+} cells [22], HCT 116 p53^{+/+} cells displayed increased complex I-supported mitochondrial respiration compared to HCT 116 p53^{-/-} cells ($p < 0.05$, Figure 6.1B), as well as greater steady-state H₂O₂ levels in HCT 116 p53^{+/+} cells relative to HCT 116 p53^{-/-} cells ($p < 0.05$, Figure 6.1C). Despite the apparent decrease in oxidative reliance in HCT 116 p53^{-/-} cells, HCT 116 p53^{-/-} cells displayed higher intracellular total glutathione levels ($p < 0.05$, Figure 6.1D). These data suggests that HCT 116 p53^{-/-} cells display an altered metabolic phenotype resulting in increased basal glutathione levels.

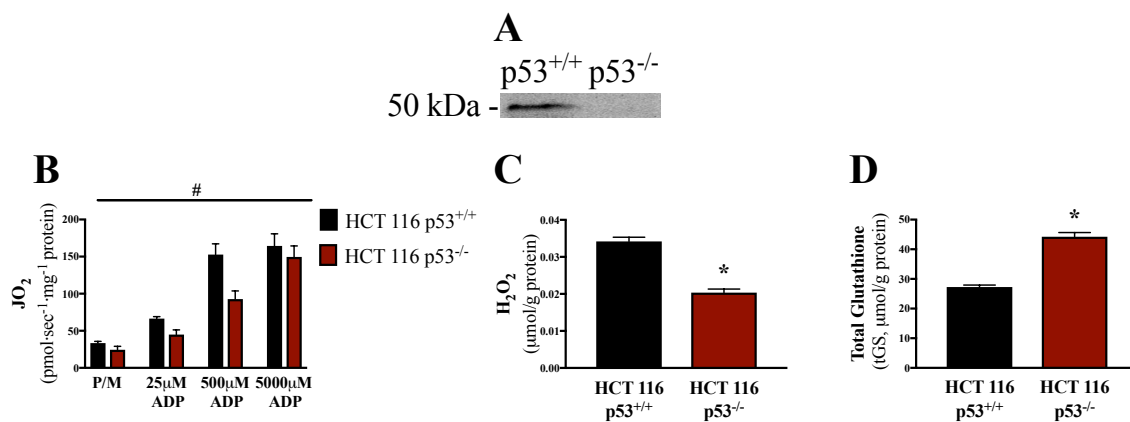


Figure 6.1 HCT 116 p53^{+/+} cells display greater oxidative characteristics despite lower glutathione relative to HCT 116 p53^{-/-} cells. **A** HCT 116 p53^{+/+} and p53^{-/-} cells were assessed for p53 protein content. **B** ADP supported mitochondrial respiration was measured in HCT 116 p53^{+/+} and p53^{-/-} cells (N=4-8). Data are reported as means \pm SEM with ‘#’ representing a main effect for p53 status. $P < 0.05$. **C** H₂O₂ emission (N=14) and **D** total glutathione (N=8-10) was assessed in HCT 116 p53^{+/+} and p53^{-/-} cells. Data are reported as means \pm SEM with ‘*’ representing a significant difference between groups. $P < 0.05$.

HCT 116 p53^{-/-} cells are insensitive to auranofin-induced cell death, yet the coordinated starvation of serine and glycine overcomes this insensitivity

As reported previously, in the presence of serine and glycine, cancer cells typically rely on anaerobic pathways of glycolysis for ATP production (Figure 6.2A). With the removal of serine and glycine, glycolytic intermediates are re-directed towards serine biosynthesis and a subsequent increase in mitochondrial activity is required in order to maintain ATP levels for cell viability. This metabolic redirection results in potential increases in H₂O₂, allowing for further decreases in glutathione levels associated with serine and glycine starvation (Figure 6.2B) [15].

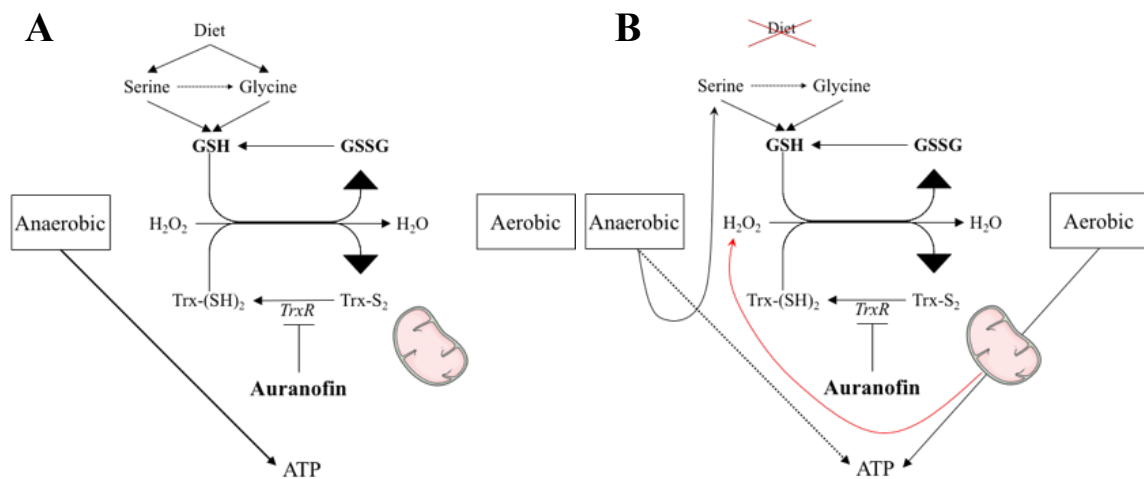


Figure 6 2 Auranofin-induced thioredoxin inhibition coupled with glutathione depletion through serine and glycine starvation renders the cell sensitive to oxidative stress. A Typical cancer cell metabolism functions through glycolytic ATP production despite the presence of oxygen, while reduced glutathione (GSH) is synthesized from serine and glycine. **B** In the absence of serine and glycine, glycolytic intermediates are shunted towards *de novo* serine production, resulting in increased mitochondrial activity. While, serine and glycine starvation renders the cell incapable of producing new glutathione, coupled with auranofin renders the cell vulnerable to oxidative stress.

HCT 116 p53^{+/+} and p53^{-/-} cells were incubated in conditioned media with or without serine, glycine and auranofin for up to 72 hours (Figure 6.3A and 6.3B). Relative to

complete conditioned media, both cell lines displayed a moderate slowing of growth in the absence of serine and glycine ($p < 0.05$), and HCT 116 p53^{+/+} cells had significantly decreased cell survival with auranofin regardless of serine and glycine status within the media ($p < 0.05$). Alternatively, HCT 116 p53^{-/-} cells were insensitive to auranofin alone as these cells still grew relative to earlier time points, yet auranofin combined with serine and glycine starvation resulted in a significant decline in cell growth and resulted in decreased cell survival relative to earlier time points ($p < 0.05$). Cell survival of HCT 116 p53^{+/+} and p53^{-/-} cells with or without auranofin and serine and glycine was mimicked using a trypan blue exclusion assay to determine cell viability ($p < 0.05$, Figure 6.3C and 6.3D). Furthermore, HCT 116 p53^{+/+} cells demonstrated an increase in phospho-p53^{ser46} content (Figure 6.3E), suggesting a likely activation of p53-mediated apoptotic signaling [23].

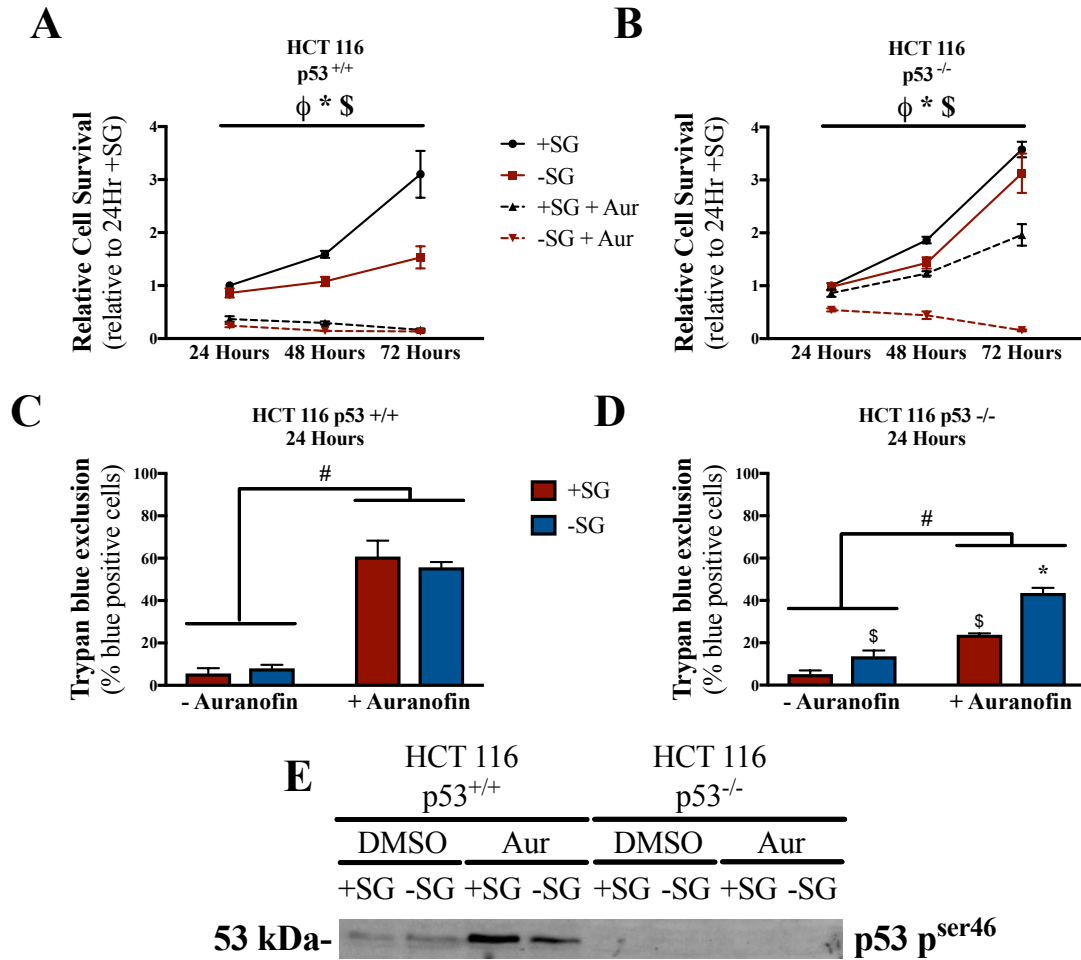


Figure 6 3 Combined serine and glycine starvation sensitizes HCT 116 p53^{-/-} cells to auranofin. **A and B** Relative cell survival of HCT 116 p53^{+/+} and p53^{-/-} cells incubated for 24 (N=9), 48 (N=9) and 72 hours (N=3) with or without auranofin (AUR) and serine and glycine (SG) Data are reported as means \pm SEM with ‘ ϕ ’ representing a main effect for time, ‘*’ representing a main effect for condition media and ‘\$’ representing an interaction. $P < 0.05$. **C and D** Trypan blue exclusion was measured in HCT 116 p53^{+/+} and p53^{-/-} cells following 24 hours of treatment (N=4). Data are reported as means \pm SEM with ‘#’ representing a main effect for auranofin, ‘\$’ representing a significant difference between all groups yet not different from each other, ‘*’ representing a significant difference from all groups. $P < 0.05$. **E** The phosphorylation of p53 at serine residue 46 was determined following 24 hours of treatment in HCT 116 p53^{+/+} and HCT 116 p53^{-/-} cells.

As auranofin coupled with serine and glycine starvation was theorized to elicit antineoplastic effects through increasing cellular susceptibility to oxidative stress, cell

survival was measured in HCT 116 p53^{+/+} and p53^{-/-} cells incubated with auranofin and starved of serine and glycine in the presence and absence of exogenous antioxidants N-acetylcysteine (NAC, Figure 6.4A and 6.4B) and reduced glutathione (GSH, Figure 6.4C and 6.4D) for up to 48 hours. Both NAC and exogenous GSH were able to rescue HCT 116 p53^{+/+} and p53^{-/-} cells from auranofin coupled with serine and glycine starvation ($p < 0.05$). This suggests that combined auranofin and serine and glycine starvation function through a ROS dependent pathway to elicit deleterious effects.

Nuclear factor erythroid-derived 2-like 2 protein (Nrf2) is a redox sensitive transcriptional regulator of glutathione synthesis as well as other antioxidant genes. In order to determine the role of Nrf2 during auranofin and serine and glycine starvation, Nrf2 was pre-activated with D3T in HCT 116 p53^{+/+} cells 24 hours prior to experimental conditions (Figure 6.4E and 6.4F). Nrf2 pre-activation dose-dependently elicited protective effects against auranofin, yet was less efficacious when auranofin was coupled with serine and glycine starvation ($p < 0.05$). Furthermore, Nrf2 inhibition by ML 385 in HCT 116 p53^{-/-} cells sensitized these cells to auranofin despite serine and glycine status ($p < 0.05$, Figure 6.4G and 6.4H). It is therefore possible that HCT 116 p53^{+/+} cells are sensitive to auranofin as they undergo oxidative stress caused by auranofin resulting in p53-mediated cell death, while HCT 116 p53^{-/-} cells are insensitive to auranofin as without p53, they likely engage Nrf2 and increase antioxidant defence mechanisms, such as glutathione, resulting in a compensatory cell protection against thioredoxin inhibition.

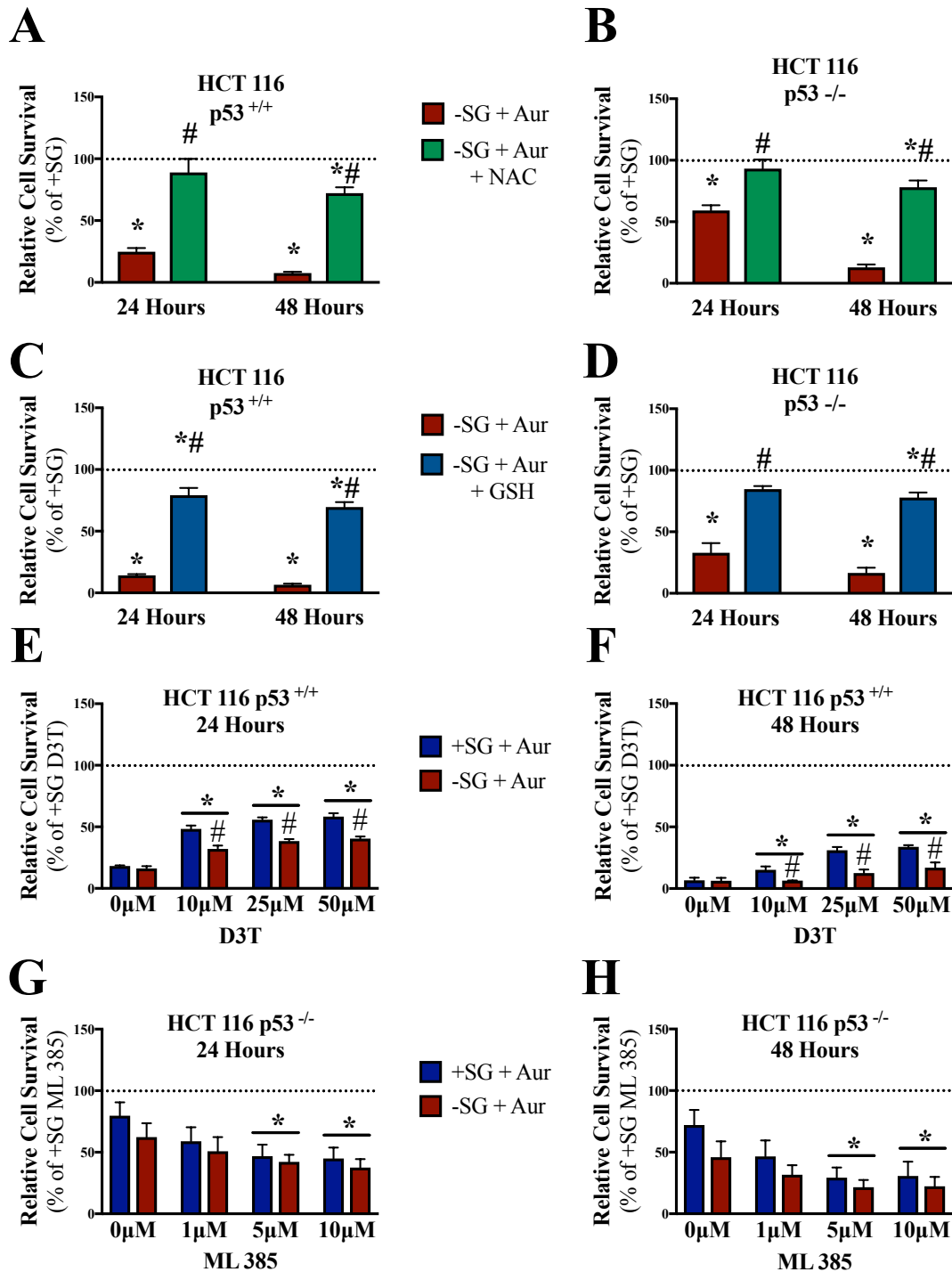


Figure 6 4 Altering cell survival through manipulating antioxidant related pathways. Relative cell survival was measured in HCT 116 p53^{+/+} and p53^{-/-} cells following incubation with or without auranofin (AUR) and serine and glycine (SG) as well as **A and B** N-acetylcysteine (NAC, N=6-9) and **C and D** exogenous reduced glutathione (GSH, N=6). Data are reported as means ±SEM, ‘*’ representing a significant difference relative to +SG without auranofin, ‘#’ representing a significant difference relative to -SG + auranofin. *P* < 0.05. **E and F** D3T stimulated Nrf2 activation (N=3) and

G and H ML 385 stimulated Nrf2 inhibition (N=3). Data are reported as means \pm SEM, ‘*’ representing a significant increase relative to 0 μ M D3T or ML 385, ‘#’ representing a significant difference between +SG and –SG of the same Nrf2 manipulating condition. $P < 0.05$.

Serine and glycine starvation resulted in elevated H₂O₂ emission regardless of p53 status, yet coupled with auranofin resulted in variable responses in glutathione

Serine and glycine starvation resulted in an increase in H₂O₂ emission regardless of p53 status ($p < 0.05$, Figure 6.5A). In conjunction with cell survival, HCT 116 p53^{+/+} cells demonstrate decreased total glutathione levels with auranofin ($p < 0.05$, Figure 6.5B and 6.5C). While HCT 116 p53^{-/-} cells respond to auranofin through increased glutathione, auranofin combined with serine and glycine starvation prevented this compensatory increase, resulting in a significant decrease in total glutathione relative to untreated cells ($p < 0.05$, Figure 6.5D and 6.5E).

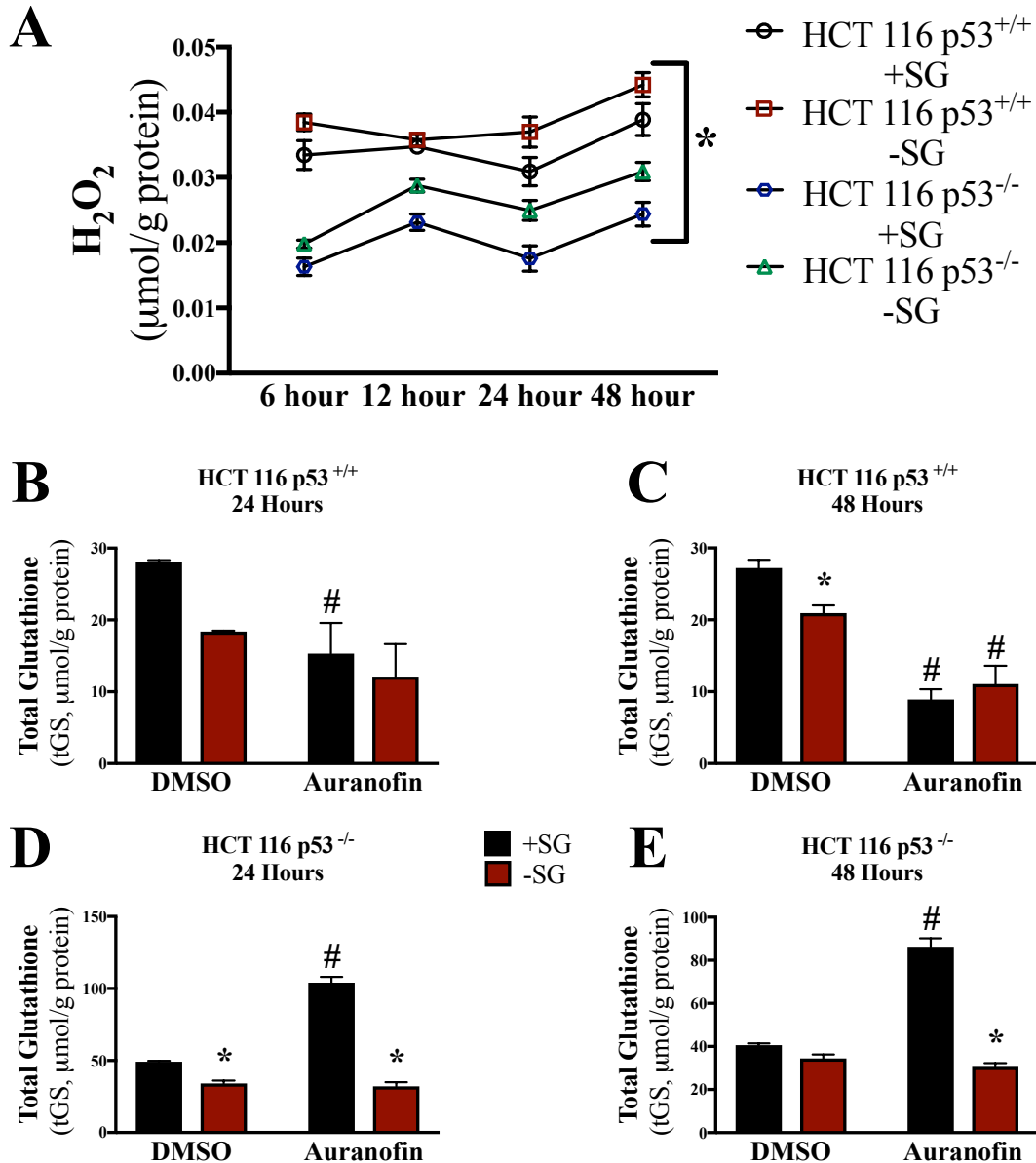


Figure 6 Serine and glycine starvation results in increased H₂O₂ emission and altered glutathione responses between HCT 116 p53^{+/+} and p53^{-/-} cells. **A** H₂O₂ emission (N=9) and **B – E** total glutathione (N=4-5) was measured in HCT 116 p53^{+/+} and p53^{-/-} cells following incubation with or without auranofin (AUR) and serine and glycine (SG). Data are reported as means ±SEM, ‘*’ representing a significant difference between adjacent groups, ‘#’ representing a significant difference relative to +SG without auranofin. *P* < 0.05.

In response to auranofin, HCT 116 p53^{+/+} cells display decreased reduced (GSH, Figure 6.6A and 6.6B) and oxidized (GSSG, Figure 6.6E and 6.6F) glutathione (*p* < 0.05). HCT

116 p53^{-/-} cells, however, display a compensatory increase in GSH (Figure 6.6C and 6.6D) and GSSG (Figure 6.6G and 6.6H), and coupled with serine and glycine starvation, GSH and GSSG responses differ. Auranofin coupled with serine and glycine starvation results in a near abolishment of GSH in HCT 116 p53^{-/-} cells ($p < 0.05$). While there is a decrease in GSSG, GSSG levels remain elevated over control, suggesting that HCT 116 p53^{-/-} cells are unable to produce new GSH, yet elevated levels of GSSG remain high.

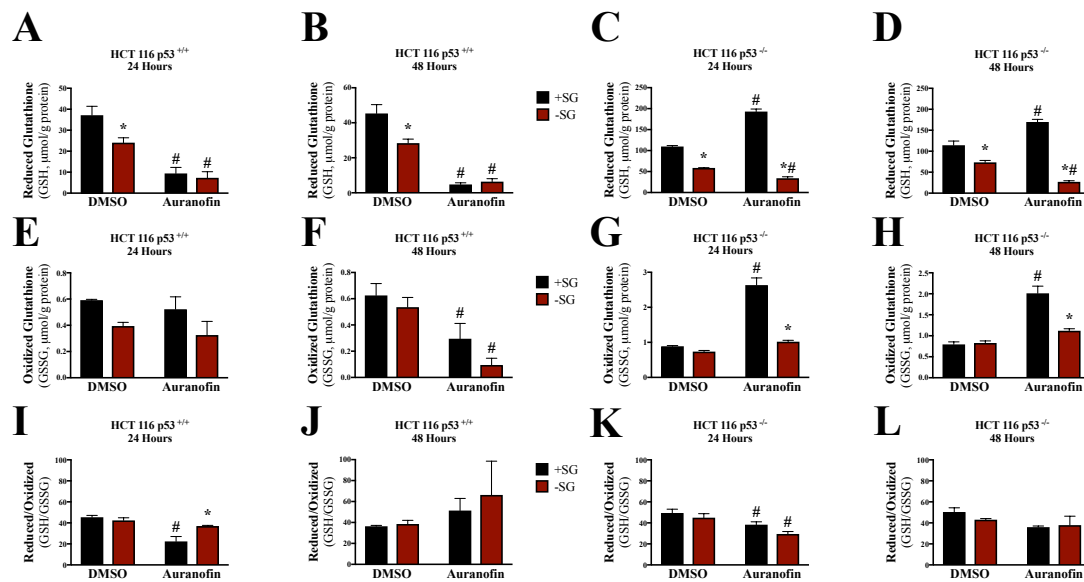


Figure 6.6 Auranofin induces a compensatory increase in glutathione in HCT 116 p53^{-/-} cells but not HCT 116 p53^{+/+} cells. A – D reduced glutathione (GSH) E – H oxidized glutathione (GSSG) and I – L GSH/GSSG ratio was measured in HCT 116 p53^{+/+} (N=4) and p53^{-/-} cells (N=5) following incubation with or without auranofin (AUR) and serine and glycine (SG). Data are reported as means \pm SEM, ‘*’ representing a significant difference within DMSO or auranofin conditions, ‘#’ representing a significant difference relative to +SG without auranofin. $P < 0.05$.

HT29 p53^{mutant} colorectal carcinoma cells display insensitivity towards auranofin, yet are sensitized through combined serine and glycine starvation

In order to further validate the role of p53 in determining cell fate when exposed to auranofin, and whether this resistance can be overridden with the coordinated removal

of serine and glycine, HT29 cells, which have mutated p53 (p53^{mutant}), were exposed to auranofin with and without serine and glycine. Similar to HCT 116 p53^{-/-} cells, cell survival was marginally influenced by auranofin or serine and glycine starvation alone, however in combination, resulted in a significant decrease in cell survival ($p < 0.05$, Figure 6.7A). This decrease in cell survival was rescued by NAC and exogenous GSH ($p < 0.05$, Figure 6.7B). Similarly, auranofin induced a compensatory increase in glutathione, which was negated when auranofin was incubated without serine and glycine, in which glutathione levels were undetectable ($p < 0.05$, Figure 6.7C and 6.7D). In conjunction with a compensatory increase in total glutathione levels, glutathione reductase was increased following auranofin treatment ($p < 0.05$, Figure 6.7F), which is indicative of Nrf2 activation in response to auranofin as glutathione reductase is a downstream target of Nrf2. Furthermore, 4-HNE (Figure 6.7G) and cleaved PARP (Figure 6.7H) protein content were solely increased in HT29 cells when exposed to auranofin coupled with serine and glycine starvation ($p < 0.05$).

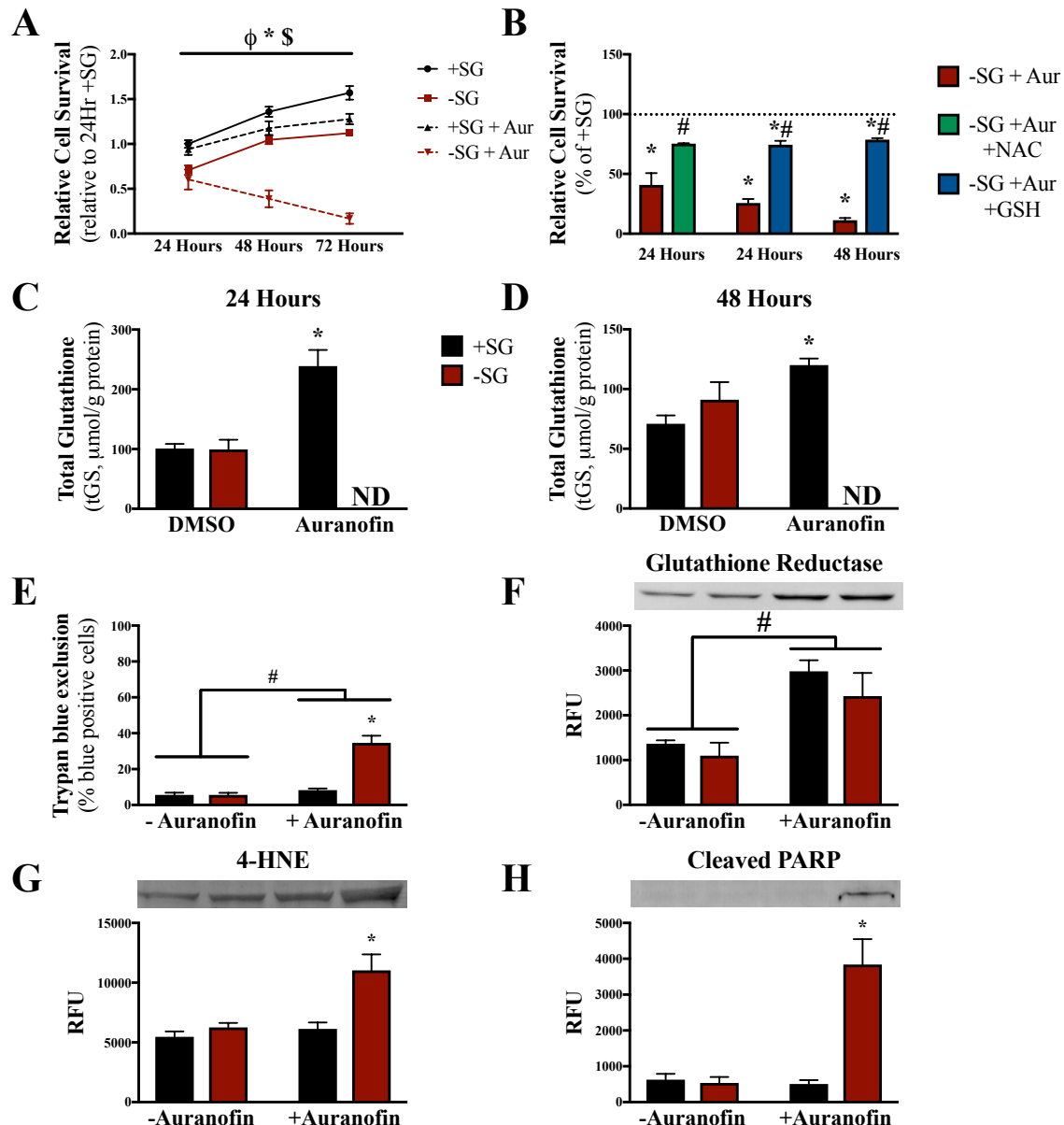


Figure 6 7 HT29 p53^{mutant} cell insensitivity to auranofin is overcome by coordinated serine and glycine starvation. HT29 p53^{mutant} cells were treated with or without auranofin (AUR) and serine and glycine (SG) and **A** relative cell survival (N=3-6). Data are reported as means \pm SEM with ‘ ϕ ’ representing a main effect for time, ‘*’ representing a main effect for condition media and ‘\$’ representing an interaction. $P < 0.05$. In addition, cell survival was also measured **B** with NAC and exogenous GSH (N=3-6). Data are reported as means \pm SEM, ‘*’ representing a significant difference relative to +SG without auranofin, ‘#’ representing a significant difference relative to -SG + auranofin. As well as **C and D** total glutathione (N=3), **E** trypan blue exclusion (N=4), protein content of **F** glutathione reductase (N=4), **G** 4-HNE (N=4) and **H** cleaved PARP (N=5). Data are reported as means \pm SEM, with ‘#’ representing a main effect for auranofin and ‘*’ representing a significant difference relative to all groups. $P < 0.05$.

Discussion

Auranofin caused marked decreases in cell survival in HCT 116 p53^{+/+} cells, however HCT 116 p53^{-/-} cells and p53^{mutant} HT29 cells were insensitive. To combat the inhibition on thioredoxin, HCT 116 p53^{-/-} cells and HT29 cells were able to increase glutathione levels, likely through Nrf2 mediated pathways. Resistance to auranofin was overcome when HCT 116 p53^{-/-} cells and HT29 cells were coordinately incubated without serine and glycine, preventing the increase in glutathione resulting in significant decreases in cell survival. The loss in cell survival appears to be driven primarily by exposure to H₂O₂ given that the antioxidants NAC and GSH were able to protect all cells from auranofin regardless of serine and glycine. The pre-incubation of HCT 116 p53^{+/+} cells with the Nrf2 activator, D3T, was able to dose dependently protect HCT 116 p53^{+/+} cells from auranofin. However, this was primarily observed in cells with serine and glycine, as the starvation of serine and glycine likely prevented Nrf2-induced increases in glutathione synthesis, therefore preventing the protective role of Nrf2 during auranofin-induced stress. The concurrent inhibition of Nrf2 along with auranofin sensitized HCT 116 p53^{-/-} cells to decreasing cell survival, regardless of serine and glycine. These results suggest that auranofin is able to influence cells in a p53 dependent manner, and this is likely related to whether a cell enters p53-mediated apoptotic signaling or whether a cell is able to increase glutathione levels likely through the activation of Nrf2, resulting in cyto-protection to auranofin.

Synergistic thioredoxin inhibition and glutathione depletion result in cell death through ROS mediated pathway

Auranofin coupled with the starvation of serine and glycine resulted in a marked decrease in cell survival in all cells. This decrease in cell survival was rescued both by the antioxidant NAC and with exogenous GSH. This suggests that H_2O_2 is a primary stressor upon the cells when exposed to these conditions. Given that cancers typically rely on non-mitochondrial glycolysis as their main source of ATP production, another possible mechanism of decreasing cell survival would be through an inability of cancer cells to produce sufficient levels of mitochondrial-derived ATP. This however does not seem to be the case as NAC and GSH effectively restored cell survival, likely pointing to H_2O_2 , not a lack of ATP, as the primary driver of decreasing cell survival. While it is possible that excess H_2O_2 can inhibit ATP production through the alteration of mitochondrial electron complexes, this data would suggest that H_2O_2 rather than metabolic redirection is the primary influencing factor mediating the deleterious effects of auranofin and serine and glycine starvation on cell survival.

The powerful efficacy in combined thioredoxin and glutathione inhibition has been previously demonstrated. Harris et al. [13] eloquently demonstrated that the combined inhibition of thioredoxin and glutathione resulted in antineoplastic properties, suggesting redundant functions of both systems. Interestingly, in a panel of over 100 non-small cell lung cancer (NSCLC) cell lines, the anticancer properties of auranofin were significantly greater in cell lines with lower or compromised glutathione pathways [24]. One possible avenue for potential therapies could be the use of intracellular glutathione as a potential biomarker to predict cell sensitivity to auranofin. However, in an attempt to

determine a cancer specific approach to glutathione depletion, Maddocks et al. [15] demonstrated that HCT 116 p53^{-/-} cells were particularly sensitive to serine and glycine starvation, and that this sensitivity was due to the inability of p53^{-/-} cells to produce glutathione when starved of serine and glycine. Current work was unable to recapitulate their findings directly, whereby HCT 116 p53^{-/-} cells were not overly sensitive to serine and glycine starvation alone. While currently still unknown, it is possible that the dialyzed FBS used in this study contained trace levels of serine and glycine preventing the full starvation these non-essential amino acids. Therefore, increasing the consumption of serine and glycine through a compensatory increase in glutathione, as triggered by auranofin, may provide a combined approach to glutathione depletion.

The cyto-protective effects of Nrf2 against auranofin require serine and glycine

Nrf2 activity is commonly promoted through oncogenic signaling resulting in enhanced protection from oxidative stress for cancer cells [25]. The pre-activation of Nrf2 was able to dose-dependently protect HCT 116 p53^{+/+} cells from auranofin. This cyto-protective effect was significantly blunted when cells were concurrently starved of serine and glycine. As it is likely that Nrf2 elicited protective effects against auranofin through a compensatory increase in glutathione, concurrent auranofin and serine and glycine starvation would prevent substrate availability for *de novo* glutathione synthesis. As many cancers display increased Nrf2 activity, serine and glycine starvation may indeed prevent increased Nrf2 chemoresistance [26]. Hayes and McMahon [27] determined that roughly 15% of lung cancer patients sampled had mutations which prevented Keap1 associated Nrf2 degradation, potentially allowing for an increase in

nuclear accumulation of Nrf2. Interestingly, certain mutant variants of p53 have been demonstrated to increase nuclear accumulation of Nrf2 as well, resulting in an increase in Nrf2 activity [28]. Given that Nrf2 activity promotes the expression of both thioredoxin and glutathione related genes, the up-regulation of the thioredoxin system has been previously demonstrated in several cancers [29, 30] whereby higher thioredoxin levels have been positively correlated with higher levels of aggression in cancers [29]. This has also been demonstrated with glutathione, where increased levels of glutathione are associated with more aggressive tumour growth [9]. Therefore, the combined inhibition of both systems appears to be critical in order to prevent redundant up-regulation of the opposing system. The concurrent inhibition of Nrf2 with auranofin was able to dose dependently sensitize HCT 116 p53^{-/-} cells to auranofin, regardless of serine and glycine status. This suggests that Nrf2 regulates the ability of HCT 116 p53^{-/-} cells to increase glutathione as a protective mechanism; therefore, whether the required precursors of glutathione are present or not is of lesser importance given that the stimulus to increase glutathione upstream was inhibited.

Perspectives and conclusions

Collectively, this data demonstrates that HCT 116 p53^{-/-} cells are insensitive to auranofin at a dose that HCT 116 p53^{+/+} cells are sensitive. This resistance is attributed to a compensatory increase in glutathione, and the prevention of this increase through combined starvation of serine and glycine renders HCT 116 p53^{-/-} cells sensitive to auranofin-induced cell death. Previous literature has demonstrated the combined effects of glutathione and thioredoxin inhibition as a potent antineoplastic therapy [13, 24],

however the possibility exists that cancers may dissipate ROS production by lowering mitochondrial H₂O₂ production [31]. Therefore, combining thioredoxin inhibition with serine and glycine starvation represents a strategy that creates redox stress through combined attenuation of thioredoxin and glutathione and increased mitochondrial H₂O₂ emission. While it is possible that the elevated H₂O₂ emission is solely in response to the coordinated decreasing glutathione, previous literature would suggest that serine and glycine starvation results in an increase in mitochondrial respiratory activity through increasing TCA cycle intermediates, thereby increasing mitochondrial H₂O₂ in coordination with decreasing glutathione levels. However, it remains to be determined whether normal non-cancerous cells can tolerate this potential therapy. These findings demonstrate a possible p53^{-/-} targeted, cancer-specific therapy, for circumventing p53^{-/-} cell induced chemoresistance towards auranofin-induced cell death. Combining auranofin with serine and glycine starvation may prove to be an efficacious anticancer therapy.

Author contributions

P.C.T. and C.G.R.P. designed the study. P.C.T., A.C.D., B.P., M.C.H., and L.D. conducted experiments and analyzed data. All authors interpreted the findings. P.C.T. and C.G.R.P. wrote the manuscript. All authors approved the manuscript.

Conflict of interest

The authors declare that they have no conflicts of interest with the contents of this article.

Funding

Funding was provided to C.G.R.P. by the National Science and Engineering Research Council (#436138-2013), with infrastructure supported by Canada Foundation for Innovation, the James. H. Cummings foundation and the Ontario Research Fund. P.C.T and M.C.H were both supported by a NSERC CGS-PhD scholarship.

References

1. Warburg, O., *The metabolism of carcinoma cells*. The Journal of Cancer Research, 1925. **9**(1): p. 148-163.
2. Liberti, M.V. and J.W. Locasale, *The Warburg Effect: How Does it Benefit Cancer Cells?* Trends Biochem Sci, 2016. **41**(3): p. 211-8.
3. Trachootham, D., J. Alexandre, and P. Huang, *Targeting cancer cells by ROS-mediated mechanisms: a radical therapeutic approach?* Nat Rev Drug Discov, 2009. **8**(7): p. 579-91.
4. Fujimori, S., et al., *The subunits of glutamate cysteine ligase enhance cisplatin resistance in human non-small cell lung cancer xenografts in vivo*. Int J Oncol, 2004. **25**(2): p. 413-8.
5. Yamada, M., et al., *Increased expression of thioredoxin/adult T-cell leukemia-derived factor in cisplatin-resistant human cancer cell lines*. Clin Cancer Res, 1996. **2**(2): p. 427-32.
6. Jia, J.J., et al., *The role of thioredoxin system in cancer: strategy for cancer therapy*. Cancer Chemother Pharmacol, 2019.
7. Kim, S.J., et al., *High thioredoxin expression is associated with resistance to docetaxel in primary breast cancer*. Clin Cancer Res, 2005. **11**(23): p. 8425-30.
8. Gamcsik, M.P., et al., *Glutathione levels in human tumors*. Biomarkers, 2012. **17**(8): p. 671-91.
9. Barranco, S.C., et al., *Relationship between colorectal cancer glutathione levels and patient survival: early results*. Dis Colon Rectum, 2000. **43**(8): p. 1133-40.
10. Finkelstein, A.E., et al., *Auranofin. New oral gold compound for treatment of rheumatoid arthritis*. Ann Rheum Dis, 1976. **35**(3): p. 251-7.
11. Roder, C. and M.J. Thomson, *Auranofin: repurposing an old drug for a golden new age*. Drugs R D, 2015. **15**(1): p. 13-20.
12. Balendiran, G.K., R. Dabur, and D. Fraser, *The role of glutathione in cancer*. Cell Biochem Funct, 2004. **22**(6): p. 343-52.
13. Harris, I.S., et al., *Glutathione and thioredoxin antioxidant pathways synergize to drive cancer initiation and progression*. Cancer Cell, 2015. **27**(2): p. 211-22.
14. Bailey, H.H., et al., *Phase I clinical trial of intravenous L-buthionine sulfoximine and melphalan: an attempt at modulation of glutathione*. J Clin Oncol, 1994. **12**(1): p. 194-205.
15. Maddocks, O.D., et al., *Serine starvation induces stress and p53-dependent metabolic remodelling in cancer cells*. Nature, 2013. **493**(7433): p. 542-6.
16. Hientz, K., et al., *The role of p53 in cancer drug resistance and targeted chemotherapy*. Oncotarget, 2017. **8**(5): p. 8921-8946.
17. Boyer, J., et al., *Characterization of p53 wild-type and null isogenic colorectal cancer cell lines resistant to 5-fluorouracil, oxaliplatin, and irinotecan*. Clin Cancer Res, 2004. **10**(6): p. 2158-67.
18. Feoktistova, M., P. Geserick, and M. Leverkus, *Crystal Violet Assay for Determining Viability of Cultured Cells*. Cold Spring Harb Protoc, 2016. **2016**(4): p. pdb prot087379.

19. Mandel, E.R., et al., *The superoxide dismutase mimetic tempol does not alleviate glucocorticoid-mediated rarefaction of rat skeletal muscle capillaries*. *Physiol Rep*, 2017. **5**(10).
20. Giustarini, D., et al., *Analysis of GSH and GSSG after derivatization with N-ethylmaleimide*. *Nat Protoc*, 2013. **8**(9): p. 1660-9.
21. Kand'ar, R., et al., *Determination of reduced and oxidized glutathione in biological samples using liquid chromatography with fluorimetric detection*. *J Pharm Biomed Anal*, 2007. **43**(4): p. 1382-7.
22. Matoba, S., et al., *p53 regulates mitochondrial respiration*. *Science*, 2006. **312**(5780): p. 1650-3.
23. Mayo, L.D., et al., *Phosphorylation of human p53 at serine 46 determines promoter selection and whether apoptosis is attenuated or amplified*. *J Biol Chem*, 2005. **280**(28): p. 25953-9.
24. Yan, X., et al., *Inhibition of Thioredoxin/Thioredoxin Reductase Induces Synthetic Lethality in Lung Cancers with Compromised Glutathione Homeostasis*. *Cancer Res*, 2019. **79**(1): p. 125-132.
25. DeNicola, G.M., et al., *Oncogene-induced Nrf2 transcription promotes ROS detoxification and tumorigenesis*. *Nature*, 2011. **475**(7354): p. 106-9.
26. Huang, Y., et al., *The complexity of the Nrf2 pathway: beyond the antioxidant response*. *J Nutr Biochem*, 2015. **26**(12): p. 1401-13.
27. Hayes, J.D. and M. McMahon, *NRF2 and KEAP1 mutations: permanent activation of an adaptive response in cancer*. *Trends Biochem Sci*, 2009. **34**(4): p. 176-88.
28. Lisek, K., et al., *Mutant p53 tunes the NRF2-dependent antioxidant response to support survival of cancer cells*. *Oncotarget*, 2018. **9**(29): p. 20508-20523.
29. Lincoln, D.T., et al., *Thioredoxin and thioredoxin reductase expression in thyroid cancer depends on tumour aggressiveness*. *Anticancer Res*, 2010. **30**(3): p. 767-75.
30. Berggren, M., et al., *Thioredoxin and thioredoxin reductase gene expression in human tumors and cell lines, and the effects of serum stimulation and hypoxia*. *Anticancer Res*, 1996. **16**(6B): p. 3459-66.
31. Derdak, Z., et al., *The mitochondrial uncoupling protein-2 promotes chemoresistance in cancer cells*. *Cancer Res*, 2008. **68**(8): p. 2813-9.

Chapter 7 Summary of findings

7.1 General findings and future directions

Cancer is a disease of uncontrollable cell proliferation brought on by selective mutations conferring a pro-growth phenotype leading to drastic cell expansion despite restraints on growth [1]. With the current practices of cancer prognosis and therapies, roughly 1 in 5 people will die as a result of cancer [2]. In order to sustain and promote cell division, apoptotic resistance and migration, cancers have evolved altered metabolic pathways resulting in sustained ATP production and the production of many biosynthetic molecules required for growth. These alterations in cancer metabolism were first observed almost 100 years ago [3, 4], and forced manipulations of cancer metabolism may lead to promising cancer-targeted therapies. An anthropomorphic view of cancer cells suggests that cancers have become ‘addicted’ to their metabolic phenotype, and that altering their metabolism may be too costly and result in either stagnation of cancer cell growth or death [5]. The classic understanding of cancer bioenergetics state that most cancers rely primarily on glycolysis ending in lactate production as their primary source of ATP production, despite the presence of oxygen, in a process coined ‘aerobic glycolysis’. Forced oxidation of pyruvate, rather than lactate production, has demonstrated the potential benefit of mitochondrial activation in lung and tongue cancers [6] among others.

In response to palmitoylcarnitine, mitochondria produce the reactive oxygen species (ROS) superoxide ($O_2^{\bullet-}$)[7] and subsequent hydrogen peroxide (H_2O_2) formation during oxidative phosphorylation [8], therefore the role of both ROS generation and ROS handling is crucial in dictating cell fate. H_2O_2 , in itself is hormetic in nature, whereby low

levels of H₂O₂ can function to increase cell proliferative rates, yet high levels of H₂O₂ can result in deleterious cellular fates. Glutathione is the main intracellular antioxidant, and functions through the direct electron donation in the reduction of H₂O₂ resulting in H₂O formation. It is the most abundant non-protein thiol present in all mammalian tissues in concentrations between 1-10mM, with the highest concentrations being noted in the liver [9]. However, glutathione has many critical functions beyond an antioxidant, such as promoting cell growth [10] through nuclear recruitment [11, 12], acting as a substrate for protein post-translational modifications [13], xenobiotic functions [14] and as a critical cysteine reservoir in the cell [15]. Consequently, in response to palmitoylcarnitine, cellular glutathione levels seemingly dictated cell survival. In HT29 cells, palmitoylcarnitine incubations resulted in reduced cell survival, increased H₂O₂ and decreased glutathione. By contrast, CCD 841 cells were insensitive to palmitoylcarnitine despite an increase in H₂O₂ as they were able to maintain glutathione levels. HepG2 cells displayed a decrease in H₂O₂ with an increase in glutathione, as this increase in glutathione appears to have promoted growth. Furthermore, combined inhibition of both glutathione (through serine and glycine starvation) and thioredoxin (through auranofin incubations), the other main intracellular antioxidant, overcame HCT 116 p53^{-/-} insensitivity to auranofin resulting in decreasing cell survival. Given the potential heightened reliance on glutathione and thioredoxin in cancers (as discussed in chapter 2), endogenous antioxidants serve as novel potential therapeutic targets for future antineoplastic treatments.

Palmitoylcarnitine elicits various responses in cell fate dictated, in part, by cellular glutathione responses

This thesis in part sought to determine the response of glutathione to increased mitochondrial activity through forced provision of a mitochondrial substrate, and whether manipulating glutathione could alter cancer cell survival. The findings of this thesis identify glutathione as a critical regulator in determining cell fate during cell exposure to the mitochondrial substrate, palmitoylcarnitine. Such that there was a relationship between cell survival and the change in total glutathione following 100 μ M palmitoylcarnitine across CCD 841, MCF7, HT29 and HepG2 cells (Figure 7.1).

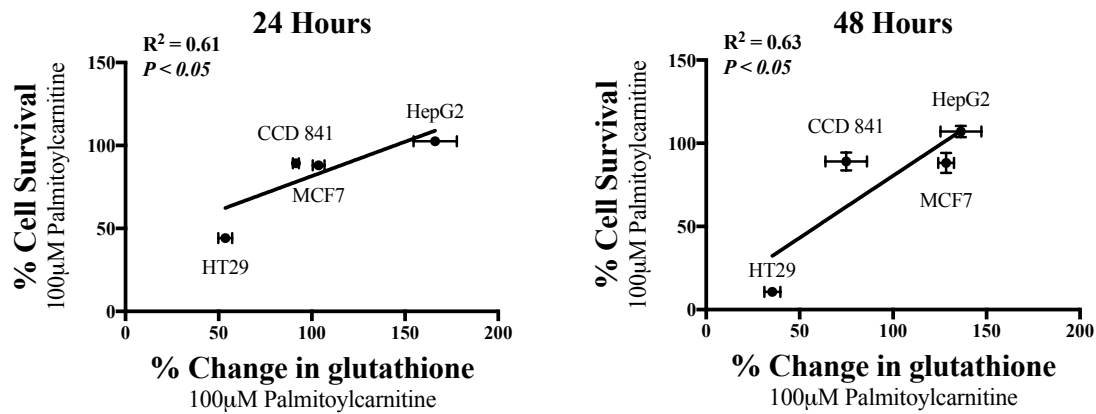


Figure 7.1 The change of glutathione in response to palmitoylcarnitine relates to the change in cell survival in response to palmitoylcarnitine. Linear regressions were performed in HT29, MCF7, CCD 841 and HepG2 cells following 24 and 48 hours of 100 μ M palmitoylcarnitine comparing the change in glutathione in cells to the change in cell survival in cells. Data are reported as means \pm SEM. $P < 0.05$.

Following both 24 and 48 hours of 100 μ M palmitoylcarnitine, the response of total glutathione mirrored that of cell survival, as larger decreases in total glutathione levels corresponded to larger decreases in cell survival. In an attempt to explain the role of glutathione during palmitoylcarnitine-induced H₂O₂ emission, glutathione was depleted using buthionine sulfoximine (BSO) concurrently with palmitoylcarnitine exposure. Interestingly, not all cells were sensitized to the deleterious effects of palmitoylcarnitine

in the absence of glutathione. There was a relationship observed between palmitoylcarnitine-induced H_2O_2 emission and the response of cells to BSO concurrent with palmitoylcarnitine, where only the cells that produced an increase in H_2O_2 emission following palmitoylcarnitine were influenced by glutathione depletion (Figure 7.2).

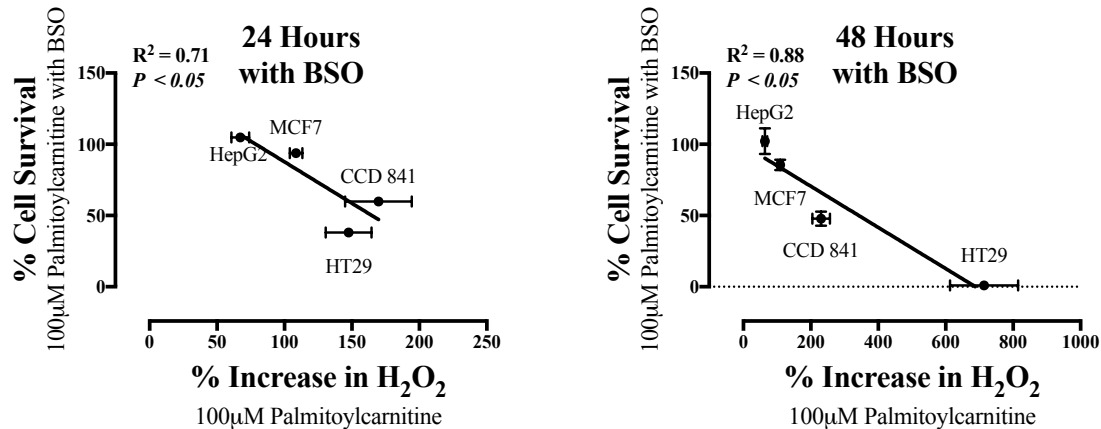


Figure 7.2 The change H_2O_2 emission in response to palmitoylcarnitine relates to the change in cell survival in response to palmitoylcarnitine concurrent with glutathione depletion by BSO. Linear regressions were performed in HT29, MCF7, CCD 841 and HepG2 cells following 24 and 48 hours of 100 μ M palmitoylcarnitine with BSO comparing the change in H_2O_2 emission in cells to the change in cell survival in cells. Data are reported as means \pm SEM. $P < 0.05$.

This demonstrates the importance of glutathione as a buffering agent to combat changes in H_2O_2 emission. With regards to the role of glutathione in promoting cell growth, it appears that an increase in palmitoylcarnitine-stimulated glutathione levels preceded HepG2 cell growth given that HepG2 cells had increased glutathione levels at 24 hours (and continued on to 48 hours), yet observable HepG2 cell growth occurred at 48 hours (Figure 7.1). In an attempt to explain the apparent lack of response of MCF7 cells to palmitoylcarnitine, it is possible that any MCF7 cell adaptation may occur past 48 hours. As redox biology is highly dynamic in nature, yet methodological sampling is temporal, early sampling times of 24 hours and 48 hours may not have been long enough to capture

any noticeable MCF7 adaptation. Interestingly, it has been previously demonstrated that low levels of chronic exogenous H₂O₂ can stimulate MCF7 cell growth despite an acute decrease in cell survival [16]. Furthermore, exogenous incubations of H9c2 cells with H₂O₂ for 24 hours resulted in an almost doubling of glutathione levels leading to enhanced cyto-protection against a further H₂O₂ challenge, however concurrent treatment with BSO rendered H9c2 cells susceptible to the latter H₂O₂ challenge [17]. While there were no observed statistical increases in glutathione, or alterations in H₂O₂ emission in MCF7 cells in response to palmitoylcarnitine, it is possible that further incubation times and more frequent methodological sampling could have resulted in observable adaptive responses to a fatty-acid stress.

Many current chemotherapies function through increasing intracellular ROS emission [18], yet following therapy, cells that survive are typically more resilient to ROS-induced cell death. It is theorized that cancers typically display heightened levels of basal ROS emission, and that successful chemotherapy treatment is aimed at pushing cancer cells passed the precipice of ROS handling resulting in ROS-induced death. However, (as previously discussed in section: *2.5.2.2 Glutathione in chemoresistance*), glutathione is a key contributor to chemoresistance in many cancers, and elevating glutathione is a critical mechanism for a cell to decrease intracellular ROS levels. Chemotherapies such as arsenic trioxide for leukemia treatment is a potent complex I-II inhibitor resulting in drastic increases in mitochondrial ROS production [19, 20], and many compounds in the anthracycline family, such as doxorubicin [18], or platinum-based compounds such as cisplatin [21], target the mitochondria to stimulate mitochondrial derived ROS resulting in cell death. A current methodological limitation in

cancer therapies is the inability to directly assess ROS levels *in vivo* during treatment. Sampling tumours during various stages of chemotherapy administration to measure glutathione levels may serve as a proxy to determine the efficacy of treatment on raising ROS to a deleterious level within a cell. One could argue that measuring intracellular glutathione, rather than ROS, may prove more beneficial, as CCD 841 cells demonstrated a significant increase in palmitoylcarnitine-induced H₂O₂, yet maintained glutathione levels, while HT29 cells increased H₂O₂ emission, palmitoylcarnitine resulted in a drastic decrease in glutathione levels as well as intracellular oxidation through decreasing the GSH/GSSG ratio. Therefore, determining the response of glutathione in cancer cells to a variety of chemotherapies may serve to expand the current understanding of whether some cancers will be susceptible to certain therapies over others.

Determining the glutathione response to a mitochondrial challenge may be beneficial in designing targeted anticancer therapies. Future work should examine expanded cell lines and the role of other mitochondrial activators, such as nicotinamide riboside (NR), a vitamin B3 analogue and a precursor to NAD⁺ production that has been demonstrated to increase mitochondrial oxidative capacity through increasing the NAD⁺/NADH ratio [22]. While NR has been demonstrated to improve mitochondrial function in a variety of murine pathologies such as advanced aging and Duchenne muscular dystrophy [23], Alzheimer's disease [24] and respiratory chain deficient mitochondrial myopathy [25], little work has been conducted on examining the role of NR supplementation towards mitochondrial activation therapies in cancers. Furthermore, there was a relationship between mitochondrial oxidative capacity and susceptibility towards palmitoylcarnitine (Figure 7.3) that warrants further exploration.

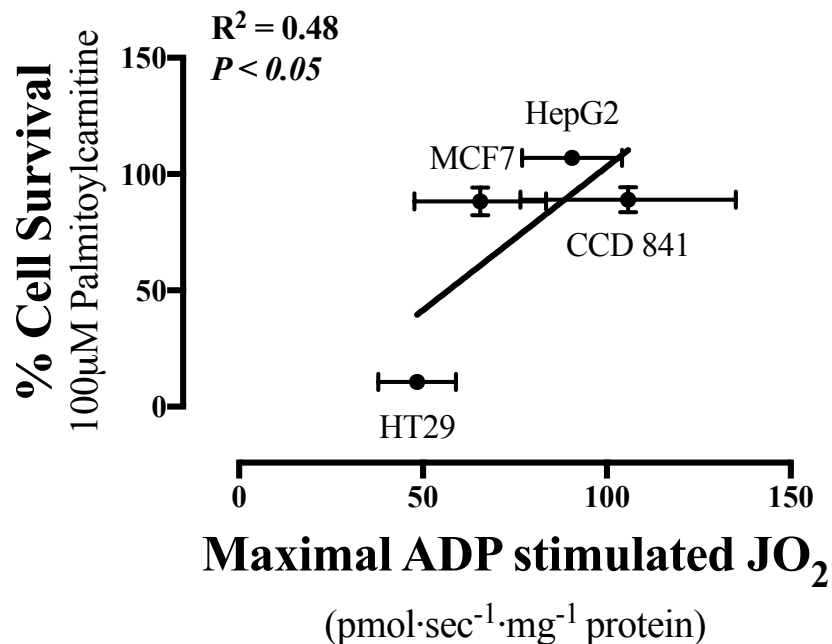


Figure 7 3 Mitochondrial respiratory capacity relates to the susceptibility of cells to palmitoylcarnitine-induced changes in cell survival. A linear regression was performed in HT29, MCF7, CCD 841 and Hepg2 cells following 24 hours of 100µM palmitoylcarnitine exposure comparing the mitochondrial respiratory capacity to the change in cell survival following palmitoylcarnitine in cells. 5mM ADP stimulated respiration was supported by 5mM pyruvate and 2mM malate. Data are reported as means ±SEM. $P < 0.05$.

As such, it would be interesting to determine whether mitochondrial depletion through ethidium bromide-induced mitochondrial depletion [26] or increasing mitochondrial capacity through PGC-1 α [27], TFAM [28] or frataxin [29] overexpression could alter sensitivity towards mitochondrial-targeted therapies. With the hypothesis being that lowering mitochondrial capacity would sensitize the cell to mitochondrial activation (rendering the cell insensitive to mitochondrial inhibition) whereas increasing mitochondrial capacity would sensitize the cell to mitochondrial inhibition (rendering the cell resistant to mitochondrial activation). To further expand on this concept, an additional study should be conducted to determine the mitochondrial capacity in many

different cancer cells and determine whether mitochondrial capacity can indeed predict sensitivity to either mitochondrial activation or mitochondrial inhibition. Cancers with low mitochondrial capacity would perhaps be successfully targeted with mitochondrial activating therapies, while cancers with high mitochondrial capacity would perhaps be successfully targeted with mitochondrial inhibition therapies. Depending on these results, mitochondrial capacity could serve as a biomarker to guide directed therapies based on where cancers fall on a ‘mitochondrial continuum’.

Dual glutathione and thioredoxin inhibition is required for potent antineoplastic function

Given that glutathione and thioredoxin increase in coordination of chemoresistance, Chapter 6 was designed in such a way that would result in increased mitochondrial ROS production while concurrently depleting glutathione and inhibiting thioredoxin. Through experimentation of the effects of BSO and auranofin on MCF7, HepG2 and HT29 cells, low doses of both BSO and auranofin individually had little influence over cell survival, however, in combination, BSO and auranofin resulted in drastic decreases in cell survival in all three cell lines (Figure 7.4).

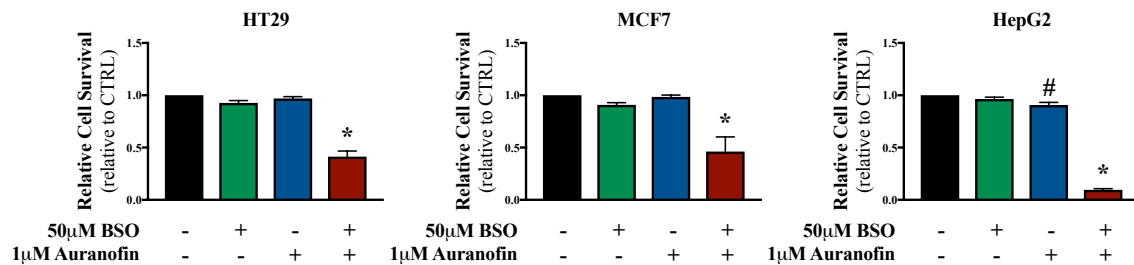


Figure 7.4 The combined effects of auranofin and buthionine sulfoximine (BSO) result in decreasing cell survival in cancer cells. Relative cell survival was assessed in HT29, MCF7 and HepG2 cells with or without 1µM auranofin and 50µM BSO (N=6). ‘*’ represents a significant difference between all other conditions. Data are reported as means ±SEM. $P < 0.05$.

These findings are in conjunction with the findings of Harris et al. [30] who noted that glutathione depletion through BSO was enough to prevent tumour formation in a mouse model of spontaneous cancer development, but once the tumour was established, both glutathione and thioredoxin inhibition (through combined BSO and auranofin) were required to elicit antineoplastic properties. However, (as previously discussed in *Chapter 2, section 2.5.4.1.1 Buthionine sulfoximine (BSO)*), the efficacy of BSO for *in vivo* glutathione depletion has been met with varied results, such that 28 patients with various cancers received 30 minutes of BSO infusions every 12 hours for up to 2 weeks, and despite a relatively safe profile, BSO infusion was unable to deplete intracellular glutathione levels below a threshold of ~30% compared to baseline [31]. However, glutathione depletion through BSO in conjunction with other compounds that stimulate mitochondrial ROS, such as arsenic trioxide, have demonstrated potent anticancer effects [32]. Additionally, the combination of BSO and auranofin likely do not stimulate an increase in mitochondrial ROS emission, therefore, it is possible that a cancer could adapt to such a therapy through decreasing mitochondrial ROS emission (through increases in UCP2 activity for example), rather than increasing ROS buffering compounds. Interestingly, Maddocks et al. [33] demonstrated that serine and glycine starvation resulted in glutathione depletion, with a preferential effect being observed in HCT 116 p53^{-/-} cells. This is critical given that ~50% of human cancers display mutations in the *TP53* gene [34], therefore serine and glycine starvation is an attractive model to induce glutathione depletion as it potentially preferentially targets cells without normal functioning p53. Typically, PKM2 is allosterically activated by serine levels [35], and during serine and glycine starvation, loss of PKM2 activity results in glycolytic

redirection towards *de novo* serine synthesis. While they did not measure H₂O₂ directly, Maddocks and colleagues [33] demonstrated that serine and glycine starvation resulted in an increase in TCA cycle intermediates suggesting an increase in mitochondrial activation for ATP production, and this current work serves to add to this literature as serine and glycine starvation resulted in an increase in H₂O₂ in both HCT 116 p53^{+/+} and p53^{-/-} cells.

Given that serine and glycine starvation has been demonstrated to deplete intracellular glutathione levels concurrent with an increase in mitochondrial activity, the purpose of Chapter 6 was to examine the combined effects of serine and glycine starvation in combination with auranofin. Interestingly, there were no differences in the responses of serine and glycine starvation alone in HCT 116 p53^{+/+} and p53^{-/-} cells, unlike previously published data, which demonstrated increased sensitivity to serine and glycine starvation in HCT 116 p53^{-/-} cells [33]. While difficult to explain, it is possible that there were trace levels of serine and glycine in the dialyzed FBS. If this is the case, this may be more representative of the whole body response to serine and glycine starvation, as tissues such as muscle are able to synthesize and release amino acids into circulation. Indeed, serine and glycine starvation resulted in a decrease in serum amino acids in mice; however, starvation did not result in the complete abolishment of serine and glycine from the serum [36]. While serine and glycine starvation yielded favorable anticancer results *in vitro*, when expanded to a murine model, serine and glycine starvation resulted in a modest slowing of cancer cell growth, however not a stagnation of growth [33, 36]. Therefore, an adjunct therapy appears to be required to increase the rate of cellular serine and glycine consumption and subsequent glutathione depletion.

While there is no direct evidence that auranofin caused an increase in serine and glycine consumption, auranofin resulted in a compensatory increase in glutathione levels in HCT 116 p53^{-/-} and HT29 cells, suggesting that HCT 116 p53^{-/-} and HT29 cells consumed greater levels of serine and glycine required to synthesize *de novo* glutathione. Furthermore, HCT 116 p53^{+/+} cells were sensitive to low concentrations of auranofin, however both HCT 116 p53^{-/-} cells and HT29 cells were resistant at similar concentrations. This is consistent with the notion that p53 mutations can confer chemoresistance [34]. It appears that auranofin induced p53-dependent cell death in HCT 116 p53^{+/+} cells, however HCT 116 p53^{-/-} and HT29 cells were insensitive to the deleterious influence of auranofin resulting in the activation of Nrf2 leading to a compensatory increase in glutathione and cell survival. These interpretations are based on the findings that auranofin stimulated an increase in p-p53^{ser46}, which has been previously demonstrated to amplify p53-dependent apoptosis [37]. Nrf2 manipulation was able to alter cell fate following serine and glycine starvation coupled with auranofin. Concurrent forced activation of Nrf2 was able to dose-dependently rescue HCT 116 p53^{+/+} cells from auranofin preferentially when serine and glycine were present suggesting the importance of glutathione synthesis in conferring cyto-protection during auranofin exposure, while Nrf2 inhibition was able to dose dependently sensitize HCT 116 p53^{-/-} cells to auranofin regardless of serine and glycine status. Interestingly, auranofin combined with serine and glycine starvation prevented the compensatory increase of glutathione in all cells resulting in decreasing cell survival, induction of cell death markers and an increase in trypan blue positive cells.

While both auranofin administration and serine and glycine starvation have been independently proven to be safe to mammals, the safety of auranofin coupled with serine and glycine starvation has yet to be proven. Therefore, future work should examine the effects of auranofin combined with serine and glycine starvation *in vivo*. This is of particular importance for two main reasons: 1) Previous work in cell culture has demonstrated that serine and glycine starvation alone elicits potent antineoplastic effects, however the strength of these findings did not translate to *in vivo* testing, therefore while these results demonstrate potent anticancer effects in *in vitro* conditions, *in vivo* experimentation is required to further elucidate the efficacy of auranofin and serine and glycine starvation; 2) Unlike previous work examining the response of cells to palmitoylcarnitine, where both transformed and non-transformed cells were exposed to palmitoylcarnitine, normal cells were unable to grow in conditions required to test the effects auranofin coupled with serine and glycine starvation. This was due to the inability of non-transformed CCD 841 cells to grow in media with dialyzed FBS. Therefore, while previous literature highlights the increased sensitivity of cancers to antioxidant depletion, there is a possibility that auranofin combined with serine and glycine starvation may result in deleterious effects in all cells, rather than cancer-specific effects.

7.2 Limitations

While careful consideration was performed during the design of the experiments, there are limitations to the experimental designs that limit the interpretation of the data. Chapter 4 attempted to re-produce the findings observed by Wenzel et al. [7], where it was demonstrated that palmitoylcarnitine in conjunction with free carnitine selectively

killed HT29 cells, but not normal NCOL-1 cells. The conditions designed by Wenzel et al. [7] were mimicked both for palmitoylcarnitine concentrations, as well as the addition of free carnitine. Wenzel and colleagues [7] demonstrated that HT29 cells have low levels of intracellular free carnitine required for palmitoylcarnitine entry into the mitochondria (see figure 2.7), therefore due to consistency across conditions, as well as uncertainty as to free carnitine levels across other cell lines, a strength of Chapter's 4 and 5 was that all conditions contained free carnitine. The cancer specific effects of palmitoylcarnitine were repeated in HT29 cells, however instead of normal NCOL-1 cells as was used previously, CCD 841 primary colon epithelial cells were used, as NCOL-1 cells may not be a suitable comparative cell line. In a response to criticism from their previous work, Wenzel and Daniel [38] addressed the possible cell line contamination of NCOL-1 cells with the cancerous LoVo cells. They addressed that NCOL-1 cells display distinct differences from LoVo and HT29 cells, however they could not distinctly identify NCOL-1 cells as non-transformed cells, rather "preneoplastic" cells. Therefore, CCD 841 primary colon epithelial cells were used as they are more commonly applied in the literature, and are readily available for purchase through the ATCC. While attention was made to closely mimic the study of Wenzel and colleagues [7], direct interpretations may be tempered, as not all cell lines were consistent between studies.

With regards to both Chapter 4 and 5, Wenzel et al. [7] used only palmitoylcarnitine as their mitochondrial substrate. While other papers have examined the effects of palmitoylcarnitine in prostate cancers and normal prostate cells, the role of exploring other mitochondrial substrates is warranted. One limitation of using palmitoylcarnitine as an exogenous substrate is that it is unknown whether

palmitoylcarnitine enters the cell, as endogenous palmitoylcarnitine is made solely within the cell. Previous work has demonstrated that exogenous palmitoylcarnitine incubations resulted in increased intracellular palmitoylcarnitine in neuroblastoma NB-2a cells [39], and has previously been demonstrated to cause an adaptive increase in oxidative capacity in mouse embryonic fibroblasts [40]. Current work demonstrated that palmitoylcarnitine resulted in an adaptive increase in mitochondrial respiratory capacity in HepG2 cells in Chapter 5. However, there is no direct evidence that proves whether palmitoylcarnitine results in a direct increase in oxidative phosphorylation. Therefore, while it is possible that palmitoylcarnitine directly enters the cell as it increases intracellular palmitoylcarnitine levels and results in adaptive increases in mitochondrial capacity, it is unknown whether these adaptations are of a direct result of palmitoylcarnitine entering the cell, or downstream adaptations.

Previous preliminary work was done using other fat sources other than palmitoylcarnitine, such as intralipid, an emulsified fat mixture, and conjugated linoleic acid/oleic acid, however these resulted in minimal effects, even in the mM dosage. HT29 and MCF7 cells were incubated in these alternative fat sources resulting in minimal changes in cell survival, H₂O₂ emission or caspase 3/7 activation. Therefore, CPT-1 inhibition likely accounts for limitations in using fat as a viable therapy, and suggests in part why a high fat diet would not be beneficial to cancer patients. Rather, palmitoylcarnitine administration would be likely as an infused compound aimed to elicit anticancer properties. Further limitations associated with Chapter 4 are that there were only a select number of cell lines, and the efficacy of palmitoylcarnitine was examined only in *in vitro* settings. Furthermore, interpretation of the data was limited as the

exogenous antioxidant N-acetylcysteine (NAC) failed to elicit a strong rescuing effect in HT29 cells following palmitoylcarnitine, only a modest protective effect (Figure A.1). While the possibility exists that glutathione depletion and decreasing cell survival associated with palmitoylcarnitine is occurring through non-ROS mediated mechanisms, it cannot be excluded that glutathione depletion is perhaps occurring through ROS mediated mechanisms. However, when comparing the effect of NAC between Chapter 4 and Chapter 6, it is possible that the varied ability of NAC to protect the cells depends on the degree of H₂O₂ emission that occurred in the respective treatments. Specifically, in Chapter 6, serine and glycine deprivation increased H₂O₂ emission in HCT 116 p53^{+/+} and p53^{-/-} cells by ~120%; by contrast palmitoylcarnitine stimulated H₂O₂ emission in HT29 cells between ~140% - 715%. Another possibility may relate to the amount of NAC taken up by cells. Both studies employed a co-incubation approach whereby NAC was applied concurrently with either palmitoylcarnitine or serine and glycine deprivation. This approach may not have permitted enough time for maximal cysteine uptake as compared to pre-treatment approaches. If cysteine uptake was sub-maximal with the co-treatment approach, this may explain why NAC was more effective with the relatively lower rates of H₂O₂ emission seen in Chapter 6 than Chapter 4. It should be noted that while developing the NAC protocol, a dose-response curve was conducted in CCD 841, HT29, MCF7 and HepG2 cells (Figure A.1) establishing a tolerable range of NAC concentrations in each cell line to avoid cytotoxicity. As such, it is unlikely that these cancer cells could tolerate higher concentrations of NAC compared to the 3mM used in Chapters 4 and 6. In this light, an alternative pre-treatment approach with NAC could be warranted to rescue HT29 cells from palmitoylcarnitine similar to what was seen with

serine and glycine deprivation. While testing the early effects of palmitoylcarnitine in Chapters 4 and 5 is a strength in determining acute responses to an oxidative challenge, it is also possible that longer exposure to palmitoylcarnitine and NAC may have resulted in a more robust protective effect of NAC in HT29 cells to palmitoylcarnitine

In Chapter 6, one main limitation of the data was that there were no differences between HCT 116 p53^{+/+} and p53^{-/-} with reference to serine and glycine starvation as previously published by Maddocks et al. [33]. While speculative, residual levels of serine and glycine found in dialyzed FBS perhaps explain this observation. However, given that there were no measures of serine and glycine in the dialyzed FBS, this remains unknown. Furthermore, there were limited comparisons as only HCT 116 and HT29 colorectal carcinoma cells were used; therefore examination in other cell lines is warranted. Certainly, further examination into non-transformed cells to determine whether normal cells tolerate serine and glycine starvation coupled with auranofin is of critical importance.

7.3 Conclusions

The findings from this thesis highlight the potential of mitochondrial and antioxidant targeting for future cancer therapies. While palmitoylcarnitine, and potentially other mitochondrial substrates and sources of mitochondrial activation, may indeed prove to be efficacious as an anticancer therapy, caution must be taken as palmitoylcarnitine resulted in a decrease in HT29 and HCT 116 cell survival; however it resulted in an increase in growth in HepG2 cells. The findings provide a foundation to explore the degree to which glutathione serves as a biomarker to predict cancer cell fate

in response to palmitoylcarnitine. If a therapy results in lower intratumoural glutathione, perhaps that is suggestive of a cancer which is sensitive to that given therapy. Furthermore, the development that serine and glycine starvation sensitize p53-null cells to auranofin offers a potential nutritional/pharmaceutical combination approach. While it remains to be determined whether this is tolerated *in vivo*, auranofin coupled with serine and glycine starvation may be a promising therapeutic option for combating cancer. Therefore, understanding the underlying mechanisms associated with cancer bioenergetics and redox buffering may be fruitful in the development of future cancer-targeted therapies aimed at manipulating the highly dynamic relationship between cancer metabolism and redox biology.

7.4 Chapter 7 references

1. Hanahan, D. and R.A. Weinberg, *Hallmarks of cancer: the next generation*. Cell, 2011. **144**(5): p. 646-74.
2. Alberts, B., *Molecular biology of the cell*, ed. A. Johnson, et al.: Garland Science, Taylor and Francis Group.
3. Warburg, O., *The metabolism of carcinoma cells*. The Journal of Cancer Research, 1925. **9**(1): p. 148-163.
4. Warburg, O., *On the origin of cancer cells*. Science, 1956. **123**(3191): p. 309-14.
5. Olson, K.A., J.C. Schell, and J. Rutter, *Pyruvate and Metabolic Flexibility: Illuminating a Path Toward Selective Cancer Therapies*. Trends Biochem Sci, 2016. **41**(3): p. 219-230.
6. Ayyanathan, K., et al., *Combination of sulindac and dichloroacetate kills cancer cells via oxidative damage*. PLoS One, 2012. **7**(7): p. e39949.
7. Wenzel, U., A. Nickel, and H. Daniel, *Increased carnitine-dependent fatty acid uptake into mitochondria of human colon cancer cells induces apoptosis*. J Nutr, 2005. **135**(6): p. 1510-4.
8. Mailloux, R.J., *Teaching the fundamentals of electron transfer reactions in mitochondria and the production and detection of reactive oxygen species*. Redox Biol, 2015. **4**: p. 381-98.
9. Lu, S.C., *Glutathione synthesis*. Biochim Biophys Acta, 2013. **1830**(5): p. 3143-53.
10. Huang, Z.Z., et al., *Mechanism and significance of increased glutathione level in human hepatocellular carcinoma and liver regeneration*. FASEB J, 2001. **15**(1): p. 19-21.
11. Vivancos, P.D., et al., *Recruitment of glutathione into the nucleus during cell proliferation adjusts whole-cell redox homeostasis in Arabidopsis thaliana and lowers the oxidative defence shield*. Plant J, 2010. **64**(5): p. 825-38.
12. Vivancos, P.D., T. Wolff, and C.H. Foyer, *A nuclear glutathione cycle within the cell cycle*. Biochemical Journal, 2010. **431**(2): p. 169-178.
13. Dalle-Donne, I., et al., *S-glutathionylation in protein redox regulation*. Free Radic Biol Med, 2007. **43**(6): p. 883-98.
14. Sipes, I.G., D.A. Wiersma, and D.J. Armstrong, *The role of glutathione in the toxicity of xenobiotic compounds: metabolic activation of 1,2-dibromoethane by glutathione*. Adv Exp Med Biol, 1986. **197**: p. 457-67.
15. Cho, E.S., N. Sahyoun, and L.D. Stegink, *Tissue glutathione as a cyst(e)ine reservoir during fasting and refeeding of rats*. J Nutr, 1981. **111**(5): p. 914-22.
16. Mahalingaiah, P.K. and K.P. Singh, *Chronic oxidative stress increases growth and tumorigenic potential of MCF-7 breast cancer cells*. PLoS One, 2014. **9**(1): p. e87371.
17. Seo, Y.J., et al., *Role of glutathione in the adaptive tolerance to H₂O₂*. Free Radic Biol Med, 2004. **37**(8): p. 1272-81.
18. Yang, H., et al., *The role of cellular reactive oxygen species in cancer chemotherapy*. J Exp Clin Cancer Res, 2018. **37**(1): p. 266.

19. Yen, Y.P., et al., *Arsenic induces apoptosis in myoblasts through a reactive oxygen species-induced endoplasmic reticulum stress and mitochondrial dysfunction pathway*. Arch Toxicol, 2012. **86**(6): p. 923-33.
20. Shi, H., X. Shi, and K.J. Liu, *Oxidative mechanism of arsenic toxicity and carcinogenesis*. Mol Cell Biochem, 2004. **255**(1-2): p. 67-78.
21. Marullo, R., et al., *Cisplatin induces a mitochondrial-ROS response that contributes to cytotoxicity depending on mitochondrial redox status and bioenergetic functions*. PLoS One, 2013. **8**(11): p. e81162.
22. Canto, C., et al., *The NAD(+) precursor nicotinamide riboside enhances oxidative metabolism and protects against high-fat diet-induced obesity*. Cell Metab, 2012. **15**(6): p. 838-47.
23. Zhang, H., et al., *NAD(+) repletion improves mitochondrial and stem cell function and enhances life span in mice*. Science, 2016. **352**(6292): p. 1436-43.
24. Gong, B., et al., *Nicotinamide riboside restores cognition through an upregulation of proliferator-activated receptor-gamma coactivator 1alpha regulated beta-secretase 1 degradation and mitochondrial gene expression in Alzheimer's mouse models*. Neurobiol Aging, 2013. **34**(6): p. 1581-8.
25. Khan, N.A., et al., *Effective treatment of mitochondrial myopathy by nicotinamide riboside, a vitamin B3*. EMBO Mol Med, 2014. **6**(6): p. 721-31.
26. Spadafora, D., et al., *Methods for Efficient Elimination of Mitochondrial DNA from Cultured Cells*. PLoS One, 2016. **11**(5): p. e0154684.
27. Wallace, M. and C.M. Metallo, *PGC1alpha drives a metabolic block on prostate cancer progression*. Nat Cell Biol, 2016. **18**(6): p. 589-90.
28. Kang, D., S.H. Kim, and N. Hamasaki, *Mitochondrial transcription factor A (TFAM): roles in maintenance of mtDNA and cellular functions*. Mitochondrion, 2007. **7**(1-2): p. 39-44.
29. Schulz, T.J., et al., *Induction of oxidative metabolism by mitochondrial frataxin inhibits cancer growth: Otto Warburg revisited*. J Biol Chem, 2006. **281**(2): p. 977-81.
30. Harris, I.S., et al., *Glutathione and thioredoxin antioxidant pathways synergize to drive cancer initiation and progression*. Cancer Cell, 2015. **27**(2): p. 211-22.
31. Bailey, H.H., et al., *Phase I clinical trial of intravenous L-buthionine sulfoximine and melphalan: an attempt at modulation of glutathione*. J Clin Oncol, 1994. **12**(1): p. 194-205.
32. Maeda, H., et al., *Effective treatment of advanced solid tumors by the combination of arsenic trioxide and L-buthionine-sulfoximine*. Cell Death Differ, 2004. **11**(7): p. 737-46.
33. Maddocks, O.D., et al., *Serine starvation induces stress and p53-dependent metabolic remodelling in cancer cells*. Nature, 2013. **493**(7433): p. 542-6.
34. Hientz, K., et al., *The role of p53 in cancer drug resistance and targeted chemotherapy*. Oncotarget, 2017. **8**(5): p. 8921-8946.
35. Chaneton, B., et al., *Serine is a natural ligand and allosteric activator of pyruvate kinase M2*. Nature, 2012. **491**(7424): p. 458-462.
36. Maddocks, O.D.K., et al., *Modulating the therapeutic response of tumours to dietary serine and glycine starvation*. Nature, 2017. **544**(7650): p. 372-376.

37. Mayo, L.D., et al., *Phosphorylation of human p53 at serine 46 determines promoter selection and whether apoptosis is attenuated or amplified*. J Biol Chem, 2005. **280**(28): p. 25953-9.
38. Wenzel, U. and H. Daniel, *Reconsidering cell line cross-contamination in NCOL-1*. Cancer Genet Cytogenet, 2005. **163**(1): p. 95-6; author reply 97.
39. Nalecz, K.A., et al., *Palmitoylcarnitine regulates estrification of lipids and promotes palmitoylation of GAP-43*. FEBS Lett, 2007. **581**(21): p. 3950-4.
40. Lin, Z., et al., *Fatty acid oxidation promotes reprogramming by enhancing oxidative phosphorylation and inhibiting protein kinase C*. Stem Cell Res Ther, 2018. **9**(1): p. 47.

Appendix A – Additional figures

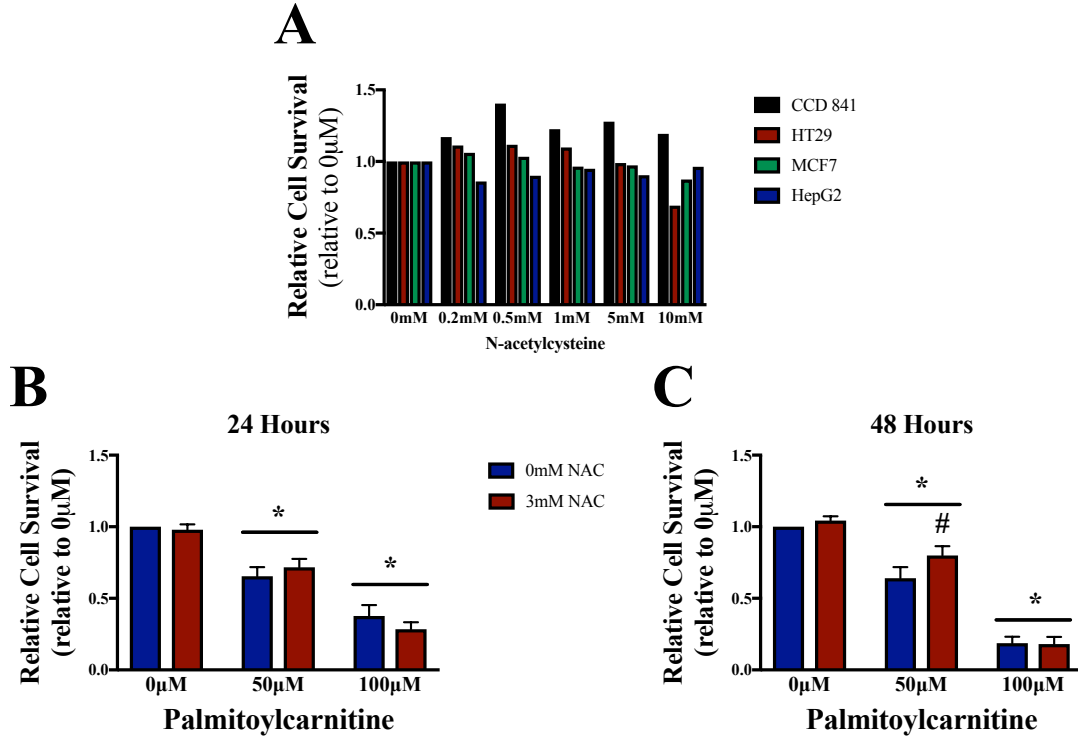


Figure A 1 N-acetylcysteine (NAC) provides marginal protection in HT29 cells against palmitoylcarnitine. A Relative cell survival was assessed in CCD 81, HT29, MCF7 and HepG2 cells were treated with increasing levels of NAC for 24 hours. **B and C** Relative cell survival was assessed in HT29 cells treated with palmitoylcarnitine and NAC for 24 and 48 hours. Data are reported as means \pm SEM. ‘*’ represents a significant difference from 0µM palmitoylcarnitine, ‘#’ represents a significant difference between the same palmitoylcarnitine concentration at the same time point. $P < 0.05$.

Appendix B – Full western blot images

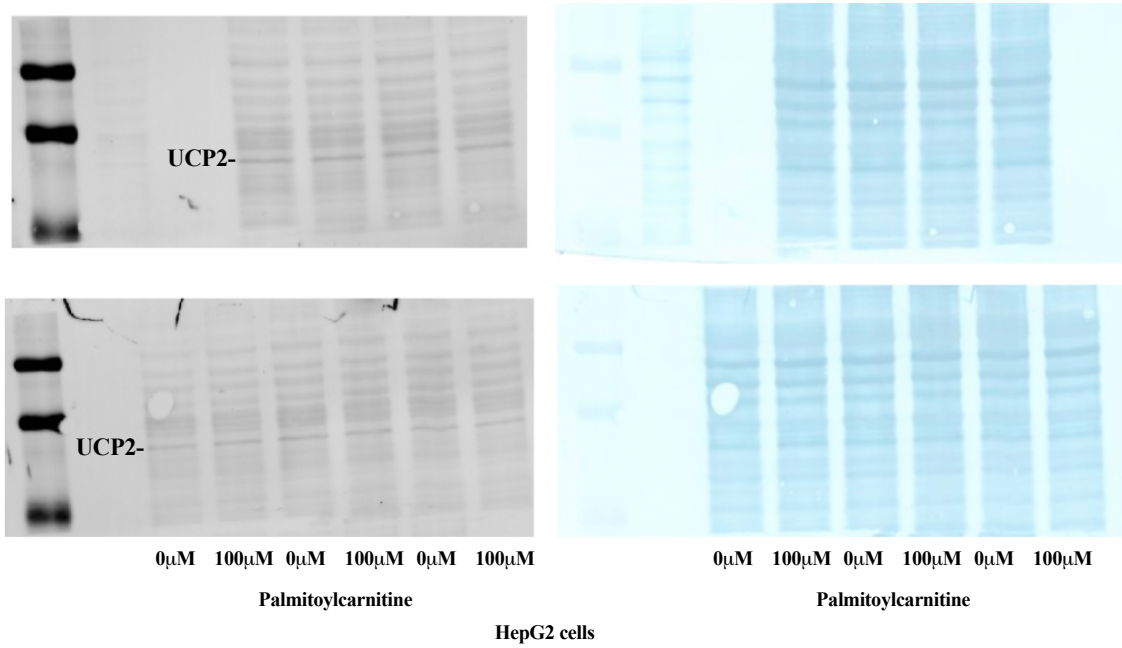


Figure B 1 Total western blot images of UCP2 protein represented in Chapter 5. Left panels Images of UCP2 protein and **right panels** total protein stains of adjacent western blots as performed using Amido black.

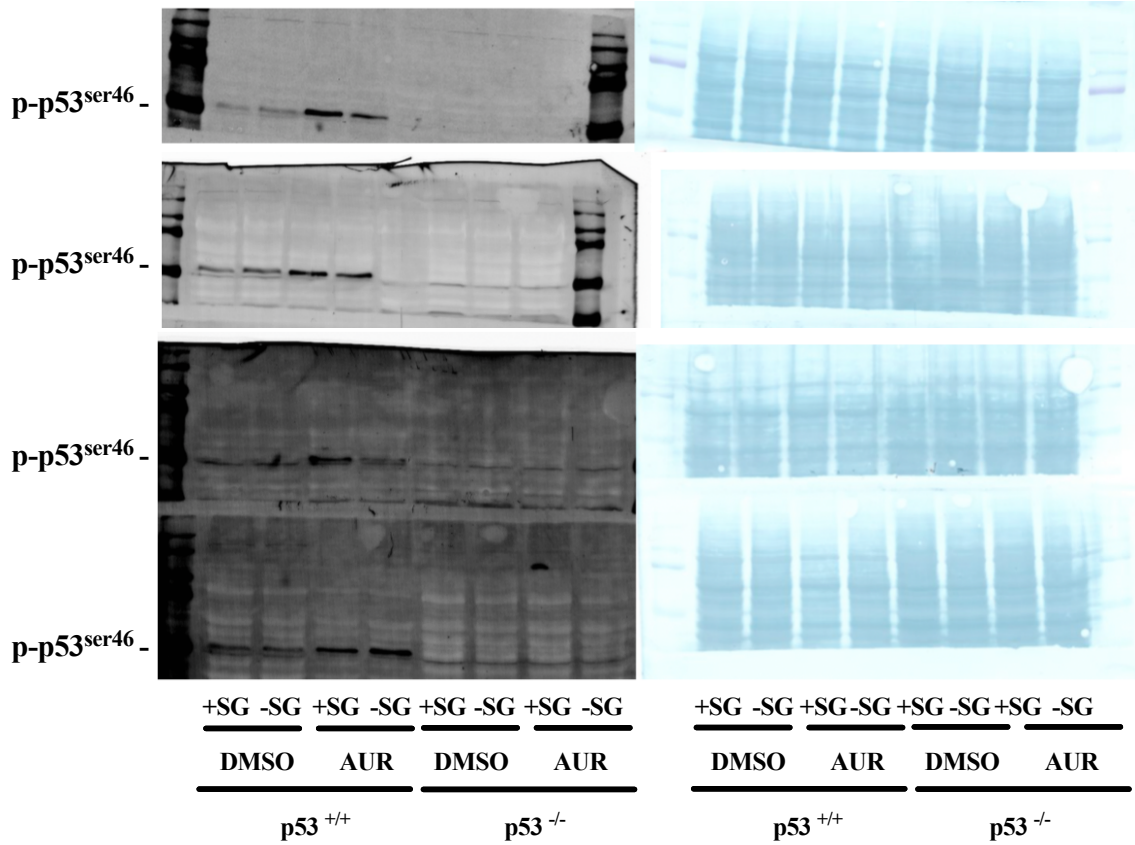


Figure B 2 Total western blot images of p-p53^{ser46} in HCT 116 cells. Left panel Images of p-p53^{ser46} protein and **right panels** total protein stains of adjacent western blots as performed using Amido black.

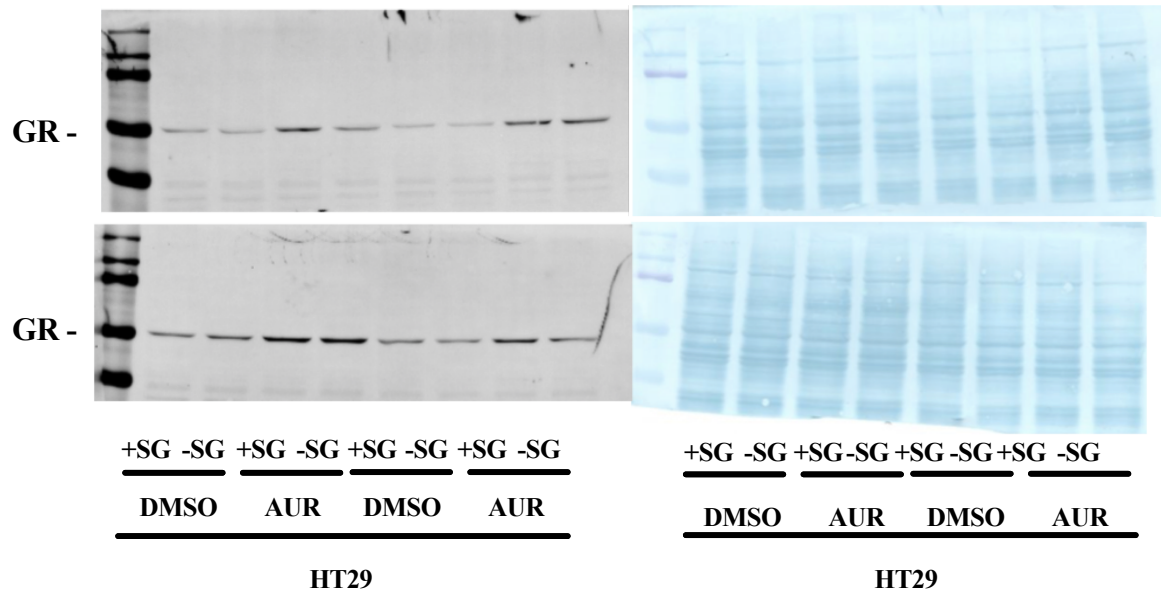


Figure B 3 Total western blot images of glutathione reductase (GR) in HT29 cells. Left panel Images of glutathione reductase (GR) protein and right panels total protein stains of adjacent western blots as performed using Amido black.

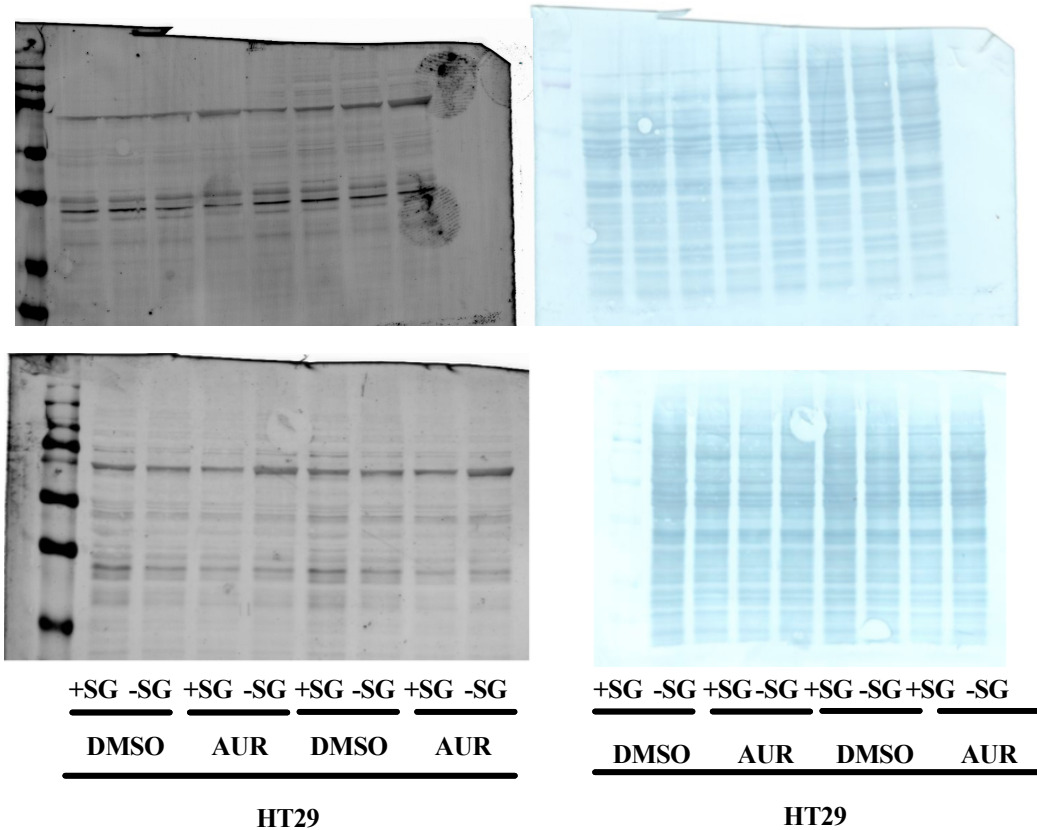


Figure B 4 Total western blot images of 4HNE in HT29 cells. Left panel Images of 4HNE protein and **right panels** total protein stains of adjacent western blots as performed using Amido black.

Appendix C – Outlined experimental methods

A.1 Cell lines:

Cell line	Origin (and ATCC reference)	Growth media
HT29	Human colon adenocarcinoma https://atcc.org/Products/All/HTB-38.aspx	DMEM 10% FBS 1% P/S
MCF7	Human breast adenocarcinoma https://www.atcc.org/products/all/HTB-22.aspx	AMEM 10% FBS 1% P/S
CCD 841	Human colon normal epithelial https://www.atcc.org/Products/All/CRL-1790.aspx#generalinformation	EMEM 10% FBS 1% P/S
HepG2	Human liver hepatocellular carcinoma https://www.atcc.org/products/all/HB-8065.aspx	EMEM 10% FBS 1% P/S
HCT 116	Human colon adenocarcinoma https://www.atcc.org/products/all/CCL-247.aspx	DMEM 10% FBS 1% P/S

A.2 Crystal violet for relative cell survival

Purpose:

Crystal violet stain is used to determine cell number in fixed adherent cells.

Make up before:

To make crystal violet staining solution:

- 0.5% (w/v) crystal violet powder (Sigma-Aldrich) in 25% MeOH in RO water

Procedure:

- Plate cells at a desired density in black-walled optical bottom 96-well cell culture plates (ThermoFisher)
- Following treatment for set time, remove media and fix cells with 10% formalin (Sigma-Aldrich)
 - o Replace media volume with same volume of formalin (100µl media aspirated off and replaced with 100µl 10% formalin)
- Following 10 minutes, aspirate off formalin and add in 50µl crystal violet staining solution for 10 minutes
- Dump out stain and carefully rinse clean with water
- Allow to dry inverted in fume hood (good air circulation)
- To analyze, scan plates using Odyssey LiCor scanner and analyze using internal software to establish fluorescent density

A.3 Digested in-well protein assay

Purpose:

Either as a crude stand alone measure of cell number, or to normalize data from live-cell assays (such as H₂O₂ and XTT)

Make up before:

Make sure we have BCA kit reagents (ThermoFisher) and RIPA buffer (Sigma-Aldrich)

- To make up BCA-RIPA solution, make up BCA reagent according to kit instructions with final volume including 10% RIPA buffer

Procedure:

- Carefully aspirate off media as to not dislodge any adhered cells
- Using a multi-channel pipette, fill up each well entirely with PBS to make sure no residual media is left in the well
- Carefully aspirate off PBS and add 200µl BCA-RIPA solution to each well
- Incubate at 37°C for 30 minutes
- Remove from incubator and carefully wipe off any precipitated moisture on the bottom of the plate
- Place plate on rocker while setting up plate reader
- Using the VICTOR³ 1420 Multilabel Counter plate reader (PerkinElmer), read plate using BCA setting

A.4 Live-cell H₂O₂ emission

Purpose:

Real time H₂O₂ emission as either static or kinetic read in live adhered cells. Ensure that whatever variable you are adding to the media does not interfere with AmplexRed signal (does not alter background signal)

Make up before:

Make stocks of AmplexUltraRED (ThermoFisher) and horseradish peroxidase (HRP, Sigma-Aldrich)

- AmplexRed at 5mM in DMSO
- HRP at 10 units/ml in ddH₂O
- Make up working solution
 - In condition media, make up working solution of AR+HRP in media
 - Add in 0.02μl of each AR+HRP per well
 - Figure out how many wells you need, make up solution such that you are adding in 10μl of working solution per well and adjust math accordingly
 - Working solution = (Final volume: Number of wells x 10μl) – (0.02μl AR x final volume) – (0.02μl HRP x final volume)
 - Final volume equation dictates how much media to add to bring up to final volume. Always make up more than you need. Example (96-wells, therefore, make up 1ml)
 - Working solution = (1000μl) – (0.22 x 1000) – (0.22 x 1000)
 - Therefore: Media added = 960μl, AR and HRP at 20μl each

Procedure

- Following desired incubation time with desired compound (example, if you are doing a 24 hour incubation time with a drug, after the 24 hours is complete)
- Quickly add in 10μl of working solution into each well and then protect from light
- Using BioTek Cytation plate reader, read plate at 568ex/581em
 - If doing kinetic read, make sure plate reader is at 37°C at 5% CO₂
- Make signal relative to an H₂O₂ standard curve
- Following read, determine well protein concentration using protocol A.3

A.5 High-resolution respirometry

Purpose:

To determine site specific mitochondrial oxygen consumption

Make up before:

- Thaw MiRo buffer
- Air phase chambers using MiRo, leave stoppers out as to minimize volume loss from liquid adhered to the stoppers
- 1mg/ml digitonin in water
- Make up protein assay tubes (45µl RIPA buffer)

Procedure:

- Plate cells in 10cm cell culture dish
- Following desired treatment or plating time, trypsin harvest cells, pellet, wash in PBS, pellet and re-suspend 1ml MiRo containing 10µl digitonin solution
- Let cells rock for 30 minutes at room temperature
 - o To validate whether the cells are permeable, take out 10µl of cells at desired times and view cells under microscope with trypan blue. If the cell membrane is permeable, cells will take up trypan blue
- Following 30 minutes and successful permeabilization, pellet cells and re-suspend in 110µl of MiRo
- Take out 5µl of cell suspension and add to protein assay tubes and freeze for later protein determination
- Add 100µl of cell suspension to the chamber and add stopper
- Follow respiration protocol as so desired
- Reference Hughes and or Ramos theses for detailed O2K protocol

A.6 Intracellular lactate determination

Purpose:

Intracellular lactate determination can be an index of glycolytic flux or pyruvate redirection. Avoid touching anything with bare skin as perspiration has high levels of lactate in it, wear clean gloves at all times. If your gloves touch your skin, change your gloves. Move fairly quickly as to avoid lactate degradation until acidification step.

Make up before:

Lactate assay buffer:

- 1M Glycine
- 500mM Hydrazine sulfate
- 5mM EDTA disodium salt
- pH to 9.5 with NaOH

NAD (make fresh)

- 25mM NAD in lactate assay buffer

Perchloric acid (PCA)

- 0.5M PCA in ddH₂O

Potassium Bicarbonate (KHCO₃)

- 2.2M KHCO₃ in ddH₂O

Protein tubes

- In order to normalize data, make up protein tubes containing 45µl of RIPA buffer per sample

Make sure you have lactate hydrogenase (LDH, Sigma-Aldrich, heart isoform)

Procedure:

- Plate cells in desired dishes (depending on cell type, this can range from 24-well plate up to a 10cm dish in my experience)
- Do the following quickly:
 - o Following cell treatment, wash cells with PBS
 - o Trypsin harvest cells, wash in PBS, pellet
 - o Carefully aspirate off PBS and re-suspend pellet in 100µl PBS
 - Take out 5µl and add to protein tube (keeping note that this is from a 100µl sample. Sample volume can be adjusted depending on cell confluence and cell type).
 - Freeze protein tube for protein analysis at a later time
 - o Following 5µl removal, bring up volume of remaining 99.5µl up to 1ml, and pellet again
 - o Carefully aspirate off PBS and add in 150µl of 0.5M PCA

- Transfer total volume into a 1.5ml eppendorf tube
 - Vortex thoroughly
 - Freeze thaw 3X
- Sample is now stable following de-proteination by PCA
- Spin at 4°C at 7,000 RPM for 5 minutes
- Collect supernatant and transfer to new tube
- On ice, add 120µl of sample to 36µl KHCO₃
 - It is the ratio that is important, so if you have less than 120µl, adjust accordingly
- This will bubble up and a precipitate will form, vortex thoroughly several times and open and close the lid to dissipate pressure
- Spin at 4°C at 7,000 RPM for 5 minutes
- Collect supernatant and transfer to new tube
 - This is now the final sample
- Per reaction:
 - 20µl sample + 20µl NAD + 2µl LDH + 258µl lactate buffer
 - Load sample in triplicate onto a 96-well plate
 - I make up 1ml per sample and load 300µl per well
 - 66.66µl sample + 66.66µl NAD + 6.66µl LDH + 860.02µl lactate buffer
 - Incubate at 37°C until reaction stops (~1hr, cell line depending. Whatever time point you decide, be consistent throughout)
 - Read on plate reader at 340nm
 - Use Beer's law to determine lactate concentration and normalize to protein values

A.7 Glutathione

Purpose:

To determine redox state and total content of intracellular glutathione levels

Make up before:

Buffer:

- **TRIS-BSA:** homogenization buffer with Trizma Base + Boric Acid/Serine/Acivicin to inhibit γ -glutamyltranspeptidase from metabolizing GSH/GSSG.
 - o 200mL HPLC grade water
 - o 50mM Trizma Base: 1.212g -- (MW=121.14g)
 - o 20mM Boric Acid: 0.248g – (MW=61.83g)
 - o 2mM L-serine: 0.042g – (MW=105.69g)
 - o 20uM Acivicin: (MW=178.57)
 - o Acivicin inhibits γ -glutamyltranspeptidase, a protein bound to the cell membrane which catabolizes glutathione upon contact
 - o pH to 8 with HCL
- DAY OF:
 - o Add 25ul 0.2M NEM for every 1ml TRIS-BSA fresh day of use (some suggest NEM is light sensitive, freeze sensitive, not sure if this is true or not, but adding it same day allows for to decide whether you would want to or not add NEM, only time you wouldn't add NEM is if you wanted to measure total glutathione)
 - NEM irreversibly binds to GSH creating a GS-NEM conjugate and inhibits glutathione reductase preventing the auto-oxidation GSH to GSSG

Making Mobile phase solvents

- **GSH mobile phase**
 - o Solvent A: 0.25% Glacial Acetic Acid in HPLC grade water
 - 2.5mL glacial acetic acid into 997.5mL water
 - Or 1.25ml glacial acetic acid into 498.75mL water
 - pH to 3.1 by adding in a couple drops of 2M NaOH to bring pH up or glacial acetic acid to bring pH down
 - **Prepare fresh every day**
 - o Solvent B: 100% Acetonitrile
- **GSSG mobile phase**
- Solvent A: 25mM Na₂HPO₄ in HPLC grade water
 - o Make 425ml
 - pH to 6.0 using phosphoric acid
 - o Add 75ml MeOH to get final 15% methanol mobile phase

Sample preparation:

- Make up 6 tubes per sample:
 - o Tube1 for homogenate/lysis

- Tube2 for protein assay
 - 5ul homogenate into 45ul buffer/RIPA buffer for cells
 - Poke hole in top of tube
- Tube3 with TCA
 - 7ul TCA into tube
- Tube4 PCA
 - 70ul PCA into tube
- Tube5 labeled GSH
 - Poke hole in top of tube
- Tube6 labeled GSSG
 - 500ul 0.5M NaOH

Procedure:

- For muscle:
 - Homogenize tissue in TRIS-BSAN at a 1mg-10ul ratio, leave on ice until all samples are done (I usually do about 10 samples at a time, do samples in random order).
 - Try and get at least 145ul final volume, otherwise need to adjust volumes of TCA and PCA, not a big deal, but adds time
 - Spin samples at 800g for 10 minutes at 4 degrees
 - Add supernatant to tube 1
- For Cells:
 - Wash cells in PBS-NEM (PBS with 0.5mM NEM – 25ul 0.2M NEM into 10ml PBS)
 - Trypsinize cells, re-suspend in media-NEM (2mM NEM in media)
 - spin at ~1000g for 5 minutes at 4°C
 - Wash cells with PBS-NEM
 - spin at ~1000g for 5 minutes at 4°C
 - aspirate off PBS-NEM carefully, re-suspend in ~155ul TRIS-BSAN
 - Add to tube 1
- Now have cells or muscle homogenate in tube 1
- Take from tube 1:
 - 5ul tube 1 -> tube 2 (protein tube)
 - Freeze in liquid nitrogen
 - 70ul tube 1 -> tube 3 (TCA tube, for GSH)
 - Put onto rocker
 - 70ul tube 1 -> tube 4 (PCA tube, for GSSG)
 - Put onto rocker
 - Vortex tubes 3 and 4
- Spin TCA and PCA tubes at 20,000g for 5minutes at 4°C
- Carefully take tubes out of centrifuge, be careful not to dislodge pellet
- From tube 3: Take off supernatant, and transfer to tube 5 (GSH tube)
- From tube 4: take 100ul of tube 4 -> tube 6 (GSSG tube)
- Freeze

Determine protein from samples using tube 2 (protein tube)

GSH determination (UV)

- GSH flow rate at 1.25 ml/min on old Agilent system (new Shimadzu HPLC down to 1.05ml/min)
- Sample detected using VWD (UV detector) detector (on HPLC stack) at 265nm
- 94% Mobile phase A, 6% acetonitrile
 - o Protocol name on HPLC is TurnbullGSH
- Take GSH tube, transfer total volume into HPLC vial.
- Have machine insert 10ul of sample into machine
 - o GSH elutes as two peaks right before NEM spike
 - Two peaks: it is because the configuration of GSH (3 amino acids) can be built in two ways depending on the specific amino acid configuration, I always use 2nd peak because 1st peak is sometimes influenced by other compounds depending on the tissue being analyzed
- **GSH Standard**
 - o Every day, run a 4 point standard
 - o 250uM GSH, 62.5uM GSH, 31.25uM GSH, 15.6uM GSH
 - o Step 1: Make 50mM GSH in TRIS-BSAN
 - o Step 2: Dilute 50mM GSH -> 5mM GSH in TRIS-BSAN
 - o Step 3: Dilute 5mM GSH -> 0.5mM GSH in TRIS-BSAN
 - o Step 4: Do serial dilutions from 0.5mM (500uM GSH)
 - 500uM GSH -> 250uM GSH -> 125uM GSH -> 62.5uM GSH -> 31.25uM GSH -> 15.6uM GSH
 - o Take 70ul of 250uM GSH, 62.5uM GSH, 31.25uM GSH, 15.6uM GSH tubes, and transfer to new tubes with 7ul TCA
 - o Transfer GSH-TCA tube to HPLC vial, ready to load

GSSG determination (fluorescent)

- Excitation/Emission 350/420nm
- Flow rate at 0.5 ml/min
- Sample elutes as a single peak
- Injection volume: 50ul
- Protocol is set up as TurnbullGSSG
- Take tube 6 out of freezer
- When thawed, add in 37.5ul of 0.1% OPA (our fluorophore, which is stored in -20°C freezer)
- Incubate samples in the dark for at least 15 minutes
- After incubation, transfer to HPLC vial, ready for run.
- **GSSG Standard**
 - o Every day, run a 4 point standard
 - o 10uM GSH, 2.5uM GSH, 1.25uM GSH, 0.625uM GSH
 - o Step 1: Make up 20mM GSSG in TRIS-BSAN
 - o Step 2: Dilute 20mM GSSG -> 2mM GSSG in TRIS-BSAN
 - o Step 3: Dilute 2mM GSSG -> 0.2mM GSSG in TRIS-BSAN
 - o Step 4: Dilute 0.2mM GSSG -> 20uM GSSG in TRIS-BSAN

- Step 5: Do serial dilutions starting from 20uM GSSG
 - 20uM GSSG -> 10uM GSSG -> 5uM GSSG -> 2.5uM GSSG -> 1.25uM GSSG -> 0.625uM GSSG.
- Step 6: Take 70ul of GSSG standard and mix with 70ul PCA
- Take 100uL from GSSG standards and transfer to new tube with 500ul 0.5M NaOH
- Add in 37.5ul of 0.1% OPA-MeOH (our fluorophore, which is stored in -20°C freezer)
- Incubate standards in the dark for at least 15 minutes
- After incubation, transfer to HPLC vial, ready for run.

Day of checklist:

- Make up TRIS-BSAN
 - Thaw 0.2M NEM stock from freezer, add 25ul NEM per 1ml TRIS-BSA
- Make up mobile phase
- Make up standard curve
- For GSH:
 - Transfer tubes into HPLC Vials
- For GSSG:
 - Incubate with OPA for 15 minutes before transfer tubes to HPLC vials

A.8 XTT for NAD(P)H determination

Purpose:

XTT is a tetrazolium salt that once reduced turns into a soluble formazan dye (it dissolves when reduced and turns red/orange). It is used as a proxy assay to determine intracellular NADH/NADPH (NAD(P)H) levels.

Make up before:

Make up XTT solution and phenazine methosulfate (PMS) solution

- XTT: 1mg/ml in condition media (this can be pre-made and frozen into stocks)
- PMS: 3mg/ml PMS powder into PBS (this can be pre-make and frozen into stocks)
- Both are potentially light sensitive
- To create detection solution: right before you are about to start, add 2.5µl/ml PMS solution to XTT solution
 - o Make sure you are constantly mixing this solution as you are loading into plates, XTT does not fully dissolve until reduced

Procedure:

- Following desired incubation time with desired compound (example, if you are doing a 24 hour incubation time with a drug, after the 24 hours is complete)
- Add 50µl detection solution into each well (bringing up the volume of each well to 150µl)
- Incubate plate for ~2-4 hours (depending on strength of signal, longer time greater signal strength. Whatever you do, be consistent throughout study)
- Measure absorbance using VICTOR³ 1420 Multilabel Counter plate reader (PerkinElmer) read at 450nm
- Normalize signal to protein content using protocol A.3

A.9 Caspase -3, -8 and -9 activity assays

Purpose:

Caspase activity is indicative of apoptotic mediated cell death. Caspase-3 is considered a final effector caspase and can act upon the entire cell; it is cleaved by various earlier caspases such as caspase-8 and -9. Caspase-8 is considered an external stimulus initiated caspase, whereas caspase-9 is triggered by mitochondrial mechanisms.

Make up before:

Homogenisation buffer: 500 ml

Chemical	Concentration	Amount added
HEPES	20mM	2.38g
NaCl	10mM	0.29g
MgCl	1.5mM	0.152g
DTT	1mM	0.077g
Glycerol	20%	100mL
Triton	0.1%	0.5mL

pH 7.4

Incubation buffer: 100 ml

Chemical	Molecular Weight	Concentration	Amount added
HEPES	283.3	100 mM	2.38g
Sucrose		10%	10g
DTT	154.25	1 mM	0.015g

pH 7.5

Fluorescent substrates for Caspase activities:

Caspase-3: AC-DEVD-AMC (Enzo - ALX-260-031-M001)

1mg into 1.48 mL DMSO for 1mM Stock

Caspase-3 Inhibitor: AC-DEVD-CHO (Enzo - ALX-260-030-M001)

1mg into 2mL DMSO for 1mM Stock

Caspase-8: AC-IETD-AMC (Enzo - ALX-260-042-M001)

1mg into 1.48 mL DMSO for 1mM Stock

Caspase-8 Inhibitor: AC-IETD-CHO (Enzo - ALX-260-043-M001)

1mg into 2mL DMSO for 1mM Stock

Caspase-9: AC-LEHD-AMC (Enzo - ALX-260-080-M001)

1mg into 1.45 mL DMSO for 1mM Stock ** Different MW from 3 and 8

Caspase 9 Inhibitor: AC-LEHD-CHO (Enzo - ALX-260-079-M001)
1mg into 1.86mL DMSO for 1mM Stock

** Aliquot Substrates into 100µl, Aliquot inhibitors into 10µl. Store in black tubes at -20°C

Procedure:

Preparation of cellular fraction:

- Scrape cells into 150µl of lysis Buffer
- Sonicate 3x3 seconds with a break in between rounds of sonication
- Freeze all fractions at -80°C

Protein determination:

- Protein determination is done with the Bradford method using a reducing agent compatible kit.
- Put a micro plate on ice (a layer of aluminium foil between plate and ice)

Caspase Activity:

- Dilute 1mM stock of each substrate into 100µM using incubation buffer
 - o make up total volume needed for all samples plus 20µl extra
- Add **40ug** of protein from S2 into the wells
 - o total of 6 wells for each sample
- Add x µl of diluted substrate (110- amount added for 30µg protein) for Caspase-3 to 2 wells
 - o Repeat step 3 using Caspase-8 and Caspase-9 substrate
- Add 3µl of Caspase-3 inhibitor to 1 of 6 wells
- Repeat step 5 for Caspase 8 and 9 inhibitor
- Read every 2 minutes for 1 hour

** Do not need to run inhibitor for every sample, just use as a check

Fluorometer measurements:

Prepare the fluorometer settings before adding standards, muscle extracts and substrates into the micro plates.

Temperatur 37°C; Excitation filter 360 nm; Emission filter 460 nm

Gain 80 % of max value

Read every 2 min for 1 hour

A.10 Trypan blue exclusion

Purpose:

To determine cell viability. As cells die, they lose integrity of outer membrane, allowing for non-membrane permeable dyes to penetrate. Trypan blue is a membrane impermeable dye, therefore, if the cell takes up trypan blue, it must have a permeable outer membrane.

Make up before:

Make up an eppendorf tube containing the desired amount of trypan blue (this ratio is important as it will dictate total number of cells). If cell number is high, a 10X to 20X dilution with trypan blue may be necessary (20 μ l cell suspension into 180 μ l trypan blue)

Procedure:

- Trypsin treat cells with 1ml of trypsin and place in incubator until cells dislodge
- Neutralize trypsin with 2ml of media (bringing total volume to 3ml)
- Remove cell suspension and place in a 15ml falcon tube
- Take out desired amount (from example before, 20 μ l) and place into trypan blue tube
- Count trypan blue-cell suspension mixture for both trypan blue negative (alive) and trypan blue positive (dead) cells
- Calculate total number of cells using standard hemocytometer practice and determine % alive and dead cells.